Grant agreement no. 776479

COACCH

CO-designing the Assessment of Climate CHange costs

H2020-SC5-2016-2017/H2020-SC5-2017-OneStageB

D3.4 Socio-economic tipping point analysis

Work Package:	3
Due date of deliverable:	M 32 (JUL/2020)
Actual submission date:	30/SEP/2020 – rev 07/MAR/2022
Start date of project: 01/DEC/2017	Duration: 42 months
Lead beneficiary for this deliverable:	VU
Contributors:	Wouter Botzen (VU), Predrag Ignjacevic (VU), Onno Kuik (VU), Max Tesselaar (VU), Timothy Tiggeloven, (VU), Gabriel Bachner (Uni-Graz), Birgit Bednar-Friedl (Uni-Graz), Wolf Grossmann (Uni-Graz), Nina Knittel (Uni-Graz), Karl Steininger (Uni-Graz), Keith Williges (Uni-Graz), Francesco Bosello (CMCC), Shouro Dasgupta (CMCC), Gabriele Standardi (CMCC), Ramiro Parrado (CMCC), Paul Watkiss (PWA), Federica Cimato (PWA), Alistair Hunt (PWA), Esther Boere (IIASA), Hugo Valin (IIASA), Jochen Hinkel (GCF), Daniel Lincke (GCF), Ana Laura Costa (Deltares), Kees van Ginkel (Deltares), Frederique de Groen (Deltares), Marjolijn Haasnoot (Deltares), Ad Jeuken (Deltares).

*This project has received funding from the European Union's Horizon 2020 research and innovation programme under the Grant Agreement No **776479.***

Disclaimer

The content of this deliverable does not reflect the official opinion of the European Union. Responsibility for the information and views expressed herein lies entirely with the author(s).

Dissemination Level		
PU	Public	X
CO	Confidential, only for members of the consortium (including the Commission Services)	
CI	Classified, as referred to in Commission Decision 2001/844/EC	

*This project has received funding from the European Union's Horizon 2020 research and innovation programme under the Grant Agreement No **776479.***

Table of contents

*This project has received funding from the European Union's Horizon 2020 research and innovation programme under the Grant Agreement No **776479.***

Version log

Version	Date	Released by	Nature of Change
0.1	09/October/18	Onno Kuik (VU)	Zero draft
0.2	18/March/20	Gabriel Bachner, Karl Steininger (UNIGRAZ)	Updated structure
1.0	6/Aug/20	Predrag Ignjacevic (VU)	Merged sections, completed summary and 1.1
2.0	12/ Aug/20	Max Tesselaar (VU)	Included flood insurance analysis
3.0	13/Aug/20	Wouter Botzen (VU)	Final check of the summary and introduction.
4.0	24/Aug/20	Onno Kuik (VU)	Final editing
4.1	18/Sep/20	Keith Williges, Karl Steininger, Wolf Grossmann (UNIGRAZ)	Revision of SETP9 (Sections 2.9 and 3.9)
5.0	30/Sep/20	Onno Kuik (VU)	Included contribution by CMCC and addressed review comments by Karl Steininger.
6.0	01/Oct/20	Francesco Bosello (CMCC)	Final check by coordinator
7.0	07/Mar/2020	CMCC	Last revision incorporating reviewer comments

*This project has received funding from the European Union's Horizon 2020 research and innovation programme under the Grant Agreement No **776479.***

Deliverable Summary

This deliverable (D3.4) substantiates that part of the activity of COACCH Task 3.4 that analyses the selected socio-economic tipping points and explores their implications on economic activity and society in general. COACCH found that a range of socioeconomic tipping points is relevant for Europe and this report identifies which tipping points are expected to materialize at which scale and when in the future, and which regions will be hit particularly. More specifically, this report elaborates on the following main findings:

- ***Impacts of migration***
  The numbers of migrants moving from African regions to Europe is expected to significantly rise over the course of the 21st century from between 0.2 and 0.4 million annually in the first two decades to up to 1.7 million annually in the 2080s. The increase is driven by population and climate change- induced drought projections in Africa. The main underlying assumptions for this finding are that the probability and conditions of access to European countries faced by migrants from Africa remain similar, on average, to those that have existed in the last 50 years. The degree to which states in Africa allow their citizens to leave is assumed to remain constant. The validity of the model depends on both the current relative levels of GDP/capita in Africa and Europe persisting over the time period as well as the personal costs to each migrant of moving.
- ***Financial tipping points***
  There is an increasing recognition that the physical risks of climate change imply a financial risk, and this is reflected in recent initiatives by the financial sector and central banks. A literature review has assessed the potential financial risks of climate change and used this to qualitatively explore potential transmission pathways including socio-economic tipping points. The study finds that large-scale climate hazards already affect credit ratings, cost of debt and of capital. Climate change is a risk for the stock of manageable assets and investment returns, and potentially financial market stability. Finally, higher climate disclosure could lead to financial market anticipation of future risks in high-risk countries, thereby leading to an occurrence of a socio-economic tipping point before the physical impacts ofclimate change occur.
- ***Food and water***
  Climate change may render agricultural production unviable, effectively abolishing farming and triggering rural abandonment, which is the analyzed socio-economic tipping point. The extent of land abandonment as a result of gradual climate change is examined as well as substantive climate-induced yield drops caused by extreme events. The largest cropland losses due to farmland abandonment found across all scenarios is 7% for Europe. Land abandonment was highest in the middle and Southern parts of Europe and showed specific concentrations in Southern Spain and Italy. From the macroeconomic assessment we find that food prices in Europe slightly increase in most of the analyzed scenarios. Cropland loss due to extreme events could (more than) offset positive effects from long-run (slow onset) higher yields.
- ***Coastal migration***
  While for inward migration from Africa, for financial risks and farmland abolishment

*This project has received funding from the European Union's Horizon 2020 research and innovation programme under the Grant Agreement No **776479.***

we identified high likelihoods of occurrence, the tipping points triggered by high levels of coastal migration in societies are not expected to occur in the EU28 due to its high existing standards of coastal protection. In the MENA region, the migration thresholds defined in the previous COACCH Deliverable D3.2 could be crossed for warming scenarios of RCP6.0 or higher in the 2050s and the 2080s. With adaptation, migration numbers are below thresholds in nearly all cases. However, additional autonomous adaptation in the form of migration further avoids impacts. We demonstrate that the simultaneous implementation of planned and autonomous measures (in the form of migration away from coastal areas) is superior to purely planned adaptation. For some developing regions autonomous adaptation might even be superior to planned adaptation. Sectoral effects can be very different between regions, depending on comparative advantages in foreign trade. Finally, the benefits of adaptation might be overestimated when using a no-adaptation scenario as a reference.

- ***Adaptation to accelerating SLR***
  For urban coastal cities, the socio-economic tipping point (SETP) is defined as an abrupt drop in the value of real estate, as a result of sharply increased risk perception of citizens and a decreased trust in the government to successfully protect against floods in the future. Tipping points in embanked urban areas such as Rotterdam can be avoided in the 21st century even in very extreme, high-end sea level rise scenarios provided that there is a sound, proactive flood management strategy. With poor, reactive flood risk management, there is a chance that in the most extreme scenarios, the first SETPs may occur by the end of the 21st century, even in cities that are currently protected with very high protection levels. The causefor these SETPs is that the implementation times of traditional dike heightening measures will become too long compared to the rate of sea level rise projected for the end of the century. However, for lowly elevated outerdike (not embanked) areas, SETPs are likely to occur in the 21st century. These areas can only be maintained by transformational response, especially in high-end sea level rise scenarios.
- ***Trade disruptions due to flooding***
  On three spatial levels, it was examined whether river floods may cause a major (SETP-like) loss of European road network functionality. First, at the level of European states we found large differences in vulnerability. Of the six examined countries, Albania is the most vulnerable, whereas Sweden and Ireland are among the most robust. Second, at the level of the national road network of Austria, we examined the economic costs of six unfavourable flood scenarios, which may happen once in 100 years in the current climate, and become up to a factor 10 more likely in the most unfavourable future climate. We did not find evidence that these unfavourable flood scenarios lead to national road disruptions with substantial macro-economic damage; the most disruptive scenario causes 101 million Euro damage. Third, at the level of individual firms, we also found that the European road network is very resilient. For an individual car and truck manufacturer, SETPs are more likely to be caused by a flood of the manufacturer itself - or a flood at one of the suppliers to the factory - than from a flood of the road network between the suppliers and the manufacturer. Detour times typically increase in a linear fashion, butspecific just-in-time characteristics of some supply chains may nevertheless cause SETPs at the level of individual firms.
- ***Collapse of insurance markets for extreme weather risks***
  Climate change will cause a rise in risk-based premiums. The thus induced decline in insurance uptake can substantially affect the viability of flood insurance markets, and

*This project has received funding from the European Union's Horizon 2020 research and innovation programme under the Grant Agreement No **776479.***

they can collapse in a range of regions across Europe. This process exacerbates the vulnerability especially in regions where insurance is voluntary and households face unaffordable premiums due to either low income or high risk. A socio-economic tipping point can occur when uptake of flood insurance diminishes as a result of rising premiums due to climate change, low income, or low willingness-to-pay for insurance. Regions where such a tipping point is projected in the future include Croatia, Bulgaria, Czech Republic, Poland and Portugal. As flood insurance markets may cease to exist in these regions, while the risk of flooding is expected to increase, households will become more financially vulnerable to flood damage. Also, from a macroeconomic perspective, the tipping regions in the Czech Republic and Poland are among the most affected. Additionally, severe impacts can be observed for the Netherlands, Germany, Austria and Italy. Especially high impacts are found for government budgets when governments are expected to take responsibility for covering uninsured flood damages. Besides this, low insurance penetration rates cause negative impacts on savings and, therefore, investments, which in turn reduces capital accumulation. Finally, negative impacts on GDP are significant across EU regions, and even larger on welfare when accounting for additional consumption for reconstruction not being welfare enhancing.

- ***Climate-induced economic shocks***

  The ToEI results for Europe imply that economically stable, developed countries are equally or even more at risk from climate change under this indicator than less economically stable, developing countries, already by their threshold of past significant shocks being lower. ToEI methodology suggests that it can be expected that the developed countries could more likely perceive the effects of climate change impacts as severe shocks to their economies are more likely than it is the case for the developing countries, as the latter have a vast experience in political conflict and economic crises.

  Through the local-scale integrated assessment model (IAM) CLIMRISK, we have shown that country-level impact data can be used to project ToEI estimates on a 0.5°by 0.5° grid in Europe. We find that severe economic shocks as measured by the ToEIoccur in a variety of regions in Europe during this century under high end emission scenarios. Even moderate mitigation efforts (e.g. RCP 4.5) could delay the ToEI by several decades, which would give time to implement adaptation policies to limit climate change risks. Scandinavian countries and Western-Europe face the highest risk, but could experience a significant delay in the ToEI from around 2080 to well past 2100. Abiding by the Paris Agreement would delay the effects even further into the 22nd century.

  Further, the analysis on climate-induced economic shocks has been also conducted with the in COAACH newly developed regional differentiated macroeconomic model, the ICES macroeconomic NUTS2 model. The assessment aims to identify how many regions and where economic shocks are larger than the 5% of regional GDP. The macroeconomic perspective of the ICES model enables to capture market adjustments triggered by climate change impacts. Furthermore, it does not rely upon a simplified modeling of the reduced form climate change damage functions, but analyses the economic consequence of each single climate change impact through its effect on the quantity and quality of production factors or changes in consumer preferences. The exercise is thus an interesting complement of the CLIMRISK assessment reported in the paragraph before. The evaluation is performed for the 9

*This project has received funding from the European Union's Horizon 2020 research and innovation programme under the Grant Agreement No **776479.***

SSP-RCP scenario combinations of the COACCH project. For each, the uncertainty range is represented considering a "low", "medium" and "high" impact case. Major findings are the following: considering a "medium impact" case, regions in the EU meeting the chosen social-economic tipping point are considerably more in high climate-change (16 to 31 regions out of the total of 138 regions) than in low climate-change scenarios (4 to 8 regions).

Nonetheless, the situation blurs when the possible "high end" of the impact uncertainty range is considered. In this case, also in low climate change scenarios many EU areas meet the tipping point in RCP2.6 and 4.5 (27 to 60 regions) in a way comparable to what occurs in RCP6.0 or 8.5 (41 to 57 regions). The factor at work is the smoothing effect of impacts on agriculture where CO_2 fertilization decreases yield losses in higher temperature scenarios. This highlights the particular care that needs to be used in the interpretation of aggregated results where the "averaging effect" can hide huge losses. The possibility of high losses in low temperature RCPs also stresses the importance to reduce emission as much as possible as, given the uncertainty, "every degree matters". Mitigation is thus essential to reduce to an acceptable level the chances of these localized high losses. Finally, adaptation also can play an important role. In the exercise it is noted that more economic "flexibility" (larger substitutability across energy and non-energy input or across domestic and imported commodities) tends to reduce the number of regions reaching the tipping point, even though more assets could be at risk compared with lower exposure, but more "economically rigid" scenarios. Although very rough, this is an indication that building adaptive capacity and flexibility is fundamental to address climate shocks.

- ***Electricity system failures***

  In our assessment of a socio-economic tipping point of major blackouts due to increasing wildfires, we use a risk-based approach to assessing the possible current impacts and effects on European countries. We find that much of the land area in Europe could see extreme increase in wildfire probability by the end of the century under different RCP scenarios.

  Focusing on blackouts due to fires, we find that across Europe, value added at risk is expected to increase strongly under three of four shared socioeconomic pathways, a concept to distinguish the main future development scenarios (SSP projections), due to a marked increase in manufacturing sector activity in all but the one pathway reflecting "regional rivalry".

  We complete our discussion of risk with a focus on the potential vulnerability to such blackouts with an overview of key traits of the electricity sector which will impact the eventual losses due to wildfires in the future. Finally, we show that the threat of major wildfires in Europe can be avoided by accelerating the investment plans for renewable energy.

Peer-reviewed papers published as a result of this study

Abadie, L.M., Jackson, L.P., Sainz de Murieta, E., Jevrejeva, S., Galarraga, I., (2020). Comparing urban coastal flood risk in 136 cities under two alternative sea-level projections: RCP 8.5 and an expert opinion-based high-end scenario. *Ocean & Coastal Management* 193, 105249. https://doi.org/10.1016/j.ocecoaman.2020.105249

*This project has received funding from the European Union's Horizon 2020 research and innovation programme under the Grant Agreement No **776479.***

Bachner, B., Mayer, J., Steininger, K.W. (2019) Costs or benefits? Assessing the economy-wide effects of the electricity sector's low carbon transition – The role of capital costs, divergent risk perceptions and premiums. *Energy Strategy Reviews* 26, 100373. https://doi.org/10.1016/j.esr.2019.100373.

Bachner, G., Lincke, D., Hinkel, J. (2021), Macroeconomic Implications of Extreme Sea Level Rise and Coastal Migration: A Global Assessment. *Nature Communications* (under review).

Borodina, O.M., Kyryziuk, S.V., Fraier, O V., Ermoliev, Y.M., Ermolieva, T.Y., Knopov, P.S., Horbachuk, V.M. (2020). *Mathematical Modeling of Agricultural Crop Diversification in Ukraine: Scientific Approaches and Empirical Results*. *Cybernetics and Systems Analysis* 56, 2, 213-222. 10.1007/s10559-020-00237-6. http://pure.iiasa.ac.at/16615

Ginkel, K.C.H. van, Botzen, W.J., Haasnoot, M., Bachner, G., Steininger, K.W., Hinkel, J., Watkiss, P., Boere, E., Jeuken, A., Sainz de Murieta, E., Bosello, F. (2020). Climate change induced socio-economic tipping points: review and stakeholder consultation for policy relevant research. *Environmental Research Letters* 15, 2, 023001. https://iopscience.iop.org/article/10.1088/1748-9326/ab6395/meta

Hinkel, J., Church, J. A., Gregory, J. M., Lambert, E., Le Cozannet, G., Lowe, J., McInnes, K.L., Nicholls, R.J., Pol, T.D., van der, Wal, R. van de (2019). Meeting user needs for sea level rise information: A decision analysis perspective. *Earth's Future* 7, 320–337. https://doi.org/10.1029/2018EF001071

Lincke, D., Hinkel, J. (2021). Coastal migration due to 21st century sea-level rise. *Earth's Future* 9, 5, e2020EF001965. https://doi.org/10.1029/2020EF001965

Scoccimarro E, Gualdi S, Krichak S. (2018). Extreme precipitation events over north-western Europe: getting water from the tropics. *Annals of Geophysics* 61, 4, OC449. https://doi.org/10.4401/ag-7772

Scoccimarro, E., and Gualdi, S. (2020). Heavy Daily Precipitation Events in the CMIP6 Worst-Case Scenario: Projected Twenty-First-Century Changes. *Journal of Climate* 33, 17, 7631-7642. https://doi.org/10.1175/JCLI-D-19-0940.1

Tesselaar, M., Botzen, W.J.W., Haer, T., Hudson, P., Tiggeloven, T., Aerts, J.C.J.H. (2020) Regional Inequalities in Flood Insurance Affordability and Uptake under Climate Change. *Sustainability* 12, 8734. https://doi.org/10.3390/su12208734

*This project has received funding from the European Union's Horizon 2020 research and innovation programme under the Grant Agreement No **776479.***

1. Introduction

1.1. Socio-economic tipping points

This section briefly recapitulates what we understand by socio-economic tipping points (D3.1), how they relate to climate change tipping points (D3.2), and what the stakeholders say about socio-economic tipping points (SETPs). It then summarizes the overall methodology by which the drivers and consequences of socio-economic tipping points have been assessed in both physical and economic terms at different sectoral and regional levels (the detailed methodological approaches are given in the respective sub-sections of section 2).

As was shown in D3.2, tipping of large elements of the climate system may cause rapid change in the biophysical system which can have profound consequences for the socio-economic structure of Europe. Moreover, SETPs can occur even in the absence of climate tipping points when climate change has large implications for socio-economic systems. More precisely, SETPs are defined as a climate change induced, abrupt change of a socio-economic system, into a new, fundamentally different state (Van Ginkel et al., 2020).

The policy stakeholders are interested in the impact of sea level rise. On a country level, they are worried about the resilience of coastal communities and the potential damage to roads and railways along the coast. At an EU level, they fear mass migration into Europe induced by climate change in other continents. The policy stakeholders in southern countries are very concerned about the impacts of droughts and extreme heat, at both local and national levels. Droughts threaten a large variety of ecosystem services in southern Europe. This would most likely lead to irreversible abandonment of rain fed agriculture and migratory flows towards cities (D3.1). Higher temperatures are likely to create opportunities for agriculture where this formerly was not possible, which could be considered a positive SETP. However, higher temperatures also have proven to negatively affect labour productivity, with temperatures above 26 degrees Celsius visibly decreasing productivity.

Business stakeholders are worried about impacts on built infrastructure that could lead to negative impacts on businesses, such as shutdown of ports or roads but also of electricity systems. In short, long-lasting disturbances in logistical systems are considered an SETP in the business sector. In the insurance industry, there could exist a climate tipping point where insured damage can become too high for the standard insurance conditions to cover.

Finally, most stakeholders agree that increasing temperatures that lead to changes in vector borne diseases would be relevant for the health care sector, especially the emergence of global epidemics.

This report presents analyses of these socio-economic tipping points and others, as summarized in the table below, which gives an outline of the report and summary of adopted methodologies per topic.

*This project has received funding from the European Union's Horizon 2020 research and innovation programme under the Grant Agreement No **776479.***

Topic	Section	Consortium partner	SETP	Short description of model approach
Impacts of migration	2.1	PWA	Climate-induced migration	Climate anomaly (rainfall & temperature) – migration relationship. Regression analysis.
Financial Tipping Points	2.2	PWA	Major downgrade of sovereign credit ratings, increasing cost of debt	A literature review to assess the potential financial risks of climate change. Qualitative assessment of potential transmission pathways.
Food and Water	2.3	IIASA	Rural abandonment, disappearance of farms	Biophysical crop model EPIC. Bio-economic model GLOBIOM, investigate the yield shock required for the tipping point. COIN-INT to investigate the implications of TP on the macroeconomy.
Coastal Migration	2.4	GCF	SETP triggered by large coastal migration	Macroeconomic CGE model COIN-INT with added coastal migration component.
Adaptation to accelerating SLR	2.5	Deltares	Abrupt drop in the real estate value	Stylized model loosely based on the City of Rotterdam.

*This project has received funding from the European Union's Horizon 2020 research and innovation programme under the Grant Agreement No **776479.***

Trade disruptions due to flooding	2.6	Deltares	SETPs triggered by decreasing road network performance due to river flooding	Three spatial levels of analysis; EU State level, national road network in Austria and individual car/manufacturer.
Collapse of insurance markets	2.7	VU	Increasing flood risks makes floods insurance unaffordable and unattractive for consumers, causing a market collapse.	Integration of partial equilibrium model of flood insurance markets in the EU (the DIFI model) with a macroeconomic computable general equilibrium model (COIN-INT).
Climate induced economic shocks	2.8	VU/CMCC	Time of emergence of impacts (ToEI) of climate change/ NUTS2 regions where economic shocks are larger than 5% of GDP.	Integrated assessment model CLIMRISK and Maddison GDP database. Comparisons between the two are drawn to create the time of emergence of impacts (ToEI)/ ICES macroeconomic NUTS2 model.
Electricity system failures	2.9	UNIGRAZ	Increasing major blackouts in terms of a disaster risk framework.	Assessment of EU's exposure to blackout risk. Production function approach assessing potential value added at risk due to power outages for EU member states.

*This project has received funding from the European Union's Horizon 2020 research and innovation programme under the Grant Agreement No **776479.***

1.2. Macroeconomic model description

1.2.1. General description of macroeconomic modelling approach

For the assessment of macroeconomic implications of selected SETPs we use two different global, multi-sectoral, multi-regional, computable general equilibrium (CGE) models: COIN-INT (developed by University of Graz) and ICES (developed by the Euro-Mediterranean Center on Climate Change, CMCC).

In general, CGE models depict the economy as an annual flow equilibrium of monetary flows across all production sectors and final demand agents. All sectors and agents are interlinked, as each economic sector delivers to other sectors and receives inputs from other sectors (described by regional input output-tables, which form the backbone of CGE models) and sectoral outputs are also delivered to final demand agents. The main idea behind CGE models is that all markets are simultaneously cleared, i.e. in equilibrium where supply equals demand. This equilibrium represents the optimal long-run equilibrium of the economy, in which all sectors/agents optimize their production costs/utility from consumption (under technological, resource and budget constraints). This equilibrium is then shocked by an intervention – e.g. by a lower sectoral productivity due to climate change – which triggers indirect effects (due to the interlinkages) and adjustments on all markets. More precisely, relative prices as well as supplied/demanded quantities adjust until a new equilibrium emerges, representing a new optimum under new conditions. From the difference between new and old equilibrium modellers can draw conclusions on how the economy would look different due to a system intervention. Comparing the differences of two different equilibria describes a comparative static approach, which can be further developed toa recursive dynamic approach to extrapolate stepwise into the future. In recursive, dynamic CGE models, annual equilibria are connected via investment and capital accumulation, where investment of one period determines the capital stock of thenext period.

Thus, the idea of CGE models is to depict long-term trends under long-term balanced macroeconomic accounts. Hence, CGE models are well suited for long-term analyses of climate change impacts and adaptation and the associated indirect effects. In fact, their multi-sectoral resolution allows for more detailed analysis than standard Integrated Assessment Models (IAMs), which work on a much coarser resolution. CGE modelling also has its limitations, though, which are specifically important for the analysis of tipping points. Most importantly, as explained, CGE models compare equilibria to each other, but do not allow for the analysis of the processes themselves that lead from one equilibrium to another. Thus, CGE models can be used to assess economy-wide effects after a system (economy) has tipped, but relies on information from other models (bottom-up models as available in COACCH) with respect to economic/sectoral parameters after the system has changed.

The CGE models were used for the analyses of 2.3 Food and water (COIN-INT), 2.4 Coastal migration (COIN-INT), 2.7 Collapse of the insurance market (COIN-INT), and 2.8 Climate-induced economic shocks (ICES). They were not used for the other analyses in this Deliverable.

*This project has received funding from the European Union's Horizon 2020 research and innovation programme under the Grant Agreement No **776479.***

1.2.2. The COIN-INT model

The COIN-INT model is based on the static version of (Schinko et al., 2014), which was originally designed to assess the economy-wide effect of climate change mitigation measures. The model is calibrated to the GTAP9 database (Aguiar et al., 2016), with the base year of 2011. For the purpose of this analysis, the model has been further developed and refined. The main characteristics are briefly summarized in this section; for details, please see the Appendix (section 5.1).

Region and sector aggregates: In COIN-INT individual countries are aggregated to 21 larger regions that share similar climatic conditions. There is a focus on the EU, hence at the EU level the regional resolution is higher than for the rest of the world; see Table 5.1.1. The EU is represented as ten regions: Germany (DEU); Austria (AUT); Italy (ITA); UK (UKD); France (FRA); Belgium and Luxemburg (BLU); Netherlands (NLD); Central EU28 + Switzerland (CEU); Northern EU28, Norway and Iceland (NEU); Mediterranean and South-eastern EU 28 (MEU).[1] The sectoral aggregations have been chosen to match sector aggregates as good as possible with the modelled impact chains throughout COACCH. In total there are 21 sector aggregates; see Table 5.1.2 in the Appendix. Special emphasis is placed on the Electricity sector which is further divided into 12 sub-sectors according to the GTAP-POWER database (Peters, 2016).

CO2 emissions: COIN-INT comprises combustion-based CO2 emissions as well as CO2 emissions arising from industrial processes.

Final demand: Within the EU there are two representative households in each region. First, a private household which is endowed with the production factors skilled labour, unskilled labour, capital as well as natural resources (fossil resources, land and CO2 emission allowances). Second, in each EU regions there is also a public household, which collects taxes and provides transfers to the private household. Net-tax income is used to finance government consumption. In non-EU regions there is only one representative regional household, aggregating public and private consumption. Investment in each region is determined via a fixed savings rate (i.e. a fixed proportion of income is devoted to savings/investments).

Dynamics: COIN-INT is available in two variants: a static comparative version which models snapshots of 2011, 2030 and 2050, as well as a recursive dynamic version that explicitly models the pathway of economic development in 5-year time steps from 2015 to 2050. Both versions are used for different purposes throughout this report. COIN-INT is calibrated to all SSP-RCP-combinations from the COACCH modelling protocol (Hof et al., 2018). The two-step calibration process is explained in detail in the Appendix.

1.2.3. The ICES model

ICES (Inter-temporal Computable Equilibrium System) is a top-down recursive-dynamic multi-sector and multi-country computable general equilibrium (CGE) model for the world economy, based upon the GTAP8.1 database (Narayanan et al, 2012). ICES has been used in climate change impact and policy assessments (Bosello et al., 2012; Eboli et al. 2010). The model structure describes domestic and international linkages between economic activities, energy use, including renewables, and CO2 emissions (Parrado and DeCian 2014). For the COACCH project the model's regional

[1] Note, that these regions do not match exactly with the member states of the EU27, but cover all regions that are part of the EU Emission Trading Scheme.

*This project has received funding from the European Union's Horizon 2020 research and innovation programme under the Grant Agreement No **776479.***

coverage for Europe has been extended to NUTS2 and NUTS1 regions (Bosello and Standardi, 2015; Pérez-Blanco and Standardi, 2019). In addition, the electricity sector has been expanded for all regions using data from PLATTS (2014) and Peters (2016).

Region and sector aggregates: The regional aggregation for COACCH covers 138 EU (NUTS0-2) regions and 18 regions from the rest of the world. The sectoral aggregation covers 24 sectors which have been tailored to fit COACCH's sectoral climate change impact assessment approach.

For a detailed description of the model, its regions and sectors please refer to the appendix of D2.7: "Macroeconomic, spatially-resolved impact assessment" (Bosello et al., 2020).

CO2 emissions: The model accounts for CO2 emissions from the combustion of fossil fuels.

Final Demand: A representative consumer in each region receives income, defined as the service value of national primary factors (natural resources, land, labor, capital). Capital and labor are perfectly mobile domestically but immobile internationally. Land and natural resources are industry-specific. Income from primary factors is used to finance three classes of expenditure: private consumption, public consumption, and savings. The expenditure shares are generally fixed, which amounts to saying that the top-level utility function has a Cobb-Douglas specification. Investment is internationally mobile: savings from all regions are pooled and then investment is allocated so as to achieve equality of expected rates of return to capital in the long term. Savings and investments are equalized at the world level, but not at the regional level. Because of accounting identities, any financial imbalance mirrors a trade deficit or surplus in each region.

Dynamics: ICES is a recursive dynamic model that runs either in 1 or 5 year time steps. The model has been calibrated to the 9 SSP-RCP combinations for the COACCH project.

*This project has received funding from the European Union's Horizon 2020 research and innovation programme under the Grant Agreement No **776479.***

2. Selected socio-economic tipping points and their implications

This chapter analyses selected socio-economic tipping points and their implications on economic activity and society in general.

2.1. Impacts of migration

2.1.1. Introduction and definition of tipping point

Migration can be voluntary or forced and can be internal (within a country) or external (from country to country)[2]. There is some evidence (IPCC, 2019) that shows that past climate extremes can be a stress multiplier for internal and external migration (medium confidence). Future climate change could also be a potential contributory factor in migration and is relevant to both mitigation and adaptation policy decisions. This is already recognised by the fact that over 50% of countries reference environmental and climate change factors in their national migration and displacement policy frameworks (IOM, 2018). Migration can be a planned adaptation strategy to changing conditions but may also involve a forced displacement. However, the role of climate change (directly or indirectly as a threat multiplier), and the level of migration that is projected, have both been sources of contention in the literature. This is particularly the case over forced displacement and international migration.

Migration of sizeable numbers of people is likely to have a range of impacts on the regions of origin as well as the destination regions. For example, movements of working age people away from rural areas will affect the demographics of those areas, leaving them with higher dependency ratios (numbers of people dependent on others' income relative to those generating income) and consequent lower tax bases with which to fund local public services such as health treatment. Conversely, migration of people to an area may impact upon housing provision, raising property prices and reducing affordability for incumbent populations. Alternatively, it may introduce new labour skills to local industries and so have a positive effect on productivity. In practice,the likely range of economic, social, cultural and environmental impacts will be much wider than these examples suggest. Consequently, understanding the potential for climate change-induced migration, and its' possible dimensions, are important for planning development strategies that help determine, facilitate and allow for the extent of such migration.

Patterns of migration to Europe, are well-established in historical data series. For example, Figure 2.1.1 shows the flow of migrants originating from countries in Africa to countries in Europe over an 18-year period to 2017. It shows an irregular

[2] Migration is defined as "The movement of persons away from their place of usual residence, either across an international border or within a State" (IOM 2019). This should be seen in relation to the broader term of human mobility which includes all the different forms of movements of persons, including tourists.

*This project has received funding from the European Union's Horizon 2020 research and innovation programme under the Grant Agreement No **776479.***

upward trend over the period, with an annual average of just under 304,000 migrants arriving in Europe.

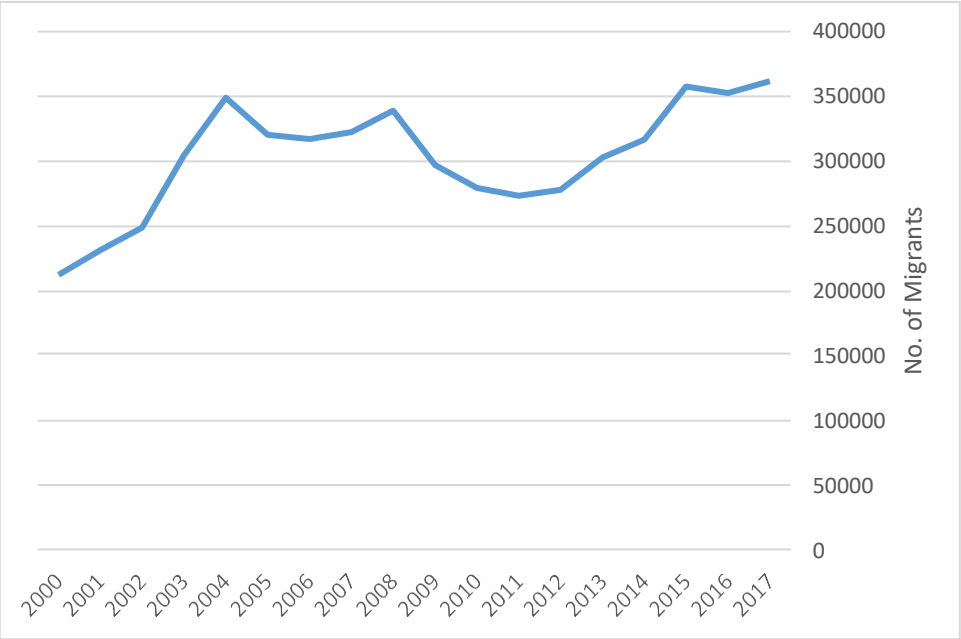

Figure 2.1.1. **Number of Migrants from Africa to Europe (2000-2017, actual)**
Source: Author's own, compiled from OECD Migration Data

Such patterns of migration, either within individual countries or between countries, can be seen as being triggered by perceived differences / opportunities in living standards between their current location and another location. Thus, there may be a range of "push" factors and "pull" factors that contribute to the decision to move. "Push" factors may include, inter alia: low and/or unpredictable income levels, social instabilities due to conflicts between population groups, environmental degradation, etc. Conversely, "pull" factors might include, for example: higher wage levels and more employment opportunities, the existence of better welfare-protecting institutions such as hospitals and schools, and political freedoms. The literature on determinants of migration highlights not only that these factors are likely to have different levels of importance across the wide range of contexts in which population movements occur (see e.g. Black, 2011). It is further complicated by the fact that the ability to migrate externally (across borders, and especially into Europe) will be affected by income and wealth, since the act of migrating itself requires resources including costs and unproductive time. Thus, where levels of impoverishment are high (or for groups in an affected community that are poor), these populations will be less able to respond by moving to areas where higher incomes may be available, i.e. they are more likely to undertake internal rather than external (international) migration (Koubi et al., 2016).

There is also substantial disagreement as to the causality of climate in migration, and subsequently whether it is feasible to quantify the size of potential migration. This involves major challenges, e.g. on whether it is possible to credibly characterise the determinants of migration, and their relationships with each other, in quantitative terms (Boas et al., 2019).

*This project has received funding from the European Union's Horizon 2020 research and innovation programme under the Grant Agreement No **776479.***

As highlighted above, there is reasonable evidence for climate extremes (e.g. droughts) being a threat multiplier for migration, and some more debated literature that attributes a more direct causality (Myers, 1997). Future climate change will affect these hazards, potentially increasing their intensity and frequency. Alongside this, it may generate new pathways for migration, notably from sea-level rise and land inundation and loss.

The casual pathways involved are, however, likely to be complex. Migration could be made more likely by prolonged periods of climate change-induced drought that adversely affects agricultural productivity and so lowers incomes in the agricultural sector, though primarily where adaptive capacity is low or other factors mean systems are already close to tolerance levels. Alternatively, sea-level rise might blight coastal settlements, either through direct impacts or by changing other factors (e.g. availability of insurance), making them effectively undesirable or even uninhabitable.

In this vein, the literature provides a wide range of quantitative estimates of numbers of possible migrants in various world regions in response to a variety of climatic variables and weather events. For example, Iqbal and Roy (2015) report that in Bangladesh a projected increase in rainfall uncertainty would increase net out-migration rates by 20% in 2030 relative to 1990. Similarly, Kubik and Maurel (2016) report in Tanzania, that for a typical household, a one-percent reduction in agricultural income induced by weather shock increases the probability of migration by thirteen percent in the following year. However, this effect is significant only for households who have average levels of wealth; having below-average levels of wealth disallows migration – both internal and external - as an adaptation strategy. At the same time, there is a significant literature that argues that climatic variables may not be dominant factors in determining decisions to migrate, (Adams and Kay, 2019) or that migration results only indirectly from climate change as a consequence of climate-induced conflict (Selby et al., 2017).

There is some analysis of migration in some modelling domains. The DIVAcoastal model used in this project includes estimates of coastal migration induced by sea-level rise and flooding. Following Tol (1995), the number of people forced to migrate is calculated as the coastal area permanently flooded times the population density in that area. The value per migrant is 3 times the per capita income. The COACCH project is looking at coastal migration as part of the socio-economic tipping points. However, it is more difficult to estimate migration in other integrated modelling assessments for other hazards, because of the extremely complex causal pathways, i.e. from a climate hazard (e.g. drought) to migration, though there are examples of the use of agent-based models to look at such responses (Thober et al., 2018). As a consequence, whilst we generate quantitative estimates of potential migrant numbers we do not attempt to attach a monetary measure of the welfare impacts of these migrant numbers.

What is the socio-economic tipping point?

Climate change-induced migration can be regarded as a tipping point since at a certain point in time people make a decision, or are forced, to move to a different

*This project has received funding from the European Union's Horizon 2020 research and innovation programme under the Grant Agreement No **776479.***

location as a consequence of climatic conditions adversely affecting their livelihoods and/or their well-being more generally. McLeman (2018) shows that migration can be seen as the consequence of a series of prior tipping points being passed. As identified in Figure 2.1.2, the first tipping point, (1), is where the need for adaptation is recognised – as in the case where a farmer needs to switch to a more drought-resilient strain of crop. The second tipping point (2) arises when the current form of adaptation is seen to be ineffective. Thus, the third tipping point (3) necessitates a change in livelihood. The migration tipping point (4) is therefore when such a change in livelihood is deemed to not be economic or feasible in the current location, e.g. thereis no alternative to farming available as a livelihood.

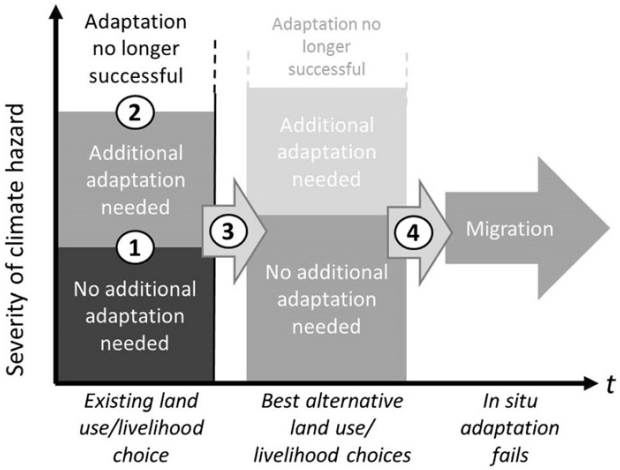

Figure 2.1.2. **Adaptation and tipping points relating to livelihoods**
Source: McLeman (2018)

Whilst our analysis below is predicated on the existence of tipping point (4), it may also be the case that tipping points exist for a wider group within a society, where – for example – news of migrants' success will result in a non-linear increase in additional migrants, and the cost of migration declines as new migrants draw upon the information and social capital provided by those who went before (McLeman, 2018). Related to this, where such non-linearities result - or are likely to result – in large numbers of migrants arriving in a specific destination, there may be tipping points in terms of provision of municipal services resulting from an expansion in housing that need to be factored into forward-looking planning processes. Similarly, there may be changes in social attitudes in indigenous populations towards migrant populations thatfoster social and political intolerance (Heinmuller & Hiscox, 2007). For example, it is notable that immigration to the EU received disproportionate attention in media coverage from 2015 when immigrant arrivals rose from 250,000 in 2014 to 1 million arrivals in 2015 (UNHCR Database).

This study utilises data from a number of recent papers in order to make indicative estimates of the potential scale of migratory movements from Africa to Europe as a consequence – directly or indirectly – of climatic change. The quantitative estimates are therefore based on the application of climate-migration functions currently published in the existing literature. These function transfers are combined

*This project has received funding from the European Union's Horizon 2020 research and innovation programme under the Grant Agreement No **776479.***

with recently published data on climate variable and population projections. The detail of this methodology is set out in the following section.

2.1.2. Contributing factors and occurrence of tipping point

Method

In order to generate estimates of potential future migration movements, we utilise the analysis undertaken in Marchiori et al. (2012). Specifically, Marchiori et al. investigate the climate anomaly (rainfall & temperature) – migration relationship, using annual data for the historical period, 1960-2000, for 39 African countries. The theoretical model is a continuous time, two-country model with a rural and an urban sector both of which are pricing competitively. Weather anomalies affect the productivity in the rural sector. The model allows for rural–urban and urban– international migration, where individuals base their decisions relating to migration on the differences in wage levels between sectors and countries.

Specifically, the model identifies two channels by which migration may be motivated. The first channel – labelled as the economic geography channel - suggests that migration from rural to urban areas occurs when weather patterns adversely affect agricultural production in rural areas and so lead to lower wage levels and a consequent larger wage level differential between rural and urban areas, thereby providing an economic motivation for migration from rural to urban areas. However, the influx of labour into urban areas is likely to have a depressing impact on urban wages, so stimulating those with international mobility to move abroad. The second channel – labelled as the amenity channel – identifies that migration might be stimulated by non-monetary reasons such as high adverse health risks resulting from the spread of vector-borne diseases facilitated by changing climatic conditions. The Marchiori et al. model utilises deviations from annual mean temperature and rainfallas measures of climate anomalies.

Figure 2.1.3 plots the climate anomaly – net migration data for Sub-Saharan Africa over the historical period 1960-2000. It shows that whilst there are clear trends in both rainfall and temperature anomalies over the period – rainfall declining and temperature increasing – trends in international migration are not so obvious. A climate-migration correlation is therefore not immediately identifiable.

*This project has received funding from the European Union's Horizon 2020 research and innovation programme under the Grant Agreement No **776479.***

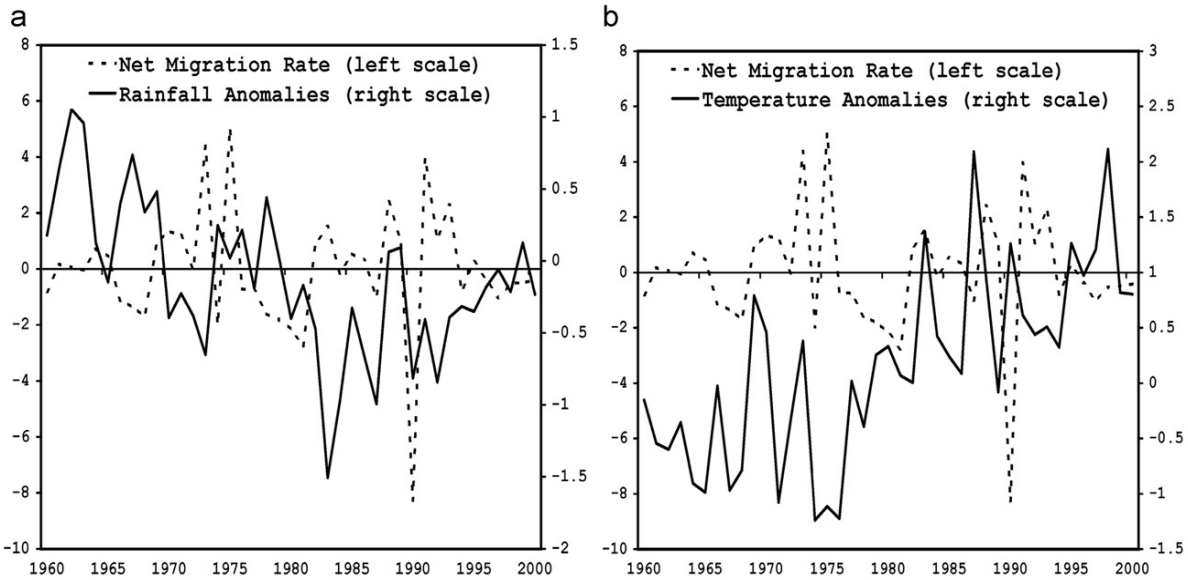

Figure 2.1.3. **Historical climate-migration data in Sub-Saharan Africa**
Source: Marchiori et al. (2012)

However, regression analysis finds that both the economic geography and amenity motivations appear to exist. The amenity-based regressions find that weather anomalies in agriculturally dependent countries induce out-migration, separately from the economic motivation. The authors speculate that there is a health-risk motivation, centered around avoidance of e.g. malaria, dengue and meningitis that could be spread by weather anomalies. There may also be an incentive to avoid future health and other non-market risks by migrating on a preventative basis. Analysis of the economic geography channel finds that wages are affected by weather anomalies and incentivise populations to migrate internationally, particularly from countries with large agricultural sectors. At the same time, urbanisation to some extent softens the motivation for rural populations to migrate internationally.

On the basis of the regression analysis, the historical data from the period 1960 to 2000 can be used to identify that 0.305 people per 1000 population migrated internationally annually as a result of temperature and rainfall events, equivalent to 128,000 migrants each year. Thus, Marchiori et al. (2012) suggest that 36% of international migration can be attributed to weather anomalies. This equates to 3% of the numbers of people who migrate from rural to urban areas. Further disaggregation shows that 0.159 per 1000 population move to other Sub-Saharan countries whilst 0.146 people per 1000 population move to countries outside Sub-Saharan Africa. Temperature is found to explain 53% of this movement whilst rainfall explains 47%.

In this analysis, we expand the geographical area for consideration to include migration from North Africa. The reason for this expansion is that whilst North Africa is not so populous as Sub-Saharan Africa, its geographical proximity increases the likelihood of migration to Europe. This rationale is borne out in the data presented in Figure 2.1.4 which plots current populations of African regions against average annual migrant numbers from those regions to Europe. Figure 2.1.4 highlights that the four regions that comprise Sub-Saharan Africa were the regions of origin for just under 126,000 migrants to Europe annually whilst North Africa is the region for just under

*This project has received funding from the European Union's Horizon 2020 research and innovation programme under the Grant Agreement No **776479.***

178,000 migrants to Europe annually over the years, 2000-2017. Thus, Africa contained the countries of origin for an annual total of around 304,000 migrants to Europe in this period. Table 2.1.1 shows that almost 80% of this total settled in one of five EUcountries.

Table 2.1.1: **Average annual number of migrants from Africa to European countries (2000-2017)**

Destination Country/Region	Average annual number of migrants from Africa (2000-2017)
Total EU	303,614
France	82,760
Germany	36,568
Italy	55,486
Spain	64,243
UK	15,969

Source: OECD Migration Database

Figure 2.1.4 shows that whilst East Africa has the highest regional population – 80% higher than North Africa – the number of migrants to Europe from East Africa is only one-sixth the number from North Africa over the 18-year period from 2000 to 2017. In order to establish a baseline of the numbers of climate-induced migrants to Europe from Africa we use a simple gravity model to reflect the fact that migrants fromNorth Africa are more likely to move to Europe than those from other African regions. In doing so we reflect the fact that migrants to Europe are more than six times more likely to originate from North Africa than Sub-Saharan Africa. In line with currentdestination patterns, we assume that Europe accounts for 40% international migrants from Africa (Afro-barometer profile of African migration, 2019).

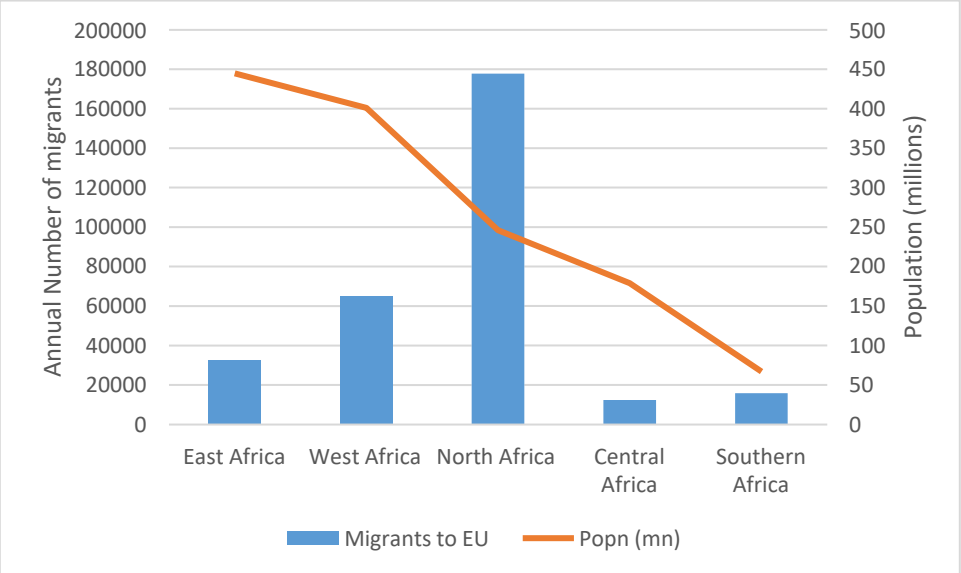

Figure 2.1.4. **Migrants to Europe and Population of African Regions – Annual Average (2000-2017)**

*This project has received funding from the European Union's Horizon 2020 research and innovation programme under the Grant Agreement No **776479.***

Source: Own calculations based on OECD Migration Data and UN Population data

On the basis of the data identified above we model the number of migrants projected to move to Europe as a result of weather anomalies. We apply the data on the fraction of climate-induced migrants to non-African destinations derived in Marchiori et al. (2012) to the population totals for Africa and its regions to establish a baseline. The baseline period is 2020 and results for this year are shown in Figure 2.1.5, disaggregated for the five African regions. The total annual number of migrants from Africa to Europe in 2020 as a result of climate anomalies is therefore estimated tobe 156,000.

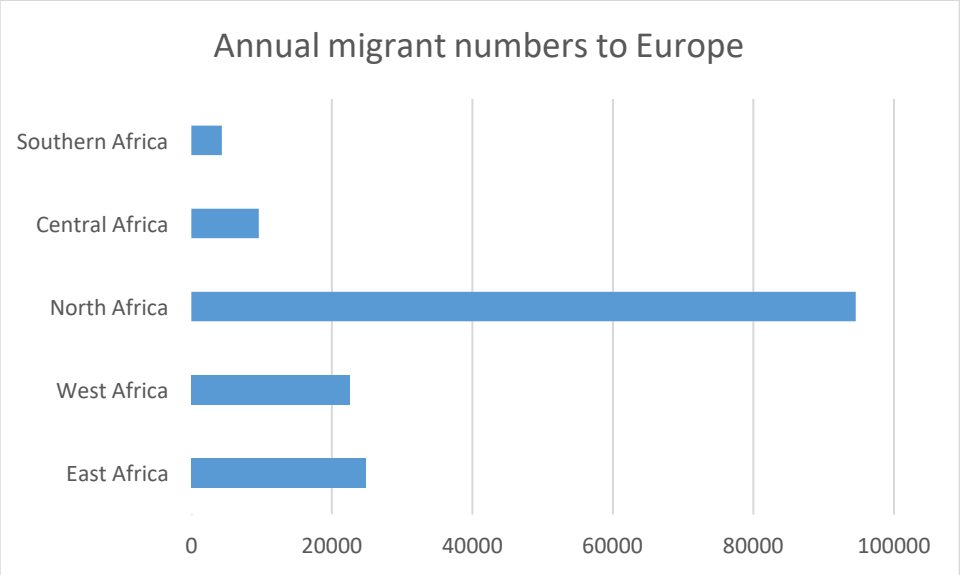

Figure 2.1.5: **Estimated Migrants: Africa to Europe associated with weather anomalies (2020, modelled)**
Source: Derived from OECD Migration database

Results

Projections of future migrant numbers due to weather anomalies are made on the basis of combining population and climate scenarios. We first identify the total population for Africa on a decadal basis, to 2100, as projected under the four SSP scenarios adopted in the COACCH project. These are presented in Figure 2.1.6. We then identify relevant climate data that may be applied to the current context. In this case, we utilise the data from Naumann et al. (2018) which provides projections of drought magnitude, using the Standardized Precipitation Evaporation Index (SPEI). We therefore assume that the length of drought is an appropriate indicator for climatic conditions likely to influence decisions within the affected population relating to migration – see e.g. Pedersen (1995) as evidence that this linkage may occur. The Naumann et al. (2018) study provides estimates of drought magnitude in all world regions for a baseline increase of 0.6^{O}C, under mitigation scenarios of 1.5^{O}C and 2^{O}C, as well as a business-as-usual scenario of 3^{O}C. These data are presented in Table 2.1.2. Under the 0.6^{O}C temperature scenario, the mean drought duration across Africa is estimated to be 7.6 months.

*This project has received funding from the European Union's Horizon 2020 research and innovation programme under the Grant Agreement No **776479.***

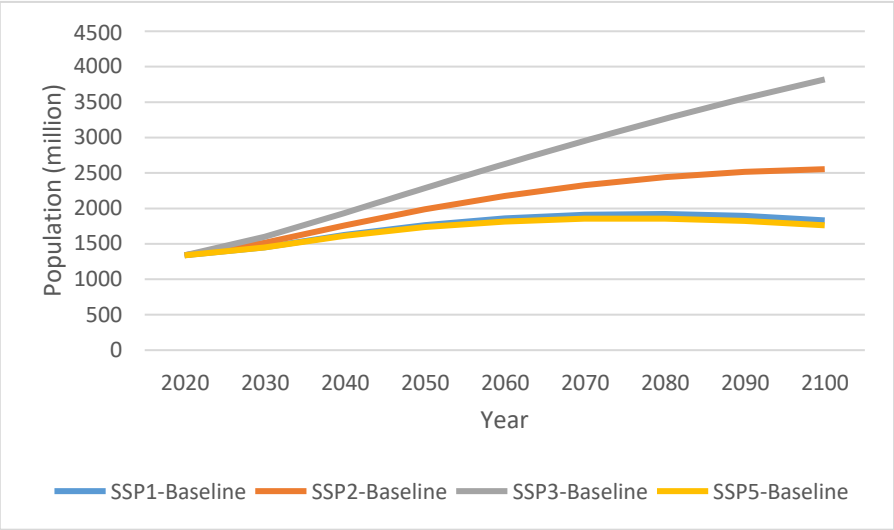

Figure 2.1.6: SSP Population projections for Africa to 2100

Source: based on the SSP database hosted by the IIASA Energy Program at https://tntcat.iiasa.ac.at/SspDb

Table 2.1.2. Mean drought length and changes from historical baseline

Mean temperature increase from 1970-2000	Drought mean length (months)	Change in drought length from 0.6^{O}C baseline (%)
1.5^{O}C	7.9	60
2^{O}C	10.9	120
3^{O}C	21.4	330

Source: Derived from Naumann et al. (2018)

We adopt the population scenarios from the SSPs as the sole aspects of socio-economic change that are considered in this analysis. Of course, this is a gross simplification of the role of socio-economics in determining migration. For example, projected increased regional or sub-regional GDP/capita may result in a greater amount of migration as people are more able to afford to travel and re-settle. Conversely, such an increase in GDP/capita may reduce the incentive to move and so result in less migration. We acknowledge these and many other possible socio- economic influences on African populations but do not include these in our quantitative analysis.

The climatic and population changes are combined according to our judgement as to how the three climatic scenarios - 1.5^{O}C, 2^{O}C and 3^{O}C – can most appropriately be mapped on to the SSP scenarios. We also indicate the RCP climate scenarios that are likely to be consistent with these temperature projections in the time periods chosen. We utilise three time periods – 2030s, 2050s and 2080s. The combinations adopted are summarised in Table 2.1.3. They are not exhaustive but are designed to explore the extent of uncertainties in these variables as well as maintaining internal consistency with each other.

Table 2.1.3. SSP-Climate Scenario combinations

Population Scenario	2030s	2050s	2080s

*This project has received funding from the European Union's Horizon 2020 research and innovation programme under the Grant Agreement No **776479.***

SSP1	1.5^{O}C RCP2.6/4.5	1.5^{O}C RCP 2.6/4.5	1.5^{O}C RCP2.6
SSP1	2^{O}C RCP6	2^{O}C RCP 2.6/4.5/6	2^{O}C RCP 2.6
SSP2	2^{O}C RCP6	2^{O}C RCP 2.6/4.5/6	2^{O}C RCP 2.6
SSP3	2^{O}C RCP8.5	3^{O}C RCP4.5/6/8.5	3^{O}C RCP4.5/6/8.5
SSP5	2^{O}C RCP8.5	3^{O}C RCP4.5/6/8.5	3^{O}C RCP4.5/6/8.5

We then model the effects of climate-induced migration under these SSP-Climate Scenario combinations. This modelling generates the set of results presented in Figure 2.1.7. This shows that in all the scenario combinations adopted there is an increase in the annual number of migrants from Africa to Europe over the course of the 21st century. Since both population numbers and climate change-induced drought lengths increase in Africa in this period this finding is not surprising. However, the range of results expands significantly, depending on the SSP-climate combination adopted, in the 2050s and - to a greater degree - in the 2080s. Most strikingly, the SSP3-3^{O}C combination in the 2080s generates an estimate of 1.7 million migrantsannually, and which contrasts with an estimate of below 0.4 million under the SSP1- 1.5^{O}C combination for that time period. Comparison of the data in Figure 2.1.5 and Table 2.1.2 highlights that whilst population is projected to increase by 150% over the 2020 baseline, drought magnitude is projected by 330% in the period to the 2080s. In this extreme example it is climatic change that is responsible for the majority of therise in estimates of migrant numbers rather than socio-economic – in this case, population - change.

*This project has received funding from the European Union's Horizon 2020 research and innovation programme under the Grant Agreement No **776479.***

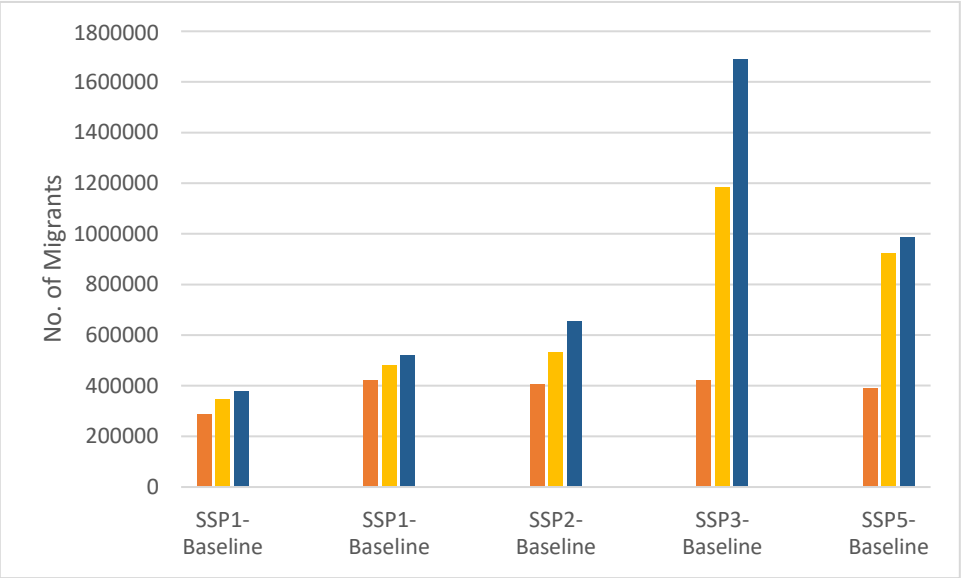

Figure 2.1.7. Africa to Europe Annual Migrant numbers associated with weather anomalies (2030s, 2050s, 2080s, modelled)
Legend: Orange – 2030s; Yellow – 2050s; Blue – 2080s

2.2. Financial Tipping Points

2.2.1. Definition of tipping point

There is an increasing recognition that climate change has large economic costs and that these could affect financial markets. This has led to the concept of climate change as a financial risk. This SETP discusses and analyses the potential likelihood and magnitude of socio-economic tipping points in the financial markets. The present analysis is based on a review of literature and a qualitative assessment of risks.

Physical Climate Risk as a Financial Risk

The Task Force on Climate-related Financial Disclosure (https://www.fsb-tcfd.org) was established by the G20's Financial Stability Board. It is developing voluntary, climate-related financial risk disclosures for use by companies in providing information to investors, lenders, insurers, and others. It defines climate risks as (TCFD, 2017):

- Transition risks, i.e. the policy, legal, technology, and market changes to transition to a lower-carbon economy and financial and reputational risk to organizations (policy and legal risks, technology risks, market risk and reputational risk).
- Physical risks, resulting from climate change from events (acute) or longer-term shifts (chronic) in climate patterns, and the financial implications for organizations, such as direct damage to assets and indirect impacts from supply chain disruption, as well as from changes in water availability, sourcing, and quality; food security; and extreme temperature changes affecting organizations' premises, operations, supply chain, transport needs, and employee safety.

*This project has received funding from the European Union's Horizon 2020 research and innovation programme under the Grant Agreement No **776479.***

There is also a further set of risks now being considered, Liability risk[3], as reported in the Bank of England (PRA, 2015). For this SETP, the focus in on **physical risks**.

The Network for Greening the Financial System (NGFS, 2019) has also identified climate change as a source of financial risk. This is being taken forward with a network of 69 members, primarily government central banks[4]. The report uses the same TCFD definitions of transition and physical risks (see Figure 2.2.1). It recognises that there is a strong risk that climate-related financial risks are not fully reflected in asset valuations. The NGFS encourages central banks to lead by example in their own operations. Interestingly, their report highlights that these risks will likely be correlatedwith and potentially aggravated by tipping points, in a non-linear fashion, and thus impacts could be much larger, and more widespread and diverse than those of other structural changes.

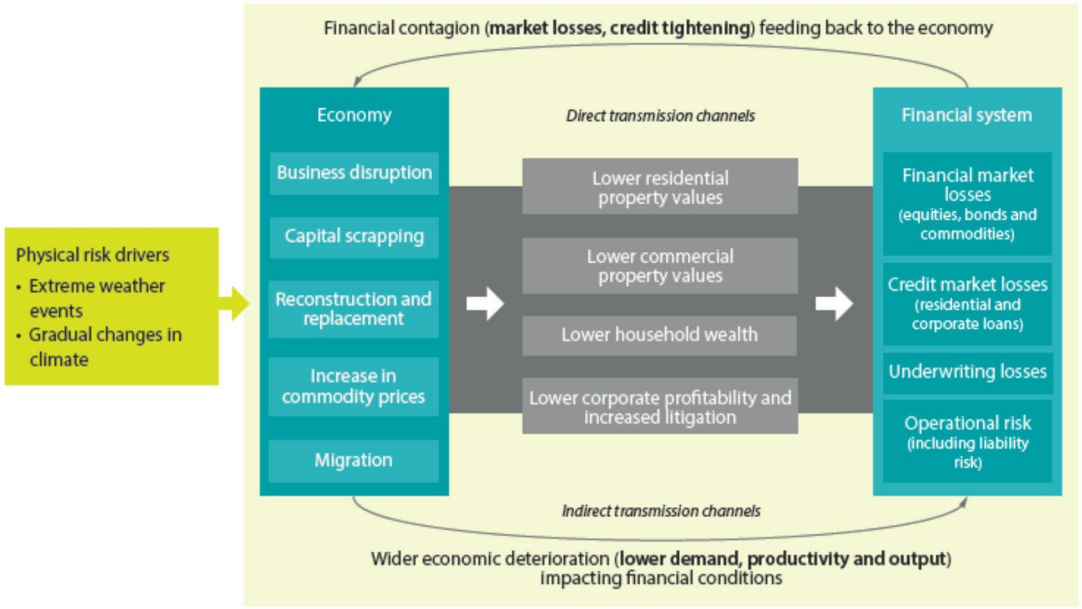

Figure 2.2.1 From physical risk to Financial Stability Risks. Source, NGFS (2019).

Climate Change and Sovereign Creditworthiness

The rating agencies have also been starting to consider climate risks. Moody's (2016a) considered the impact of natural disasters on credit ratings. It reports that natural disasters can have a large negative impact on government finances and economic growth and are the major cause of materialization of contingent liabilities for emerging market sovereigns, after banking crises. Further, on occasion, natural disasters have been the direct cause of sovereign defaults. The analysis combined EM-DAT data with sovereign ratings and identified that emerging economies are significantly more exposed than developed countries, particularly Emerging Asia and

[3] which comes from people or businesses seeking compensation for losses they may have suffered from the physical or transition risks from climate change outlined above. The issue of liability risk raises the important question of who will be held responsible

[4] https://www.ngfs.net/en/about-us/membership

*This project has received funding from the European Union's Horizon 2020 research and innovation programme under the Grant Agreement No **776479.***

the Caribbean. It reports the average annual damage from natural disasters over 1980-2015 was 1.5% of GDP in emerging markets vs. 0.3% of GDP in developed economies.

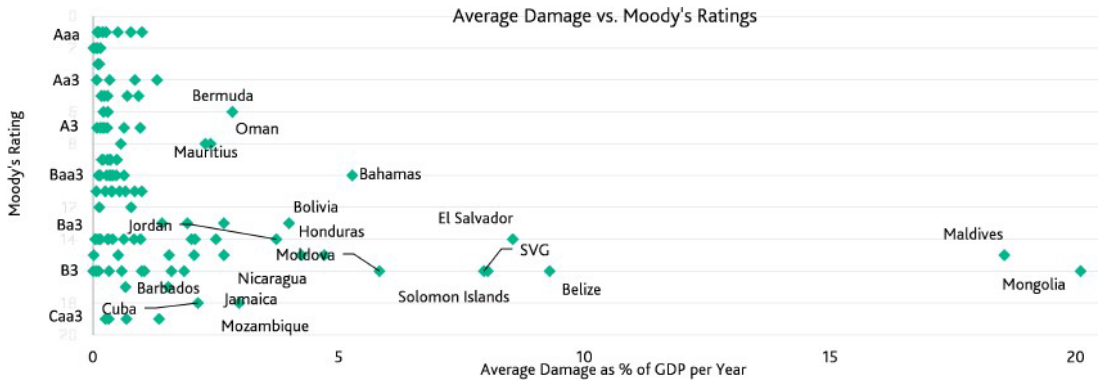

Figure 2.2.2 Average Damage versus Moody's Ratings. Source Moody, 2016a, using EM-DAT.

Most importantly, this study highlights that natural disasters have severe macroeconomic impact and can affect sovereign creditworthiness through several channels, including directly impacting a country's economic strength, government fiscal strength and external vulnerability (Figure 2.2.2). It highlights natural disasters are frequently associated with:

- contracting economic output, potentially followed by a short-term boost to growth from reconstruction efforts;
- increasing poverty, as natural disasters have a disproportionate impact on the poorer segments of the population;
- worsening external balances, as imports of reconstruction materials increase and exports tend to suffer;
- downward pressure on the exchange rate and upward pressure on prices;
- deteriorating fiscal balances, as tax revenues shrink due to the decline in economic activity but government expenditures rise due to emergency assistance and reconstruction efforts; and
- increasing debt-to-GDP levels, which results from both the decrease in GDP and from an increase in borrowing to finance the recovery and reconstruction activity.

The macroeconomic costs of natural disasters, including the immediate decline in GDP and then potentially the cumulative, permanent GDP loss during the years following a major disaster, can also have a second-round effect on the government's budget. In addition, natural disasters can escalate government borrowing costs, especially for already highly indebted nations. The report concludes that natural disasters can therefore affect a sovereign's debt repayment capacity by affecting a country's economic resilience, fiscal strength and susceptibility to event risk. It found that sovereigns that are more susceptible to natural disaster risks generally have weaker debt repayment capacity, and lower ratings. Natural disasters are also a cause of contingent liabilities for emerging market sovereigns –when government act as a (re)insurer of last report, without knowing precisely its disaster risk exposure.

*This project has received funding from the European Union's Horizon 2020 research and innovation programme under the Grant Agreement No **776479.***

Moody's (2017) also published a note on assessing the effects of climate change on sovereign issuers. It sets out that the sovereign bond rating methodology does not account separately or explicitly for the credit risks posed by climate change, but climate risks are already broadly captured in the four key risk factors they use in (their) analysis – economic strength, fiscal strength, institutional strength and susceptibility to event risk – either directly or indirectly through a variety of indicators. Thus, the credit implications of physical climate change are captured in a broad set of rating factors that influence a sovereign's ability and willingness to repay its debt. This paper also sets out how the rating agency sees the four primary channels by which the effects of physical climate change are transmitted to sovereigns' credit profiles. These are:

- the potential economic impact (for example, weaker activity due to a loss of agricultural production);
- damage to infrastructure assets as a direct result of the physical destruction incurred from climate shocks;
- rising social costs brought about, for example, by a health crisis or food security concerns; and
- population shifts due to forced displacements resulting from climate change.

It highlights that sovereign susceptibility will depend on an issuer's exposure and resilience to climate change. The analysis considers resilience (sovereign's adaptive capacity and fiscal flexibility, as well as the country's income levels) andwhether there are government policies to mitigate climate change risks (for example, natural disaster insurance or a savings funds). In general, the paper concludes that sovereign issuers with smaller, less diversified economies and geographies, lower incomes and quality of infrastructure, and lower fiscal flexibility are more susceptible to the credit implications of climate change.

The study used the Notre Dame Global Adaptation Index (ND-GAIN) Vulnerability country indices to assess potential susceptibility, combining this with a number of indicators used in their sovereign bond methodology that are specifically linked to climate change susceptibility (including the scale of the economy (as measured by nominal GDP), national income (GDP per capita), and Fiscal Strength). It found that sovereigns' ratings are quite strongly correlated with their susceptibility to climate change, due to the overlap between the factors for assessing sovereign credit profiles and those driving exposure and resilience to climate change. However, it also reflects the fact that countries with an overarching reliance on agriculture and where the quality of infrastructure is typically weaker (important aspects of susceptibility to physical climate change) tend to be lower rated already (Figure 2.2.3 and Figure 2.2.4).

*This project has received funding from the European Union's Horizon 2020 research and innovation programme under the Grant Agreement No **776479.***

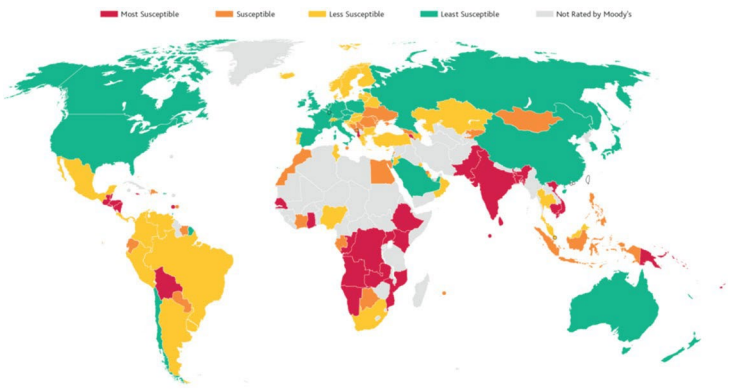

Figure 2.2.3 Susceptibility to Physical Climate Change of Moody's-Rated Sovereigns Based on Illustrative Data

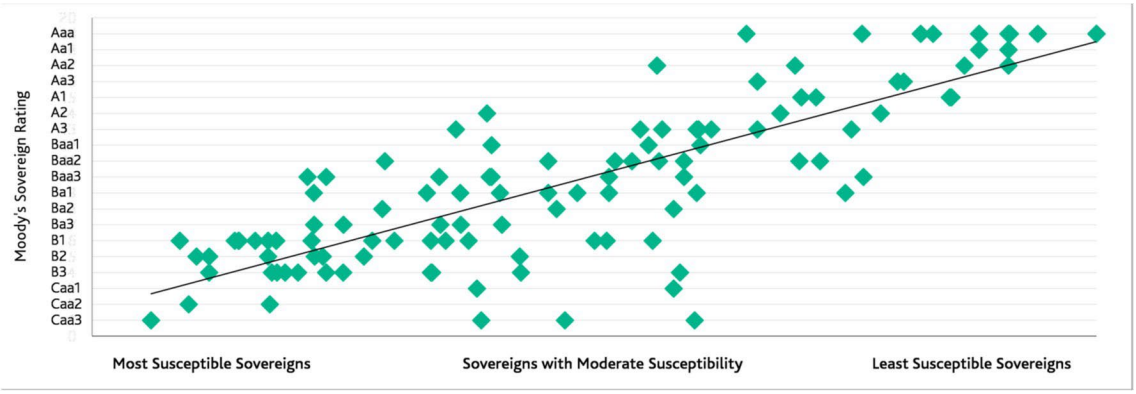

Figure 2.2.4 Correlation between Climate Change Susceptibility and Sovereign Creditworthiness Moody's Sovereign Ratings vs. Climate Change Susceptibility. Source Moody's 2016b

Moody's (2016b) also published a report on climate risks on small island nations, which highlights potential effects from climate change in the long-run. Severe extreme events can be a direct cause of sovereign defaults. For example (Moody's 2016a) report that Hurricane Ivan in 2004, which resulted in damages of over 200% of GDP, was the direct cause of Grenada's subsequent debt restructuring. Further, hurricanes in 2003 and 2004, which damaged the agricultural sector, were contributing factors in the Dominican Republic's debt restructuring in 2005

Standard & Poor's have assessed natural hazard (Standard & Poor's, 2014) and the impact on sovereign creditworthiness. It expects the poorest and lowest rated sovereigns will bear the brunt of these impact. This is in part due to their reliance on agricultural production and employment, which can be vulnerable to climate patterns and extreme weather events, but also due to their weaker capacity to absorb the financial cost. Overall, the report concludes that climate change is likely to be one of the global mega-trends impacting sovereign creditworthiness, in most cases negatively. This will be felt through various channels, including economic growth, external performance, and public finances. Standard & Poor's uses a ratings methodology (Sovereign Government Rating Methodology And Assumptions) that incorporates the specific assessment of five key factors: institutional and governance effectiveness, economic structure and growth prospects, external liquidity and

*This project has received funding from the European Union's Horizon 2020 research and innovation programme under the Grant Agreement No **776479.***

international investment position, fiscal performance and flexibility, and monetary flexibility.

The main factors through which climate change could feed through to sovereign creditworthiness are considered to be:

- economic performance, i.e. the growth prospects of national economies and eventually levels of prosperity, including labour productivity, as well as impacts on infrastructure and thus productivity;
- fiscal performance, from potential negative impacts on growth weighing on public finances as tax revenues decline if national economy reduces, and there is additional government budget (disaster recovery, reconstruction) spent on major extremes.
- external performance, e.g. exports of agricultural products for foreign currency.

Standard & Poor's also assessed countries at risk, using the Share of the population living in coastal regions, the Share of agriculture in national GDP and the ND-GAINS index. This does not include an analysis of the effect on the sovereign rating,but the analysis found lower-rated sovereigns tend on average to be more vulnerable (Figure 2.2.5).

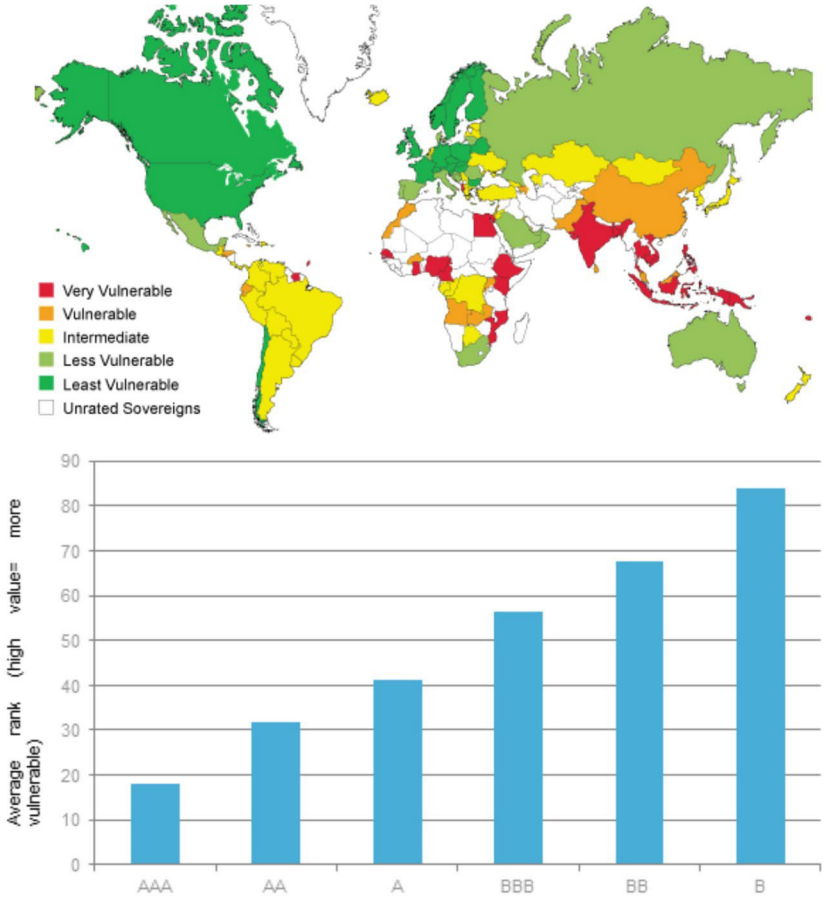

Figure 2.2.5 Potential vulnerability to climate change, and correlation between vulnerability and rating. Source: Standard & Poor's, 2014.

*This project has received funding from the European Union's Horizon 2020 research and innovation programme under the Grant Agreement No **776479.***

Standard & Poor's (2015a) considered that the creditworthiness of certain governments could be downgraded due to climate-related extreme events, but not to an extent that would be relevant for financial stability[5]. Nonetheless, this represents a potential mechanism, which if extreme, could form a tipping point. Standard & Poor's (2015b) considered the potential risk of downgrading of companies (the creditworthiness of companies), noting that some environmental and climate events have led to downgrading of companies (e.g. hurricanes and storms in the Gulf of Mexico). Standard & Poor's have recently revised the way they factor climate risks into corporate ratings (2017).

Standard & Poor's (2015c) assessed the potential effects of natural disasters on downgrades (see Figure 2.2.6). The report uses examples of 250 year return periods for extreme events to look at potential downgrades. This uses the credit rating methods, adjusting down one notch when the risk that "the occurrence of a rare but severe natural catastrophe could also lead to a material deviation from the indicative rating level, depending on the extent of damage." and another, less powerful, negativeadjustment to the economic assessment to any sovereign whose "economic activity … (is) vulnerable due to constant exposure to natural disasters or adverse weather conditions'. However, it does highlight that the most likely effect of naturalcatastrophes on sovereign ratings would be indirect rather than direct, through a weakening of the fundamental factors that determine the rating of a sovereign. A natural disaster can hit economic output and growth potential as well as external finances through hampering export performance and requiring additional food and reconstruction-related imports. The report highlights that there have been few downgrades to date as a result of natural events (the exception being the tropical storm in Grenada). It finds that the top five catastrophes for both perils (measured in damages as share of value) could lead to downgrades of around 1.5 notches for the sovereigns affected. Floods and European winter storms are generally unlikely to, by themselves, lead to downgrades.

In terms of transmission, the analysis looked at the direct property damage as a share of property and infrastructure values following a disaster of a severity thatwould be expected to occur once every 250 years, then looked at the effects on key macroeconomic variables: GDP growth, the balance of payments, as well as on general government debt and deficits. The economic outcomes were then converted into a proprietary simplified sovereign rating tool. This reports examples such as a 1 in 250 year flood in Thailand or a 1 in 250 year storm in the Caribbean, noting the downgrades are higher in developing and emergent countries than in developed OECD countries. Sovereigns most vulnerable to natural hazards are likely to be small island states with next to no "geographical diversification" and a narrow economic base. Extreme examples include a 4 point downgrade from a 1 in 250 year event in the Caribbean, as compared to less than 1 point downgrade for a 1 in 250 year flood in a European country. The conclusion is that for industrialised countries, which are the

[5] The rate scale moves down: AAA, AA+, AA, AA-, A+, A, A-, BBB+, BBB, etc. A downgrade by one notch e.g. is a change from AAA to AA+.

*This project has received funding from the European Union's Horizon 2020 research and innovation programme under the Grant Agreement No **776479.***

relevant countries for financial market in Europe, that there is hardly any risk of financial market instability.

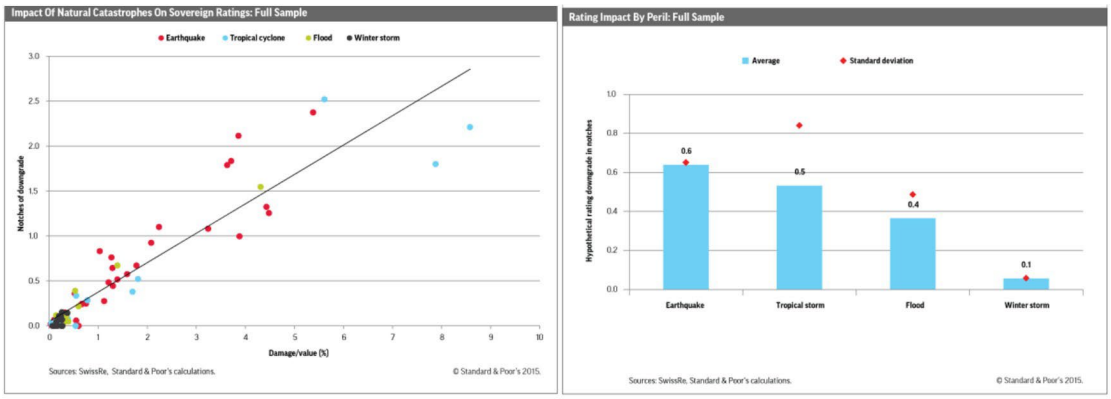

Figure 2.2.6 Impact of Natural Catastrophes on Sovereign Rating. Source: Standard & Poor's 2015c.

Climate risks to the private sector

Climate risks also apply to private companies and the flows of private investment: accounting for physical climate risks could - on average – reduce company enterprise values by 2-3% due to the risk costs of insuring assets, and more than this in some sectors[6]. Further work analysing this area has been advanced in the ClimINVEST Project. This has produced two reports on physical climate risks (Romain et al., 2018;de Bruin et al., 2019).

Previous estimates

A study by ICBS and SOAS (2018) undertook an econometric analysis to look at the relationship between climate vulnerability, sovereign credit profiles, and the cost of capital in developing countries. This found that countries with higher vulnerability to climate change risk bear an incremental cost on government-issued debt. These costs are above and beyond the rates attributable to macroeconomic and fiscal fundamentals. This incremental debt yield carries over into the cost of private debt. It highlights that a high cost of capital in the public sector constrains social investmentsin areas such as infrastructure, education and public health. The governmental cost of borrowing also acts as a proxy for the country risk premium, which has direct ramifications on investments undertaken by the private sector. The most critical variable affecting the Weighted Average Cost of Capital – which is a key variable for investment appraisal – is the sovereign risk assigned to each country. The analysis focused on how climate vulnerability impacts the sovereign cost of borrowing.

The study looked at the rate at which countries can borrow from international debt capital markets, and how physical climate risks could affect a country's sovereign credit profile. It also assessed whether physical climate risks are currently incorporated in country-level credit ratings and sovereign bond yields. The relationships are shown below. The analysis again used the EM-DAT database. To do this the econometric analysis compared the cost of debt with the ND-GAINs index. Countries with greater sensitivity to climate impacts tend to have higher sovereign borrowing costs, while

[6] https://www.economist.com/business/2019/02/23/business-and-the-effects-of-global-warming

*This project has received funding from the European Union's Horizon 2020 research and innovation programme under the Grant Agreement No **776479.***

countries that are well prepared to deal with the risks of climate change enjoy low borrowing costs.

The study found that climate vulnerability – as assessed by ND GAINS - has already raised the average cost of debt in a sample of developing countries by 117 basis points (V20 countries, i.e. 20 highly vulnerable countries). This increase is considerable, representing an uplift of nearly 10% on overall interest costs. In absolute terms, this translates into USD 40 billion in additional interest payments over the past 10 years on government debt for these 20 countries (estimated from the total additional interest payments by multiplying the marginal cost of debt to the stock of external debt outstanding). It also estimated that this has led to higher sovereign borrowing rates into the cost of private external debt, such that climate vulnerability has cost these countries USD 62 billion in higher interest payments across the public and private sectors for these 20 countries (Figure 2.2.7).

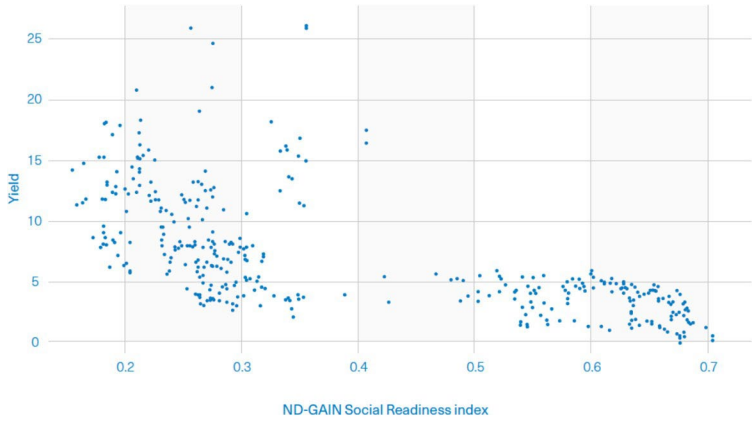

Figure 2.2.7 Cost of debt and ND-GAIN readiness index. Source ICBS and SOAS (2018)

The study did some forward-looking analysis to 2030 and estimated the additional interest payments attributable to climate vulnerability to increase to between USD 146 – 168 billion over the next decade for these 20 countries. The overallfinding is that climate change increases the cost of capital, and can have effects on financial health. The report sets out that credit ratings are an assessment of the credit risk of a borrower, and that there is a strong relationship between sovereign credit ratings and the market rate of interest. Sovereign issuers, particularly in emerging markets, are potentially vulnerable to negative rating actions as a result as climate shocks. The analysis also did some country and risk case studies that provided impact pathways, shown below.

South Pole Group (2016) investigated whether climate change could lead to risks in financial market stability, primarily looking at German equity funds, based on a literature review and analysis. This looked at physical and transition risk. The South Pole Group analysis used information from the IPCC 5th Assessment Report (global and Europe chapter). The study concluded that physical risks represented a very low risk for financial market stability in Germany and Europe in the short to medium term, i.e. it is very unlikely that the physical effects of climate change could cause a significant risk for the financial market stability. Transition risks were considerably more relevant.

*This project has received funding from the European Union's Horizon 2020 research and innovation programme under the Grant Agreement No **776479.***

However, these conclusions were largely based on the assumption that the insurance industry can adapt relatively well to direct risks since insurance premiums can be adjusted on an annual basis and the risk capital can be adapted continuously. However, this is not necessarily the case, because insurance is a risk spreading mechanism – it cannot adjust to changes in trends. This is being captured in the later SETP, based on insurance modelling.

De Nederlandsche Bank (2017) undertook a study (Waterproof?) on the Dutch Financial sector, again, looking at physical climate risks and transition risks. For the former, this included the consequences of climate change for insurers, and the impact of large-scale flooding on the financial sector. The analysis finds climate change will put an upward pressure on insurance premiums, which could moreover lead to shock-induced price increases. The lack of climate change in catastrophe models could also increase risk exposure. There was also considered to be a risk from uninsured losses, notably those covered by Government - the financial sector may incur losses through their exposures to these parties. Looking internationally, the study found Dutch financial institutions appear to have only limited exposures in countries that are most vulnerable to climate change.

A further analysis was developed by Covington and Thamotheram (2015). This 'dividend approach' estimates the present value loss of future dividends from the current stock of investments. Using a relationship between dividends and GDP, they estimated the impact of climate change on assets at particular confidence levels (including Value at Risk). They estimated the value at risk in 2030 (from climate change) may be equivalent to a permanent reduction of between 5% and 20% in portfolio value.

The Economist Intelligence Unit (2015) assessed the value at risk (value at risk measures the size of the loss a portfolio may experience, within a given time horizon, at a particular probability) from climate change. This built on the study by Covington and Thamotheram (2015). The analysis used estimates made directly by the DICEmodel (thus with no regional or sector breakdown). It also used a wider definition of manageable assets, to cover all assets held by non-bank financial institutions, reporting these were US$143trillion in 2013. The dividend approach was discounted from both the perspective of a private investor and a government. The analysis estimated the value at risk, as a result of climate change, to the total global stock of manageable assets ($143 trillion) as $4.2 trillion (mean expected losses, discounted in present valueterms using private sector discount rates [5.5%]), between now and the end of the century. This translates into climate change causing permanent, present value losses to current manageable assets of 3% on average ($4.2 Tr) and up to 10% at extreme outcomes, when discounted at a private sector discount rate. Much higher values were derived across the full range, and when public discount rates are used. It also reported that warming of 5°C is consistent with US$7trn in losses—more than the total market capitalisation of the London Stock Exchange— while 6°C of warming is consistent with a present value loss of US$13.8trn to manageable financial assets, roughly 10% of their global total. The results (as in Figure 2.2.8) show that the asset management industry is particularly subject to tail risks: lower probability but higher impact losses.

*This project has received funding from the European Union's Horizon 2020 research and innovation programme under the Grant Agreement No **776479.***

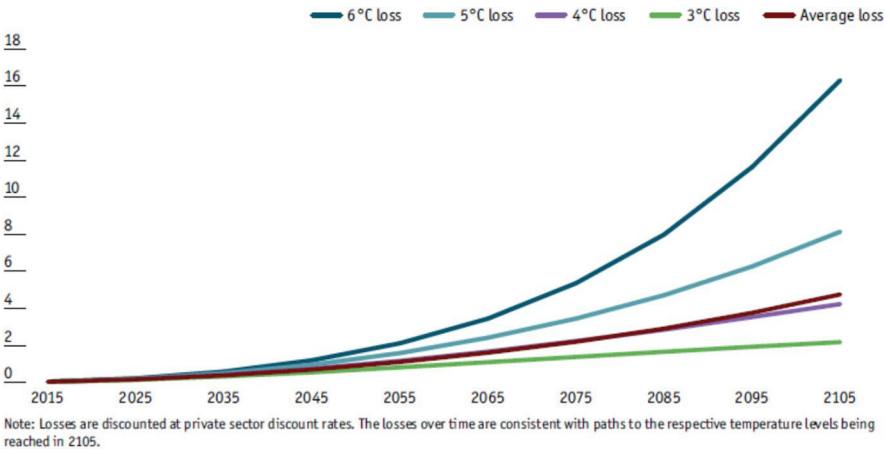

Figure 2.2.8 Present value loss to current manageable assets (trillion $, 2015 prices). Source EIU, 2015.

The method for this analysis was based on the present value of global financial assets and value at risk, where the PV of global financial assets is the discounted cash flow arising from holding these assets. The underlying approach was that as the present value of a portfolio of equities is just the discounted cash flow of futuredividends, then in the long run (this century), dividends in a diversified portfolio shouldgrow at the same rate as GDP. Further, in a well-functioning financial market, the samerelationship with GDP growth should hold for cash flows from other kinds of assets, such as bonds. The DICE model was used to forecast the effect of climate change on GDP, and in turn on cash flows from assets.

The analysis supporting this analysis (using DICE) was produced by Dietz et al (2016), who report that the expected 'climate value at risk' (climate VaR) of global financial assets today is 1.8% along a business-as-usual emissions path ($2.5 trillion). However, they also highlight that much of the risk is in the tail. For example, the 99th percentile climate VaR is 16.9%, or $24.2 trillion. The approach uses Value at risk (VaR) as a metric to quantify the size of loss on a portfolio of assets over a given time horizon, at given probability, and thus a measure of the potential for asset-price corrections due to climate change. The study used the DICE model to estimate the impact of climate change on financial assets, rather than damages per se.

A separate analysis was undertaken by Mercer (2015). This looked at both the physical risks but also opportunities. It found that climate change risks will impact investment returns. For a 2°C pathway, it reports that investors could see a negative impact on returns, especially in the most affected sectors. However, this scenario would be likely to lead to gains in infrastructure, emerging market equity, and low- carbon industry sectors. Under a 4°C pathway, chronic weather patterns pose risks to the performance of asset classes such as agriculture, timberland, real estate, andemerging market equities. The analysis used FUND and adapted an existing investmentmodel to allow model inputs for different scenarios, and to allow a climate sensitivity adjustment for different asset classes and industry sectors (i.e. the asset sensitivity to the TRIP factors). Note that the analysis used the WITCH model, as the source of mitigation cost estimates. It also ran a FUND run where damages where scaled up

*This project has received funding from the European Union's Horizon 2020 research and innovation programme under the Grant Agreement No **776479.***

(based on DICE). The analysis also added in additional estimates for coastal flood and wildfires: it also adjusted the agricultural values (as these dominate FUND outputs). The analysis looked at four aspects, two of which are relevant for physical impacts.

- Resource availability, defined as the impact on investments of chronic weather patterns (e.g. long-term changes in temperature or precipitation), e.g. onagriculture, energy, water.
- Impact, defined as the physical impact on investments of acute weather incidence/severity (i.e. extreme or catastrophic events).

For resource risks, the study quotes examples on crop yields (positive or negative) and water availability (and effect on industries). For impact, the study identifies increased property damage and business interruption as a result of more volatile extreme flooding. The two categories broadly reflect the long-term trends and short-term extreme weather patterns, respectively.

The results were input into Mercer's investment modelling tool to estimate the climate impact on return. The analysis looked at the effect on equities, as these comprise a significant proportion of most institutional investment portfolios. Emerging market equities are more sensitive to the climate change risk factors associated with physical damages of climate change. Indeed, in terms of the results, only the developed market global equity was found to experience a reduction in returns across all scenarios. For the other asset classes, climate change was found to either have a positive or negative effect on returns dependent on the future scenario. It also looked at the potential effects on bonds. The risk for developed market sovereign bonds was considered low. It also looked Investment-grade credit (corporate bonds), as well as other growth fixed income opportunities. It concluded emerging market sovereign bonds are more vulnerable to the potential impacts of climate change.

What is the tipping point?

The analysis above indicates there are several potential tipping points, affecting sovereigns, private companies and the financial markets, although these are all closely inter-linked and involve complex pathways.

Climate change can impact on sovereigns (countries). The pathway includes:

- Climate impacts, including slow onset and extreme events, that affect national economic performance and the public finances (and public financial management).
- These then affect a number of criteria that are important in how the financial markets and credit agencies assess governments, and thus the cost of capital.
- This leads to changes in the credit agency rating and the cost of borrowing.
- This leads to subsequent effects on the private sector, and in extreme cases, risks for the financial markets.

In practice, these linkages could be extremely complicated, as illustrated below (Figure 2.2.9).

*This project has received funding from the European Union's Horizon 2020 research and innovation programme under the Grant Agreement No **776479.***

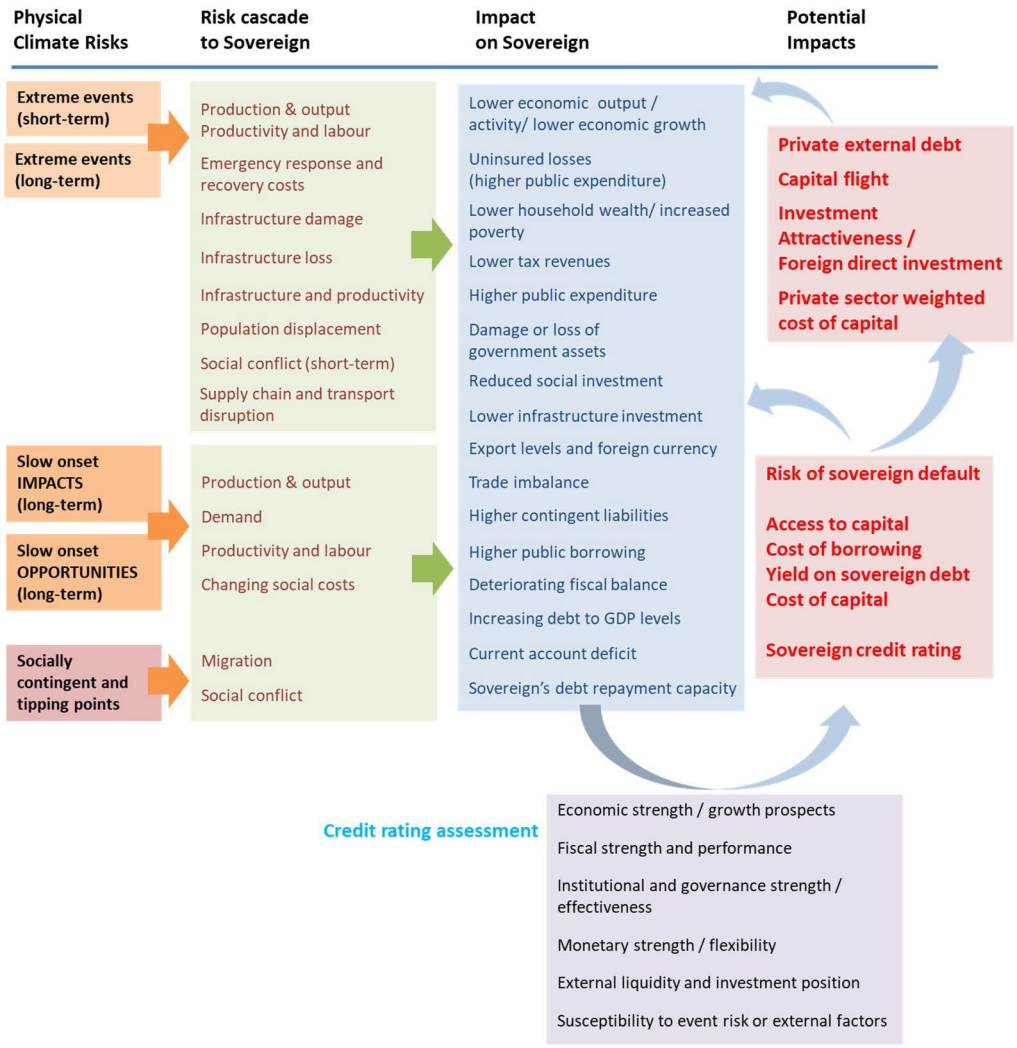

Figure 2.2.9 Potential pathways for climate change on sovereigns.

The analysis has also analysed the potential for socio-economic tipping points, using the framework developed in WP3. This identifies that under more extreme conditions, this pathway could lead to a major tipping point. This might be experience as a major downgrade in credit ratings (e.g. by multiple levels, including down to junk status), followed by the changes in the cost of borrowing/additional cost of interest on government borrowing, and with feedback loops that would exacerbate these impacts on public finances, and cascade through to the private sector.

An interesting issue here is that greater transparency on potential risks will lead to financial market anticipation. Financial impacts are likely to propagate through the insurance, investment and financial markets before the actual climate change of impacts occur, because of this anticipation to future impacts. This market anticipation will effectively bring forward the timing of climate change impacts. There is very little literature on this, although one study has assessed the potential effect (Kemp et al., 2019). This looks at Barbados and shows how anticipatory behaviour changes the damage to infrastructure for the same degree of climate change, i.e. damage depends on behaviour. This creates an extremely interesting (and perverse) tipping point where the economic impact and major downgrade happens before the actual impacts of

*This project has received funding from the European Union's Horizon 2020 research and innovation programme under the Grant Agreement No **776479.***

climate change occur, because of market anticipation of future impacts. In the absence of support and adaptation, this could be a real concern for highly vulnerable states (e.g. small island developing countries).

To date, most of the analysis of climate change and sovereigns has used the ND-GAINS Index. This does not capture economic and financial risk, and it would be useful to explore the impact of direct economic models from COACCH into the sovereign analysis.

A second area concerns the financial markets (Figure 2.2.10). Financial markets play a large number of roles, but this includes the provision of capital and liquidity, investment, asset and equity management, financial stability, and include the financial markets, credit markets, commodity and trading markets, insurance and re-insurance markets, etc. Climate change could affect the portfolios and investments of the financial institutions, the interactions between financial institutions (between financial institutions themselves, but also between these and sovereigns and companies), and the overall financial markets (and financial market stability).

In theory, if the effects above are big enough, they could affect financial markets. They could potentially lead to: Increased volatility; Financial and credit market losses; Credit tightening; Financial contagion; Capital and asset destruction; Price and equity shocks; Illiquidity of capital (reduction in interbank transfer); Insolvency of key financial actors; Reduced financial stability.

There might also be effects on specific high-risk sectors, e.g. commodity trading markets or some vulnerable sectors, e.g. real estate investors (residential and commercial property investment) especially for some parts of the portfolio, e.g. coastal investments. There is the potential that at the global level, these types of effects could lead to financial market instability. Previous studies have highlighted the impacts on investment returns as well as the stock of capital.

However, we consider that the financial markets overall would be unlikely to be dramatically affected in this way, because they would de-risk investments. The more likely consequence is that there would be sovereign and financial market instability in particular high-risk locations or market segments

*This project has received funding from the European Union's Horizon 2020 research and innovation programme under the Grant Agreement No **776479.***

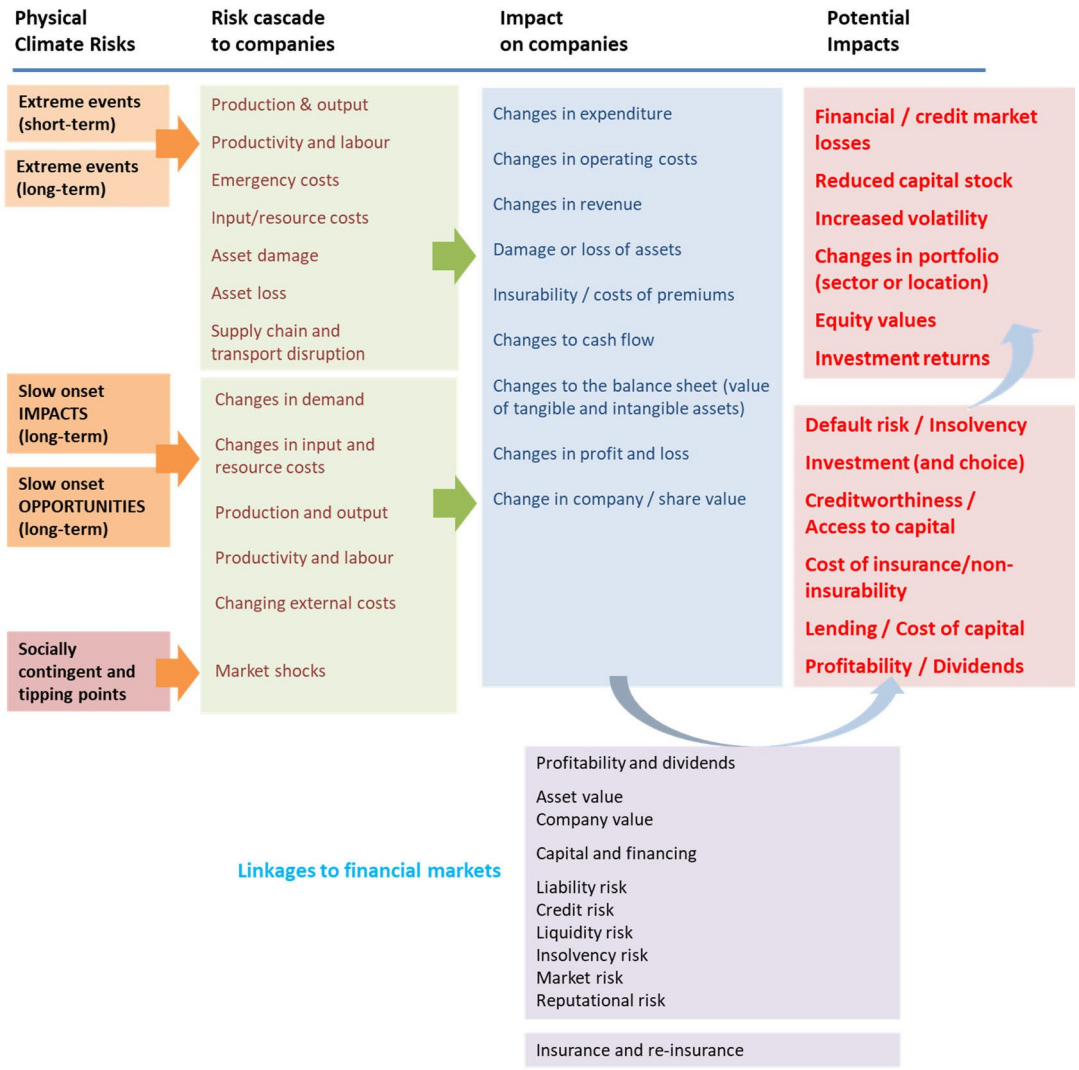

Figure 2.2.10 Potential pathways for climate change on companies and through to financial markets.

Previous studies have looked at these pathways using FUND and DICE models. However, these show very modest damage costs, and this if reflected in the results, which while large, do not indicate the level of tipping points of interest here. The use of COACCH results, including with more categories of damage, and more disaggregated information, could provide new information on likely risk.

2.2.2. Contributing factors and occurrence of tipping point

The analysis above highlights that these effects primarily involve complex and often indirect pathways. Most of the modelling undertaken in the sector, such as provided by the credit agencies, is also proprietary.

COACCH is producing new estimates that would provide the information to feed into these models, and could replace the current use of ND-GAINS, and FUND/DICE models. However, for the present analysis we have not been able to make use of these new estimates, but used information from the literature review to

*This project has received funding from the European Union's Horizon 2020 research and innovation programme under the Grant Agreement No **776479.***

undertake a qualitative assessment of the potential importance of these socio—economic tipping points in Tables 2.2.1 and 2.2.2 below.

The information above clearly indicates a differentiated risk:

- For Europe, studies to date have indicated low risks, both in terms of sovereign risk, insurance market risk and financial stability risk (Table 2.2.1).
- Globally, smaller sovereigns with less diversified economies, lower incomes and quality of infrastructure, and lower fiscal flexibility are most susceptible to the financial risks of climate change. These will include small island developing countries and smaller least developed countries (LDCs), which will include countries in Africa and Asia (Table 2.2.2).

In terms of hazards and sovereign and credit rating risks, drawing on the review above:

- Existing natural hazards have been linked to credit downgrades, with the largest impacts (average 0.5, but up to 1.5 notches) are from tropical storms. Current floods and European winter storms are generally unlikely to, by themselves, to leadto downgrades.
- Increases in hazard intensity could increase these impacts. A major extreme (1 in 250 year flood or storm) in a vulnerable country (e.g. SIDS or LDC) could be associated with a 4 point downgrade, as compared to less than 1 point downgrade for a 1 in 250 year flood in a European country.
- While an individual event may lead to a major downgrade, such effects would be reversible over time. However, a change in the frequency of large events would alter such recoveries and could lead to a persistent downgrade that lasts over time (a tipping point).

Table 2.2.1 Europe. Illustrative Risk of Financial Tipping Point.

	2050s	2080s
RCP8.5	Very low	Low
RCP4.5	Very low	Very low
RCP2.6	Very low	Very low

Table 2.2.2 Global hotspots (SIDS, small LDCs). Illustrative Risk of Financial Tipping Point.

	2050s	2080s
RCP8.5	High	Very high
RCP4.5	Medium	High
RCP2.6	Low	Low

Assumed SSP2 (Middle of the road)

2.3. Food and Water

2.3.1. General definition of the socio-economic tipping point

Climate change and extreme weather events can increase the intensity and likelihood of short-term variability and shocks to agricultural supply, impacting the entire food system and posing threats to food security. Furthermore, instability in the food system may disturb other systems such as energy and water. Food supply shocks due to crop losses inside Europe may thereby lead to socio-economic tipping points

*This project has received funding from the European Union's Horizon 2020 research and innovation programme under the Grant Agreement No **776479.***

that can be measured both on the producer, as well as on the consumer side. Eventually, such tipping points might lead to significant macroeconomic effects.

On the producer side, crop losses may become of such a magnitude and frequency that farms structurally experience that their costs are larger than their benefits of production. In case this happens, several adaptation options may be possible. Extreme droughts may eliminate the possibility of rain-fed agriculture, leading to a shift in crop management from rain fed to irrigated agriculture. It may alsobe that irrigation is not a possibility due to the available water, or not the mostprofitable option in the specific location. In this case, farmers may stop growing the crop at the location and turn to a more profitable crop that is more resistant to extreme weather events. In case these two adaptation options - a shift in cultivation practices and a change of crops - may not be a viable option, producers may be forced to leave a certain area, leading to farms to cease to exist and land abandonment. Inthis study, we define the socio-economic tipping point of climate-induced land abandonment as the change in cropland area in a certain location, due to the climate stressors above impacting farming economic viability. In this tipping point, we are not looking for certain thresholds to be passed but looking for a substantial reduction in cropland area extent that is a result of gradual and extreme climate events.

Methodological approach

The analysis of climate change impact requires mobilizing different models and tools, each of those looking at different systems and informing on how these respond to changes in their environmental variables. First, trajectories of GHG emissions define different levels of radiative forcing, and the impact of these on temperature and precipitation patterns are studied via General Circulation Models (GCMs). Second, the change in temperature and precipitation patterns, as well as the atmospheric concentration in CO_2, are used as input in the biophysical model related to crop growth EPIC. The productivity impact of these models is integrated into the bio-economic model GLOBIOM, to analyze the occurrence of the socio-economic tipping point of land abandonment. In a last step along the modeling chain, COIN-INT – a global, multi-sectoral, multi-regional computable general equilibrium (CGE) model – is deployed to analyze the implications of local land abandonment on a macroeconomic scale. Figure 2.3.1 summarizes the model chain of the methodological approach.

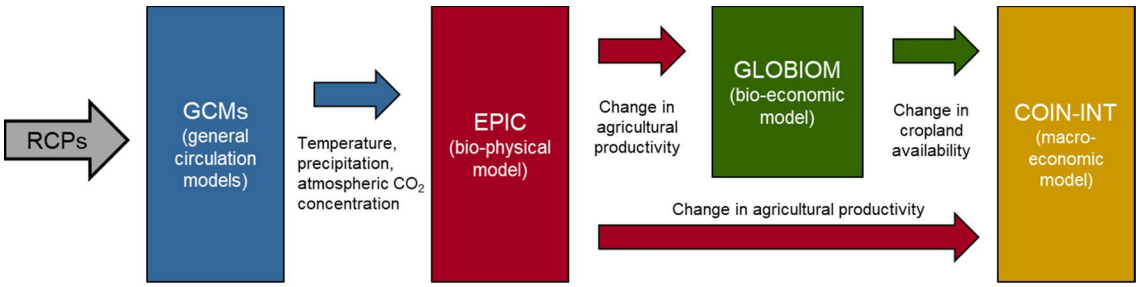

Figure 2.3.1: Conceptual overview of the model chain.

*This project has received funding from the European Union's Horizon 2020 research and innovation programme under the Grant Agreement No **776479.***

GLOBIOM (Havlík et al. 2014) is a partial equilibrium model that covers the agricultural and forestry sectors, including the bioenergy sector. Commodity markets and international trade are represented at the level of up to 58 economic regions. The spatial resolution of the supply side relies on the concept of Simulation Units (SimU), which are aggregates of 5 to 30 arcmin pixels belonging to the same altitude, slope, and soil class, and also the same country (Skalský et al. 2008). For crops, grass, and forest products, Leontief production functions covering alternative production systems are parameterized using biophysical models like EPIC (Williams 1995), G4M (Kindermann et al. 2008; Gusti 2010), or RUMINANT (Herrero et al. 2013). The biophysical models allow a precise calculation of agricultural GHG emissions (N2O and CH4).

For the European Union, GLOBIOM has been enhanced to make use of available European datasets (Frank et al. 2015, Frank et al. 2016). A more detailed SimU architecture (Balkovic et al. 2009) is used and the unit of analysis of the model is the NUTS 2 level. Information on land cover is based on CORINE land cover map (CLC2000) and crop sector representation includes alternative tillage systems (conventional, reduced, and minimum tillage), crop rotations, residue management and additional crops i.e. sugar beet, rye, oats, flax, fallow, green fodder and corn silage. In terms of trade and demand, every country in the EU is represented by its own demand and trade flows. All countries in the EU can trade with other countries in the EU or with regions in the rest of the world through a common EU market. Hence, trade flows go towards or away from a single EU country, to an EU-level market, and subsequently to another EU country or a world region outside Europe.

For this study, GLOBIOM is enhanced to be able to deal with extreme events that may be particular for the occurrence of socio-economic tipping points. To allowfor these extreme events, a “short run” response to yield shocks is implemented by limiting the possible production response to the shock. These limitations to the production responses include the restriction of land reallocation per sector for all land use sectors to reflect short-term adjustments and the reduction of possibilities for substitution between land and other inputs for crops. More specifically, GLOBIOM is adjusted to allow for a short-run response in the years 2030 and 2050, when a production shock is modelled. Up till these two time-steps, GLOBIOM is run normally with the exogenous model parameters, and land conversion and conversion of landuse is set to reflect 10-year periods. Subsequently, we run the year 2030 and 2050 again and adjust exogenous model parameters and land conversion and conversion of land use in such a way that they reflect a yearly response. In the case of GLOBIOM, exogenous model parameters include population, GDP, and income elasticities. Land conversion and conversion of land use include coefficients for maximum and minimum expansion and reduction of crops and livestock activities and management changes. In the year of the shock, these coefficients are set to reflect yearly adjustments.

The reasoning behind these model adjustments is that the extreme events that are implemented are selected to happen only once with this order of magnitude, and not 10-years in a row, which is the normal time-step of GLOBIOM. At the same time, GLOBIOM is a linear optimization model, meaning that, without setting certain bounds, the effect of introduced shocks may lead to corner solutions that might overestimate

*This project has received funding from the European Union’s Horizon 2020 research and innovation programme under the Grant Agreement No **776479.***

the true magnitude of the climate-driven land abandonment. It is therefore of importance to parameterize the cost of land conversion correctly.

For the major crops grown in Europe (rapeseed, rye, rice, soybeans, sugar beet, sunflower, corn, potato, winter wheat and barley), EPIC model outputs based on Euro-Cordex climate data were produced for the GCM-RCP climate scenarios. All runs consider simulations with explicit accounting for CO2 fertilization.

Both the climate-induced yield impact of gradual change as well as the yield impact induced by weather variability are implemented in GLOBIOM. The climate-induced yield impact of gradual change is implemented for the time-period between 2000 and 2050 following the procedure outlined in D2.2 (Boere et al., 2019). For the historical baseline (1986-2015) and each 30-year time-slice for decades between 2000 and 2050 a growth rate is computed for each crop at the NUTS 2 level. This growth rate captures the yield changes that are due to the gradual change in climate.

Extreme yield losses are implemented around the year 2030 and 2050. The yield losses implemented are selected following the procedure outlined in deliverable D3.2 (Scoccimoro et al., 2020). The extreme yield losses of the year 2030 are based on data of the time-slice 2016-2045 and the extreme yield losses of the year 2050 are based on data of the time-slice 2035-2065. For each of the 30-year time slices we compare the difference between the annual yield and the mean yield level of that timeslice. For an aggregation of impacts of the shocks across individual crops, the yields arecomputed as weighted averages of all crops weighted by their area. As the focus is on the extremes and inter-annual variability, we select from every GCM-RCP combination,and for each time slice, the year which represents the largest negative deviation between the weighted yield over all crops of that year and the weighted yield over all crops of the historic baseline of 1985-2015. To retain the inter-crop correlation, all crop-specific yield deviations of the selected year are implemented in GLOBIOM at the NUTS 2 level.

The analytical approach to the occurrence of the tipping point of land abandonment is summarized in Table 2.3.1. Temperature and precipitation stresses provide the main climatic indicators to analyze the magnitude of yield impacts that leads to farm exit and land abandonment.

Table 2.3.1: Flow, indicators and methods used to analyze tipping points due to yield supply shocks in Europe

	Climatic / weather event	**Input indicators: Agriculture**	**Output indicators: Socio-economic tipping point**	**Expected indirect and economy-wide impacts**
Indicator	Temperature and precipitation stresses (heatwaves and droughts)	Crop-specific yield impact based on climatic/weather events	Land abandonment / farm exit	Large increases in prices; Welfare and GDP losses; Changes in international trade patterns
Tool	Climate model projections with Euro-Cordex downscaling	Process-based crop-model EPIC based on climate model projections with Euro-Cordex downscaling	Bio-economic model GLOBIOM	Global, multi-regional, multi-sectoral CGE model COIN-INT

*This project has received funding from the European Union's Horizon 2020 research and innovation programme under the Grant Agreement No **776479.***

To study in a final step the macroeconomic implications of farmland abandonment, we deploy the COIN-INT CGE model. The main model properties were described in section 1.2.2 as well as in the Appendix. For this assessment we use the comparative static version of COIN-INT and look at effects in 2050, relative to a 2050 baseline (i.e. SSP development only). We thus analyze a new long-term equilibrium in 2050, after new land allocation has happened, which was induced by extreme drought over Europe. Note, that we exclude SSP4 from the analysis, as this development is not part of the COACCH modeling protocol (Hof et al., 2020).

The implementation of climate-induced farmland abandonment in COIN-INT works via two channels. First, the change in cropland availability from GLOBIOM is aggregated to the COIN-INT CGE model regions. The aggregated change in cropland availability is then implemented as a change in the agricultural land endowment of COIN-INT. Second, the slow onset climate change impact on agricultural crop yields is implemented via changes in land productivity in the production function of the agricultural crop sector in COIN-INT (i.e., in case of lower/higher productivity more/less land is needed to achieve the same output as without the productivity change).

Scenario selection

In line with the COACCH framework, the identification and verification of climate conditions leading to a tipping point of land abandonment is based on shortfalls in production within the GCM-RCP-SSP framework. The following options are selected for further investigation of the tipping point of land abandonment to occur:

- Socio-economic scenario: pathways SSP1 to SSP5
- Mitigation scenario: no climate policy
- RCP scenario: no climate shock (baseline), RCP 2.6, RCP 4.5 and RCP 8.5
- GCM scenario: The climate models that are available under Euro-Cordex runs: EC-EARTH, HadGEM2-ES, REMO2009, IPSL-WRF33-CM5A.

Due to data limitations, not all GCMs are available for all RCPs. Our sample is therefore limited to the GCM-RCP combinations in Table 2.3.2:

Table 2.3.2: GCM-RCP combinations using Euro-Cordex data available for the analysis of the socio-economic tipping point of land abandonment

GCM	RCP
EC-EARTH	2.6
EC-EARTH	4.5
EC-EARTH	8.5
HadGEM2-ES	4.5
HadGEM2-ES	8.5
REMO2009	2.6
REMO2009	4.5
REMO2009	8.5
IPSL-WRF33	4.5

*This project has received funding from the European Union's Horizon 2020 research and innovation programme under the Grant Agreement No **776479.***

2.3.2. Contributing factors and occurrence of tipping point

To verify the occurrence of climate conditions within the current century, D3.2 analyzed the climate impacts on yields along the RCPs, time, and geographical dimensions, as well as whether differences in yields are likely caused by temperature stress or water stress. It concluded that along the RCP axis, clear differences in the magnitude of yield shocks could not be observed. However, regional differences were identified, with larger magnitudes of yield shocks in Southern and Eastern Europe, compared to Northern and Western Europe.

Although the severest magnitude of extreme events may not show significant differences between RCP2.6 and RCP8.5, the likelihood of severe yield losses may differ depending on the RCP. Recent advances in the field of attribution of extreme events in the context of climate change will help future research about the extent to which climate change influences the probability of occurrence of specific types of extremes, such as heatwaves, cold spells, floods or droughts. As event attribution capabilities continue to improve, the outcomes of global circulation models (GCMs) will allow defining all four moments of the statistical distribution of climatic variables, which can then be used to infer the attributes (e.g., frequency, intensity) of extreme events. However, based on currently available information, this study limits itself tothe occurrence of these events under different SSP-RCP-GCM combinations and does not analyze the frequency of return of these events. This is the main reason for thelack in significant difference that is observed between RCP2.6 and RCP 8.5. Even though we find evidence for large yield shocks to occur under both RCPs, the likelihood of occurrence – which is not considered here – may be much higher under RCP 8.5 compared with RCP 2.6.

There are a few reasons why we do not focus on the likelihood of large yield losses to occur. The EPIC runs supply a broad set of simulations, but for a robust analysis of extreme events, the sample is too small and also problematic to analyze as distributions are subject to trends (caused by trends in climate variables and atmospheric CO2 concentrations) and different biases related to models, crops and regions selection (Rosenzweig et al., 2014). This leads to the inability to represent the full range of representative climate change projections from a small set of climate models (McSweeney and Jones, 2016). Also, the strong differences in climate patterns between GCMs (McSweeney and Jones, 2016) and yield responses between crop models (Rosenzweig et al., 2014; Müller et al., 2015) complicate the delineation of probabilities from individual events.

The changes in yield can be further mapped at the NUTS 2 level. Figure 2.3.2 shows the average factor change in weighted yields that is due to the yield shock for REMO2009 under RCP2.6 and RCP8.5. Note that the eventual yield changes due to climate that is implemented in GLOBIOM will differ from that reported in Figure 2.3.2 because of the additional effect of gradual climate change on yields. Figure 2.3.2shows a clear pattern of neutral or slightly positive yield effects in the North of Europe and negative yield impacts in the South of Europe for REMO2009. A clear difference in magnitude of yield change between the 2030 period and the 2050 period cannot be observed across GCMs and RCPs. In the case of REMO2009 both RCP 2.6 and RCP 8.5

*This project has received funding from the European Union's Horizon 2020 research and innovation programme under the Grant Agreement No **776479.***

show a slightly more diverging picture between the North and South of Europe in terms of yield impacts. In 2050, the year with the largest negative yield impact shows aslightly more positive picture for the North of Europe and a slightly more negative picture for the South of Europe compared to the year with the largest negative impact around 2030. However, these differences are not large enough and vary too much across GCMs to draw any conclusions between the two time slices.

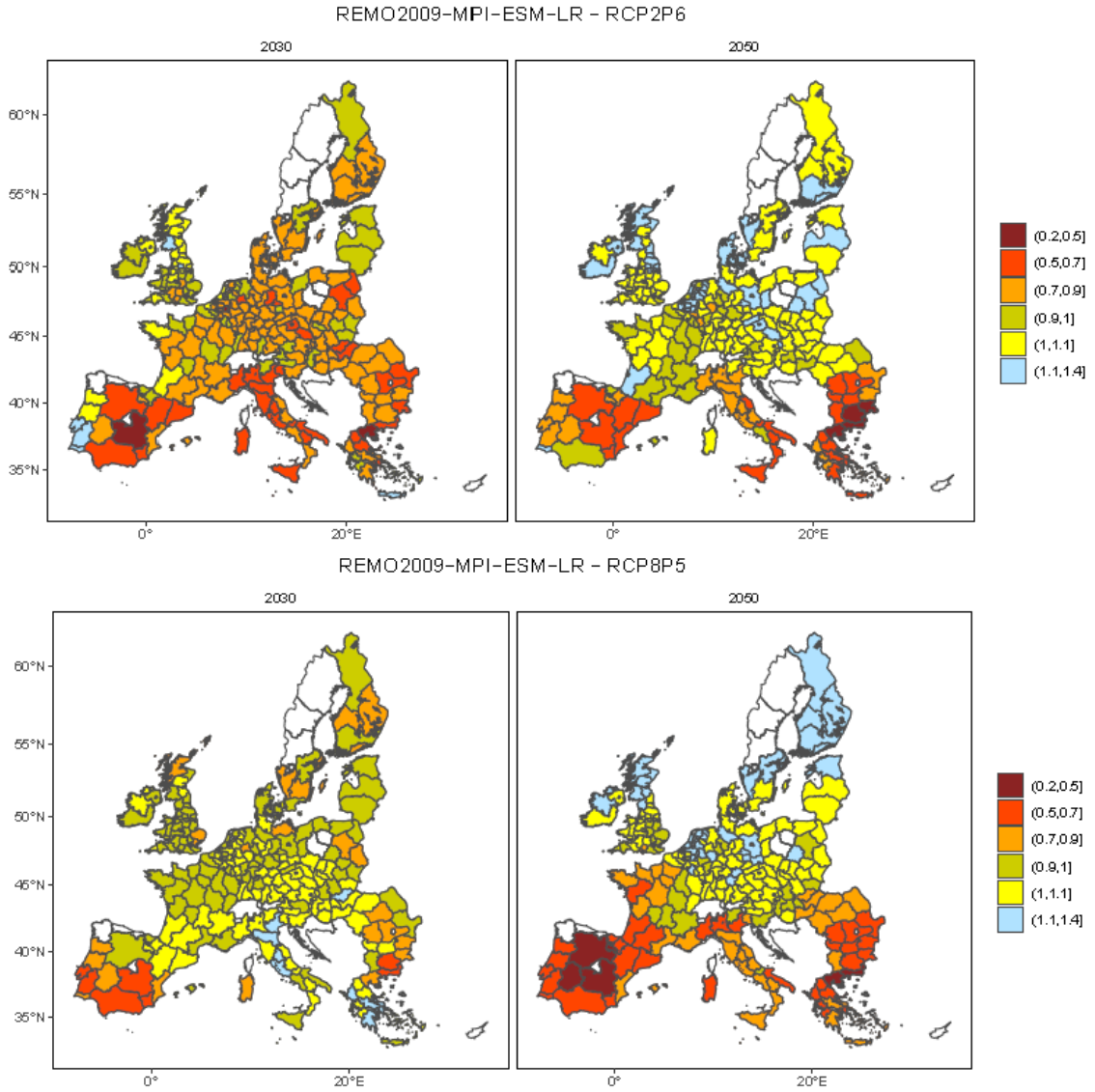

Figure 2.3.2: Average factor of yield changes across crops around the 2030 and 2050 time-slice at the NUTS-2 level.

The socio-economic tipping point of land abandonment due to the decline in farm profitability and the lack of suitable adaptation options may be quite local in its nature. Tipping points may be most obvious at the community scale, where an interplay of different mechanisms can rapidly change the socio-economic structure ofa local area to a state of abandonment (van Ginkel et al., 2020).

In Southern Europe, the higher temperatures and lower precipitation caused by climate change may have large impacts on the agricultural sector (Ciscar et al. 2014).

*This project has received funding from the European Union's Horizon 2020 research and innovation programme under the Grant Agreement No **776479.***

With water availability becoming scarcer, and therefore irrigation not being an adequate adaptation mechanism for the future, this may lead to rapid patterns of farm abandonment. Indeed, Figure 2.3.3 shows that especially in the Southern part of Europe, all five selected scenarios show localized patterns of land abandonment that are more concentrated and of higher magnitude compared with other areas in Europe and could therefore be considered as tipping points. Figure 2.3.3 shows that the locations that are especially vulnerable to experience a withdrawal of arable farming are all located in Italy or Southern Spain. Besides this common characteristic, the localized tipping points do not seem to aggravate along the axes of RCPs or SSPs anddo not show a striking difference between the GCM REMO2009 and the GCM EC- EARTH.

The abandoned farmland found in this section is the result of the analysis using a partial-equilibrium model that describes the land in economic terms and therefore does not consider how the interplay with other sectors and socio-economic variables may accelerate or discourage the process of land abandonment. GLOBIOM determines the viability of cropland farming at a certain location by the change in output in combination with changes in land, input, and production costs. The most profitable farming activity at a given location depends on the local climate and biophysical context, and alterations to these may make the area more favourable (unfavourable) for certain types of arable farming if, on average, the climatic conditions move closerto (further away) from the optimum conditions of cultivating (Prishchepov et al. 2013). However, as highlighted in van Ginkel et al. (2020), farmland abandonment is in reality the outcome of many individual choice processes, and is also influenced by several feedback mechanisms. After a certain degree of migration is reached, a rural area gets less attractive to live in, which may further accelerate the process of ruralabandonment. These social processes are not considered in the identification of the tipping point in this analysis. This may also influence the time-dimension of abandonment and may lead to a more sudden abandonment.

*This project has received funding from the European Union's Horizon 2020 research and innovation programme under the Grant Agreement No **776479.***

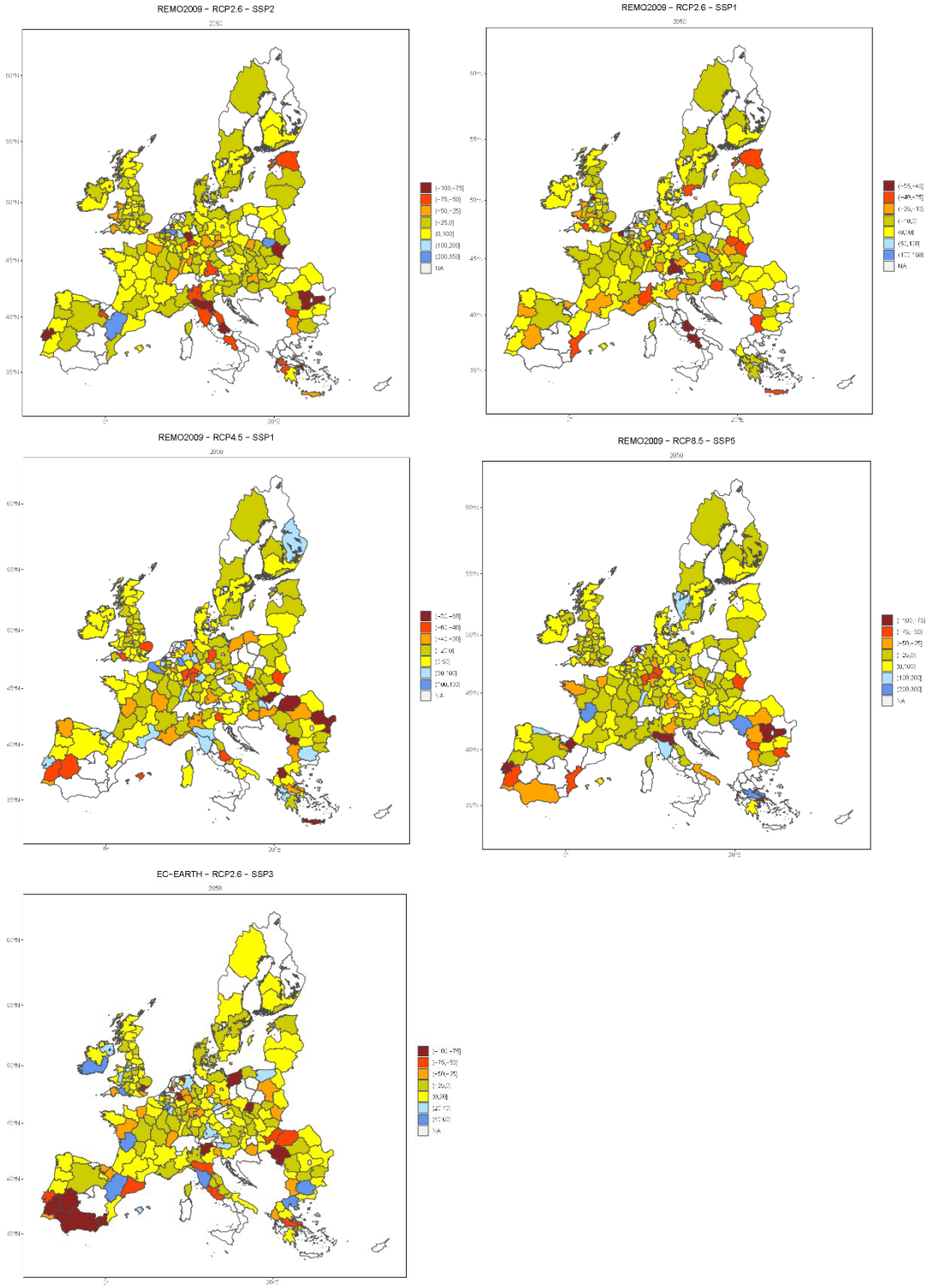

Figure 2.3.3: Relative change in cropland under the five selected scenarios compared to a no climate change scenario in 2050

2.3.3. Macroeconomic implications

Selection of tipping point scenarios for macroeconomic assessment

*This project has received funding from the European Union's Horizon 2020 research and innovation programme under the Grant Agreement No **776479.***

Since the effects on cropland changes do not coincide with the typical RCP impact logic (i.e. stronger effects the higher the RCP) and since there is no clear picturealso from comparison across SSPs, we choose a different approach for the identification of tipping points and selection of scenarios for the macroeconomic assessment. That is, we look for the worst cases in terms of EU-wide land loss as coming from GLOBIOM and use the "Top 5"-scenario combinations (GCM-RCP-SSP) to be further analysed. This approach of selecting the worst cases might not be representative, but as we are interested in possible large-scale socio-economic tipping points, or large-scale reconfigurations in the socio-economic system, it gives a good impression of what could happen in extreme cases. Figure 2.3.4 shows the ranking ofall 36 cases by GCM-RCP-combination (a), SSP (b) and RCP (c). We see that the EU-wideeffect is negative in most cases (only three combinations show EU-wide positive effects). The worst five combinations are specified as follows:

1. REMO2009-MPI-ESM-LR_rcp2p6-SSP1: -7.1% EU-wide cropland loss
2. REMO2009-MPI-ESM-LR_rcp4p5-SSP1: -6.9% EU-wide cropland loss
3. REMO2009-MPI-ESM-LR_rcp2p6-SSP2: -6.6% EU-wide cropland loss
4. REMO2009-MPI-ESM-LR_rcp8p5-SSP5: -6.6% EU-wide cropland loss
5. RCA4-EC-EARTH_rcp2p6-SSP3: -6.5% EU-wide cropland loss

We see that in the worst cases, EU-wide long-term cropland loss due to farmland abandonment is about -7%. It also becomes clear that the REMO2009-MPI- ESM-LR is strongly represented in the worst five combinations.

We also find that the worst cases are not all connected to the strongest forcing scenario (RCP 8.5), but also to RCP 2.6 and RCP 4.5. This is because, as already discussed in section 2.3.2 and Scoccimarro et al. (2020, section 3.3), we do not observea significant difference in the climatic factors driving the largest negative yield shock between RCPs.

When comparing the five selected scenario combinations across CGE model regions (Figure 2.3.5, the presented data is GLOBIOM model output and serves asinput for the COIN-INT model), we see that the EU-wide cropland loss (which is about - 7% for all five scenarios) can be distributed very differently among regions. We alsosee that for the European regions Austria (AUT), Italy (ITA), Netherlands (NLD) and Northern Europe (NEU) the effects can even have different signs. Note, that we assume in this analysis extreme events to happen in Europe (DEU: Germany; AUT: Austria; ITA: Italy; UKD: United Kingdom; FRA: France; BLU: Belgium and Luxemburg; NLD: Netherlands; CEU: Central Europe; NEU: Northern Europe; MEU: Mediterranean and South-Eastern Europe), not in other regions of the world.

The reconfiguration of cropland availability due to farmland abandonment is triggered by single year extreme events over Europe. This new configuration is however still confronted with annual variability as well as slow-onset biophysical climate change impacts, i.e. changes in crop yields on the land remaining in production. Thus, for each of the five scenario combinations, we also implement changes in crop yields from slow-onset changes in the CGE model, to capture the whole effect of climate change. For each of the five scenario-combinations, the associated changes in crop yields measured as relative changes in tonnes of dry-matter

*This project has received funding from the European Union's Horizon 2020 research and innovation programme under the Grant Agreement No **776479.***

crops relative to the baseline are given in Figure 2.3.6 (the presented data is GLOBIOM model output and serves as input for the COIN-INT model), again for the CGE model regions. We see that changes in crop yields for the five selected cases are (strongly) positive for most European regions and scenario combinations. Only ITA and Mediterranean and South-Eastern Europe (MEU) show positive and negative effects in yield changes.

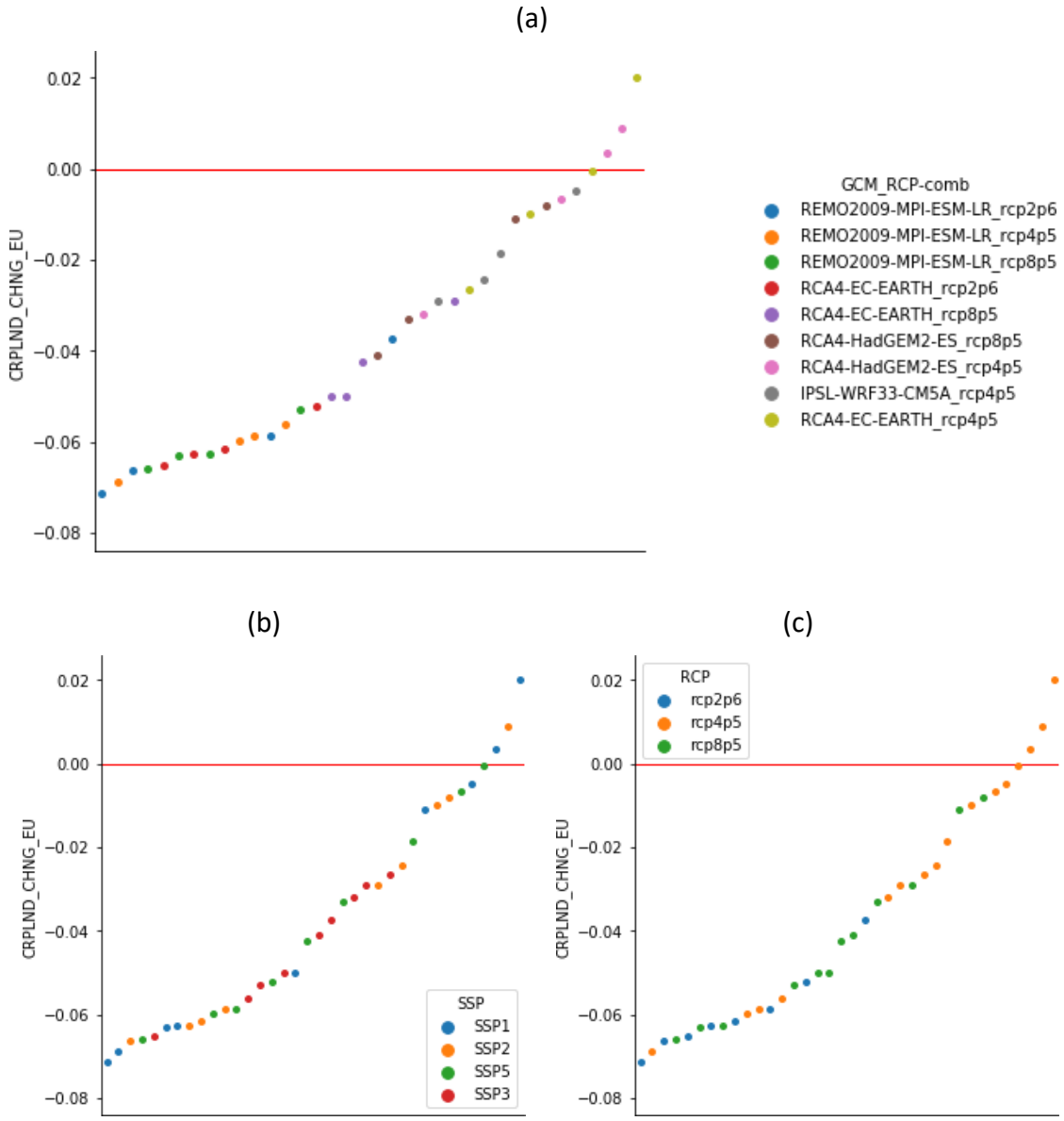

Figure 2.3.4: Ranking of EU-wide cropland change due to farmland abandonment in 2050, by GCM-RCP combination (a), by SSP (b) and by RCP (c).

*This project has received funding from the European Union's Horizon 2020 research and innovation programme under the Grant Agreement No **776479.***

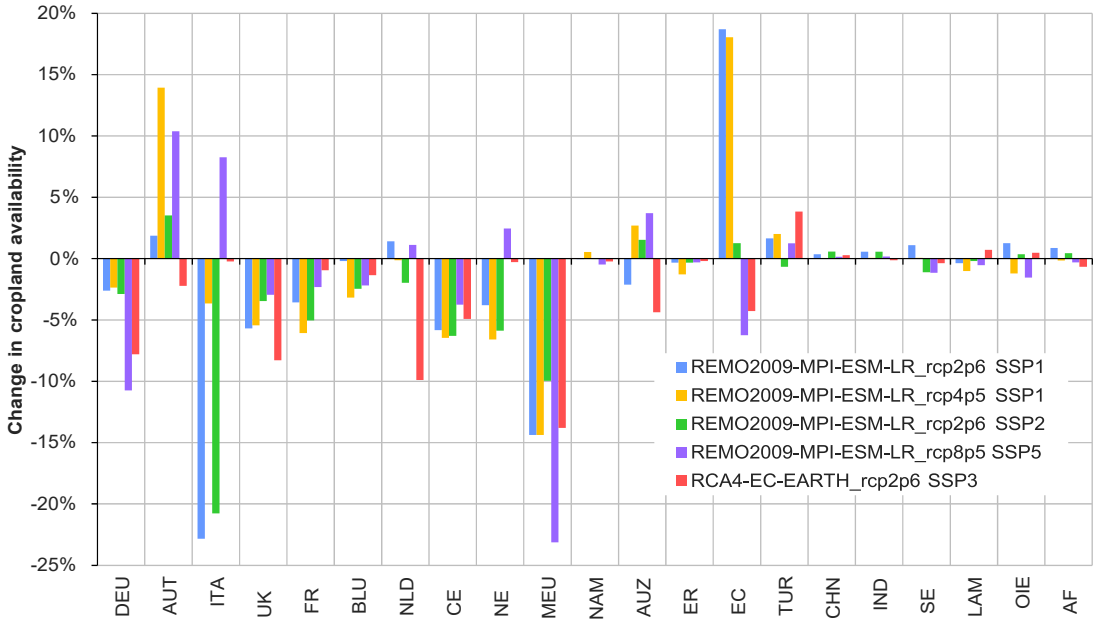

Figure 2.3.5: Regional change in cropland availability of EU-wide worst five scenarios from the scenario-space (changes in cropland area relative to the baseline). The regions abbreviations are as follows: DEU: Germany; AUT: Austria; ITA: Italy; UKD: United Kingdom; FRA: France; BLU: Belgium and Luxemburg; NLD: Netherlands; CEU: Central Europe; NEU: Northern Europe; MEU: Mediterranean and South-Eastern Europe; NAM: North America; AUZ: Australia and New Zealand; ERA: Eurasian countries; ECA: Emerging economies-Asia; TUR: Turkey and Israel; CHN: China; IND: India; SEA: South-East Asia; LAM: Latin America; OIE: Oil exporting countries; AFR: Africa.

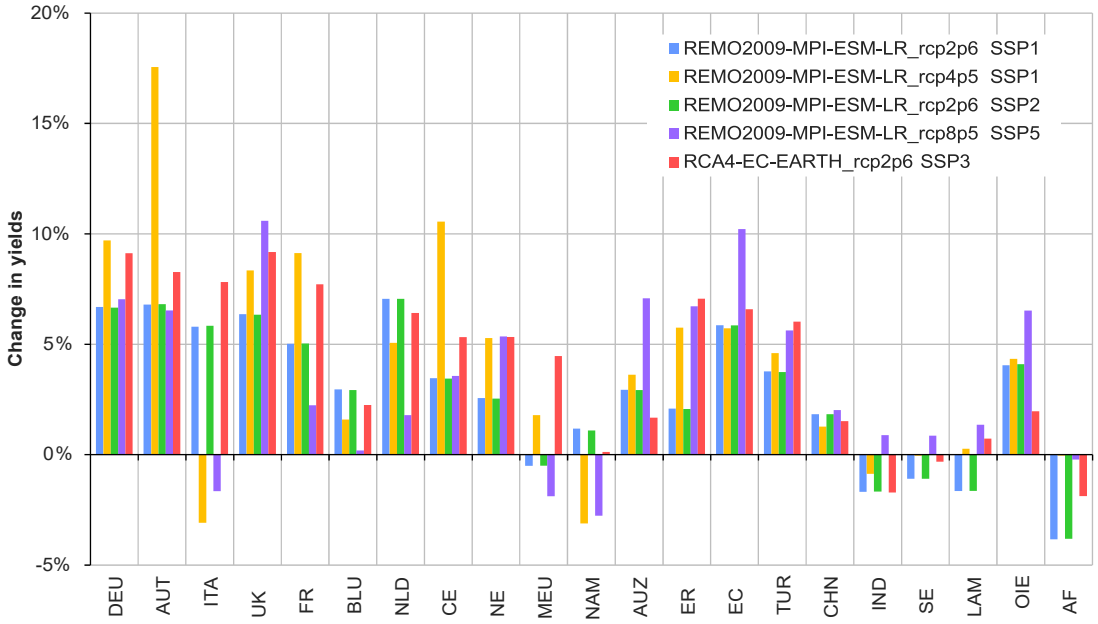

Figure 2.3.6: Regional change in crop yields for the selected scenario combinations (changes in tonnes of dry-matter crops relative to the baseline). The regions abbreviations are as follows: DEU: Germany; AUT: Austria; ITA: Italy; UKD: United Kingdom; FRA: France; BLU: Belgium and Luxemburg; NLD: Netherlands; CEU: Central Europe; NEU: Northern Europe; MEU: Mediterranean and South-Eastern Europe; NAM: North America; AUZ: Australia and New Zealand; ERA: Eurasian countries; ECA: Emerging economies-Asia; TUR: Turkey and Israel; CHN: China; IND: India; SEA: South-East Asia; LAM: Latin America; OIE: Oil exporting countries; AFR: Africa.

*This project has received funding from the European Union's Horizon 2020 research and innovation programme under the Grant Agreement No **776479.***

Results from macroeconomic assessment

Figure 2.3.7 shows the combined effect of changed yields and changed farmland availability on land rents as a result from COIN-INT. For European regions, wemostly see positive effects on rents. There are two opposing effects, determining the effect on land rents. First, as cropland gets scarcer, rents would increase. Second, with rising yields, less land is needed for satisfying demand and thus rents would decrease. The former effect dominates and thus we see mostly increasing land rents.

The changed land rents in turn affect crop and food prices, which are given in Figure 2.3.8 and Figure 2.3.9. We see that the effect of changing land rents does not translate 1:1 to crop and food prices. This is because of foreign trade, as crop and food markets are highly globalized. By importing cheaper crops to Europe from non-European regions (where yields are also increasing strongly), crop prices are even slightly below baseline levels. Regarding food prices, we do see a slightly different picture, with slightly higher food prices in most EU regions and scenarios.

Note, that for these scenarios, it is assumed that an extreme weather event occurs over Europe (with farmland abandonment as a consequence) but not in other world regions. The effect from foreign trade would thus be different, when at the same time also extreme weather would occur in the rest of the world.

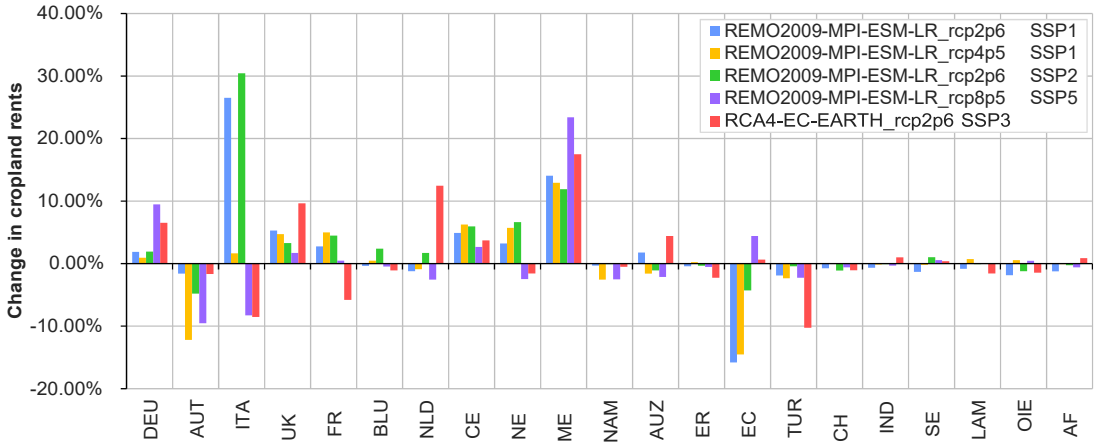

Figure 2.3.7: Changes in cropland rents due to the combined effect of changed cropland availability and yield changes.

*This project has received funding from the European Union's Horizon 2020 research and innovation programme under the Grant Agreement No **776479.***

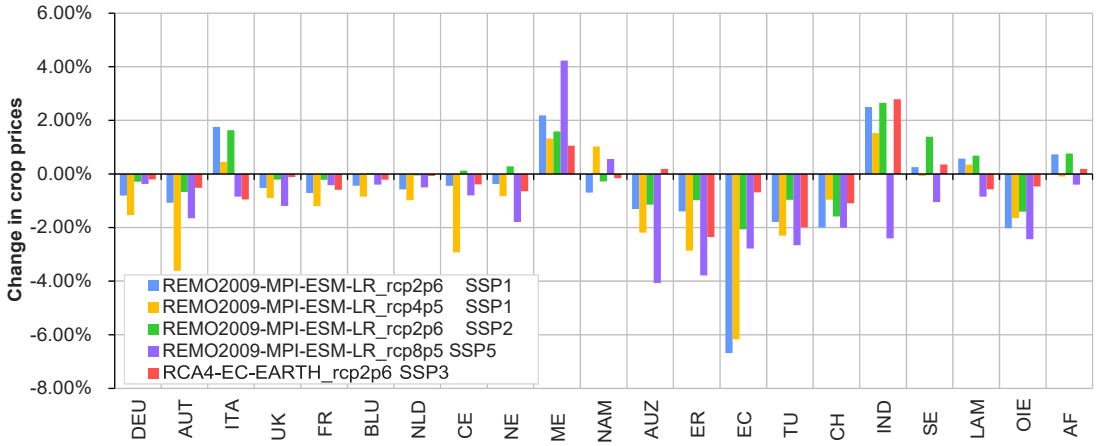

Figure 2.3.8: Changes in crop prices due to the combined effect of changed cropland availability and yield changes.

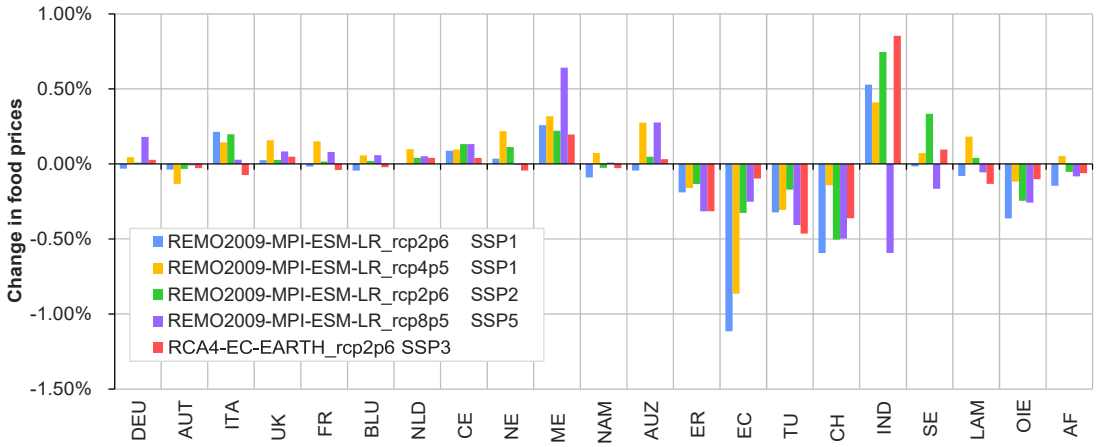

Figure 2.3.9: Changes in food prices due to the combined effect of changed cropland availability and yield changes.

Eventually the described effects translate into GDP effects, which are given in Figure 2.3.10. We see that GDP effects of European regions turn out to be positive in most cases, except for the more vulnerable regions ITA and MEU, where we canobserve relatively strong negative effects of up to -0.5% lower GDP in 2050. The mostlypositive effects on GDP are clearly driven by the strong increases in yields. We see this when running the same scenario combination without changes in cropland availability (Figure 2.3.11, i.e. only yield changes) and calculating the differences of %-changes in GDP; i.e. measuring the difference in terms of %-points (Figure 2.3.12). It becomesclear that when including changes in cropland availability due to extreme events, the potential positive gains from higher yields are partly set off and in some cases even more than compensated (i.e. switching from a positive effect in Figure 2.3.11 to a weaker or even negative effect in Figure 2.3.10). We see that for regions ITA and MEU the isolated effect of yield changes is clearly misleading, when changes in cropland configurations are omitted.

*This project has received funding from the European Union's Horizon 2020 research and innovation programme under the Grant Agreement No **776479.***

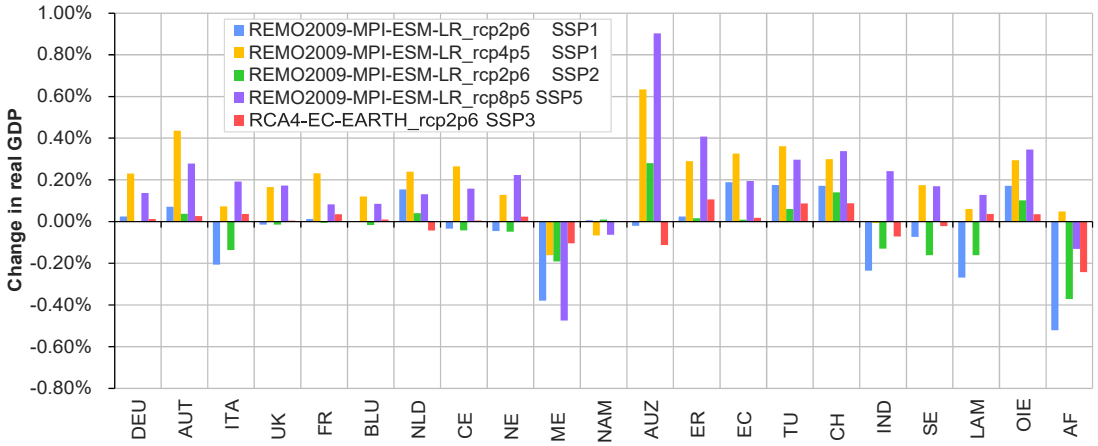

Figure 2.3.10: Changes in real GDP due to the combined effect of changed cropland availability and yield changes.

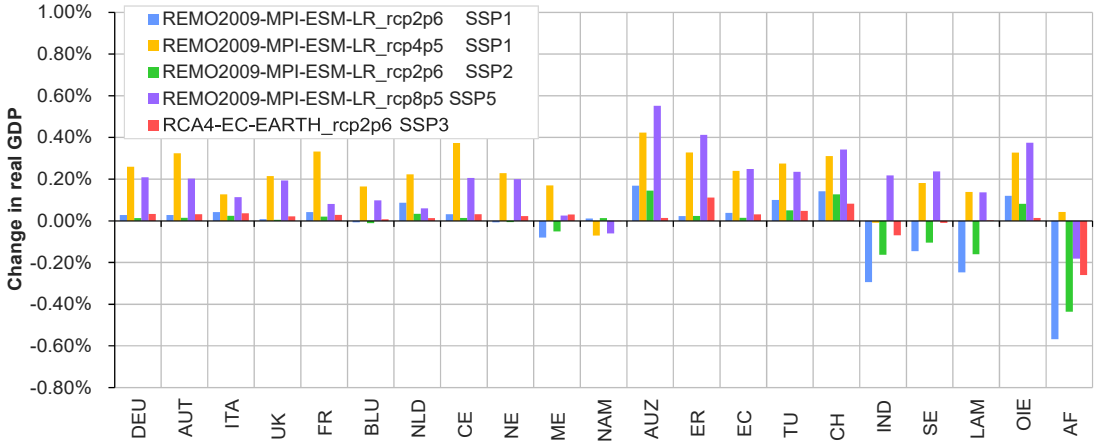

Figure 2.3.11: Change in real GDP due to the isolated effect of yield changes.

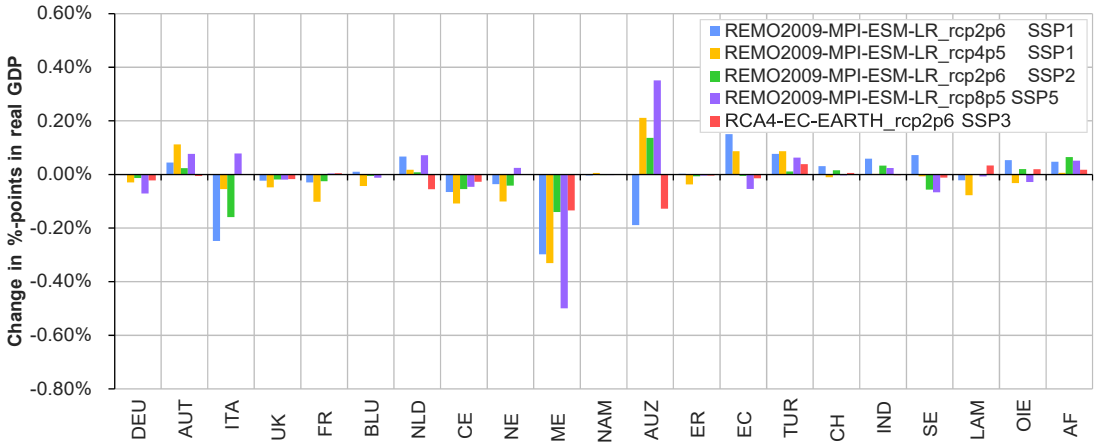

Figure 2.3.12: Percentage point difference between GDP effects due to isolated yield changes and due to the combined effect of yield and cropland changes. Negative (positive) effects show that GDP effects are reduced (increased) by also including changes in cropland.

*This project has received funding from the European Union's Horizon 2020 research and innovation programme under the Grant Agreement No **776479.***

2.4. Coastal migration

Mean and extreme sea-levels are projected to rise substantially during the 21st century (see D2.3 and D3.2), and such substantial sea-level rise (SLR) will trigger different human responses including adapting in situ through increasing coastal protection or retreating from the coastal floodplain. In particular coastal retreat and the associated migration of people has received increasing attention in the literature and media, with accelerated sea-level rise and increased coastal flooding potentially displacing millions of people from coastal areas (Hauer 2017, Hauer et al. 2019, Hino et al. 2017, DeConto and Pollard 2016, Nerem et al. 2018). A recent Worldbank study, for example, conjectures that by 2050 140 million people could migrate due to water stress, crop failure and sea level rises in Sub-Saharan Africa, South Asia and Latin America alone (Rigaud et al. 2018). A forthcoming study by COACCH researchers estimates that even under cost-benefit optimal protection decisions globally 17 to 72 million people will have to migrate from coastal areas during 21st century (Lincke and Hinkel, forthcoming).

In this deliverable we explore the macroeconomic effect of coastal migration. Coastal migration is modelled using the DIVA model for coastal impact and adaptation modelling (see COACCH Deliverable D2.3 for a detailed description). Population migrates from coastal areas only if they are not protected by protection infrastructure such as dikes. If population is not protected, they migrate when they fall below the water level of the 1-in-1-year event. This models a rather reactive form of migration: population stays until it gets flooded regularly. The two migration scenarios (migration/no migration) are combined with the two adaptation scenarios (BAU adaptation/no further adaptation) described in D2.3.

2.4.1. Definition of tipping point

In the previous deliverable D3.2 we analyzed the potential tipping point characteristics for three regions:

1. Within the EU28 we analysed coastal migratrion for member countries. There we have chosen thresholds of 0.1 and 0.05 percent annual coastal migration of total population. To tip the system these thresholds need to be crossed over a longer time period, in our case we define a tipping point for a country if the average annual coastal migration relative to the countries population in one of our three time periods (2030s, 2050s, 2080s) crosses the threshold. The 0.1 percent might seem low but it would imply about 8,000 coastal migrants every year in Germany and about 6,000 every year in France and Italy. Such a constant stream of coastal migrants might have severe consequences as the population could loose trust in the ability of a country to deal with rising sea- levels.

*This project has received funding from the European Union's Horizon 2020 research and innovation programme under the Grant Agreement No **776479.***

2. To analyze external pressures to the EU we analysed coastal migration from the Middle-East-North-Africa region. We selected thresholds of 100,000 and 200,000 annual coastal migrants in the MENA region, as such a constant stream of coastal migrants might have severe consequences within the region, but also for Europe if we assume that the majority of these people targets the EU countries.
3. In order to assess global disruptions that could trigger tipping points we defined thresholds of one million and two million annual coastal migrants globally. Such a constant stream of coastal migrants might have severe consequences within countries or regions.

2.4.2. Contributing factors and occurrence of tipping point

There are two major contributing factors to the occurrence of tipping points listed above. One is the sea-level rise itself, the other is the successful adaptation to rising sea-levels. As shown in Deliverable 3.2, the defined tipping point thresholds can only be reached in the scenarios with no adaptation (except from the MENA-tipping point that can be reached also without adaptation under high-end sea-level rise). In terms of sea-level rise, the lower thresholds for each regional tipping point can be crossed even under RCP 2.6, while the higher threshold can usually only be crossed from RCP 6.0 onwards (Table 2.4.1).

Table 2.4.1: Crossing of the tipping point thresholds defined in COACCH Deliverable D3.2 under the climate scenarios used in COACCH without adaptation. Green dots mean that no thresholds are crossed, yellow dots mean that the lower threshold is crossed and red dots mean that the higher threshold is crossed. ForEU28 yellow and red dots mean that the threshold is crossed for at least five of the countries.

RCP	Region	2030s	2050s	2080s
RCP 2.6	EU28	🟢	🟢🟢	
	MENA	🟡	🟡	🟡
	global	🟢	🟡	🟡
RCP 4.5	EU28	🟢	🟢	🟢
	MENA	🟡	🟡	🟡
	global	🟢	🟡	🟡
RCP 6.0	EU28	🟢	🟢	🟢
	MENA	🟡	🔴	🟡
	global	🟡	🔴	🟡
RCP 8.5	EU28	🟢	🟡	🟡
	MENA	🟡	🔴	🟡
	global	🟡	🔴	🟡
RCP 8.5	EU28	🟢	🟡	🟡

*This project has received funding from the European Union's Horizon 2020 research and innovation programme under the Grant Agreement No **776479.***

(high end)	MENA			
	global			

2.4.3. Macroeconomic implications

Definition and selection of scenarios

Coastal migration, defined as a retreat of people and assets from the coastline, can also be interpreted as "autonomous adaptation." In contrast, building sea dikes (which are mostly funded by the public sector) in order to prevent rising sea levels from creating damages to the assets and people located at the coasts, can be interpreted as "planned adaptation" (see e.g. Filatova, 2014). Of course, both types of adaptation aim at reducing direct damages but are differently characterised in terms of costs. Whereas planned adaptation is a top-down approach that focuses primarily on engineered flood protection (or "grey" adaptation measures), autonomous adaptation works bottom-up and leaves the decision on how to react to climate change to individuals.

The recent macroeconomic literature on sea level rise (see e.g., Bosello et al. (2012); Parrado et al. (2020) or Bosello & De Cian (2014) for a review) includes adaptation in the form of planned adaptation and compare the economy-wide impacts from sea level rise to a no-adaptation scenario. This approach is however problematic, due to two reasons: First, a no-adaptation scenario is highly implausible (Hinkel et al., 2014), as societies will adapt in any way; be it autonomously or planned. Second, the planned adaptation scenario is assumed to be a perfect adaptation scenario, in which planned adaptation is put in place globally; even in e.g. least developed countries, where public funds might be very limited and autonomous adaptation might be more realistic.

In the here presented analysis we contribute to the literature by introducing an autonomous adaptation scenario; i.e. coastal migration (or coastal retreat) into the macroeconomic CGE model COIN-INT (see section 1.2 and the Appendix for details).

Looking at Table 2.5.1 we choose RCP8.5 with high end ice melting in combination with SSP5 as the main scenario for the macroeconomic analysis and compare macroeconomic effects between three cases: (i) no further adaptation, (ii) BAU (planned) adaptation (without migration) and (iii) autonomous adaptation (migration). In addition a combined scenario is presented (iv) in which planned and autonomous adaptation are combined. To put the results into perspective we complement the analysis by showing also results for RCP8.5-SSP5 with medium ice melting and for a standard scenario; i.e. RCP4.5-SSP2 (medium ice melting).

All results are given as relative change to a baseline scenario, which includes only the socio-economic development of the world, but no climate change (and thus no climate-induce sea-level rise). By comparing the climate change impact scenarios to the baseline, the pure effect of climate change can thus be analysed in isolation.

Model implementation

*This project has received funding from the European Union's Horizon 2020 research and innovation programme under the Grant Agreement No **776479.***

The following DIVA model output indicators are used as input for the COINT-INT CGE model:

- Annual land loss due to submergence (km²/year)
- Expected annual damages to assets by sea floods (million US$/year)
- Total capital stock (million US$/year)
- Expected annual number of people flooded per year (thousands/year)
- Protection costs (million US$/year), split into an investment fraction and a maintenance cost fraction.
- Migration costs (million US$/year)

Migration costs capture two aspects. First, the costs of leaving immobile assets behind, i.e. full depreciation of assets that are lost due to coastal retreat. Second, the costs of moving mobile capital away from the coastlines further inland. Both aspects fall into the broad category of capital costs and are treated as such in the CGE model.

The impacts of sea level rise are implemented in COIN-INT via six channels:

1. Sea flood damages reduce the physical capital stock (capital costs).
2. We assume that each person that is flooded within a year, is not able to provide labour to the labour market for 2 out of 48 working weeks a year (labour costs).
3. The annual land area that is lost due to SLR is translated into lower cropland availability for agricultural crop production (land loss).
4. Investment costs for renewing sea dikes or for upgrading them (in the case of BAU (planned) adaptation) is modelled as forced investment activity of the government agent (investment cost fraction of DIVA's protection costs).
5. Maintenance costs for sea dikes are implemented as forced government consumption for construction activities (maintenance cost fraction of DIVA's protection costs).
6. Migration costs are included as capital costs and reduce the accumulation of productive capital (i.e. capital stock).

For a consistent flow of information across the CGE model and DIVA, all values from DIVA, expressed in US$ PPP (Purchasing Power Parity) are converted to US$ MER (Market Exchange Rates), the CGE model's reference, using the conversion factors from the World Development Indicators (World Bank, 2020). Please see the Appendix of COACCH Deliverable D3.3 for a more detailed description of the implementation of impacts.

Results

Figure 2.4.1 shows changes in real GDP relative to the baseline scenario for RCP8.5-SSP5 (high end ice melting) for the European model regions (top) and non-European regions (bottom). Clearly the effects on real GDP are very strong, when no

*This project has received funding from the European Union's Horizon 2020 research and innovation programme under the Grant Agreement No **776479.***

further adaptation is taken in place (first column). In the European regions[7], GDP lowers by up to -4.5% in 2050 in regions such as Italy (ITA) and Northern Europe (NEU).On the other hand for landlocked regions such as Austria (AUT) and Central Europe (CEU) we even see slight increases due to comparative advantages over the rest of the word. In the non-European regions the negative effects are even stronger, with GDP losses of up to -11% in Asia's Emerging economies (ECA).

With BAU (planned) adaptation (second column in Figure 1) GDP losses can be reduced significantly; i.e. below 1% in European regions and below 2% in non- European regions. Interestingly we see that the ranking of regions changes, when compared to the no further Adaptation scenario.

When implementing autonomous adaptation instead of planned adaptation (third column in Figure 2.4.1) we see that impact are higher than with BAU (planned) adaptation, but still lower than without further adaptation. What also becomes visible is, that autonomous adaptation is more of a reactive process to rising sea levels, since in the first year of the time horizon until 2035 the shape of the curves is very similar to the no further adaptation scenario. Only then sea levels have risen strongly enough to trigger migration, which becomes visible as a slight flattening of the curves, or in some cases even a reversing of the trend (see e.g. ITA or ECA). Such a reversal in trend is possible due to comparative advantage effects.

The last column in Figure 2.4.1 shows the combined case of autonomous and planned adaptation. For the European regions the results are not very different from the BAU (planned) adaptation case, since the protection measures (sea dikes) in this case protect most inhabited areas and thus prevent people from migrating. Interestingly, for the non-European regions, we see that the combination of planned and autonomous adaptation is still much better than the pure planned adaptation scenario (e.g. for South-East Asia (SEA), or the Oil-Exporting regions (OIE)). This shows in Europe more populated areas are protected by dikes than in other regions.

Figure 2.4.2 shows relative GDP effects for RCP8.5-SSP5 with medium ice melting. In general, the effects are much weaker than with high end ice melting, but still significant. The qualitative findings from Figure 2.4.1 also apply here. Again, the no-Adaptation scenario shows the strongest effects, which can be reduced by both planned and autonomous adaptation.

Figure 2.4.3 again shows relative GDP effects, but now for RCP4.5-SSP2 medium ice melting; a standard scenario. Here the story is again similar as for the former two scenarios. There is one difference though, namely that some regions tend to regain some of their GDP losses with on-going sea level rise. This becomes visible as the upward turn of the curve for Mediterranean and South-Eastern Europe (MEU) at the end of the time horizon. Again, this can be explained by emerging comparative advantages, which get stronger when sea level rise is increasing. Apparently by 2045 a

[7] The regions abbreviations are as follows: DEU: Germany; AUT: Austria; ITA: Italy; UKD: United Kingdom; FRA: France; BLU: Belgium and Luxemburg; NLD: Netherlands; CEU: Central Europe; NEU: Northern Europe; MEU: Mediterranean and Southeastern Europe; NAM: North America; AUZ: Australia and New Zealand; ERA: Eurasian countries; ECA: Emerging economies-Asia; TUR: Turkey and Israel; CHN: China; IND: India; SEA: South-East Asia; LAM: Latin America; OIE: Oil exporting countries; AFR: Africa.

*This project has received funding from the European Union's Horizon 2020 research and innovation programme under the Grant Agreement No **776479.***

point is reached where other regions suffer much more than MEU and thus this region can improve again.

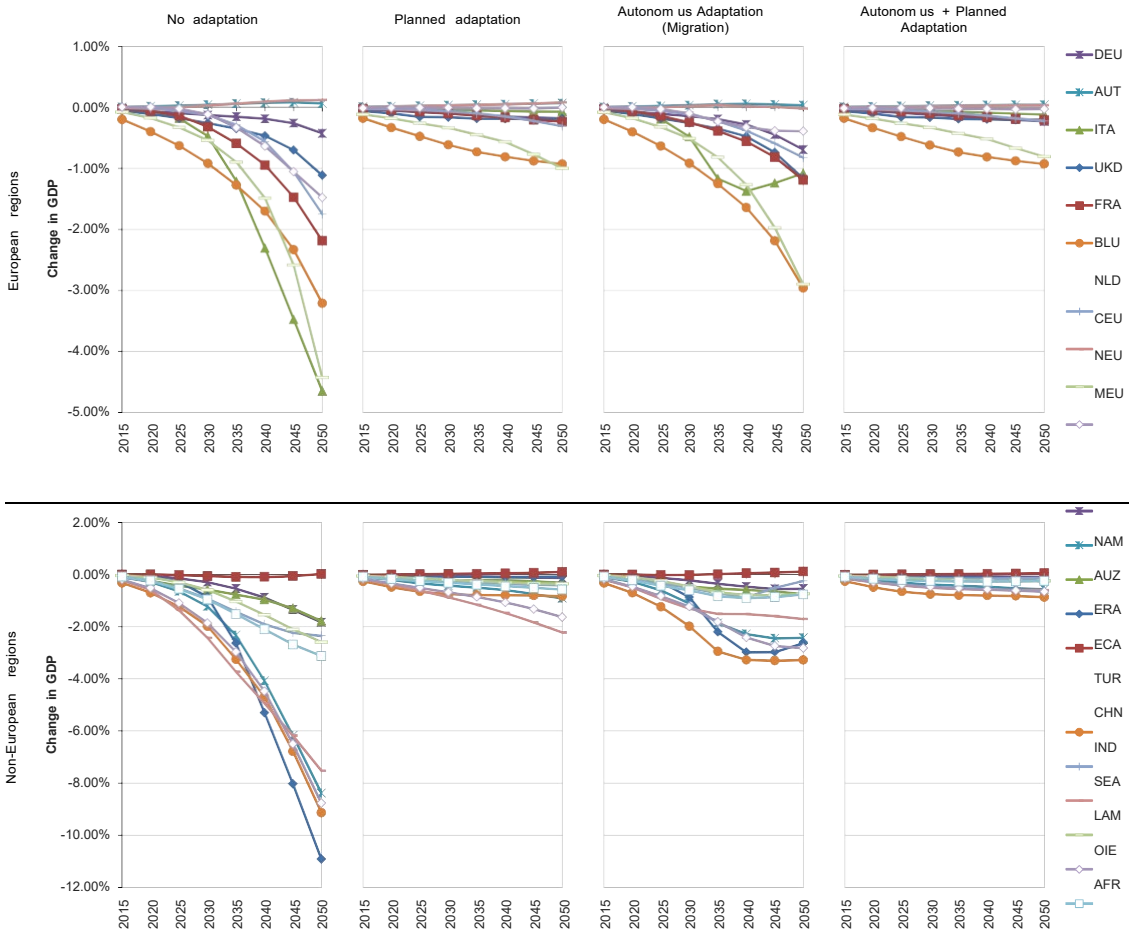

Figure 2.4.1: Change in real GDP relative to Baseline scenario (SSP5-RCP8.5) for high end ice melting. Top: European regions, bottom: regions of the rest of the world.

*This project has received funding from the European Union's Horizon 2020 research and innovation programme under the Grant Agreement No **776479.***

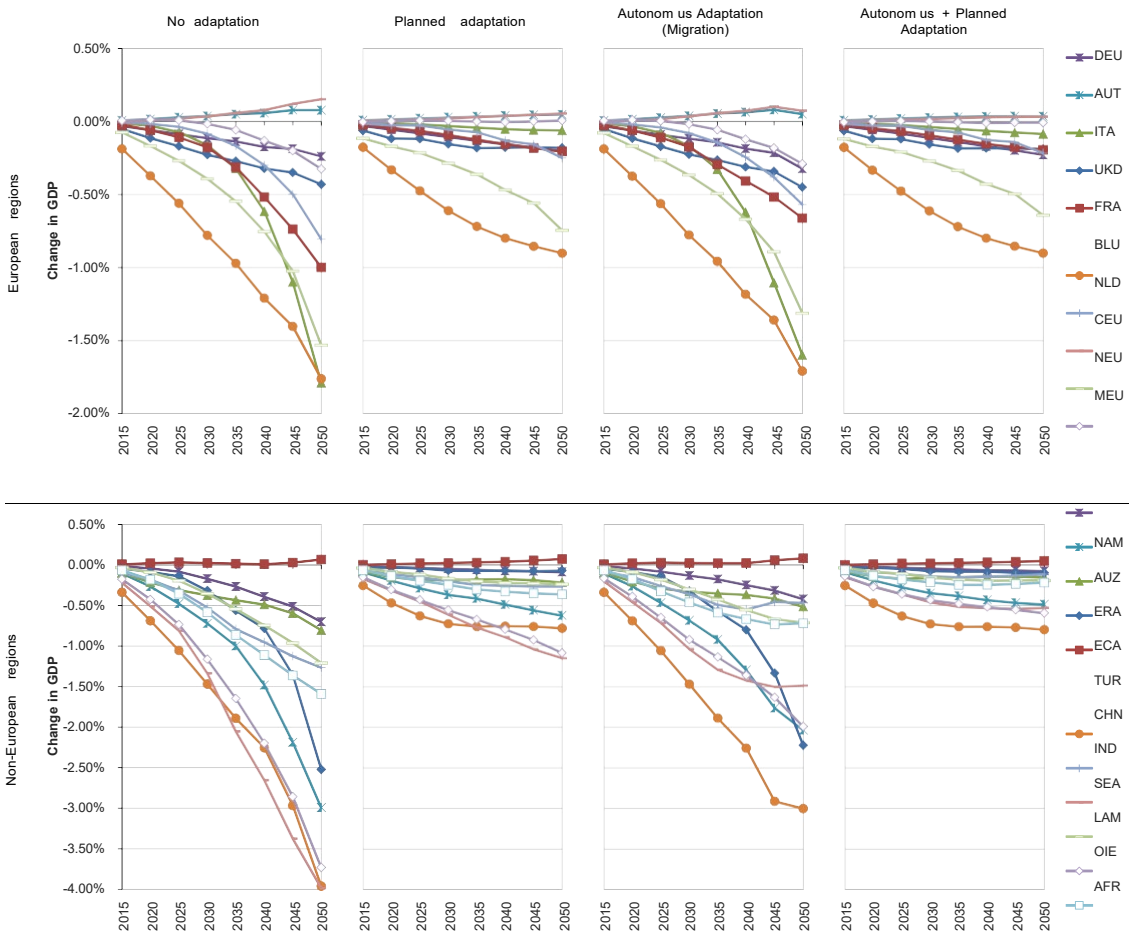

Figure 2.4.2: Change in real GDP relative to Baseline scenario (SSP5-RCP8.5) for medium ice melting. Top: European regions, bottom: regions of the rest of the world.

*This project has received funding from the European Union's Horizon 2020 research and innovation programme under the Grant Agreement No **776479.***

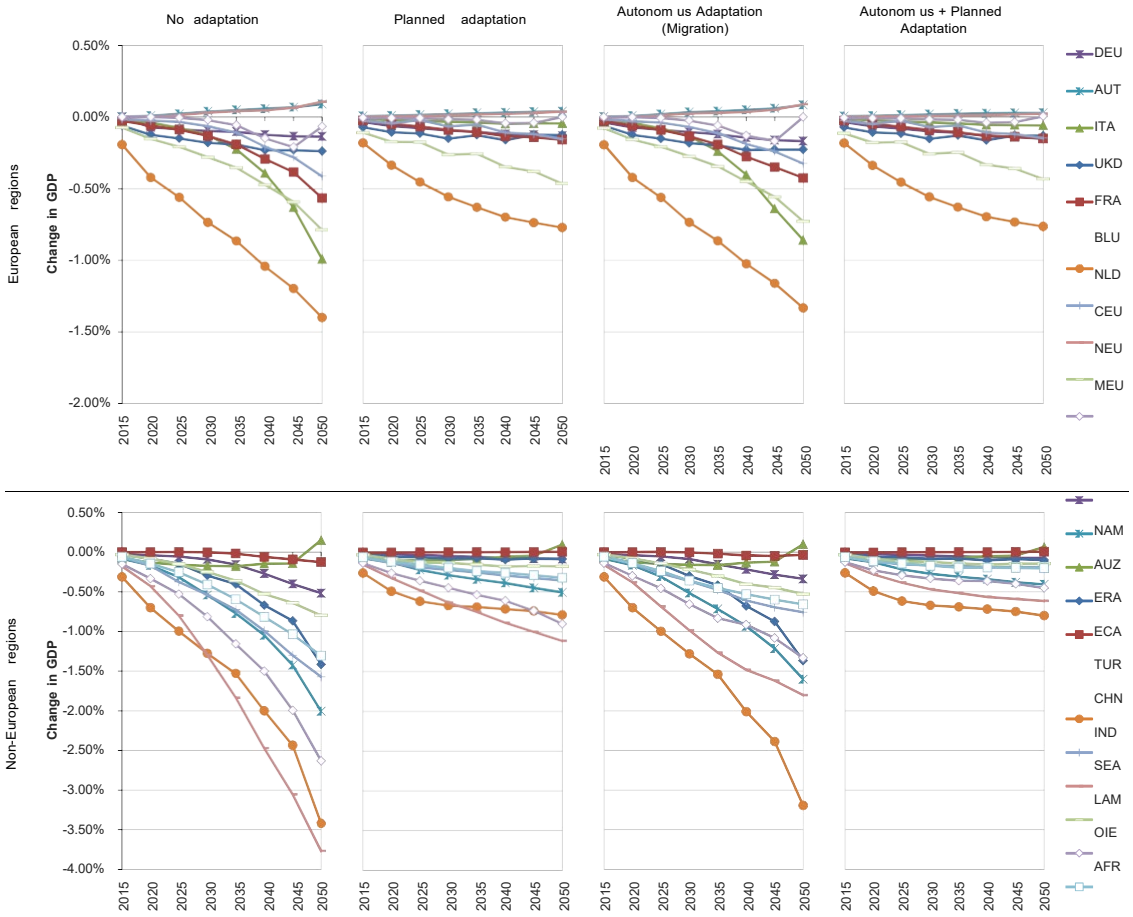

Figure 2.4.3: Change in real GDP relative to Baseline scenario (SSP2-RCP4.5) for medium ice melting. Top: European regions, bottom: regions of the rest of the world.

We now investigate closer the difference between planned and autonomous adaptation. Figure 2.4.4 shows the percentage point difference of GDP changes between the planned and the autonomous adaptation scenario (RCP8.5-SSP5, high end ice melting and medium ice melting). We see that the bars are mostly positive, which means that GDP losses with planned adaptation are smaller than with autonomous adaptation. Interestingly, for India (IND) and SEA this is not the case under high end icemelting. This might be explained by very high investment expenditures for planned adaptation which do not unfold as productive capital.[8]

[8] Note that we assume that this investment is only effective in the short term, i.e. it has a positive effect on GDP in the year of investing (at the cost of government consumption, though), but it does not build up the productive capital stock as sea dikes cannot be regarded as a production factor that earns a rent (as opposed to other capital such as machinery or buildings)

*This project has received funding from the European Union's Horizon 2020 research and innovation programme under the Grant Agreement No **776479.***

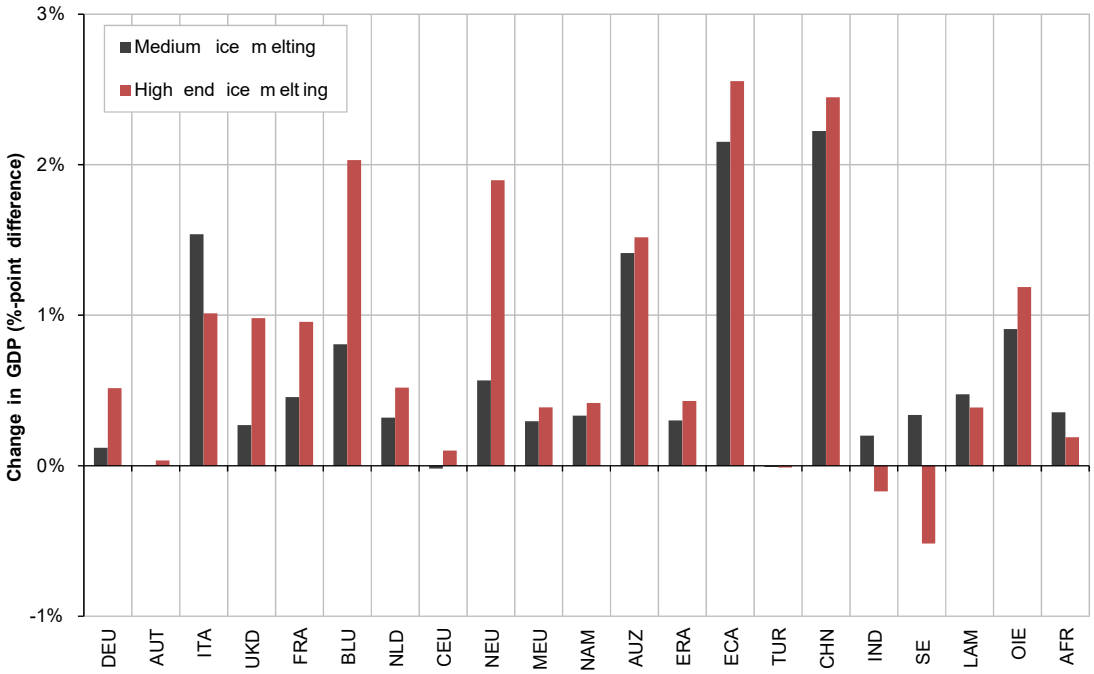

Figure 2.4.4: Percentage point difference of changes in real GDP (SSP5-RCP8.5) between planned and autonomous adaptation.

Finally, in Figure 2.4.5 we show sectoral effects under RCP8.5-SSP5 high end ice melting. We aggregate the total of 21 COIN-INT sectors to four macro-categories: Primary, Energy, Industry, Services (see Table 1 in the Appendix for details).

First, we can see that sectoral effects are in most cases stronger (to the negative) with autonomous adaptation, which is consistent with the GDP effects presented above.

We see that effects for the primary sector are negative in mostly all regions. This is due to sea level rise-induced agricultural land loss, combined with lower global demand due to lower general economic activity.

Looking at the energy sector we observe that in many regions sectoral activity increases. We explain this by substitution effects in production. As capital is getting more scarce due to sea level rise, capital rents (or "capital prices") are higher and thus, production sectors tend go for higher energy intensities instead of capital usage. This effect might be outweighed, though, by very strong economy-wide effects, such as for NEU or other strongly affected non-European regions (e.g. SEA).

For industry the regional effects are mostly negative. We can observe that in non-European regions the effects are more severe than in the European regions. In Europe we see also positive effects in Industry output for some regions, especially those which are amongst the least affected regions of sea level rise (or landlocked regions) and which can take advantage of their highly competitive industries; e.g. AUT, Netherlands (NLD) and to some extent CEU (including Switzerland), United Kingdom (UKD) and MEU.

For the Service sector we see negative or zero effects throughout all regions, which can be explained by lower demand for services since in general economic activity is lower due to lower economy-wide income.

*This project has received funding from the European Union's Horizon 2020 research and innovation programme under the Grant Agreement No **776479.***

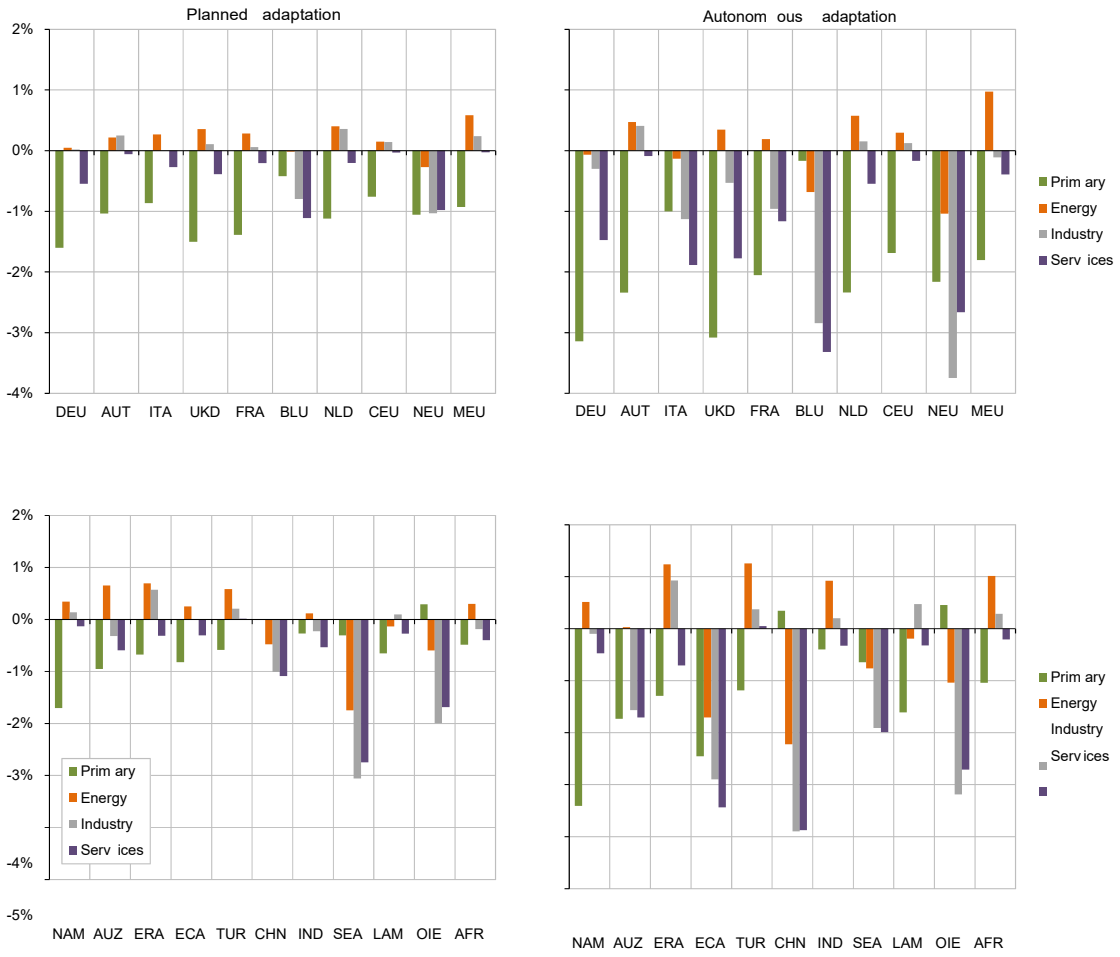

Figure 2.4.5: Change in sectoral activity relative to Baseline scenario (SSP5-RCP8.5) for high end ice melting. Left: BAU Adaptation (only planned adaptation by dikes), right: No further adaptation (no dike height increase), but autonomus adaptation by migration, top: European regions, bottom: regions of the rest of the world.

2.5. Adaptation to accelerating sea level rise in a coastal city

The global mean sea level (GMSL) is rising, and there is high confidence that this rise is accelerating (IPPC, 2019). In the SROCC report, the IPCC projects a GMSL rise of 0.29-0.59 m in RCP2.6 and 0.61-1.10 in RCP8.5, in 2100 compared to 1995 levels (likely range: 17-83% confidence interval). However, SLR could rise beyond the likely range and a GMSL rise of 2 m in 2100 is considered possible (IPCC, 2019).

Expert judgments of ice sheet and sea level rise experts (e.g. Bamber et al., 2019) reveals that higher levels of SLR may occur (Figure 2.5.1, Grinsted, 2020). A major source of uncertainty is the potential instability of the Antarctic ice sheet, which is recognized as a COACCH climate tipping point (Scoccimarro et al., 2020). Studies accounting for these instabilities find a GMSL rise of up to 1.24-2.46 m (likely range) corresponding to a 0.72-3.18 m (5-95% CI) for RCP8.5 (Le Bars et al., 2017). For decision makers with a low risk tolerance it is beneficial to consider SLR beyond the likely rise of the SROCC

*This project has received funding from the European Union's Horizon 2020 research and innovation programme under the Grant Agreement No **776479.***

report (IPCC, 2019). As having the risk of an SETP is highly

*This project has received funding from the European Union's Horizon 2020 research and innovation programme under the Grant Agreement No **776479.***

unappreciated, it is beneficial to explore if and under what circumstances a SETP could be triggered under SLR.

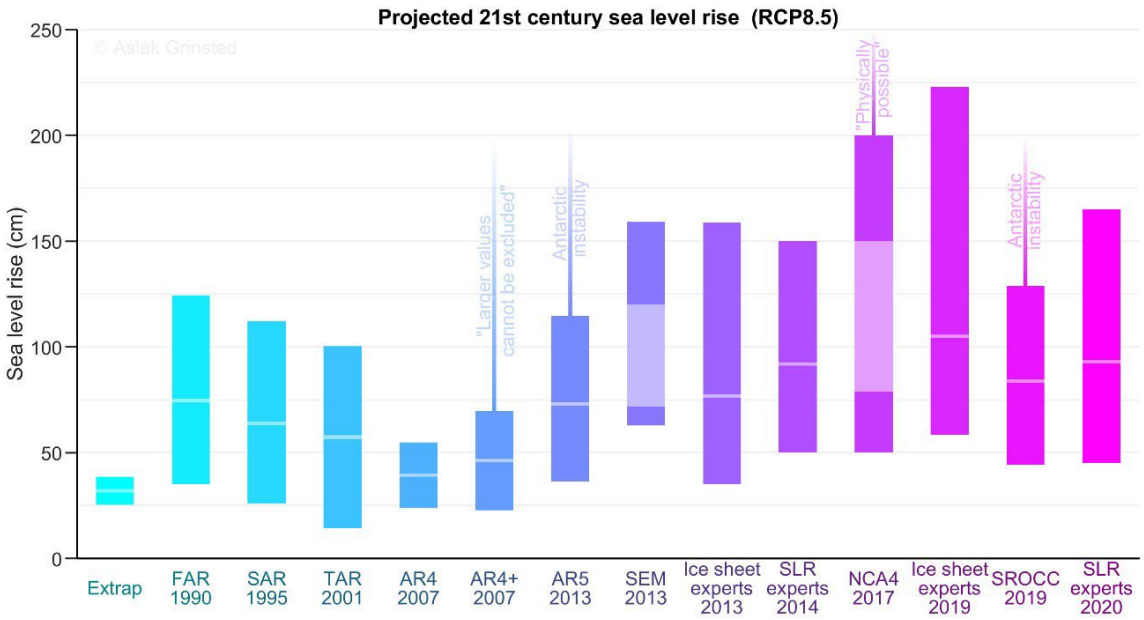

Figure 2.5.1: Estimated 21st century sea level rise under RCP 8.5 (Grinsted, 2020).

The previous section (2.4) assessed the implications of sea level rise for the European coastline from a macro-perspective. This chapter investigates on a more local level, the mechanisms that might lead to socio-economic tipping points on the urban scale. We investigate if, and through which mechanisms, a high-end sea level rise may lead to a socio-economic tipping point for European coastal cities. We develop a stylized model loosely based on the City of Rotterdam, to investigate the interaction between physical drivers and socio-economic mechanisms that may lead toa climate change induced socio-economic tipping point.

The objective of the study is to identify if these coupled dynamics may lead to socio-economic tipping points on the urban scale. In particular we investigate whether fast rates of sea level rise (beyond just investigating the magnitude of sea level rise), may trigger SETPs. Our model describes an archetypical coastal city with one outerdike residential area and one inner dike residential area protected by an engineered coastal defense. Both parts of the city are at risk of flooding from coastal storm surges. The flood risk increases over time due to sea level rise. The flood risk perception of the city residents is influenced by the objective flood risk but also by recent experiences of floods and near misses. These perceptions have an impact on the supply and demand of real estate in the residential areas. The government can anticipate on the development of the flood risk by upgrading the protection infrastructure.

To study the occurrence of SETPs in our study area, we explore the model outputs under the wide variety of input parameters. From the scientific field “decision making under deep uncertainty”, which focusses on (quantitative) policy support under uncertain future conditions, we use an approach called ‘scenario discovery’ (Bryant and Lempert, 2010). Scenario discovery is a vulnerability analysis tool, used to

*This project has received funding from the European Union’s Horizon 2020 research and innovation programme under the Grant Agreement No **776479.***

identify subspaces of the uncertainty space in which conditions of interest occur (Kwakkel and Haasnoot, 2019), in our case: the occurrence of SETPs. In other words: we are looking for the combination of model input parameters (sea level rise projections and other uncertainties) under which SETPs may occur.

2.5.1. Definition of tipping point

Three types of socio-economic tipping points can be distinguished: adaptation tipping points, socio-economic impact tipping points and socio-economic response tipping points (). The focus here is on the second and third type: socio-economic tipping points in terms of impact and response.

The SETP in terms of impact is defined as: the point where an indicator of the socio-economic structure rapidly alters, indicating an abrupt shift from one socio-economic state A to another, fundamentally different state B. The selected indicator is the price of real estate; a rapid drop of which indicates a shift from an attractive to a very unattractive real estate investment climate. The price of real estate is assumed to be strongly correlated to the risk perception of the residents, and their trust in the government to successfully protect the city against floods. Therefore, the SETP occurrence is derived from the trust metric; when the trust is below 50%, an SETP occurs.

The SETP in terms of response is defined as: the point where the flood protection strategy needs to be abruptly transformed from one policy A to another, fundamentally different policy B.

Table 2.5.1: Three types of tipping points, after Deliverable 3.2 (Scoccimaro et al., 2020)

Adaptation tipping point. This is the point where a certain flood protection measure, or a portfolio of actions, does no longer meet a formal or informal performance threshold (Kwadijk et al., 2010, Haasnoot et al. 2013). Adaptation tipping points may, but do not necessarily, coincide with SETPs. For example, if no incremental adaptation measures are available when flood protection fails, one may need to switch to a radically different adaptation strategy (such as managed retreat). This can be considered an SETP in terms of transformational response to climate change. However, in many cases, an adaptation tipping will not necessarily lead to a socio-economic tipping point, because incremental adaptation (without significant socio-economic impact) may still be possible. Adaptation tipping points qualify as SETPs when they correspond to an abrupt, non-linear reconfiguration of the socio-economic system (Van Ginkel et al., 2020a).
Socio-economic impact tipping point. For example, if flood protection fails and a large-scale flood disaster occurs, the Delta may not recover to the original state. In the direct aftermath of a disaster, many citizens will be displaced and not everybody will return after the event. This has happened to the city of New Orleans, which did not return to the original state after Hurricane Katrina (DeWaard et al., 2016). However, an impact SETP may also result from voluntary migration out of regions with high flood risk. This may happen well before an actual event strikes, for example because of increasing concerns about the state of the flood protection.
Socio-economic response tipping point. Whereas the cause of the previous 'impact' tipping point was unplanned and autonomous change beyond control of the government, it is also possible that a rapidly changing, transformational response is causing an SETP. An example is an accommodate strategy in which the government would enforce a managed retreat from regions with economic stagnation and population decline. Some characteristics of such a transformational response to worsening environmental conditions can be seen in Indonesia's capital Jakarta, where severe land subsidence and floods made the national government decide to relocate the capital.

*This project has received funding from the European Union's Horizon 2020 research and innovation programme under the Grant Agreement No **776479.***

2.5.2. Method: contributing factors and occurrence of tipping point

Overview of the model

In Figure 2.5.2 an overview of the physical model components is given. It shows a coastal city, threatened by storm surges from the sea which are aggravated by sea level rise. Residential area A is an outer-dike area with an elevation well above sea level. Residential area B is located in a polder below sea level, but is protected by a dike.

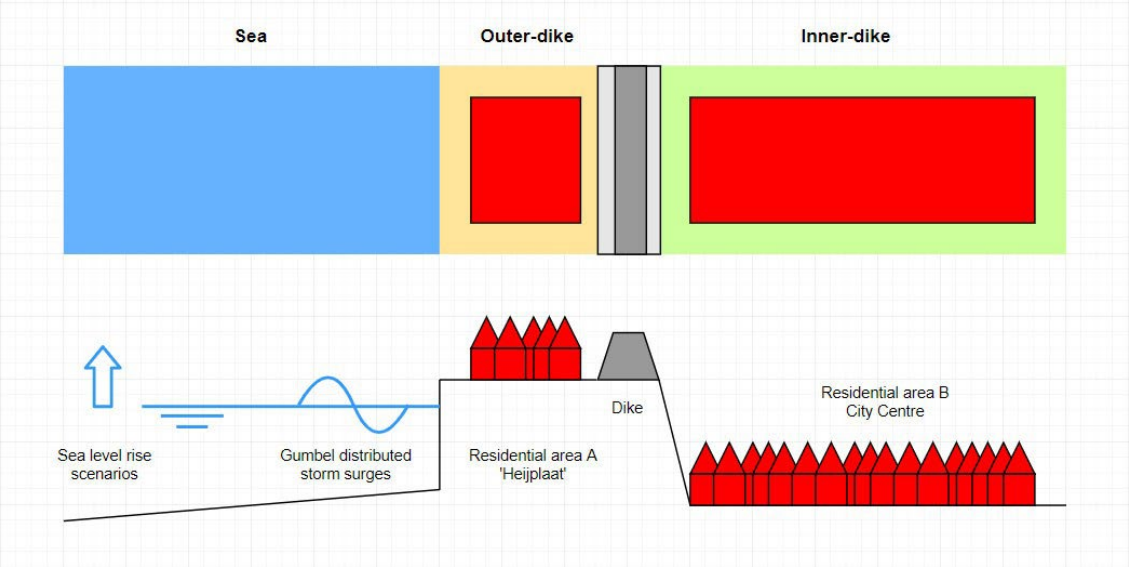

Figure 2.5.2: Schematic overview of the city, not to scale.

The model simulates the development of the flood risk over time in the residential areas of the city, for a large variety of sea level rise and storm surgescenarios. The objective is to identify potential socio-economic tipping points. Different management strategies can be chosen to adapt components of the city orthe flood protection over time. These management strategies are taken by 'mayors' with different perspectives on when to adapt to the changing conditions, and with different type of adaptation measures. The system performance is evaluated for 4 different mayors.

The model runs on a yearly timestep; the focus is on the most extreme water level occurring in each year. The simulation starts at present (2020) and continues for 100 years (2120). In each timestep, the following steps are taken (further detailed below):

- The degree of sea level rise is determined from the climate scenario, and the maximum storm surge level is drawn from the extreme value distribution;
- The water levels are compared to the flood protection levels, and when the dikes are overtopped the resulting flood depths are calculated. Failure due to fragility of the dikes is thus not considered here;
- A flood risk assessment for the sea level and storm conditions is carried out to calculate the annual expected damage for the climatic conditions

*This project has received funding from the European Union's Horizon 2020 research and innovation programme under the Grant Agreement No **776479.***

in the timestep (accounting for the SLR that already took place until that timestep);

- The recent experiences with floods (including near-misses) per residential area feed (together with some other factors outlined below) into the risk perception module, which calculates the development of the perceived or subjective flood risk as a function of the objective floodrisk;
- The risk perception (among other factors) causes a shift in the supply and demand for real estate, which is used to calculate a new equilibriumprice in the housing market. In this version of the model the price of realestate is assumed to be strongly correlated to the risk perception of the citizens. Accordingly, the SETP-occurrence is evaluated from the trust indicator rather than directly from the price of real estate. It is assumed that a collapse of trust corresponds to a collapse of the real estate market.
- The mayor of the city evaluates the above state parameters and decides on the implementation of new measures to manage the flood risk of the city.

A schematic overview of the model components is given in Figure 2.5.3.

*This project has received funding from the European Union's Horizon 2020 research and innovation programme under the Grant Agreement No **776479.***

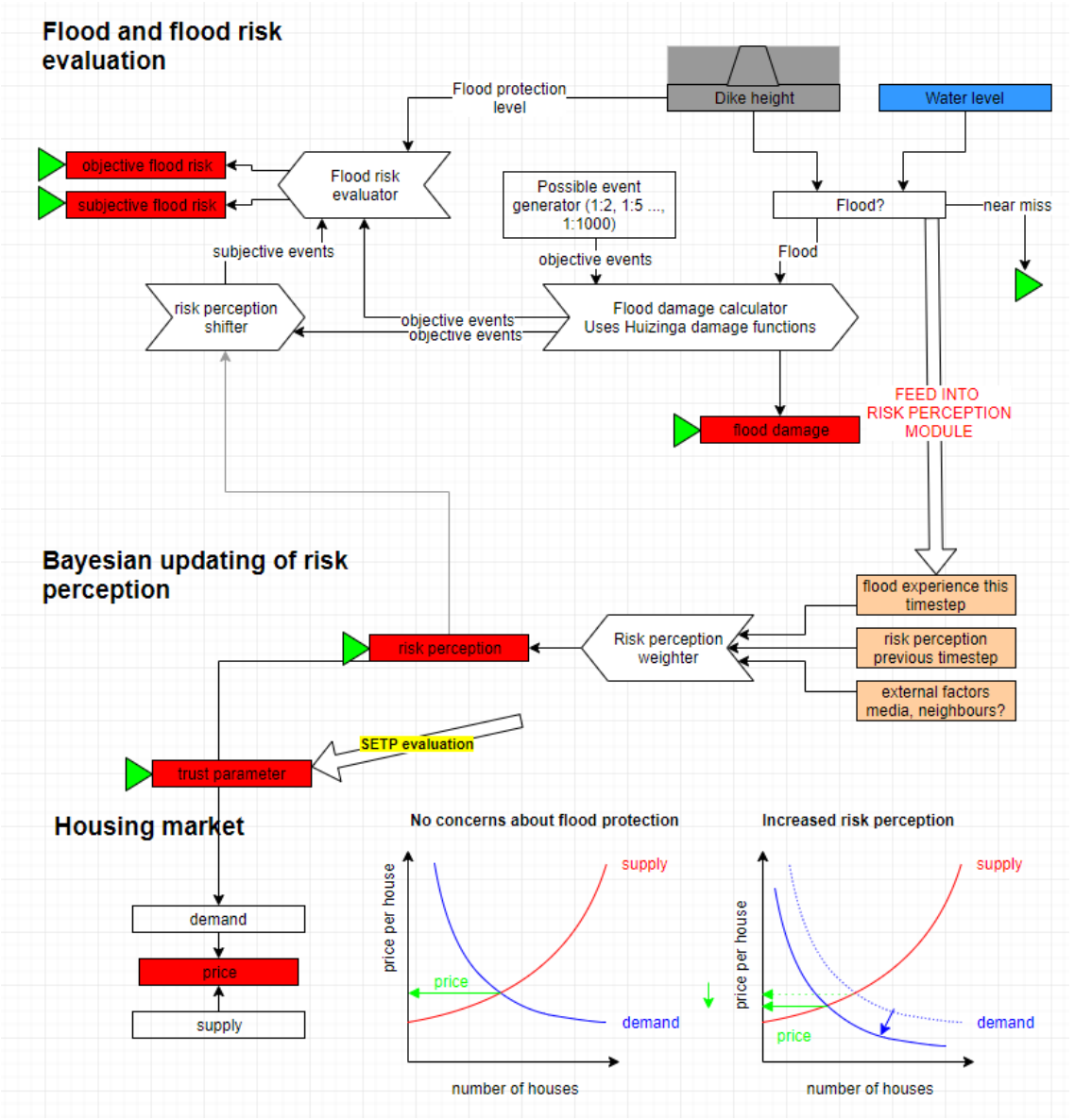

Figure 2.5.3: Schematic overview of model components

Sea level rise and storm surge levels

Water level simulations are assumed to be the sum of two independent components: sea level rise scenarios and storm surge levels. Two sets of sea level rise scenarios are considered: (1) global mean sea level rise scenarios from the SROCC report (IPCC, 2019), without Antarctic ice sheet instability, and (2) extreme globalmean sea level rise scenarios including Antarctic ice sheet instability from Le Bars et al. (2017). Storm surge levels are taken for each model experiment from a Gumbel extreme value distribution. The Gumbel distribution represents annual-maximum water levels at Hoek van Holland (Port of Rotterdam, The Netherlands) based on 118 observations from 1888-2005 (Sterl et al., 2009). We assume these annual storm surge extremes to be independent from the degree of sea level rise.

*This project has received funding from the European Union's Horizon 2020 research and innovation programme under the Grant Agreement No **776479.***

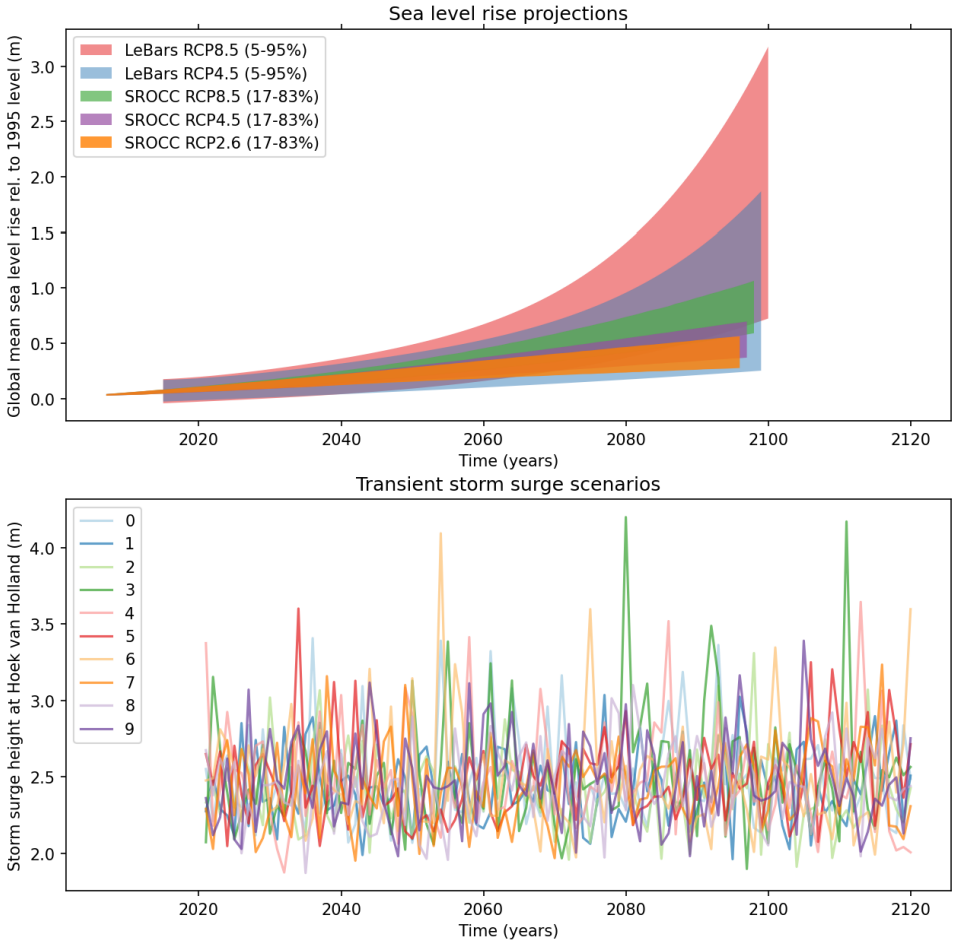

Figure 2.5.4: Global mean sea level rise projections and the 10 transient storm surge scenarios used in the model

*This project has received funding from the European Union's Horizon 2020 research and innovation programme under the Grant Agreement No **776479.***

Residential areas

The model contains two residential areas: one outer-dike and one inner-dike area. The innerdike area is protected by a dike.

The characteristics of the outer-dike area are loosely based on the Heijplaat neighbourhood of Rotterdam. We assume a residential area of 40 ha (ha = 104 m2), of which 5 ha is covered with houses. The 1500 residents live in 750 houses costing € 300,000 (2020-euros) per house. The area is elevated 3.0 m above mean sea level in 2020.

The characteristics of the inner-dike area are loosely based on the embanked (but flood-prone) neighbourhoods of Rotterdam. This is referred to as the city centre, with 500,000 inhabitants living in 250,000 houses. The price of a house is € 350,000. The elevation of the city centre is -1 m.

Flood protection

The flood protection consists of a system of dikes protecting the inner dikearea. Flood protection objects can be updated with a certain lead-time. A minor dike heightening of 0.5 m takes 7 year to implement. A major dike heightening of 1 m takes 12 year to implement. When a minor dike heightening is still being implemented, the implementation of the mayor dike heightening is finished 5 years faster.

Inundation and flood damage

Floods occur when the storm surge level (sum of sea level of the sea level rise scenario and the storm surge height from the Gumbel distribution) exceeds the level of the flood protection. In these overtopping cases, we assume a bath-tub inundationwith a depth of: storm surge level – residential area level. The associated flood damageis calculated using the Huizinga et al. (2017) land-use based damage function forresidential areas, which has a maximum damage of 168 €/m2 (2010 price level) upon an inundation of 6 m.

Objective flood risk and expected annual damage

In each time step, the model calculates the objective flood risk for the sea level and storm surge conditions in that moment of time. This also accounts for the SLR that took place until the time step for which the flood risk calculation is done, but does not anticipate any future SLR. The flood risk is calculated by trapezoidal integration of the damage per return period while accounting for the flood protection in place (figure 2.5.3). This gives the expected annual damage in €/year per residential area.

Risk perception

The risk perception per household may differ from the objective flood risk, depending on (the absence of) recent flood experiences and other factors such as the public opinion and media. At maximum, the subjective probability weighting of a possible event may differ a factor 10 from the objective probability of an event (Botzen et al., 2009). This is represented by assigning a subjective probability π to the damages corresponding to the event with objective probability p, as follows (Haer et al., 2017):

*This project has received funding from the European Union's Horizon 2020 research and innovation programme under the Grant Agreement No **776479.***

$$\pi_i = \frac{(10^{2RP_t-1}p_i)^{\delta}}{((10^{2RP_t-1}p_i + (1-(10^{2RP_t-1}p^{i}))^{\delta})^{1/\delta}}$$

The variable δ is used to represent a heterogeneous population. For now, we assume a homogeneous population per residential area (δ = 1), so that the equation reduces to:

$$\pi_{\mathrm{i}} = 10^{2\mathrm{RP_t}\text{-}1}p_{\mathrm{i}}$$

In the above equation, the risk perception RPt can fluctuate between 0 and 1, with RP = 0.5 indicating that the risk perception equals the objective flood risk. The RPt updated in each time step by Bayesian weighing, as follows (Haer et al., 2017):

$$RP_t = \frac{aRP_{t-1} + bI_{experience} + cI_{social} + dI_{media}}{a+b+c+d}$$

In this equation, a, b, c, d represent the weighting factors of the risk components RP_{t}, $I_{\mathrm{experience}}$, I_{social}, I_{media}. The values of the risk components area always vary between 0 and 1, as follows:

$RP_{\mathrm{t\text{-}1}}$ the risk perception in the previous timestep.

$I_{\mathrm{experience}}$ the flood or near miss experience in the current timestep
in case of a flood: linear interpolation between no flood $I_{\mathrm{exp,d=0\ m}}$ = 0 and the maximum experience $I_{\mathrm{exp,d=1\ m}}$ = 1 on the basis of flood depth d.
in case of a near-miss: linear interpolation between no impact $I_{\mathrm{exp,ll=0.5\ m}}$ = 0 and the maximum experience $I_{\mathrm{exp,ll=0\ m}}$ = 1 on the basis of the height difference Δ between the flood protection level and the storm surge level.

I_{social} impact on the risk perception from social interactions such as the flood experience in a neighbouring residential area:
in Heijplaat: I_{social} = 0;
in the City Centre: $I_{\mathrm{social}} = I_{\mathrm{experience,Heijplaat}}$.

I_{media} impact on risk perception from external factors such as the media and scientific communication about the risk.

The value of weighting factors a, b, c, d depend on flood experience in themodel timestep, see Table 2.5.1. They should be interpreted as follows (Haer et al. 2017): in 'no flood' conditions, the risk perception is mainly determined by the historic experiences. As a result, the risk perception will steadily decrease to low equilibrium conditions as long as the 'no flood' conditions persist. In case of a near-miss in the Heijplaat, the local residents are not very much concerned. Since this is an outerdike area, the inhabitants are used to having the flood waters close to their houses.

*This project has received funding from the European Union's Horizon 2020 research and innovation programme under the Grant Agreement No **776479.***

Moreover, they have some flood proofing in their housing, which mitigates the damage if the water would flood their residential area. In the city centre, the situation is different: a near miss has a strong effect on the risk perception. High water nearly overtopping the dike will create awareness that the polder nearly had flooded, and that such an event could have had catastrophic consequences. Similar dynamics were observed in Dutch polders following near misses in 1993 and 1995. In case of a flood, the historic risk perception (factor a) only has a small influence on the new risk perception, because the historic experiences are overruled by the impact of the new experience, which weighs heavily (factor b). This creates a period of strongly elevated risk perception after an event, which may create a policy window for implementing drastic flood protection measures ('never waste a good crisis'). Over time, this effect will decay towards the equilibrium conditions. These equilibrium conditions strongly depend on social interactions between residents, and how residents weigh the information from science and media. The factor c indicates that the risk perception in the Heijplaat may spill-over to the risk perception in the city centre due to social interaction. This is not yet implemented in the current version of the model.

Table 2.5.2: Bayesian weighting factors to calculate risk perception (freely after Haer et al., 2017)

		Heijplaat			City Centre		
		No flood	Near miss	Flood	No flood	Near miss	Flood
a	Previous experience	1	1	0.1	1	0.1	0.1
b	Current experience	0.04	0.04	1	0.04	0.5	1
c	Social interaction	0	0	0	0.04	0.2	0.1
d	Science and media	0	0	0	0	0	0

For each time step, the subjective flood risk is calculated by trapezoidal integration of the damage per return period. This resembles the calculation of the objective flood risk, but now using the subjective probability πi rather than the objective probability pi. Figure 2.5.5 gives a computational example of the conversion from objective to subjective flood risk, for the situation where the risk perception doubles the actual risk of the flood events, i.e. πi = 2 pi. Botzen et al. (2009) find that Dutch citizens have a realistic perception of the damage that may occur during a flood event, but that their perception of the likelihood of these events may strongly deviate from the actual likelihood. Accordingly, the damage per event is kept constant, but the likelihood of the events is shifted representing the subjective probability weighing.

*This project has received funding from the European Union's Horizon 2020 research and innovation programme under the Grant Agreement No **776479.***

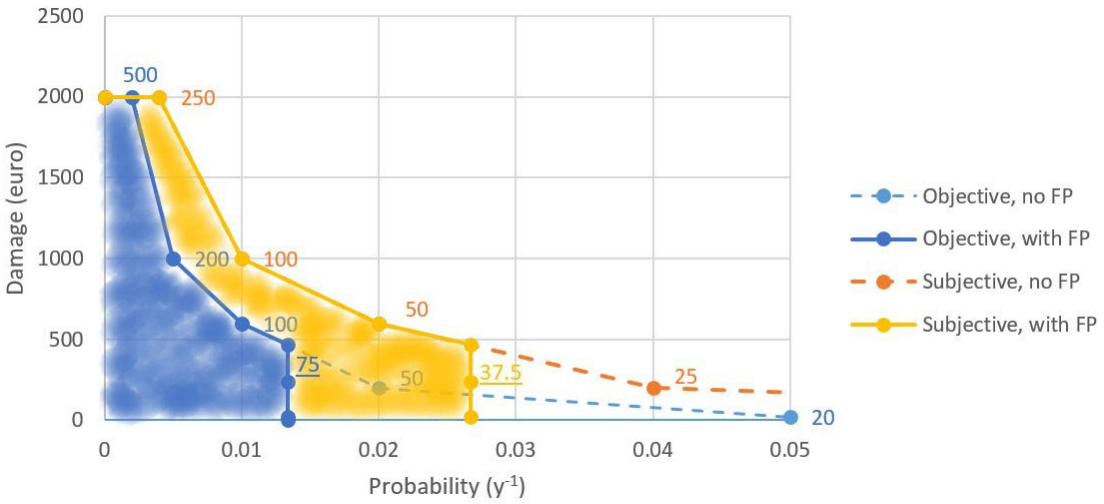

Figure 2.5.5: Calculation of the objective (blue) and subjective (yellow) flood risk, in case that the likelihood of flood events is overestimated by a factor 2. The areas under the curves represent the expected anual damage (euro/year). The area is calculated using trapezoidal integration up till the flood protection level. Labels to points in the figure indicate the return periods of the (perceived) events. Underlined labels indicate the flood protection level.

Management strategies

The government can intervene in the system by updating the flood protection or by changing the residential area. These interventions can be implemented according to different management strategies. These strategies prescribe when measures need to be implemented, depending on threshold conditions in monitoring variables such as occurrences of flood events, protection level of flood protection objects in terms of return periods, objective flood risk, or subjective flood risk.

Management strategies are represented by mayors in the model. The following archetypical management strategies were implemented (Table 2.5.3).

Table 2.5.3: Archetypical management strategies represented by different mayors

Mayor name	Mr. Re Active	Ms. H. Economicus	Mr. P. Sentiment	Ms. A.L.L Lawkeeper
Summary	Reactive management strategy. Only takes action upon the occurrence of near misses or actual flood events.	Management strategy on the basis of the objective flood risk. Takes action when the flood risk is above a threshold (which might e.g. follow from CBA).	As Mr. Economicus, but on the basis of the perceived flood risk rather than actual flood risk.	Strategy that strictly follows the flood risk standards. When dikes fail to meet formal risk criteria, they are upgraded.
Strategy	Minor dike heightening (0.5 m) if a near-miss happened Major dike heightening (1 m) if a flood happened	Minor dike heightening (0.5 m) if the objective flood risk exceeds 5 million euro/year Major dike heightening (1 m) if the objective flood risk exceeds 10 million euro/year	As economicus, but thresholds for perceived rather than objective flood risk	Minor dike heightening (0.5 m) if the return period (RP) of the flood protection level is below 10,000 year Major dike heightening (1 m) if RP < 2,000 year

*This project has received funding from the European Union's Horizon 2020 research and innovation programme under the Grant Agreement No **776479.***

2.5.3. Results

The results will be presented as follows. First, we will examine some illustrative model runs to show the impact of sea level rise and management strategy in detail. Note that the results of this model run are very sensitive to the random realisation of the storm surge series, which in this case is the transient storm surge scenario 1(Figure 2.5.4). To enable mutual comparison between the mayors, this transient storm surge scenario is used for all mayors. Second, we present the results of the vulnerability analysis, with the results for all 10 transient storm surge scenarios.

Results part 1: occurrence of SETPs under different management strategies

In Figure 2.5.6-Figure 2.5.9 the behaviour of the model under 4 sea level rise scenarios, the transient storm surge series 1, and the 4 mayors of Table 2.5.3 is illustrated[9].

Outerdike Area A

The outerdike area A is not protected by a dike system, but only by its elevation above sea level. Since no dike heightening measures are taken, the behaviour of the model is similar irrespective of the mayor. In 2020, the elevation protects against a 1:100 year flood, but as can be seen in panel 3A, the protection level rapidly declines.In the worst-case scenario (orange), the remaining protection level in 2065 is only 1:10 years. Floods start to occur on a regular basis from 2070, leading to a very rapid increase of risk perception. Within a decade, the frequently occurring floods have ledto a rapid decline of trust. A socio-economic impact tipping point occurred. In the blue and green scenario, the system dynamics are more or less similar, but the SETPs occur later, in 2080 (blue) and 2090 (green). In the red scenario, no SETP occurs in the 21st century.

Innerdike Area B

The innerdike area B is protected by dike system, which can be upgraded by the Mayor. Figure 2.5.6-Figure 2.5.9 show that the behaviour of the mayor is decisive for the dynamics in this area.

Under mayor 'Re Active' (Figure 2.5.6) and a worst-case scenario (orange), the first near-miss takes place in 2082, after which a small dike heightening is implemented. In 2088, before the implementation of the measure is finished, disaster strikes and the area floods, at which it is decided to implement a large dike heightening rather than a small one. At this point, the flood protection level has

[9] For interpretation of these figures, be aware of the following interpretation of the sea level rise scenarios (compare with figure 2.5.x):

- LeBars_2017_RCP45_05 (red) is just below the SROCC_RCP2.6_CI17, which corresponds to the lower bound of the complete uncertainty space. Corresponding to a GMSLR of only 26 cm by 2100, this is the most optimistic case.
- LeBars_2017_RCP45_med (green) corresponds roughly with SROCC_RCP_85_CI83, which is the upper bound of RCP8.5 without Antarctic ice sheet instability.
- LeBars_2017_RCP85_med (blue) represents the median of RCP8.5 with Antarctic ice sheet instability
- LeBars_2017_RCP85_95 (orange) represents the upper bound of RCP8.5 with Antarctic ice sheet instability. This corresponds to the upper bound of the complete uncertainty space, the worst case.

*This project has received funding from the European Union's Horizon 2020 research and innovation programme under the Grant Agreement No **776479.***

lowered to an extremely low value, below 1:10 year. When the large measure is implemented, the flood protection recovers to above 1:100 but continues to show a very rapid decline. In the blue scenario, the dynamics are similar, but occur later. In thegreen and red scenario, no SETPs occur in the displayed realisation of the storm surge levels. However, since the flood protection levels in the green scenario also have rapidly declined, it is not unthinkable that a flood occurs in other realisations of the extreme value distribution.

Under mayor Economicus (Figure 2.5.7), action is taken much earlier. In the worst-case scenario (orange) by 2063, the flood risk has risen so high that a small dike heightening is planned, and before this dike heightening is implemented it is decided to change it into a major dike heightening. This causes the flood protection level to recover to above 1:10,000 years before the year 2080. However, by the end of the century the rate sea level rise is so high that also the strategy of mayor Economicus fails. The next major dike heightening is not finished in time, and disaster strikes a couple of times in a row. This can be seen as an SETP in terms of impact. Another interesting phenomenon is that the near-miss events before the actual floods have caused a strong increase in risk perception prior to the disaster. However, this does not necessarily mean that taking action on the basis of risk perception (rather than actual risk) is more effective, as we will see for the next mayor.

Under mayor Sentiment (Figure 2.5.8), action is taken on the basis of similar risk thresholds as for mayor Economicus, but now applied to the perceived rather than the actual risk. Until 2075 (orange scenario), the risk perception is significantly lower than the actual risk, because of the absence of near-misses or actual events. This causes mayor Sentiment to take much later action than mayor Economicus. As a result,more flood disasters strike the city centre; and SETPs occur. Also, the SETPs do notonly occur in the orange scenario, but also in the blue scenario, just before the end of the century. An interesting finding is that Sentiment takes later action thanEconomicus, but when the first action has been taken, Sentiment earlier decides to take follow up action as well, because the elevated risk perception will persist for sometime.

Under mayor Lawkeeper (Figure 2.5.9), a small dike heightening is implemented when the flood protections fails to protect against the 1:10,000 year event, and a large dike heightening is implemented when the flood protection fails to protect against the 1:1000 year event. This strategy has best resemblance with the current Dutch flood protection strategy. The figure shows that in the first time step of the model, it is directly decided to upgrade the flood protection in 3 of the 4 sea level scenarios. Consequently, in the first half of the 21th century the flood protection levelsare well above the formal standards. If the protection level starts to fail the formal requirements, the protection level is dropping below the requirement for the time it takes to implement the measure. This causes the sawtooth shape of the flood protection standards. In the second half of the 21th century, the rate of sea level risein the orange scenario becomes so high that small dike heightening does no longer suffice to keep up with the sea level rise.

*This project has received funding from the European Union's Horizon 2020 research and innovation programme under the Grant Agreement No **776479.***

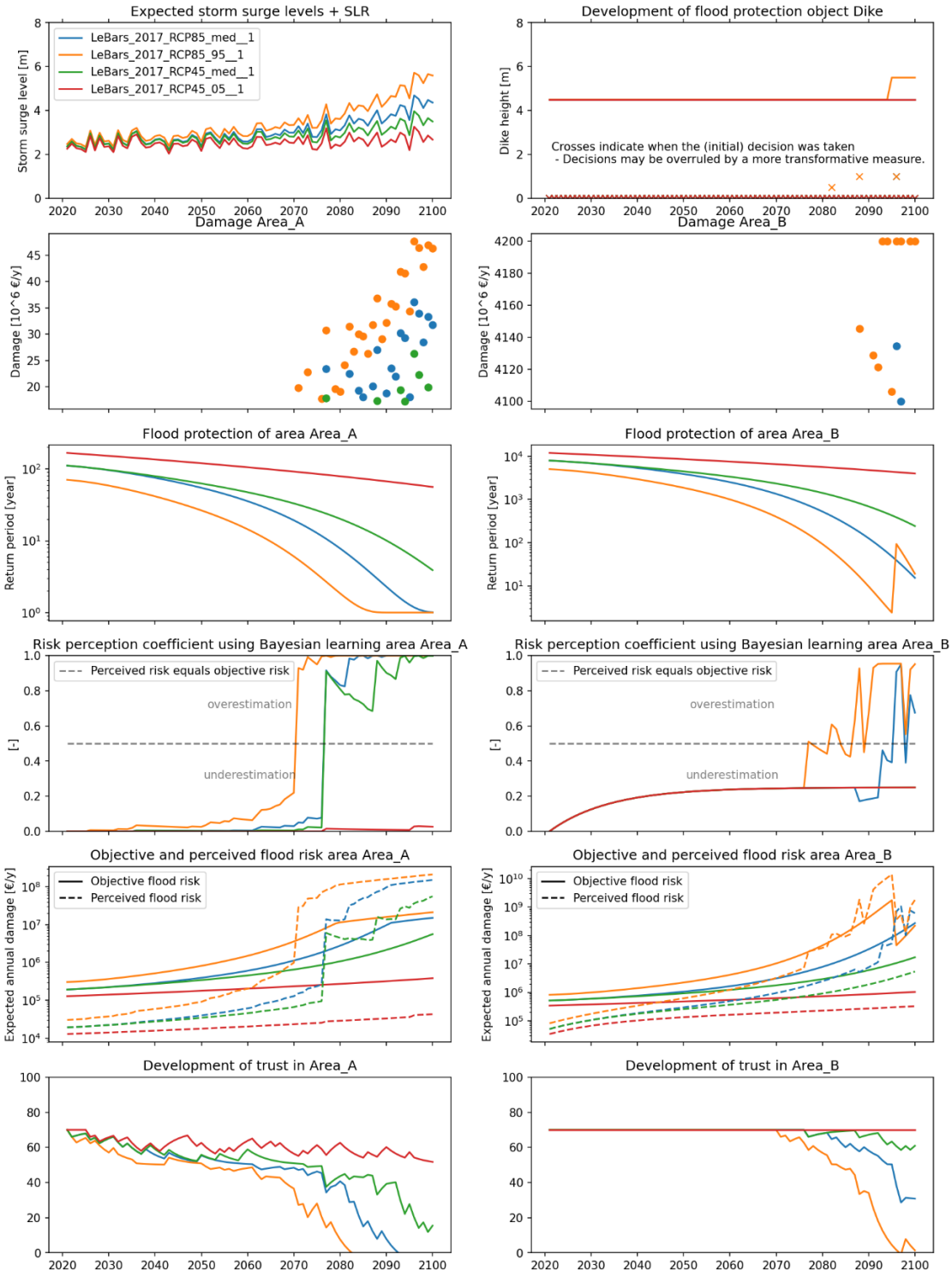

Figure 2.5.6: Model behaviour under mayor 'R. Active', 4 SLR scenarios and transient scenario #1

*This project has received funding from the European Union's Horizon 2020 research and innovation programme under the Grant Agreement No **776479.***

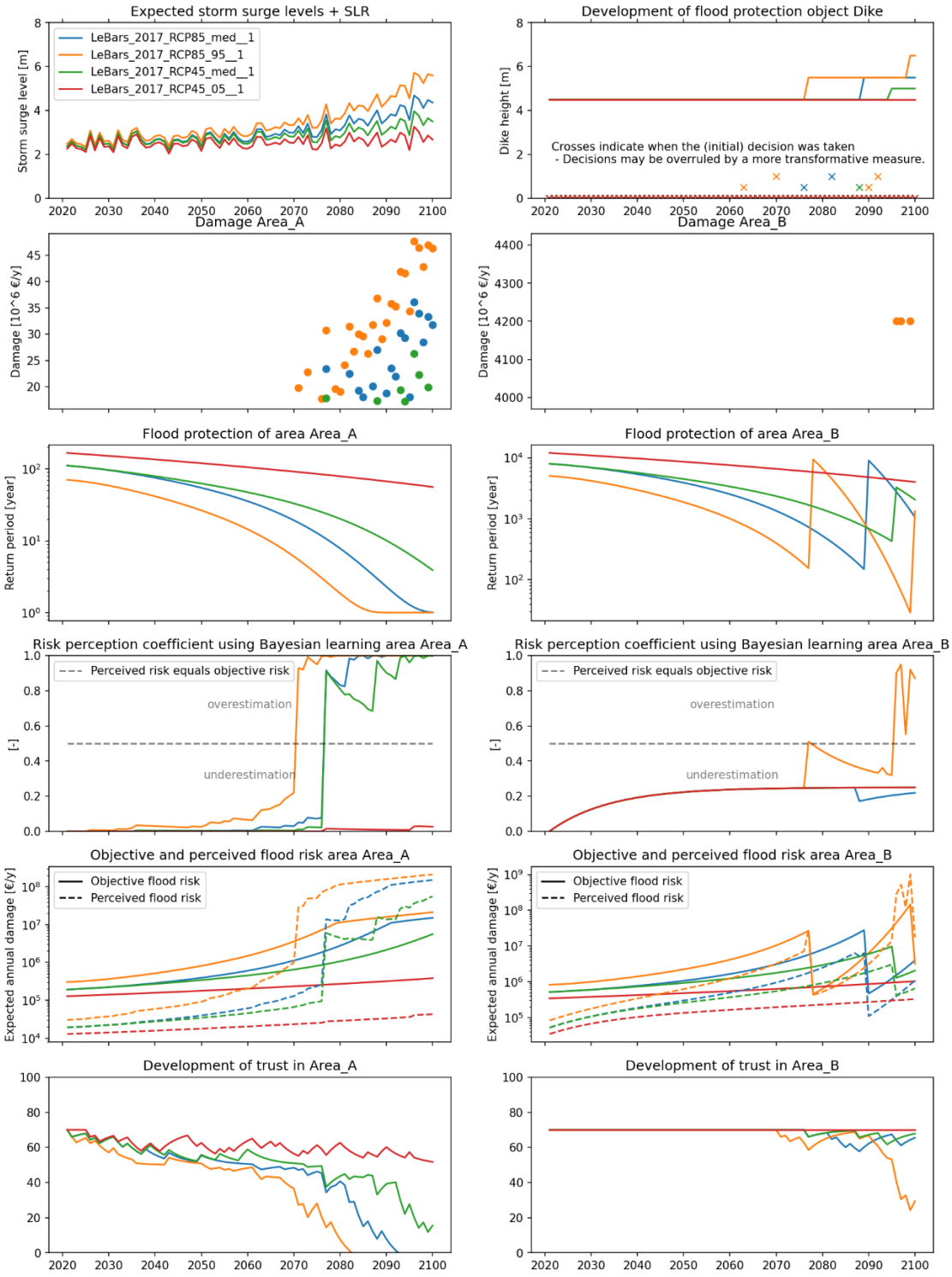

Figure 2.5.7: Model behaviour under mayor 'H. Economicus', 4 SLR scenarios and transient scenario #1

*This project has received funding from the European Union's Horizon 2020 research and innovation programme under the Grant Agreement No **776479.***

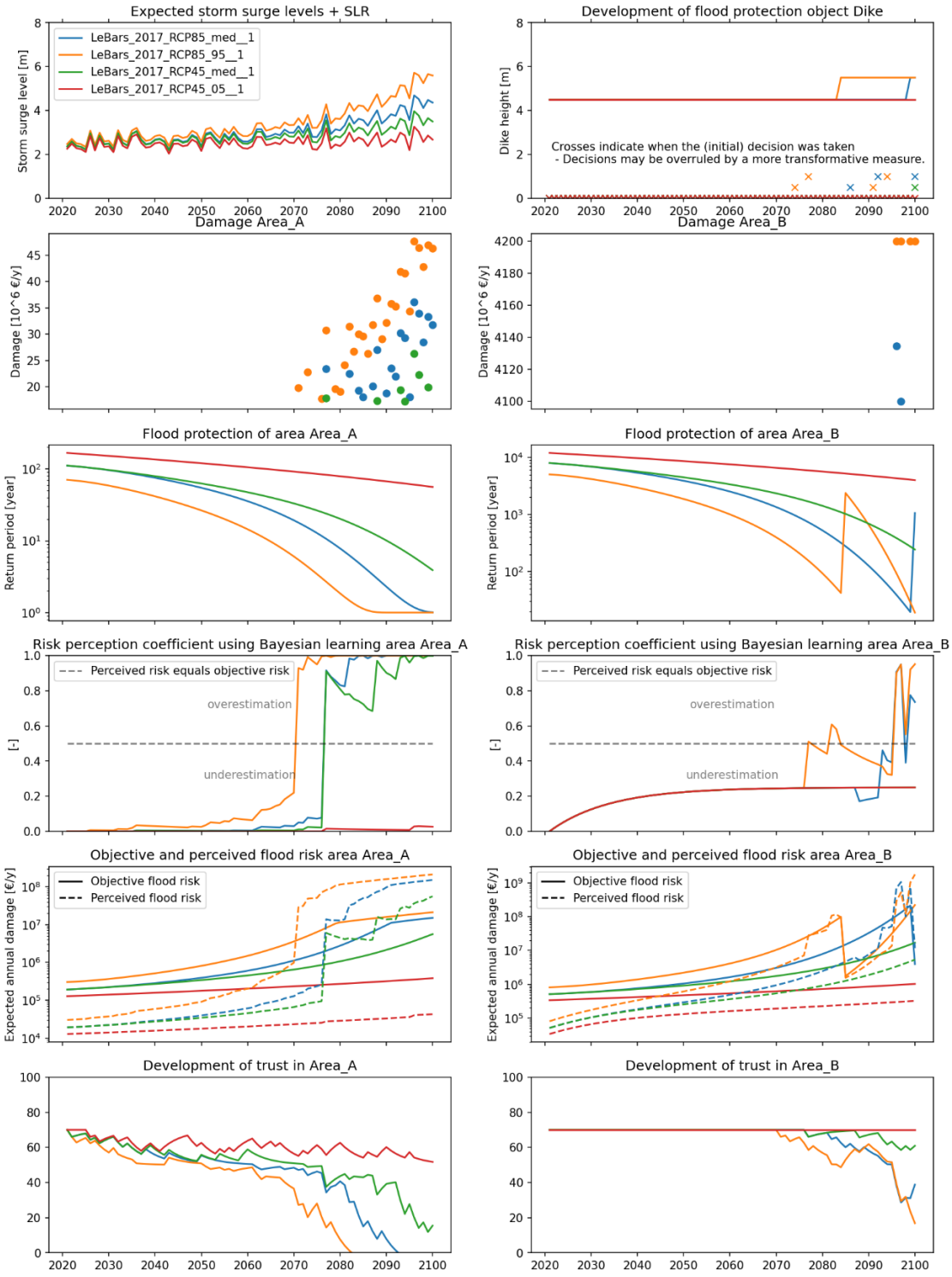

Figure 2.5.8: Model behaviour under mayor 'Sentiment', 4 SLR scenarios and transient scenario #1

*This project has received funding from the European Union's Horizon 2020 research and innovation programme under the Grant Agreement No **776479.***

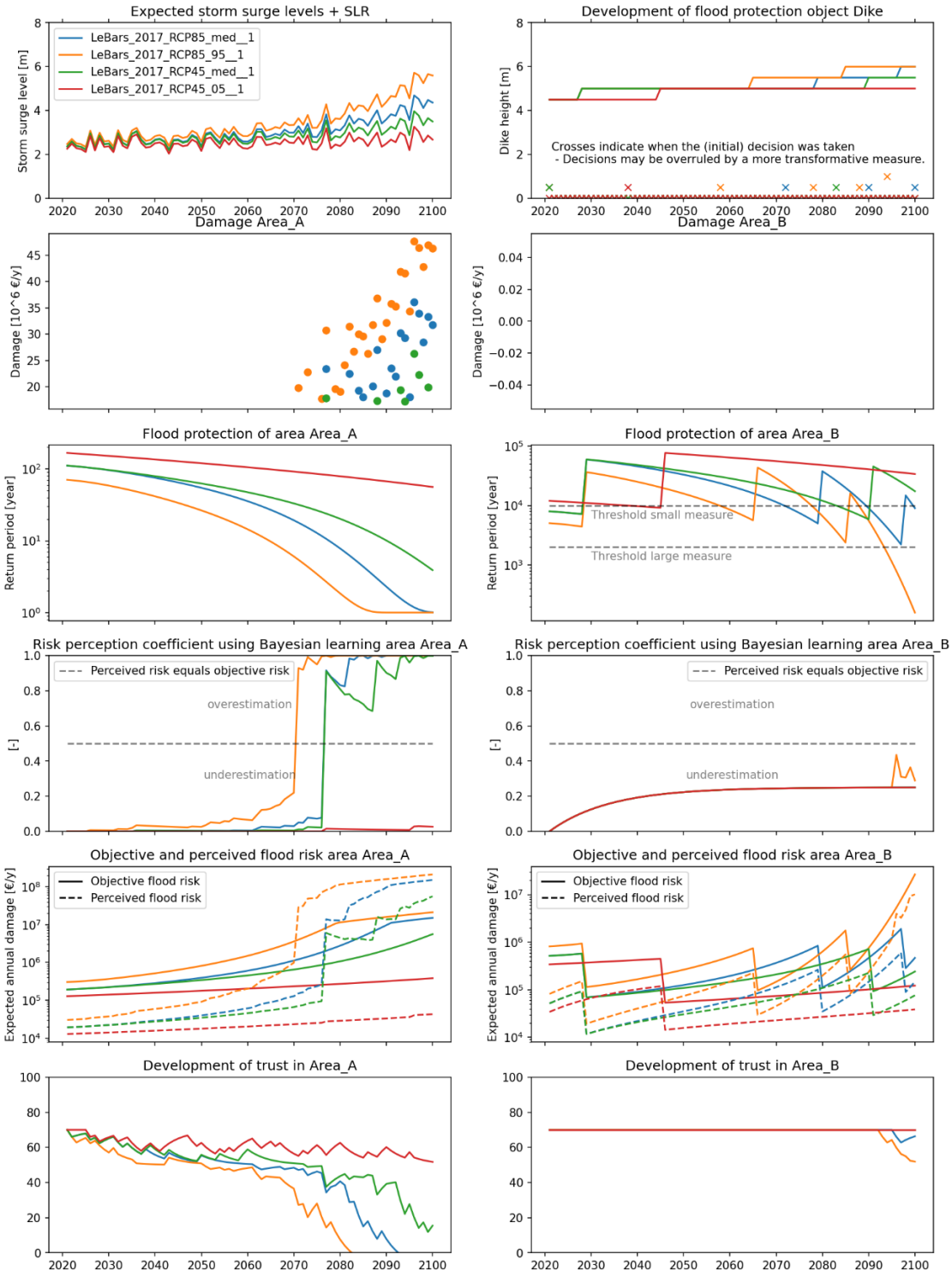

Figure 2.5.9: Model behaviour under mayor 'Lawkeeper', 4 SLR scenarios and transient scenario #1

*This project has received funding from the European Union's Horizon 2020 research and innovation programme under the Grant Agreement No **776479.***

Results part 2: exploratory modelling of many possible futures

In the previous section, we investigated the model behaviour in detail for 4 sea level rise scenarios, 1 transient scenario representing a realisation of the storm surge extreme value distribution and the 4 different mayors. In this section, we will more thoroughly investigate the entire uncertainty space, spanned by the following dimensions:

- Sea level rise scenarios:
    - SROCC (no instability of the West-Antarctic icesheet):
        - RCP2.6 (17% CI, 50% CI, 83% CI)
        - RCP4.5 (idem)
        - RCP8.5 (idem)
    - LeBars (instability of the West-Antarctic icesheet):
        - RCP4.5 (5% CI, 50% CI, 95% CI)
        - RCP8.5 (idem)
- 10 realisations of the Gumbel extreme value distribution describing the storm surge heights
- The 4 different mayors

To assess the model performance, we evaluate the following metrics, which quantitatively indicate when SETPs occur:

- For residential area A: the year when the trust goes below 50% (corresponding to a collapse of the real estate market)
- For residential area B: the year when the trust goes below 50% (corresponding to a collapse of the real estate market)

For a schematic overview of the exploratory modelling experiment, see Figure 2.5.10.

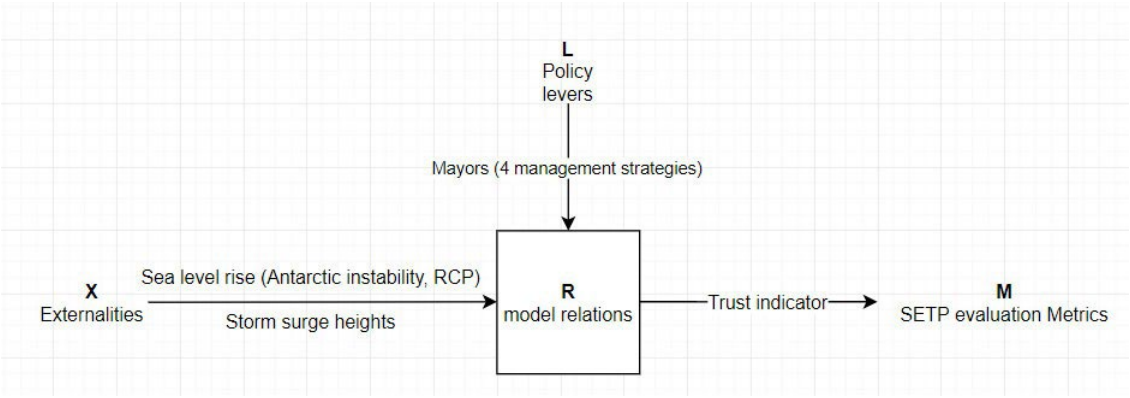

Figure 2.5.10: XLRM scheme describing the uncertainty space (spanned by X and L) and the evaluation metrics (XLRM scheme adapted from Kwakkel, 2017)

*This project has received funding from the European Union's Horizon 2020 research and innovation programme under the Grant Agreement No **776479.***

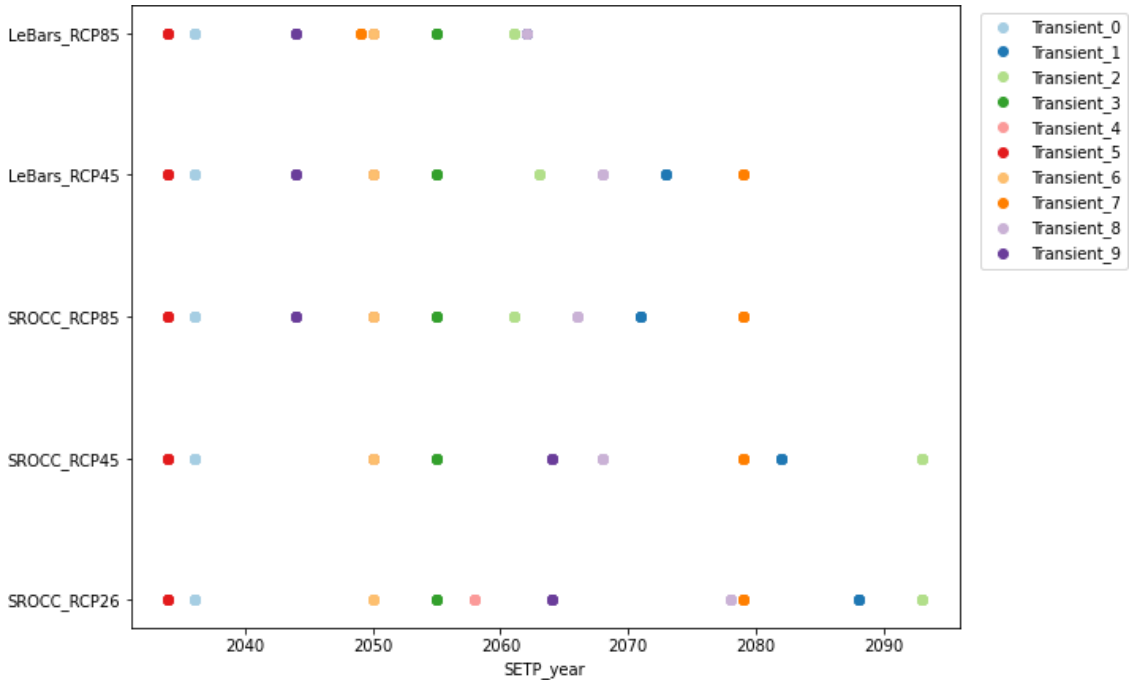

Figure 2.5.11: The occurrence of socio-economic tipping points in residential area A over time, dependent on the transient storm surge scenario (colored dots) and the SLR scenario (y-axis) (50% CI). In this figure, the tipping point is defined as the first time that the trust of the residents is below 50%. Note that for this area there is no difference between the mayors, because in this version of the model mayors can only raise the dikes, which does not benefit the outerdike area.

Figure 2.5.11 shows the timing of the SETPs in time, for the outerdike Heijplaat area. In all these simulations, the tipping points occurs in the 21st century. The large scattering of the dots over time indicates that the choice for the transient scenario is very important for the timing of the SETP. This means that the order in which the storm surges will arrive, is as much an explanatory variable for SETPs as the climate change (sea level rise) signal. For example, in the transient scenario 5 (red dot, Figure 2.5.11), an SETP will occur in 2034 irrespective of the climate scenario.

The figure also shows that the transient storm surge series chosen in the previous section (where different Mayors were compared) is among the more favourable series, with the SETPs happening relatively late in the 21st century. In most other series, the SETPs will occur earlier.

Finally, it is clear that, despite this sensitivity to the storm surge series, there is a clear sensitivity to the climate scenarios as well. In the high-end sea level rise scenario (Le Bars, RCP8.5) all SETPs occur before 2065. In contrast, under a low-end sea level rise scenario, the last SETPs occur just before 2100.

*This project has received funding from the European Union's Horizon 2020 research and innovation programme under the Grant Agreement No **776479.***

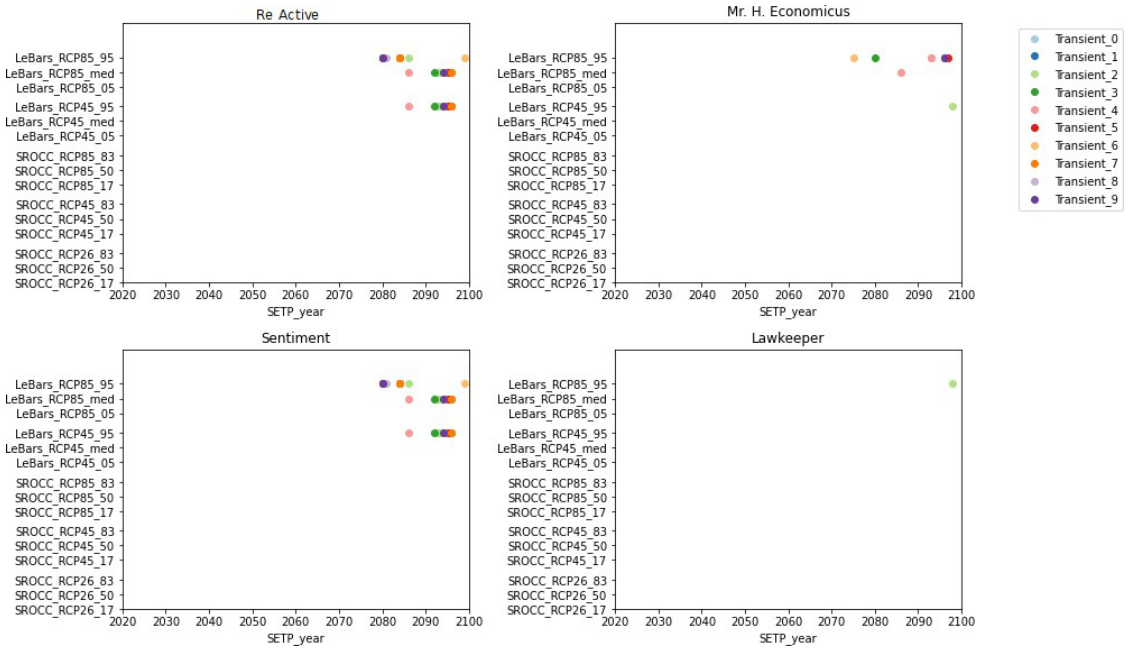

Figure 2.5.12: The occurrence of socio-economic tipping points in residential area B over time, dependent on the transient storm surge scenario (colored dots) and the SLR scenario (y-axis) including confidence interval, for different mayors. In this figure, the tipping point is defined as the first time that the trust of the residents is below 50%.

Figure 2.5.12 shows the occurrence of SETPs for the innerdike (City Centre) area. Not surprisingly, the SETPs in this area (if any) occur significantly later than in the outerdike area, due to the protection by the dike. The first SETPs happen around 2075. Moreover, they only occur in the Le Bars, i.e. the extreme sea level rise, scenarios. This means that the socio-economic tipping points will only happen if the climate tipping point 'rapid melting of the Antarctic Ice Sheet' also happens. The climate tipping point is the trigger for the socio-economic tipping point. Without this climate tipping point, the socio-economic tipping point will not happen within the 21st century. For a detailed study confirming this finding for The Netherlands, see Kwadijk et al., 2010.This is also in line with the findings of the DIVA model (see previous section).

There are significant differences in SETP timing between the different mayors. Under the reactive management strategy (Mayor Re Active), the situation is the worst, because action is then only taken when the first impacts are already felt. At this point, new measures can no longer be implemented fast enough to keep up with the high rate of sea level rise. The performance of Mayor Sentiment, who anticipates on the perceived flood risk, is comparable. Again, action is only triggered by near-miss events, but now via the elevated risk perception caused by the near-miss event. Mayor Economicus, who anticipates on the objective flood risk rather than the subjective flood risk, performs better, because the decisions to heighten the dikes are made earlier. Economicus does not wait for the 'policy window' of increased risk perception to implement the measures, but instead anticipates to the rapidly increasing risk also ifthis is not accompanied with the near misses warning signs. In that sense, Economicus is less sensitive to randomness in the storm surge series than Sentiment. Finally, under mayor Lawkeeper, SETPs are almost completely avoided. There is only one SETP for a

*This project has received funding from the European Union's Horizon 2020 research and innovation programme under the Grant Agreement No **776479.***

very extreme sea level rise scenario (Le Bars, 95% CI), combined with an unfavourable storm surge series. Since the policy of Lawkeeper best resembles the current management practice, it can be concluded that even with the climate tipping point of very rapid sea level rise occurring, the SETP for the innerdike area can be avoided with the proactive dike management as displayed by Lawkeeper.

An interesting observation from comparing Figure 2.5.11 (innerdike) to Figure 2.5.12 (outerdike) is that the timing of the SETPs are much more clustered in the innerdike area. This indicates that for embanked areas, the sea level rise signals start dominating over the randomness of the storm surges when it comes to explaining why an SETP happens.

The reason for the SETPs to occur in the high-end sea level rise scenarios is that the implementation time of the measures becomes too long compared to the rate of sea level rise.

2.5.4. Discussion and further work

The used approach has two important limitations. Firstly, in reality, the flood risk strategy may also change over time, which is not fully captured by the current model. For example, the strategy displayed by the mayor Re Active can probably only be justified in a decision making context where a high rate of sea level rise can be denied with some certainty. However, it is hard to imagine how this viewpoint couldbe held if the city would indeed find itself in the year 2050, with RCP8.5 combined witha clear disintegration of the Antarctic Ice sheet. At this point, the sea level would have already risen with some 50 cm, and the first signs of an acceleration should be clearly detectable from the water level time series. It is hard to imagine how a city with a strong institutional setting would not act more radically upon such a clearly looming disaster. Secondly, in case of actual disasters or near-misses, flood risk measures may be implemented faster than displayed by the implementation measures in the model. These are currently derived from a business-as-usual decision-making context rather than an urgent disaster-management setting. With faster adaptation, many of the SETPs may be avoided.

Further work could focus on applying the model framework with theshowcased dynamic adaptivity to other cities. Each city has its own unique characteristics and barriers to adaptation, such as financial, technical or social constraints. For example, in certain socio-economic contexts raising dikes may nolonger be attractive from the perspective of cost-benefit analysis. Another possibility isthat construction of high sea dikes may destroy the unique beach front of a city or require the relocation of unique cultural heritage. One could argue that some of these impacts are so large that their mere implementation can be seen as an SETP.

2.6. Trade disruptions due to flooding

This section focusses on the indirect impacts of flood damage to the road network. It builds on the analysis of direct flood damage as presented in COACCH Deliverable 2.3 (Lincke et al., 2019) and presented with extended domain in Van Ginkel

*This project has received funding from the European Union's Horizon 2020 research and innovation programme under the Grant Agreement No **776479.***

et al. (2020b, under review). Furthermore, it uses a scaled-up version of the method used to assess trade disruptions in the road network of Austria in COACCH Deliverable 3.2 (Scoccimarro et. al., 2020).

In the current deliverable, we explore whether and under what conditions disruptions of the road network due to river floods may cause socio-economic tipping points (SETPs). In earlier COACCH work, we found that the stakeholder perspective and the scale of analysis is decisive for determining whether a tipping point occurs (van Ginkel et al., 2020a). To represent different stakeholder perspectives and scales of analysis, this deliverable examines the impact of river floods to the road level network at three levels of abstraction.

Level 1: we take a pan-European viewpoint to examine the degree to which national road networks may be vulnerable to river floods. We compare the road networks of the following European territories: Albania, Austria, Belgium, the island of Ireland (consisting of the Republic of Ireland and Northern Ireland, further referred to as island of Ireland), Italy and Sweden. Approaches from percolation theory[10] are used to assess the performance of the national road network when road segments are inaccessible due to river floods. The analysis shows which countries have the largest likelihood of 'tipping point like' disruptions of their national networks. We reflect on the network characteristics explaining the differences between countries. The results are mainly useful for mutual comparison of European countries rather than for gaining in-depth understanding of the situation in one country.

Level 2: we zoom in on the road network of Austria. For this country, we move beyond percolation analysis to gain a better understanding of the traffic dynamics and impacts that are associated with road disruptions. This implies that we move from a pan-European perspective to the perspective of a national road operator, or national transport planner, who wants to know which parts of the network are most vulnerable, and what traffic flows are impacted with what economic consequences.

Level 3: we zoom in even further on a vulnerable industry in Europe: car and truck manufacturing, which relies heavily on just-in-time deliveries to sustain the production process. COACCH stakeholders pointed out that individual factories may exhibit abrupt strong non-linear (tipping point-like) impacts due to supply chain disruptions from natural disasters (Tröltzsch et al., 2019). These local-scale impacts often disappear in (inter)national risk metrics such as GDP-shocks, but nevertheless are highly relevant; not only because they may hit regional economies very hard, but also because they may receive disproportionally large attention in the media and may steer public opinion. Therefore, local tipping points from disruptions of the supply chain are an important story to tell.

2.6.1. Definition of tipping point

Level 1: Pan-European assessment of national road networks

[10]Percolation theory is applied in many different fields. In case of road networks, it aims to assess the robustness of those networks when nodes or edges are removed (Li et. al., 2015).

*This project has received funding from the European Union's Horizon 2020 research and innovation programme under the Grant Agreement No **776479.***

The percolation graphs (Figure 2.6.3 and 2.6.4) indicate the potential loss of functionality (% of NUTS-3 origin-destination pairs) due to combinations of flood events. From these graphs, the following insights about tipping points can be obtained:

- High impact flood events (disproportionally large loss of functionality compared to the extent of the flood) can be considered as tipping point events, because their occurrence leads to an abrupt, extensive drop in network functionality. In the graphs shown, these events show as outliers above the 95% range.
- By comparing the shape of the graphs for different countries, we can qualitatively indicate the likelihood of a tipping point in the sense of 'severe disruption of the network performance'.
    - The steepness of the percolation function is a metric for the resilience of the network. A steeply increasing function is an indication for less resilience; tipping points are more likely to happen.
    - For countries with very resilient road networks and little floods, this graph could proof that SETPs cannot happen. In a recent example by the Word Bank of a percolation analysis of road networks (e.g. Hallegatte, 2019), the graph goes up to 100%, because all the road segments were taken out at x=100%. Since we only take out those segments that can be inundated, our graph might not go up to 100%: there will be some regions that stay connected, even if all the possible flood events happen at the same time. If y gets close to 100% (such as in Austria), SETPs could theoretically happen, if y stays low even for large x, SETP cannot happen.

Level 2: Tipping point for freight and personal vehicle transport in Austria

For the national government or road operator in Austria, the tipping point is defined as the points where river floods cause a sudden severe disruption of commuter and commercial traffic, expressed by costs of travel time lost. In addition to level 1 tipping points, the costs of rerouting or delays of actual cars and trucks usingthe road network are estimated.

To investigate potential 'tipping point behaviour' for this level of analysis, we follow the following steps:

- we start with selecting six scenarios from the earlier work on the Austrian road network as outlined in deliverable 3.2 (Scoccimaro et al., 2020). These six scenarios represent: 1, 2, 3, 4 or 5 combinations of 1/100y micro floods (of which we do not know the likelihood of coincidence) and a combination of 5 spatially correlated micro floods (of which we expect the likelihood of coincidence is high).
- After, a detailed visual inspection of the flood locations the scenarios served as input to an Austrian traffic model, VMÖ 2025+[11] (VPO2025+, 2009), that calculates detours and time per car and truck and includes limitations by road capacity (i.e. allows for traffic jams). The model consists of a multi-modal

[11] This is the official Austrian national transport model. It has been developed by TRAFFIX within the context of the national traffic forecast Verkehrsprognose Österreich 2025+. The model is used by the main Austrian transport sector players.

*This project has received funding from the European Union's Horizon 2020 research and innovation programme under the Grant Agreement No **776479.***

network model and of traffic demand models for passenger and freight transport. The demand for trips is calculated by a profound economic model that based on population distribution and economic exchange between areas.

- In a next step, the demanded trips are attributed to the network optimizing across transport modes, distance, time and costs. The spatial scope of VMÖ covers continental Europe with a focus on Austria and its surroundings regarding spatial resolution. VMÖ covers 2,628 traffic zones (2,412 of which within Austria) and all motorways, arterial roads, collectors as well as all main local roads.
- The differences in travel time between the base case scenario of no floods and those with 1 to 5 floods and spatially correlated floods are being valued according to aggregated travel time values for trucks and cars from literature.

Level 3: Tipping point for a car & truck manufacturer

As a case study, we take a typical European car & truck manufacturer[12], a branch of industry known to be quite dependent on just-in-time delivery (see textbox 2.6.1). We use the current supply structure, with 10 suppliers geographically dispersed across a number of European countries, each supplying a component that is critical for some product produced in the factory. For this case, the tipping point is defined as the point where river floods cause a severe disruption of the supply chain so that production is significantly hindered. More quantitatively, we search for combinations of floods that either (1) completely block the access to the factory or supplier, (2) cause a steep increase of travel time or (3) push travel times to the factory over legal thresholds for truck drivers.

Textbox 2.6.1

The car & truck manufacturing industry is a typical example of an industry operating with a just-in-time (JIT) inventory system. This means that input products are delivered just before they are needed in the production process, keeping a minimum amount of stocks and inventories. JIT-manufacturing is also called the 'Toyota Production System', referring to the first car manufacturer who adopted the system in the 1970s (Banton, 2020). JIT-manufacturing is generally known to be very sensitive to disruptions in the supply chain. If the supply chain of one critical input product to the production process is disrupted, the whole production process needs to be stopped as soon as the (typically small) inventory is depleted.

A recent example of a car & truck manufacturing supply chain disruption occurred during the first months of the Covid-19 crisis, early 2020. Car manufacturers in the European Union had to close for 30 working days, on average (ACEA, 2020). Many factors contributed to these shutdowns, including a decreasing demand for products. However, among the main contributing factors were two that are highly relevant for our case study: (1) a shortage of input products because of problems in the supplying factories (from labour restrictions or lacking crucial inputs) and (2) strongly delayed freight due to intensified border controls and sometimes even border closures.

[12] The analysis is done with real-life data for an existing car and truck manufacturer and actual suppliers somewhere in Europe. The authors verified the credibility of this data. To guarantee confidentiality about the supply chain of this factory, the data (and visualisations) shown are manipulated, but in such a way that the results of the analysis are not effected.

*This project has received funding from the European Union's Horizon 2020 research and innovation programme under the Grant Agreement No **776479.***

2.6.2. Method of analysis

Method level 1: assessment of multiple national road networks

The level 1 method is adopted from COACCH Deliverable 3.2 (Scoccimarro et. al., 2020), where it was used to assess network disruptions due to flooding of roads in Austria. Now, it analyses the disruption impact of flooding on the optimal routes connecting the NUTS-3 regions within Albania, Austria, Belgium, the island of Ireland, Italy and Sweden. The studied territories are mapped in Figure 2.6.1. Where possible, the road network used for the analysis includes a buffer around the country itself, to enable short cuts through neighbouring countries. Rerouting is not considered in this first level of analysis but is used in the nation-wide analysis (level 2) and the factory specific analysis (level 3).

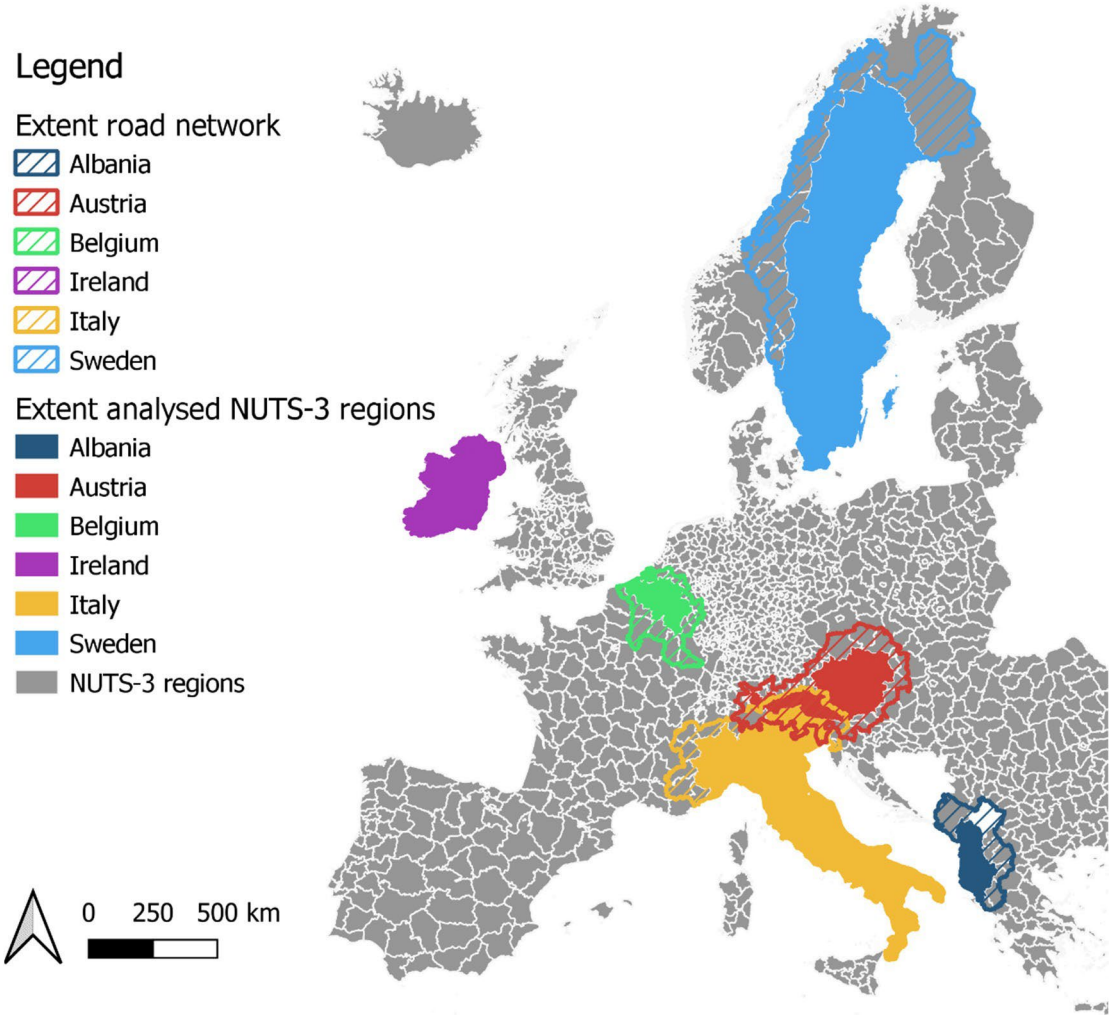

Figure 2.6.1: The extent of the road network and extent of the analysed NUTS-3 regions for Albania, Austria, Belgium, the island of Ireland, Italy and Sweden.

The analysis performed consists of a stochastic percolation for the 'micro- floods' in each country. It compares the performance of the different national road networks for multiple flood events, even if some have low correlations of happening

*This project has received funding from the European Union's Horizon 2020 research and innovation programme under the Grant Agreement No **776479.***

simultaneously. A similar approach is used by the World Bank in their report "Lifelines: The Resilient Infrastructure Opportunity" (Hallegatte, 2019). The methodology here proposed further introduces the link to the hazard disruption, making a concrete link with the physical triggering condition. Furthermore, the proposed methodology is flexible and in future analyses, search algorithms could be used to more quickly find potential tipping points, while considering only highly correlated flood events or compound events.

In the countries under study, there are too many (e.g. 498! = 4.890327959x101128 for Austria) possible combinations of micro-floods to perform an exhaustive analysis of all combinations. Instead, 1000 samples[13] were considered for each case of simultaneous impact of 2 to a maximum number of floods, see Table 2.6.1. In the case of 1 flood event, the impact of each single flood is analysed. The maximum number of floods - i.e. the impact of all possible flood events – is just calculated once. The result of this approach is shown in Section 2.6.2.2.

Table 2.6.1: The number of sampled combinations of micro-floods per country. The maximum number of micro-floods per country is the last number each list.

Country	Number of sampled combinations of micro-floods
Albania	1, 2, 3, 4, 5, 10, 20, 30, 40, 50, 100, 175
Austria	1, 2, 3, 4, 5, 10, 20, 30, 40, 50, 100, 200, 300, 400, 498
Belgium	1, 2, 3, 4, 5, 10, 20, 30, 40, 50, 100, 179
Island of Ireland	1, 2, 3, 4, 5, 10, 20, 30, 40, 50, 100, 200, 225
Italy	1, 2, 3, 4, 5, 10, 20, 30, 40, 50, 100, 200, 300, 400, 500, 1000, 1350
Sweden	1, 2, 3, 4, 5, 10, 20, 30, 40, 50, 100, 200, 300, 400, 500, 1000, 1810

Method level 2: tipping points for freight transport in Austria

For this level of analysis for Austria the 6 scenarios as presented in section 2.6.1 ranging from 1 to 5 simultaneous floods and one with spatially correlated flood are used to remove roads in the network from the traffic model. The traffic model calculates (alternative) routes for passenger vehicles and trucks, and associated travel times. We calculate for each flooding scenario:

- the aggregated excess distance of trucks (and similarly for cars) as ***SUM(distance per link*number of trucks per link)$^{disruption\ situation}$ - SUM(distance per link*number of trucks per link)$^{base\ case}$***
- the aggregated excess time of cars (and similarly for trucks) as ***SUM(time per link*number of cars per link)$^{disruption\ situation}$ - SUM(time per link*number of cars per link)$^{base\ case}$***

During the execution of the analysis it appeared that the floods were completely blocking off some destinations (no rerouting possible). The traffic modelershad to take out these specific zones and associated trips with cars and trucks from the analysis in order to prevent run-time errors. This causes the number of trips to be different in the base case and the various flood scenarios. To account for this

[13] For all countries except Italy; because of insufficient computational power on average 213 samples are considered for each case of simultaneous impact of micro-floods.

*This project has received funding from the European Union's Horizon 2020 research and innovation programme under the Grant Agreement No **776479.***

mismatch, we apply a correction factor to the excess distance and time calculations. In addition, we assume that the trips taken out also represent a real economic disturbance as goods may not be delivered and employees are not able to travel to work or students to school. We assume that this represents a disruption of a day, though we realize that a blockage due to river floods may last longer in most cases.This day is further translated into 8 (working) hours for cars and 24 hours for trucks(the time that goods cannot be delivered).

The excess time per disruption scenario was multiplied with a value of time (2015-Euros per hour) to value the delay caused by the disruption. The value of time was 53 euro for trucks and 25 euro for cars, these were derived as follows. Warman et al. (2016) value 23 euro (2010 Euros) for employer's business trips in Austria. RAND (2003) use 44 (2002) euros for all different types of goods transported in the Netherlands. The above numbers have been scaled to 2015 and to Austria using historic inflation rates[14] price correction and GDP/capita ratio between the Netherlands and Austria for 2015.

The values obtained are daily costs of disruption for work days. During weekends and holidays, different patterns of traffic exist for both light and heavy vehicles. The workday disruption situation is assumed to be the worst case. Additional indirect costs can arise from the delays that are not accounted for in these estimates. The just in-time supply chain disruption exemplifies such situations (see level 3 analysis).

On the other hand, the traffic model does not only include business trips but also leisure and other types of trips. Therefore, the damage estimates will provide an upper limit for a day's disruption.

Method level 3: tipping points for car manufacturer in Austria

In the first step of this chapter we studied the robustness of the national road networks of member states by randomly sampling possible disruptions between NUTS-3-regions. In this third step, the sampling procedure is different. First, we calculate the preferred route from the supplier (origin) to the car & truck manufacturer (destination). Then, rather than sampling a random subset of micro-floods (as in the first step) we find all the possible disruptions caused by one micro flood (Area of Influence, AoI) on the preferred route. For all these disruptions we calculate the fastestdetour, if any exists. We then select the three micro floods leading to the largest detour; these are the three micro floods causing the largest disruption of the preferredpath. For these three detours (level 1, Figure 2.6.2) the analysis is repeated for a second micro flood. For each detour, we study all the possible disruptions caused by the second micro flood and calculate all fastest detours for these. This procedure is continued on each next level, up till level 7, where 7 AoIs are sampled at the sametime. For an illustration of the first five steps, see Figure 2.6.15. Because the search is directed towards the worst-case alternatives, 7 AoIs already corresponds to a very unlikely coincidental situation; a 'perfect storm' with very unfavourable impact for this particular car manufacturer. This is comparable to the 'low #AoI, large loss of network functionality' outliers in the first step of this section (Figure 2.6.3).

[14] https://www.inflation.eu/inflation-rates/austria/historic-inflation/hicp-inflation-austria.aspx

*This project has received funding from the European Union's Horizon 2020 research and innovation programme under the Grant Agreement No **776479.***

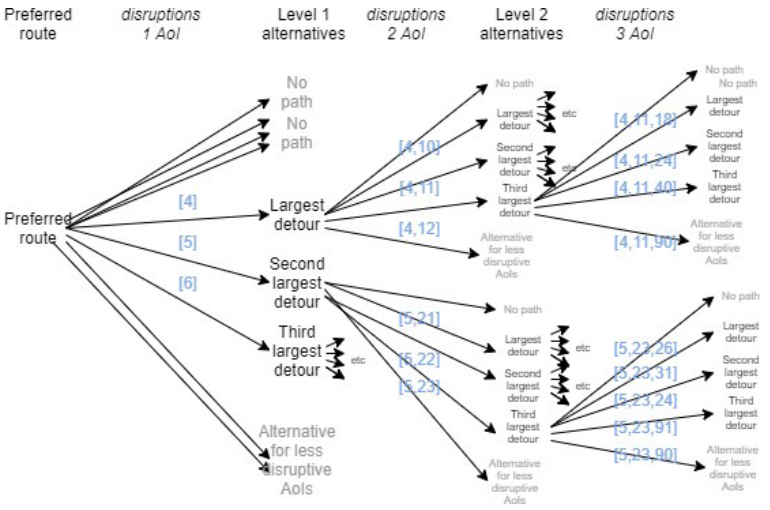

Figure 2.6.2: Algorithm used to identify the worst-case combinations of micro-floods causing the largest increase in travel time

2.6.3. Results

This section presents the results of the assessment of national road networks (level 1), the in-depth assessment of the Austrian road network (level 2) and the disruption of deliveries to the car and truck manufacturer.

Level 1 results: stochastic percolation analysis for national road networks

The results of the stochastic percolation analysis (Figure 2.6.3) are visualised twofold: with the absolute (left-hand panel) and the relative (right-hand panel) number[15] of combinations of micro-floods on the x-axis. Both graphs depict the percentage of loss of optimal network functionality between NUTS-3 regions on the y-axis.

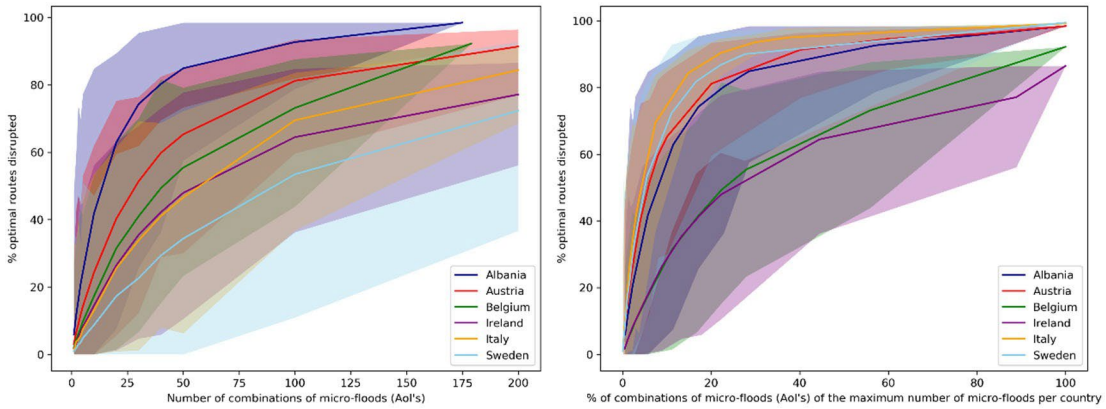

Figure 2.6.3: Average loss of optimal network connectivity. The colours around the lines represent the minimum and maximum of the % optimal routes disrupted for the country indicated with the same

[15] We also use the relative number of combinations to the maximum number of micro floods to account for the size of the country. A larger country potentially has more locations where flooding might occur. The missing parameter in this analysis is the likelihood of concurring events in one country. Therefore both views are presented.

*This project has received funding from the European Union's Horizon 2020 research and innovation programme under the Grant Agreement No **776479.***

colour. The graph on the left displays for visual inspection purposes the % optimal routes disrupted for Albania, Austria, island of Ireland, Italy and Sweden until combinations of 200 micro-floods, yet, the maximum number of micro-floods is respectively 175, 498, 225, 1350 and 1810.

Least and most vulnerable countries

Comparing all six countries, Albania has the most vulnerable road network, considering simultaneous micro-floods. The steep curve of Albania also indicates that it is the country where it is most likely for SETPs to occur. In Albania, already for 5 possible combinations of 2 micro-floods, 50% or more of the optimal routes are disrupted (Figure 2.6.4). When the percentage of combinations of micro-floods is considered (right plot, Figure 2.6.3) instead of the absolute number, Italy is mostvulnerable concerning road network functionality. This differs because the maximum number of potential micro-floods in a country increases with the size of a country16. For example, 10% of all potential flood events in Italy corresponds to 135 simultaneous floods, whereas in Albania the same percentage corresponds to only 18 simultaneous floods. Albania's area measures 12% that of Italy and accordingly, Albania has 13% the number of micro-floods of Italy. In line with this, Italy, Sweden and Austria perform worse than Albania in the comparison of relative combinations of flood-events, amongst others because they are countries with more potential micro-floods.

Sweden's road network is least susceptible to loss of functionality due to floods. However, still more than 50% of the road functionality in Sweden can bedisrupted due to very unfavourable combinations of 4 and 5 simultaneous micro-floods (Figure 2.6.4.). This indicates that the possibility of an SETP cannot be excluded. However, most combinations of 1-5 simultaneous floods disrupt only a small percentage of all optimal routes. With at least 50% of the flood samples disrupting less than 7% of the optimal routes, the chance for SETPs to occur is low. In relative terms ofcombinations of micro-floods, the island of Ireland is least susceptible to loss of road functionality due compared to the other five countries.

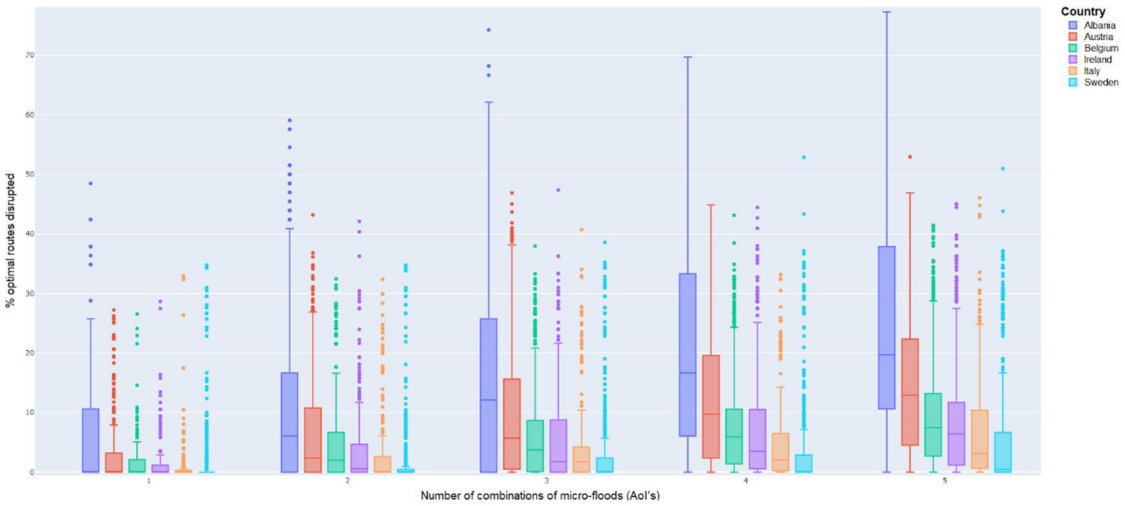

[16] Not in all cases, it also depends on a lot of other factors like the number and size of mountains, lakes and rivers.

*This project has received funding from the European Union's Horizon 2020 research and innovation programme under the Grant Agreement No **776479.***

Figure 2.6.4: Loss of optimal network functionality up to combinations of five micro-floods simultaneously. The boxes indicate the median, 25th and 75th percentiles (respectively Q2, Q1 and Q3). Whiskers indicate 'minimum' (Q1-1.5*IQR) and 'maximum' (Q3+1.5*IQR) where IQR=Q3-Q1. Outliers to 'minimum' and 'maximum' are represented as points.

Mutual comparison of the countries' network characteristics

Comparing the countries' network characteristics gives insight into why some countries are more susceptible to micro-floods than others. Albania and Italy are identified as countries with road networks that are most vulnerable to river floods, compared to Austria, Belgium, the island of Ireland and Sweden. Albania is a small, mountainous country, with the main corridor located near the coast where the country is flatter (see Figure 2.6.5). The roads that are located more land-inwards cross through mountains. This forces the quickest way to move from one NUTS-3 region to another to always be the main corridor near the coast, where also most of the micro- floods potentially occur. Therefore, large network disruptions can be expected with only a few simultaneous flood events.

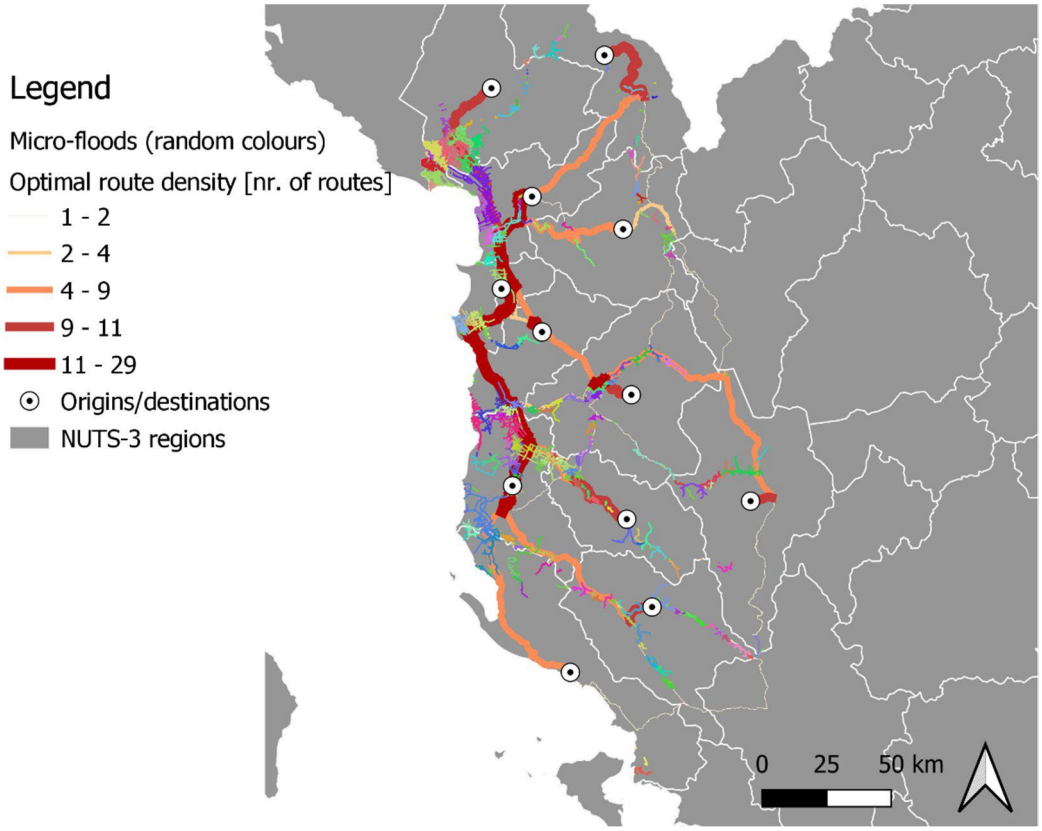

Figure 2.6.5: Number of times a road stretch is used for the optimal quickest routes connecting NUTS-3 regions in Albania.

Italy is much larger than Albania and has more potential micro-floods (see Table 2.6.2). Furthermore, Italy is much less vulnerable than Albania up to 175 micro-floods occurring simultaneously. This can be explained by the many, relatively small, NUTS-3 regions and potential micro-floods in Italy. Multiple main corridors are identified: the roads connecting the east and west in the most northern part of the country and two

*This project has received funding from the European Union's Horizon 2020 research and innovation programme under the Grant Agreement No **776479.***

routes connecting the north of the country with the south (see Figure 2.6.6). As for the main corridor in the north, it runs through the Po Valley. This Valley receives alldischarge from the Alps and is an economic hotspot: one-third of the 93 NUTS-3regions that are assessed for Italy are there. Hence, there are many connections between NUTS-3 regions which can be disrupted by many micro-floods. The other two main corridors from north to south Italy are roads located on either side of the Apennines, also receiving discharge from that mountain range. Since those two main corridors are also motorways, most of the optimal routes from north or south or vice versa could be disrupted by those micro-floods.

Table 2.6.2: Characteristics of the studied countries and its NUTS-3 regions.

Country	Area [km^2]	Nr. of potential micro-floods	Nr. of NUTS-3 regions	Nr. of origin-destination pairs
Albania	28,800	175	12	66
Austria	83,945	498	35	595
Belgium	30,666	179	44	946
Island of Ireland	84,098	225	19	171
Italy	250,394	1350	93	4278
Sweden	449,655	1810	21	210

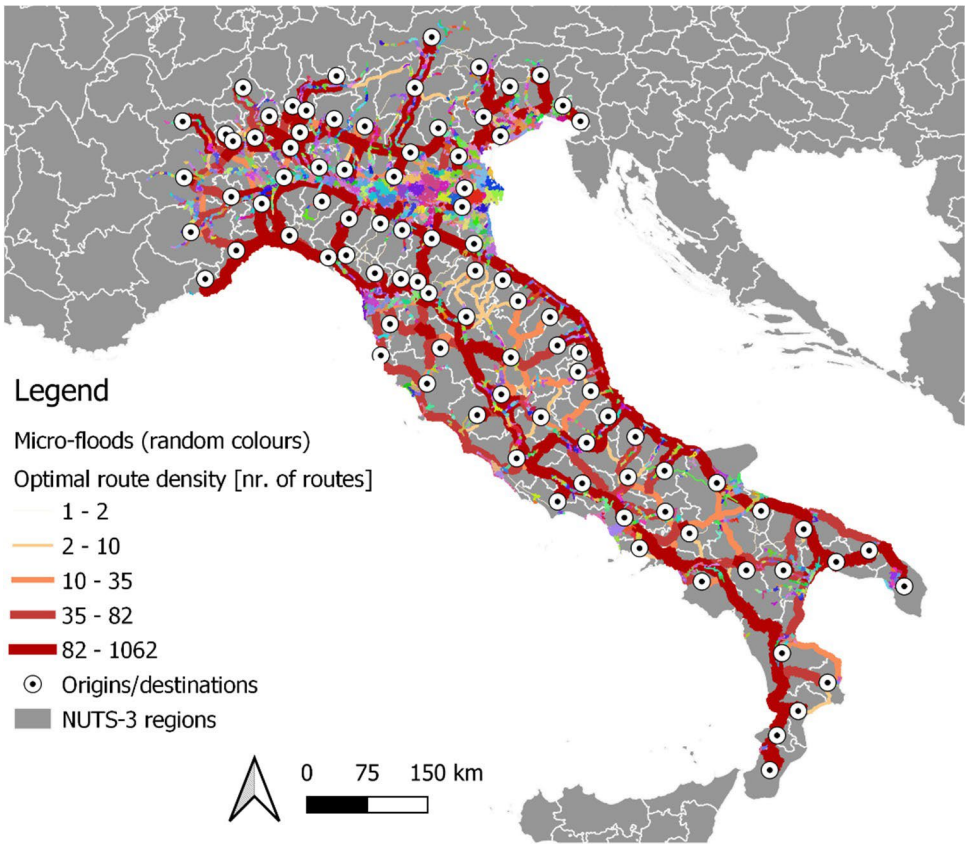

Figure 2.6.6: Number of times a road stretch is used for the optimal quickest routes connecting NUTS-3 regions in Albania.

*This project has received funding from the European Union's Horizon 2020 research and innovation programme under the Grant Agreement No **776479.***

Sweden and the island of Ireland are identified as territories with road networks that are least susceptible to river floods, compared to Albania, Austria, Belgium and Italy. Sweden has the largest area of the six (see Table 2.6.2) with only one-sixth of the population of Italy. Therefore, there are not many NUTS-3 regions and especially in the north, they are large compared to the regions in Italy (see Figure 2.6.7Figure 2.6.6). The main corridor runs from north to south, although there are also many other roads that have a higher optimal route density. This makes the road network of Sweden less susceptible to river floods. Indeed, there is a low chance that one or a few of the 1810 micro-floods disrupt all the roads that have a high optimal route density. On the other hand, when many flood events occur simultaneously, i.e. from 181 flood events, chances are more likely that those will cause large disruptionsin road functionality.

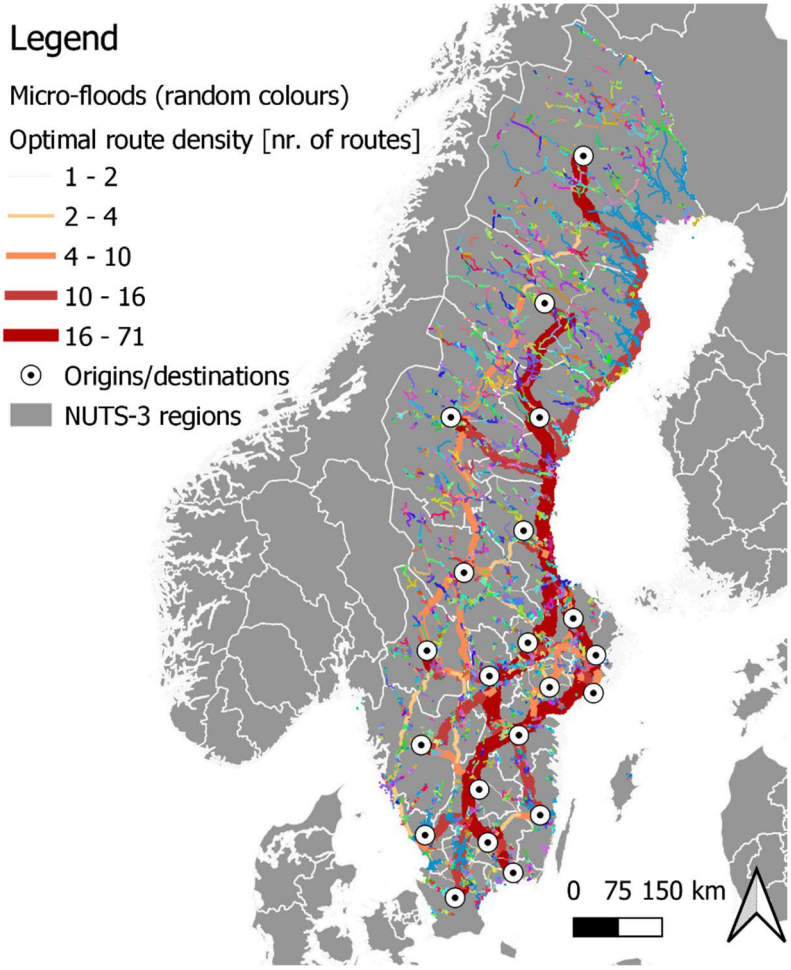

Figure 2.6.7: **Number of times a road stretch is used for the optimal quickest routes connecting NUTS-3 regions in Sweden.**

The island of Ireland measures approximately three times the size of Albania (see Table 2.6.2) with only around 1.3 times as many potential micro-floods. LikeSweden, the island of Ireland has a more evenly divided optimal route density (see Figure 2.6.8). This can be caused by the relatively rounder shape of the country that is

*This project has received funding from the European Union's Horizon 2020 research and innovation programme under the Grant Agreement No **776479.***

as well much flatter than Italy and Abania. The main corridor runs from south-west to north-east, mainly over the Irish and UK motorways. A lot of the micro-floods are not intersecting with this main corridor, hence the low average disruption of road network functionality.

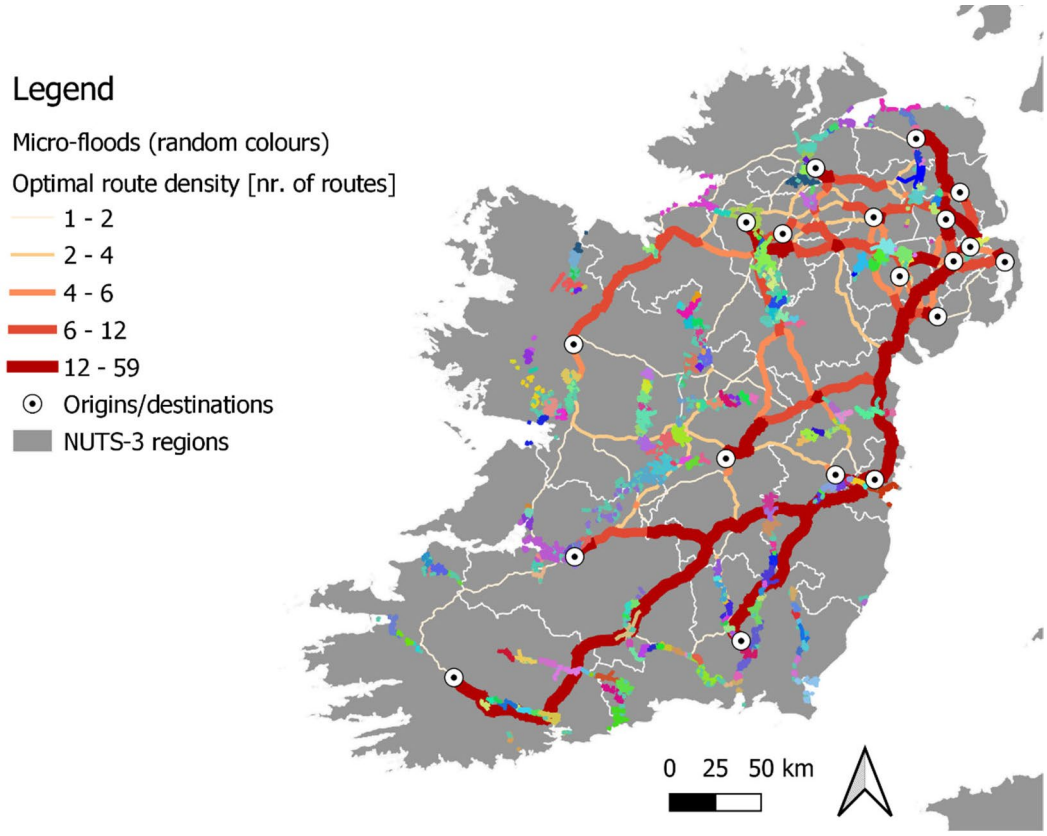

Figure 2.6.8: **Number of times a road stretch is used for the optimal quickest routes connecting NUTS-3 regions in the island of Ireland.**

Level 2 results: costs of travel delays in worst-case flood scenarios

In COACCH Deliverable 3.2 (Scoccimarro et. al., 2020) we identified six flood risk scenarios with potential SETP-characteristics for Austria. In this section we present the economic evaluation of these six events. Table 2.6.3 shows that in the worst scenario, the total extra travel time for cars and trucks may increase with respectively 106,000 and 44,500 hours due to flooding. This extra time is valued as a loss of 2.7 million euros for cars and 2.4 million euros for trucks. Note that for cars, the potential flood situation of 2 simultaneous floods (see Figure 2.6.10) is most disrupting, whilst for trucks this is the scenario of 3 simultaneous floods (see Figure 2.6.11). These numbers have been corrected for the total number of trips (see Table 2.6.4).

Table 2.6.3: Total extra time needed for road traffic in Austria, for cars and trucks under 6 flood scenarios compared to a baseline of no flooding. The flood scenarios are shown in .

Scenario	Total excess time for cars (hours)	Total excess time for trucks (hours)
1	44,848	16,751
2	106,102	40,832

*This project has received funding from the European Union's Horizon 2020 research and innovation programme under the Grant Agreement No **776479.***

3	79,665	44,510
4	64,916	40,072
5	76,772	24,369
Correlated	65,870	36,101

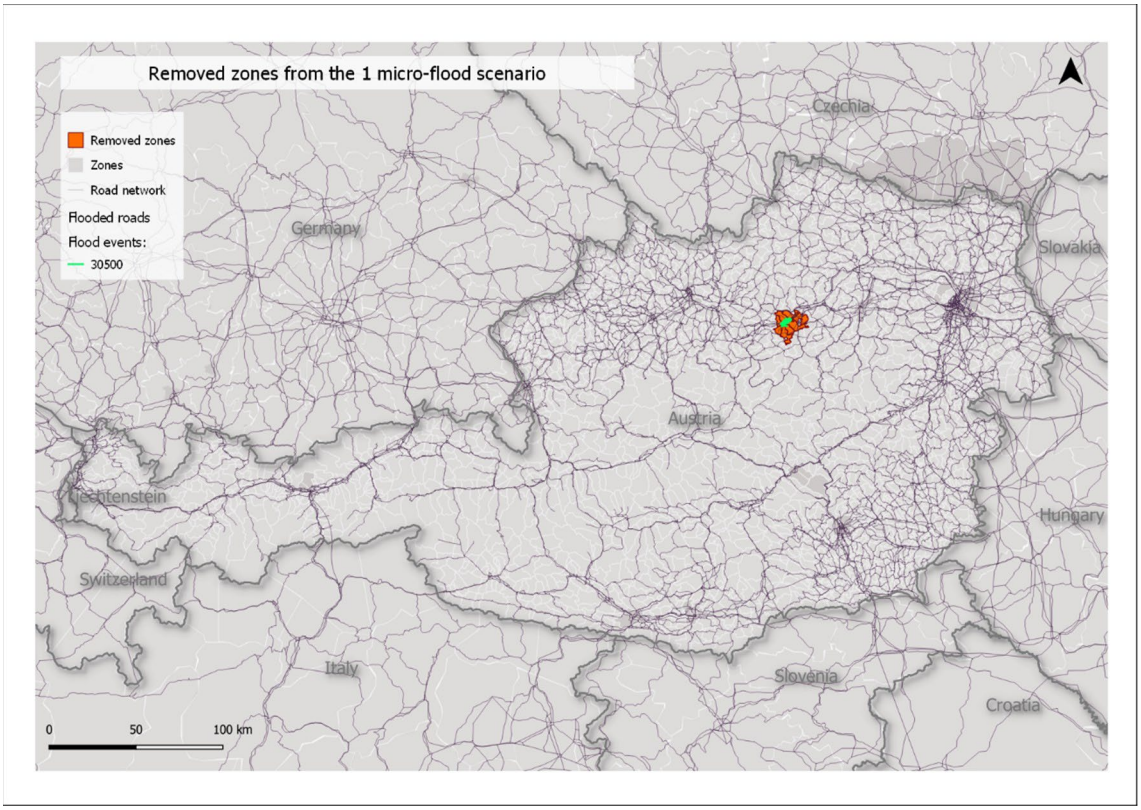

Figure 2.6.9: Flooded road segments and removed zones for the 'single flood' scenario.

*This project has received funding from the European Union's Horizon 2020 research and innovation programme under the Grant Agreement No **776479.***

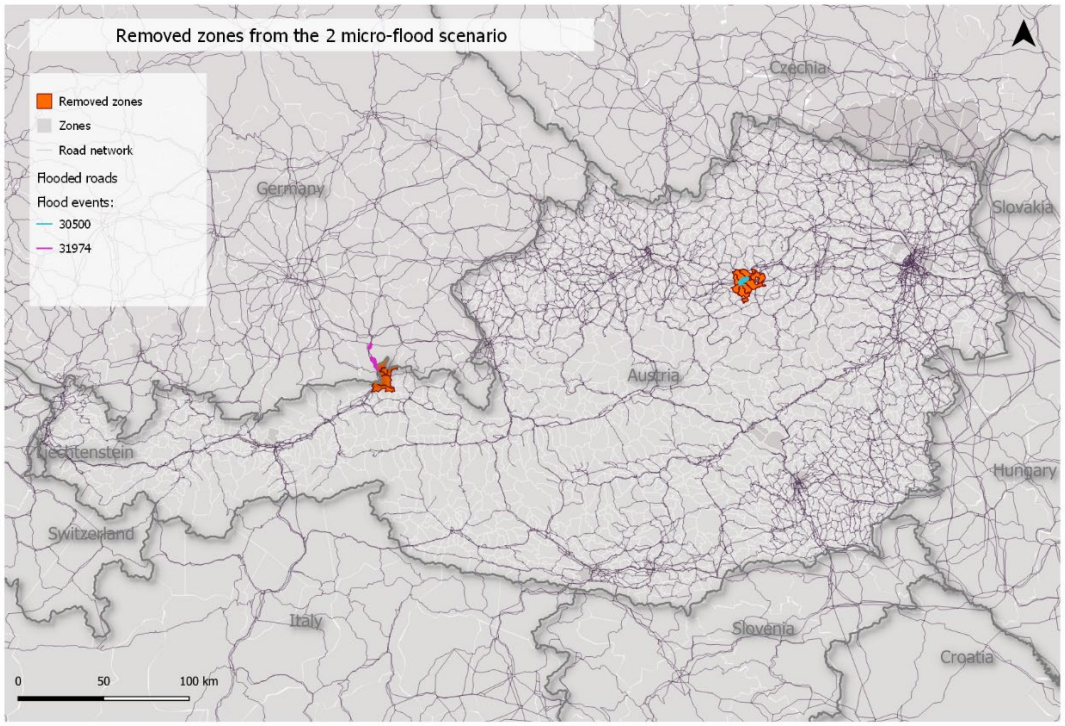

Figure 2.6.10: Flooded road segments and removed zones for the '2 simultaneous floods' scenario.

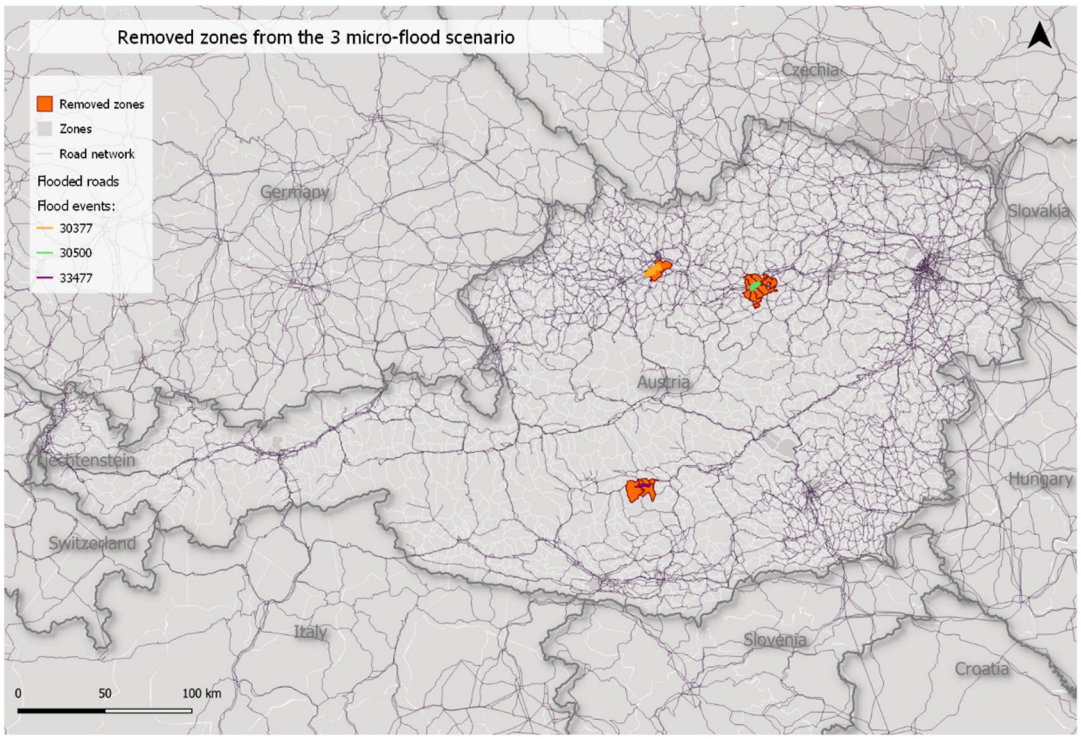

Figure 2.6.11: Flooded road segments and removed zones for the '3 simultaneous floods' scenario.

*This project has received funding from the European Union's Horizon 2020 research and innovation programme under the Grant Agreement No **776479.***

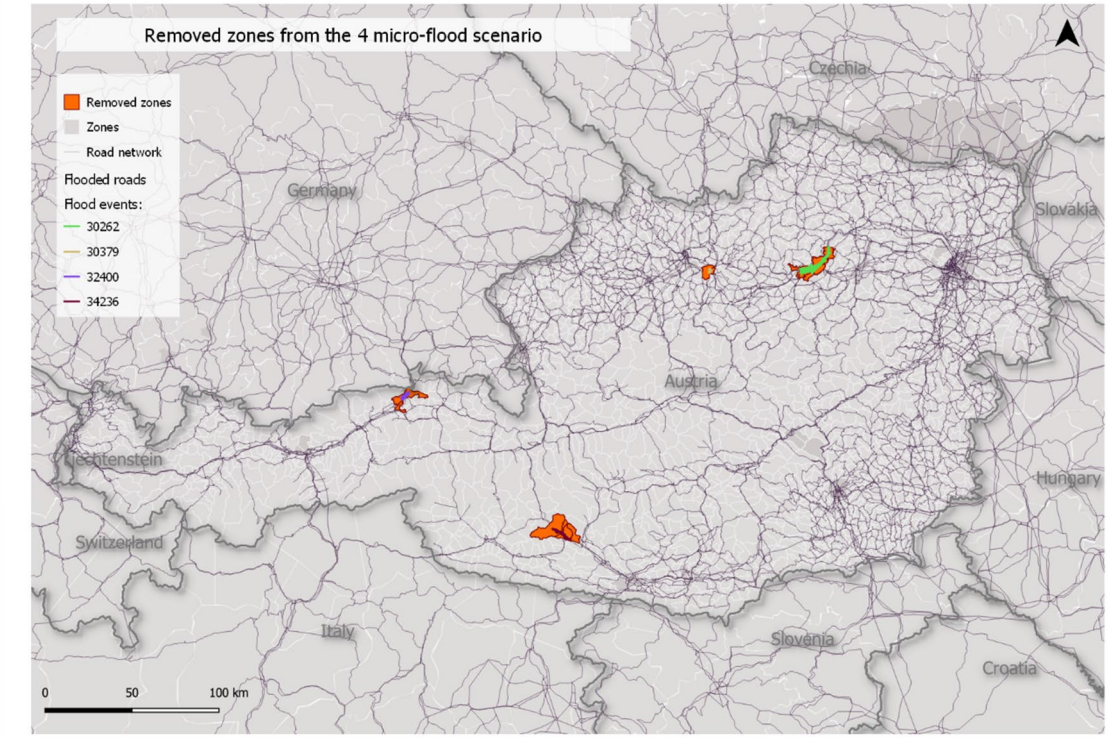

Figure 2.6.12: **Flooded road segments and removed zones for the '4 simultaneous floods' scenario.**

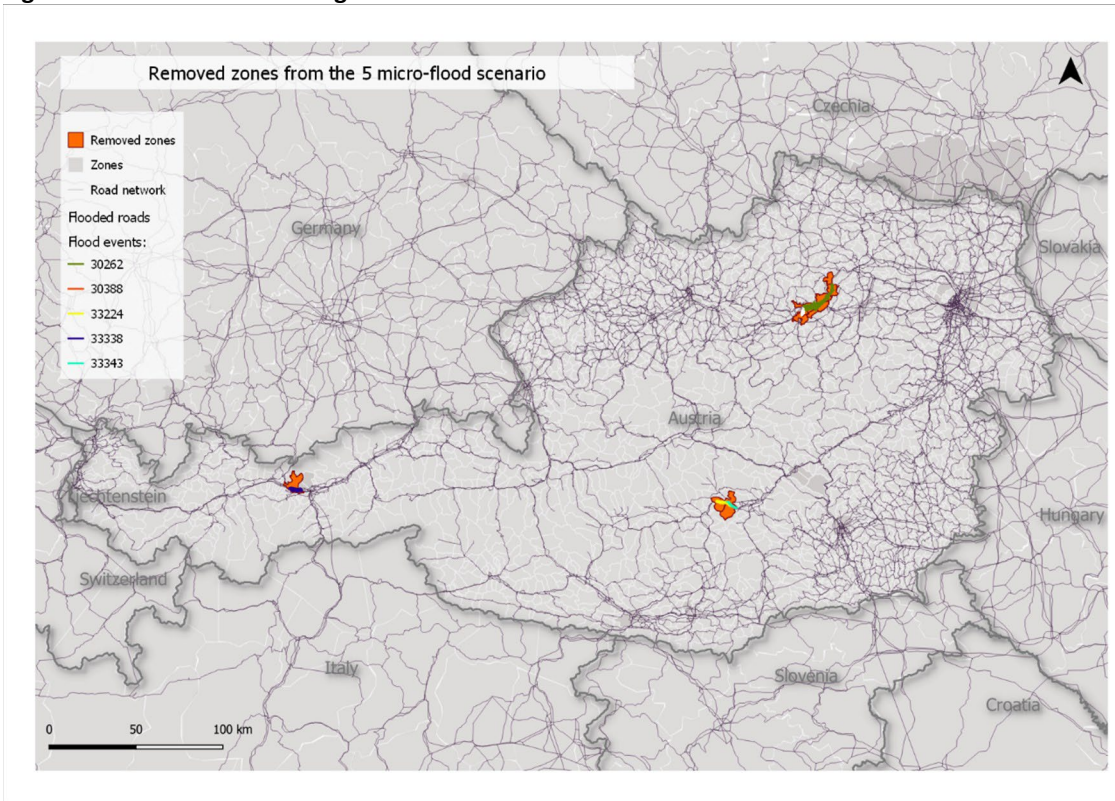

Figure 2.6.13: **Flooded road segments and removed zones for the '5 simultaneous floods' scenario.**

*This project has received funding from the European Union's Horizon 2020 research and innovation programme under the Grant Agreement No **776479.***

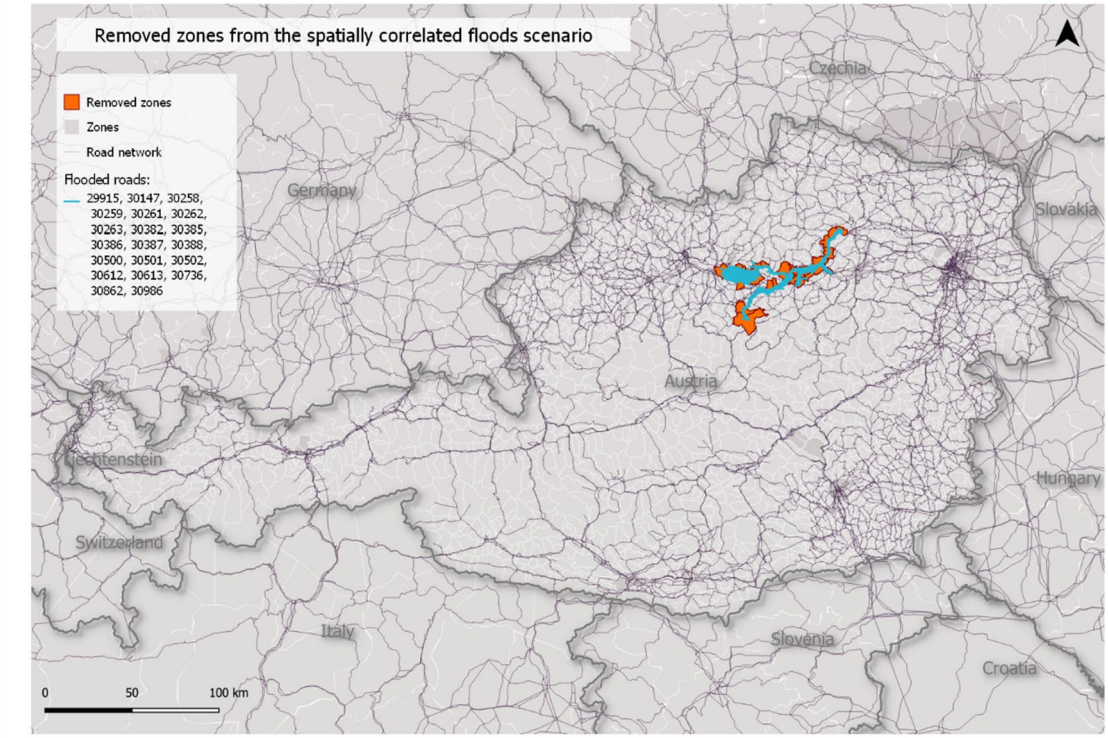

Figure 2.6.14: Flooded road segments and removed zones for the 'correlated floods' scenario.

*This project has received funding from the European Union's Horizon 2020 research and innovation programme under the Grant Agreement No **776479.***

Table 2.6.4*:* Percentage decrease of trips compared to a baseline of 'no flooding'. The flood scenarios are shown in Figures 2.6.9 - Figure 2.6.14. These percentages are used to correct the excess time values (see section 2.6.2)

Scenario	% trips taken out due to floods	
	cars	trucks
1	0.02%	0.40%
2	0.05%	1.16%
3	0.15%	2.73%
4	0.07%	1.87%
5	0.05%	1.16%
Correlated	0.08%	1.74%

In addition to excess travel time, some zones were removed from the analysis, including the connected trips. If we assume that these trips cannot take place within a full day, a loss of a business day of 8 hours and non-delivery of freight for 24 hours can be valued. The results are shown in Table 2.6.5. These results show that the cancelled trips, especially for cars, represent a much higher value than the excess time costs ranging from 1-11 Million for trucks and 13-86 Million euros for cars.

Table 2.6.5: Valuation of travel time lost due to detour and delay. The flood scenarios are shown in Figures 2.6.9 - Figure 2.6.14

Scenario	Cars time excess value	Trucks time excess value	Car trips cancelled (1 day) value	Truck trips cancelled (1 day) value	Total cost for cars	Total cost for trucks
1	1,127,505	894,078	13,544,061	1,600,980	14,671,566	2,495,058
2	2,667,453	2,179,363	27,606,658	4,681,795	30,274,112	6,861,158
3	2,002,813	2,375,699	86,037,859	11,033,293	88,040,672	13,408,992
4	1,632,011	2,138,832	40,826,553	7,534,732	42,458,564	9,673,564
5	1,930,076	1,300,666	28,575,352	4,687,083	30,505,428	5,987,749
Correlated	1,655,994	1,926,881	48,489,988	7,005,916	50,145,981	8,932,797

Discussion

In addition to the percolation analysis of national road networks (level 1), this level 2 analysis for Austria has shown what these interruptions imply for the actual traffic flows over the network, and the associated travel time losses.

The major share of costs originates from cancelled trips rather than from detour times. The total costs can add up to 88 million euro for cars and 13 million for trucks. So in total, the most disruptive event has a societal cost of 101 million Euro.The question is whether the severity of the disruptive impacts can be qualified as a climate induced socio-economic tipping point. For that, we also need to consider the likelihood of the event, which is less than 1:100 year. We then need to acknowledge that the damage found is less than 1% of the climate and weather induced damages currently observed annualy in Austria (Steininger et al., 2015, 2016, 2020), and can therefore not be considered as a 'real' tipping point like event with large macro- economic consequences. Climate change may cause an increase of this return period with a factor 2 to 10, or even a similar decrease, depending on which climate model projections are used (see Scoccimaro et al., 2020).

*This project has received funding from the European Union's Horizon 2020 research and innovation programme under the Grant Agreement No **776479.***

With respect to the modelling approach, the following issues need to be considered. First, the share of commercial travel compared to leisure, education etc. needs to be investigated, to attach better matching values of time. Now the values chosen are for business travel, which will lead to an overestimation. Second, the consequences of taking out zones needs extra consideration: what sort of trips are not happening and can they be valued similarly as the trips still occurring in the traffic model? Third, what will be the impact of accounting for modal split in the approach? For example, what if we also included railways in the analysis and allowed for alternative routing of goods when a road is blocked and vice versa? Finally, additional uncertainty to the damage costs in Table 2.6.4 is caused by the assumption made thata major flood event blocks traffic for only one day. In reality, this could be an underestimation, depending on the amount of adaptation that is taking place duringan event. As indicated in Section 2.6.2, additional indirect costs can arise from the delays that are not accounted for in these estimates. The just in-time supply chain disruption exemplifies such situations (see level 3 analysis).

Level 3 results

The product produced by the car & truck manufacturer relies on just-in-time deliveries from 10 different sites. The sites are located within a 2 to 8-hour drive from the factory. We have examined the risk that one of these inputs cannot be delivered in time, because the route between the factories is disrupted by a flood. As outlined in the method section, for each input product we first identify the most disruptive micro- flood (AoI) for the preferred route, then we iteratively find the additional micro-floods that cause the worst-case disruptions of the alternative routes. This search process is repeated until the worst combination of 7 micro-floods, with the most detrimental effects on the routes between the supplier and the car manufacturer.

The first finding is that for all suppliers, the most critical part of the route to the car and truck manufacturer are the direct access roads to the production site. These access roads are exposed to a flood risk in two different micro-flood scenarios. These two AoIs most likely will occur at the same time, during the same peak flow through the river adjacent to the site. In case of inundation of these roads, none of the goods can be delivered to the manufacturer because no detouring is possible. The flood causing the inundation of these roads will most likely also flood a small part of the manufacturing site itself. This seems to be a clear example of a socio-economic tipping point from the perspective of the manufacturer. It, however, does not so much result from a disruption of the supply chain, but rather of the production site itself.

The second finding is that one of the suppliers (supplier 1) is exposed to a flood risk as well. The model behaviour here is similar to the behaviour described under the first finding. When the access road to the supplier is flooded, there no longer is a way to reach the supplier, also not through any alternative.

When ignoring the micro-floods blocking access roads to either the supplier or the car and truck manufacturer, the increases of travel time due to other micro-floods look as in Figure 2.6.15. These travel times typically increase in a linear fashion, indicating that the road network is rather resilient in the sense that fairly good alternatives remain when the preferred routes are disrupted. For seven micro floods at

*This project has received funding from the European Union's Horizon 2020 research and innovation programme under the Grant Agreement No **776479.***

the same time, the absolute increase in travel time is 1 to 4 hours. The linear shape of the functions indicates that for each detour that needs to be taken caused by a disruption of an AoI, the travel time typically increases by some 8 to 35 minutes (Figure 2b). There are, however, some exceptions to this observation. The routes from suppliers 3, 5 and 6 have a relatively steep increase of travel time in both an absolute and relative sense. These three suppliers are located close to each other. The largest increase of travel times towards these suppliers already occurs for one AoI, which apparently hits a critical part of the route, for which a large detour is required.

The black lines in Figure 2.6.15(a) indicate max daily driving periods for truck drivers according to Regulation (EC) No 561/2006 (EC, 2006). Under normal conditions, a truck driver can drive a maximum of 9 hours per day. Two days per week, anexception to this rule can be made, and a drive of 10 hours is allowed. When this period is exceeded, a minimum of 9 hours rest is to be taken. In practice, this means that freight is delayed a full day.

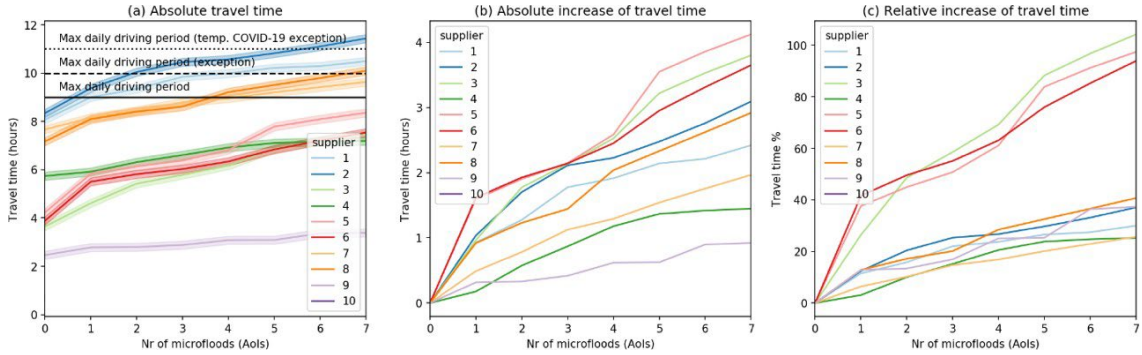

Figure 2.6.15: Increase in travel times for the worst-case flood disruptions from 10 suppliers delivering inputs for product 1, excluding congestion.
Panel a: black lines indicate max daily travel times according to Regulation (EC) No 561/2006, and its exceptions. The shaded areas around the lines indicate the margin for unloading time which also falls under the regulation.
Note that supplier 10, which is a stock building very close to the factory, is only affected by the two AoIs that were already filtered out, because they block all access to the factory.

Most suppliers in Figure 2.6.15 have a travel time below the maximum allowed driving times. In case of an exceedance of these thresholds, freight is delayed with a full day, because the driver will need to take a 9-11 hour rest and then needs to wait till the factory staff is present on the site again. A freight delay of one day will already cause a standstill in the production process because only 1 day of stock is held in the factory. Moreover, there can be additional spill-over effects from the car and truck manufacturer back to the suppliers, caused by the specific way in which the input products are packed and produced. Input products are not only packed, but alsoproduced in a very specific type of container, which is emptied at the destination site and then returned to the supplier. If these containers are not returned in time, the supplier cannot continue production of the input products.

Let us now zoom in on the results for supplier 6, to gain a better understanding of what is causing the relatively large increase in travel time on this route. Figure 2.6.16b shows that the first AoI corresponds to a large micro flood caused by the

*This project has received funding from the European Union's Horizon 2020 research and innovation programme under the Grant Agreement No **776479.***

flooding of a large river. This flood disrupts a major motorway used for transport from the supplier to the car manufacturer. The fastest detour when this part of the network is disrupted is 1 hour and 11 minutes routes longer than the preferred route. As shown in the other panels (a-f) of Figure 2.6.16, the detours for extra micro-floods are not adding as much travel time as this first one.

*This project has received funding from the European Union's Horizon 2020 research and innovation programme under the Grant Agreement No **776479.***

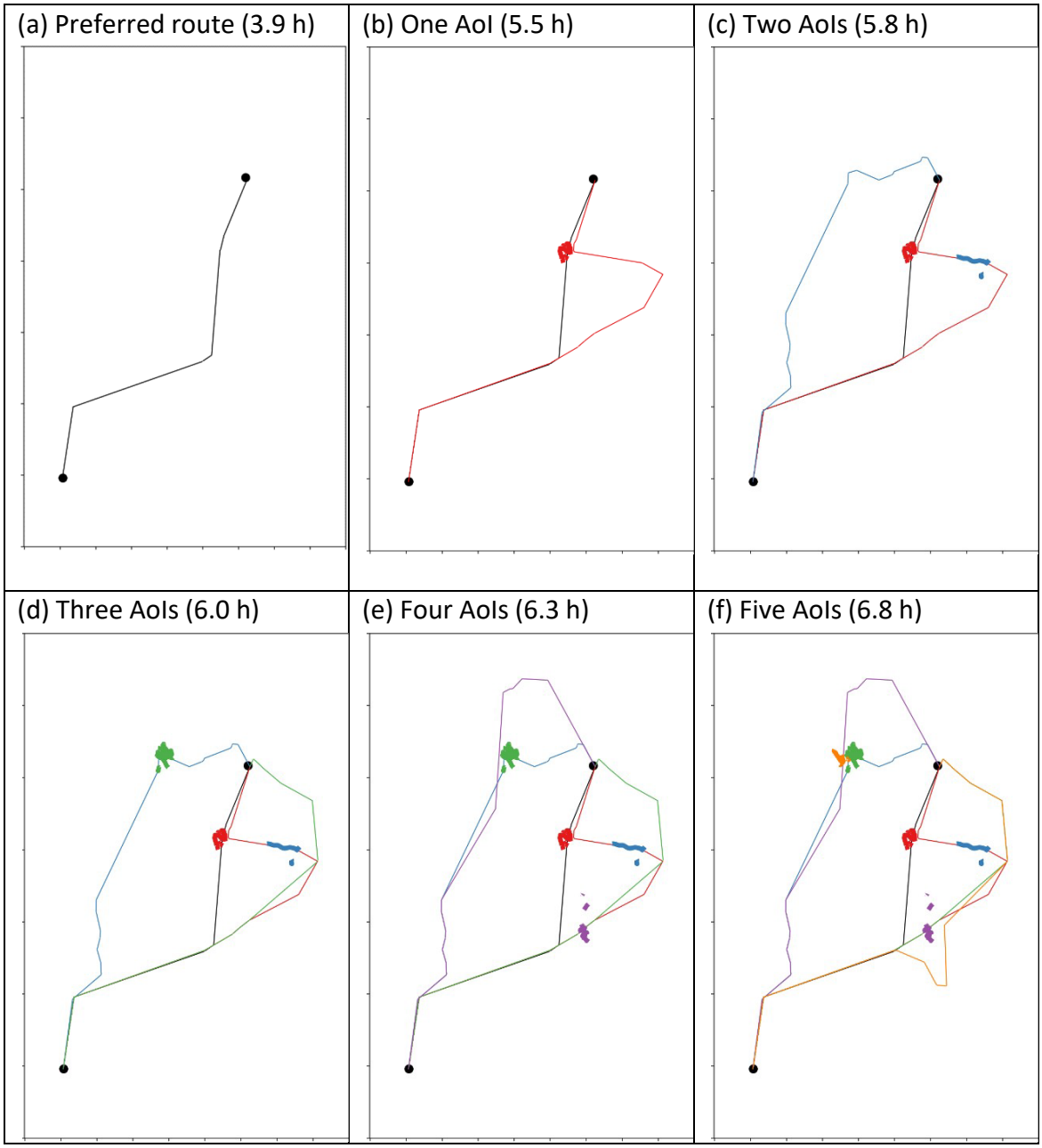

Figure 2.6.16: Illustration of the (re)-routing procedure for routes from supplier 6 to the car manufacturing factory. Colored thick lines (clusters) indicate the parts of the network disrupted by one micro flood (AoI). Colored thin lines indicate the alternative route that is taken when the network disruptions are taking place.

Discussion

The above analysis does show that a full delay due to flooding may be possible when legal driving times are exceeded for a few suppliers. The increases in travel time do currently not account for any congestion. Congestion effects on alternative routes in case of disruption of the preferred route may contribute largely to the travel time. However, for truck transport these effects may be partly mitigated by adapting driving and unloading times.

*This project has received funding from the European Union's Horizon 2020 research and innovation programme under the Grant Agreement No **776479.***

Although the search algorithm seemed successful in identifying combinations of micro-floods leading to relatively large disruptions, there is no guarantee that it identifies all the worst-case examples, because the complete uncertainty space is extremely big and increases when more detour options are considered, because each detour also may introduce new micro-floods on previously unused alternative routes. For example, there are 1.11 * 1013 combinations of 7 micro-floods out of 250 AoIs.

The locations of the car and truck manufacturing site and the suppliers seem to be chosen such that they are very well connected to the main road network. These choices also guarantee a large degree of resilience with regard to road network disruptions.

More importantly we also found that flooding at production and assembly side probably has the largest disruptive effects. From case studies in the literature we know that there are examples were SETP-like event occurred. One frequently mentioned example in the literature are the 2011 Thailand floods which inundated more than 800 industrial factories and estates, among which were many manufactures of car partsand electronic communications equipment17. When these manufacturers were asked to indicate the factors that contributed to losses in their supply chain, only 5% indicated that disrupted logistic channels were a factor, whereas 55% indicated that inundation of production facilities played a major role (Haraguchi and Lall, 2015).

2.7. Collapse of insurance markets for extreme weather risks

2.7.1. Definition of tipping point

Insurance uptake can decline when natural disaster risk increases as a result of climate change. Here we examine impacts of climate change on flood insurance markets in particular. Such problems with declining uptake of flood insurance mainly arise in voluntary flood insurance markets, when risk-based premiums become unaffordable or exceed perceived benefits of flood insurance, which are related to risk perceptions. Such a process may be exacerbated by climate change as this can cause risk-based premiums to rise sharply in certain areas, while flood risk perceptions and the related benefits from insurance are underestimated, as is often the case for low- probability- high-impact risk (Kunreuther & Pauly, 2004). In a worst case scenario, the lack of insurance uptake can result in a collapse of the flood insurance market in certain areas, which has been referred to in the literature as posing limits on the use ofinsurance as an instrument to adapt to climate change (Klein et al., 2015). Such a collapse can also be interpreted as a climate induced socio-economic tipping point, which is defined as "*a climate induced, abrupt change of an established socio- economic system's functioning into a new functioning of fundamentally different quality*" (van Ginkel et al., 2020).

[17] Most notorious is the inundation of the Western Digital factory, producing a large share of the world's hard disk. Production stopped for 46 days. Globally the price of hard disk surged (Haraguchi and Lall, 2015).

*This project has received funding from the European Union's Horizon 2020 research and innovation programme under the Grant Agreement No **776479.***

2.7.2. Contributing factors and occurrence of tipping point

The occurrence of an insurance tipping point is caused by declining demand, as a result of rising premiums and lacking willingness-to-pay for coverage. The demand for flood insurance is simulated in the "Dynamic Integrated Flood Insurance" (DIFI) model, which is a partial equilibrium model that uses climatic and socio-economic data projections, premium setting rules of the insurance industry, and household behavioural rules and decision models, which are assessed for various stylized flood insurance systems in EU countries up to 2080. A detailed description of the model and the output of insurance penetration rates is given in deliverable D3.2: Tipping point likelihood in the SSP/RCP space of the COACCH-project. A concise explanation of the tipping point is given here in order to improve understanding of the macroeconomic implications it can have for EU regions, which we describe afterwards.

In deliverable D3.2 the flood insurance tipping point is defined as projected flood insurance penetration falling below a threshold of 10% of the population in high- risk areas (1/100 year floodplains), and where the penetration rate in 2010 is above 20%. This definition shows how future climatic and socio-economic conditions can leadto a significant reduction of insurance demand, up to the point that it almost disappears. When flood insurance penetration declines to such an extent, insurance is no longer able to provide households with adequate financial protection against the growing threat of flooding as a result of climate change.

Table 2.7.1, below, shows the amount of NUTS2 regions per flood risk scenario and per country where an insurance tipping point is projected to occur between 2010 and 2080. The country name is followed by two numbers, the left number states the amount of NUTS2 regions where a tipping point is expected, and the number on the right gives the total amount of NUTS2 regions in that country. Most tipping point regions are projected under RCP4.5-SSP2 (10 regions), which may seem surprising, as the high-end climate change scenario RCP8.5-SSP5 (9 regions) is also considered. However, SSP5 projections predict a future with high income growth compared toSSP2, which reduces unaffordability of insurance and, therefore, can trigger a higher penetration rate. Despite small differences between the two scenarios, the results shown in Table 2.7.1 are quite robust to variations in climate- and socio-economic change. Furthermore, it can be seen that Eastern European regions are overrepresented in the table, which indicates that the most significant problems with low insurance uptake are found there. This can be explained by a combination of a high rise in riverine flood risk in these regions, as well as relatively low economic growth rates compared to Western European regions, as follows from the GLOFRIS output.

Table 2.7.1: Regions where a tipping point in flood insurance occurs by 2080, per scenario. The first number in brackets gives the amount of regions where a tipping point is projected, while the second number gives the total amount of NUTS2 regions in that country.

RCP4.5-SSP2	RCP8.5-SSP5
Croatia (1/2)	Croatia (1/2)
Bulgaria (1/6)	Bulgaria (1/6)

*This project has received funding from the European Union's Horizon 2020 research and innovation programme under the Grant Agreement No **776479.***

Czech (1/8)	Poland (6/16)
Poland (6/16)	Portugal (1/5)
Portugal (1/5)	

The tipping point regions identified in Table 2.7.1 are where flood insurance markets are expected to collapse due to disappearing demand for coverage, resulting from rising costs of insurance due to climate change. Because flood insurance markets may cease to exist in these regions, while the risk of flooding is expected to increase, households will become more financially vulnerable to flood damage. Instead of formal insurance arrangements, households will have to rely on possibly less reliable sources of funding, such as compensation by governments, which can be dependent on political motives, or private savings, which can be insufficient. The identification of these problems for future scenariossubstantiates the need for reforms of flood insurance systems. For example, insurance purchase requirements can prevent the demand for flood insurance from collapsing, while higher cross-subsidization of risk between risk groups can increase affordability. Also, replacing a private with a public reinsurer can suppress the costs of reinsurance. Although these reforms can be especially urgent for the identified tipping point regions, for other regions they may also be beneficial. In the following section we further assess the implications of an insurance tipping point using a macroeconomic general equilibrium model.

2.7.3. Macroeconomic implications

The macroeconomic analysis of the insurance tipping point considers all European regions but focusses particularly on those regions and scenario combinations, where tipping points occur as presented in Table 2.7.1. To be precise,we consider the two scenario combinations where the highest number of tippingpoints are projected, that is a socioeconomic development according to the SSP2 storyline with climate change according to the RCP4.5 and the SSP5 scenario with the RCP8.5 scenario (both concentrations pathways are forced with the HadGEM2-ES GCM). As the COIN-INT model is consistently used for multiple analyses in the project, there is a trade-off with respect to the detail on the regional and sectoral aggregation as it cannot be the optimal for every scientific question. This implies that the individualtipping regions from the bottom-up analysis are not modelled as separate countries in the COIN-INT CGE model. However, the relevant countries (Croatia, Bulgaria, Czech Republic, Poland and Portugal) are included in two aggregates: the Mediterranean and South-Eastern EU 27 (MEU) entails Portugal, Bulgaria and Croatia, and the Central EU 27 + Switzerland (CEU) entails the Czech Republic and Poland. It is important to note that the MEU in addition includes Cyprus, Greece, Malta, Spain, Romania, Albania and the Rest of Europe (Bosnia and Herzegovina, Macedonia, Serbia and Montenegro,Faroe Islands, Gibraltar, Monaco, San Marino) and the CEU additionally contains Hungary, Slovenia, Slovakia and Switzerland. Thus, model results for the two relevant aggregates are moderated by less severe effects in these other regions of the aggregates. Moreover, as the DIFI model is restricted to EU regions, we also do not have insurance data for some countries in the aggregate such as Albania or Switzerland.

*This project has received funding from the European Union's Horizon 2020 research and innovation programme under the Grant Agreement No **776479.***

In the following, we describe the specific modelling approach for the macroeconomic insurance tipping point analysis and give the details on the operating principles of the performed scenario analysis as well as on the implementation of data stemming from the hydrological impact model GLOFRIS (Ward et al, 2017; Winsemius, 2016) and the partial equilibrium model of the flood insurance sector (DIFI). Figure 2.7.1 gives a conceptual overview of the interaction of the applied models and which type of data is used for further procedure in the subsequent model. The common features of the COIN-INT model have been described in section 1.2.2 and in more detail in the Appendix section 5.1.

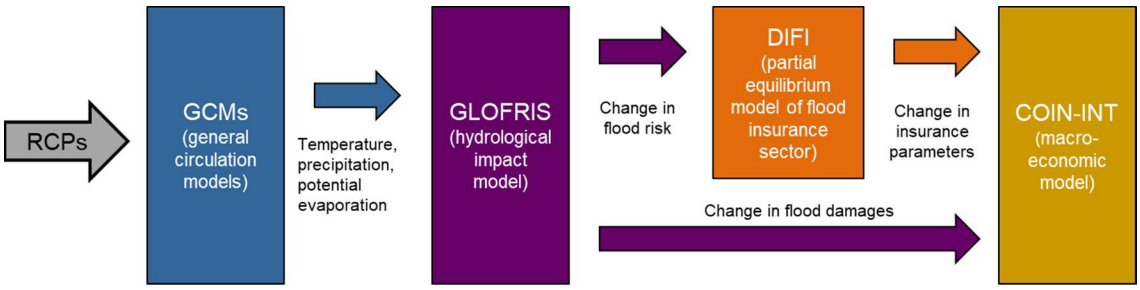

Figure 2.7.1: Conceptual overview of the model chain in the insurance tipping point analysis.

As the macroeconomic model entails two agents, the private and the public agent, flows can be modelled between these two agents but not within one agent. Thus, insurance premiums (consumption of a private household from the insurance sector) are only explicitly modelled for a change in premiums due to climate change or due to a change of the underlying insurance market system. The difference of the paid premium is modelled as a shift in consumption patterns (increasing or reducing the demand for insurance output and respectively reducing or increasing other consumption equally). With an insurance coverage of 100%, the premiums always cover the incurred damage. However, in an insurance system where uptake is voluntary, the insurance penetration rate is usually much lower than 100%, which means that uninsured households affected by flooding require alternative funds to recover the damage. The private agent either needs to reduce its savings or receives compensations payments by the public household via transfers. Transfers range from zero to the total of uncovered risk, depending on the insurance market system and the common practice of the regions' government as to how it handles disaster losses.

In the countries where an insurance tipping point is projected (Croatia, Bulgaria, Czech Republic, Poland, and Portugal) governments have provided ex-post disaster relief for riverine floods in the past (OECD, 2016; Le Den et al., 2017; Maccaferri et al., 2012). However, with the exception of Poland, where government compensation for flood losses is considered a form of social assistance, ex-post government compensation for damage caused by floods are not explicitly mentioned in national law, and is therefore risky to fully rely upon. Besides the probability that governments of these countries will provide damage relief, the amount of damage thatwill be covered is uncertain.

Some insurance market systems might incentivize policyholders to engage in private adaptation measures, such as dry-proof or wet-proof measures. Expenditures

*This project has received funding from the European Union's Horizon 2020 research and innovation programme under the Grant Agreement No **776479.***

for these adaptation measures are modelled as consumption from the construction sector (shift in consumption patterns) and can decrease the extent to which the expected annual damage (EAD) translates into destruction of capital in the first place. The reduction of damages is calculated based on the benefit-cost ratio introduced in Aerts (2018). Whatever is destroyed, however, needs to be replaced. This replacement enters the model as consumption from the construction sector and is not welfare enhancing as it only restores the original state of welfare and individuals are not better off by this consumption. Also depending on the insurance market system, the public household may provide reinsurance to private insurers. In that case, there is a reinsurance premium paid by the private agent to the public household in form of a transfer.

An important assumption is that in the long run and on the aggregate level insurance companies pay out slightly less than what they collect through premiums as they would otherwise go out of business. They charge an additional fee for administration costs and to cover their risk aversion to be prepared for unexpectedly large floods. Insurers base their premiums on the EAD, while pay-outs after a flood can clearly exceed or fall below premiums collected throughout a year. As insurance is meant to spread the risk over time and space, damages in a certain year or location may exceed the collected premiums, however the insurer can recover from this loss by surpluses in other regions or in the past and future.

Climate impact data is provided by the GLOFRIS model for the years 2010, 2030, 2050 and 2080. The exposure relies on SSP scenarios: Exposed assets and household income growth are estimated using GDP growth, and exposed population is determined by population growth. For some regions projections suggest a reduction ofdamages despite the growing assets at risk, as the combination of certain emission scenarios and GCMs entail less precipitation and result in some regions getting dryer. Flood impacts enter the model in three different ways:

- For every SSP-RCP combination, flood damages reduce the effectively usable capital stock by reducing the capital endowment of the private household representing the destruction of assets. The amount of damage is based on data from the GLOFRIS model and reflect average effects (EAD, expected annual damages).
- The costs of dikes and other flood protection structures are depicted as investments to maintain the current level of protection that crowd out other investments. The investment and maintenance costs of flood protection standards are also obtained from the GLOFRIS model.
- Ongoing maintenance costs to prevent a decay of protective structures amount to 1% of annual investment costs and are modelled as consumption expenditures that crowd out other consumption possibilities of the governmenthousehold as this is usually the entity taking care of large protective structures.

The definition of the tipping points as they are described in Section 2.7.1 include dynamic elements, i.e. change of penetration rate over time, and apply for the period of 2010 to 2080. The macroeconomic model, however, has not been set up togo beyond 2050 as socioeconomic developments thereafter are highly uncertain. In

*This project has received funding from the European Union's Horizon 2020 research and innovation programme under the Grant Agreement No **776479.***

order to still be able to model the implications of the identified insurance tipping points and to capture dynamic developments, we performed some adjustment on the output data from the DIFI model and complemented the comparative static version of the COIN-INT CGE model by an exogenously calculated capital accumulation path.

With respect to the time-steps used in the DIFI model, which shows the occurrence of insurance tipping points mainly in 2080 and not in 2050, we had to adjust the macroeconomic analysis to be able to capture the relevant parameters for 2080 that flow from the DIFI model to the COIN-INT model. To do this, we computed the ratios of the data for the state of the climate in 2080 (for the two RCPs 4.5 and 8.5) relative to the GDP in 2080 based on SSP aligned GDP projections and applied the same ratio to the 2050 GDP as the impact shock in 2050. The purpose was to shock the economy adequately in proportion and not with the values from 2080 that are too high for 2050. Considering the exogenously calculated capital accumulation path, we compute two types of pathways: one with no climate change but socioeconomic change, i.e. for SSP2 and SSP5 scenarios, and one with both socioeconomic and climatechange, i.e. RCP4.5-SSP2 and RCP8.5-SSP5. The development of the climate change capital stock is based on the amount of uncovered risk in each country and whether governments compensate for the damages. In case repair costs need to be financed by households themselves, we assume that savings are reduced accordingly. As savings equal investments in one period and translate into capital stock in the following period, the reduction of savings lead to a lower capital stock. In line with the sectoral tipping point analysis, we consider the development until 2080, calculate the ratio of the lower capital stock to the GDP in 2080 as a scaling factor and apply the same ratio to the GDP in 2050 to obtain the equivalent reduction of the capital stock in 2050. The lower capital stock is then implemented in the CGE model via a reduction of the capitalendowment of the private household.

At this point, it is important to note that the analysis of macroeconomic effects further differs from the sectoral tipping point analysis with respect to the point of reference. As stated earlier, the definition of an insurance tipping point is based on a dynamic element, where a potential state in 2080 with a given socioeconomic and climate development is compared to a starting point in 2010. Then, the different developments across multiple scenario combinations are compared with each other. In contrast, the macroeconomic scenario analysis compares two potential states at the same point in time, one with socioeconomic but no climate change (baseline scenario) and the other with socioeconomic and climate change (impact scenario) and thus the implemented shock only represents the deviation from the counterfactual.

Results of macroeconomic assessment

While the detailed analysis on the NUTS2-level shows that there are several regions severely affected by climate change induced decline of insurance uptake, the macroeconomic analysis suggests that from a comprehensive perspective, tipping points do not necessarily transform into a “macroeconomic” tipping point. One reason for that is that regional differences are large within countries and even more so within model aggregates and therefore effects tend to balance on the aggregated level. Another reason is that the economy and the model alike are composed of multiple

*This project has received funding from the European Union’s Horizon 2020 research and innovation programme under the Grant Agreement No **776479.***

interacting sectors, where relative prices allow (and force) agents to adjust without abrupt and fundamental changes. However, when implementing the cumulative effects over time of reducing savings and thereby the capital stock (to be more consistent with the insurance tipping point definition), macroeconomic impacts can become quite extreme considering typical CGE modelling results.

We first describe overall results patterns and then look into details on the differences between regions based on their insurance system background as well as differences between the two chosen scenarios RCP4.5 with SSP2 and RCP8.5 with SSP2, where most tipping points occurred under the sectoral assessment. Finally, we also investigate the effects on the public budget.

Figure 2.7.2 shows the effects on the main macroeconomic indicators GDP and welfare, whereby we differentiate between private and public welfare as we are interested in both agents. The underlying shock includes both the direct climate change impact on flood damages (data from GLOFRIS) as well as the change in insurance parameters (data from the DIFI model). For each region, the figure shows first effects in the lower emission scenario with average socioeconomic development (RCP4.5-SSP2) and then in the higher emission scenario with low socioeconomic development (RCP8.5-SSP5). The impact is negative for all indicators in all regions and all scenario combinations, except for negligible positive impacts on UK's GDP in the lower emission scenario, where impacts are small anyway and after-flood repair activities can contribute positively to GDP.

In general, an important differentiation between GDP and welfare effects is that construction activities increase GDP but do not increase welfare if it is considered to restore the original state before a flood event occurred. Thus, negative effects on welfare (considering the sum of private and government welfare) are much larger than on GDP. While GDP effects range from 0% to -3.2%, private welfare losses range from -0.4% to -3.5% and government welfare losses from -0.8% to -7% with the minimum always for the UK and the maximum always for the Netherlands.

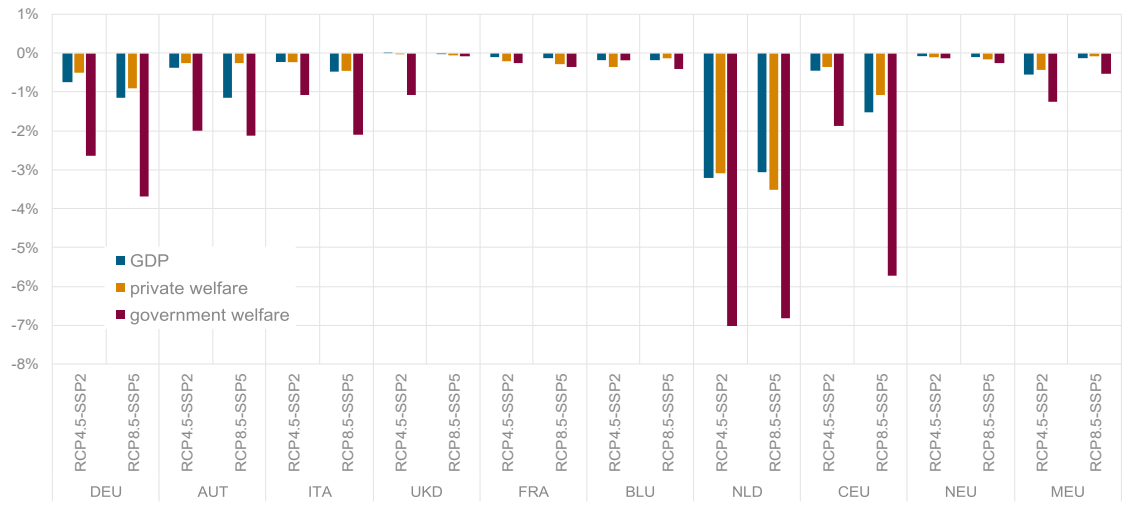

Figure 2.7.2: Effects on macroeconomic indicators: GDP, private welfare and government welfare for European model regions in the two tipping point scenario combinations RCP4.5-SSP2 and RCP8.5-SSP5.

*This project has received funding from the European Union's Horizon 2020 research and innovation programme under the Grant Agreement No **776479.***

Comparing the severity of effects across regions, the strongest impacts as just stated occur in the Netherlands, where flood damages strongly increase with climate change for a given socioeconomic development. In the higher emission scenario (RCP8.5-SSP5) also the CEU region is heavily affected, including the tipping countries from the sectoral analysis Czech Republic and Poland, with GDP losses up to -1.5% and total welfare losses up to -6.8% (sum of private and government welfare). Also, Germany, Austria and Italy experience large impacts in the climate change scenarios, RCP4.5-SSP2 and RCP8.5-SSP5, compared to the baselines with no climate change, SSP2 and SSP5 respectively: Germany incurs GDP losses up to -1.2% and total welfare losses up to -4.6%, Austria GDP losses up to -1.2% and total welfare losses up to -2.4% and Italy GDP losses up to -0.5% and total welfare losses up to -2.6%.

Differences across regions occur to a large extent based on the different insurance market systems in place and the different practices when it comes to handling uncovered risk. While we for example assumed, that 30% of private damages in Austria are covered by the government as there is the established system of a disaster fund, damages in most CEU regions need to be covered by private households themselves. Besides the CEU region, the second relevant regional aggregate for the insurance tipping regions MEU shows GDP losses up to -0.6% and total welfare losses up to -1.7%, with larger damages occurring in the lower emission scenario as SSP2 income growth is projected to be lower than in SSP5, which can imply higher rates of unaffordability of insurance premiums, lower uptake of flood insurance, and thushigher uncovered risk. As there are compensation payments in most MEU regions with an assumed compensation coverage of around 20% and as the insurance system in these regions does not incentivize adaptation measures, the incentivized adaptation benefit decreases in the climate change scenarios implying higher damages.

Overall, regions with the lowest impacts include the UK, France and the BLU regions entailing Belgium and Luxembourg, where the insurance system is either a public-private partnership or a solidarity system, both of which systems maintain mandatory insurance uptake. This implies that there is no uncovered risk and households do not need to reduce savings to finance repair costs nor do governments have to issue compensation payments.

Considering the magnitude of effects, impacts tend to be stronger with the higher emission scenario (RCP8.5) and the SSP5 development, however, this is not necessarily the case for all regions. As has been described in the sectoral tipping point analysis (see deliverable D3.2), socioeconomic developments according to SSP5 project a future with higher income growth as compared to SSP2, which can reduce the unaffordability of insurance and, therefore, can trigger a higher penetration rate. As a consequence, there are less uninsured damages that reduce savings and the capital stock in a voluntary system.

An important driver of the results is the change in the rental rate of capital. Figure 2.7.3 shows how climate change induced flooding affects the price of capital across model regions and for the two scenario combinations RCP4.5-SSP2 and RCP8.5- SSP5. Changes range from below 1% increase in the UK, France (FRA), Belgium and Luxembourg (BLU) and the Northern EU countries (NEU) to an increase of 10% in the Netherlands (NLD). A substantial rise can also be observed for Germany (DEU) and the

*This project has received funding from the European Union's Horizon 2020 research and innovation programme under the Grant Agreement No **776479.***

Central European region (CEU). The patterns of clearly resemble the patterns in Figure 2.7.2 showing the overall economic effects.

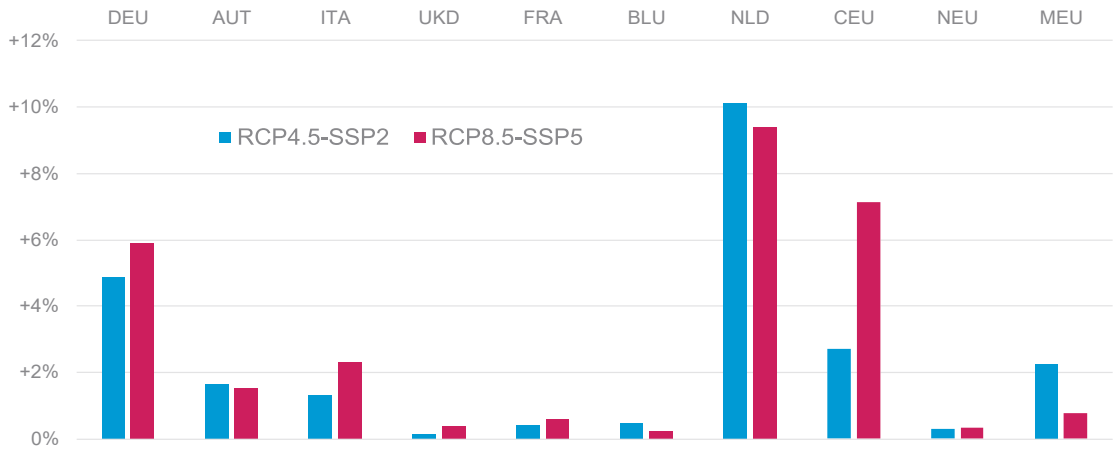

Figure 2.7.3: Change in the rental rate of capital in model regions and for the two tipping point scenario combinations RCP4.5-SSP2 and RCP8.5-SSP5.

As a consequence of the increased capital price, the production activity ofcapital-intensive sectors decreases in the respective regions. Depending on the severity of effect and the (forced) demand for reconstruction activities, overall production can be partly compensated by increased production in the construction sector and in other competitive sectors. However, overall consumption also declines in the climate change scenarios compared to the baseline scenarios. This is also visible in Figure 2.7.4, which presents a decomposition of the GDP effects for the contributions of private consumption, government consumption, investments, exports and imports. Thus, investigating the effects on GDP reveal that the reduction in private and government consumption is a large negative contributor in all regions. Figure 2.7.4 alsoshows the net effect of the GDP change as imports increase in most regions. Asdomestic production becomes more expensive, regions tend to import from other countries, where the costs of production have in relative terms improved. The opposite is true for exports, less goods are exported as their prices must increase based on the risen costs of production.

*This project has received funding from the European Union's Horizon 2020 research and innovation programme under the Grant Agreement No **776479.***

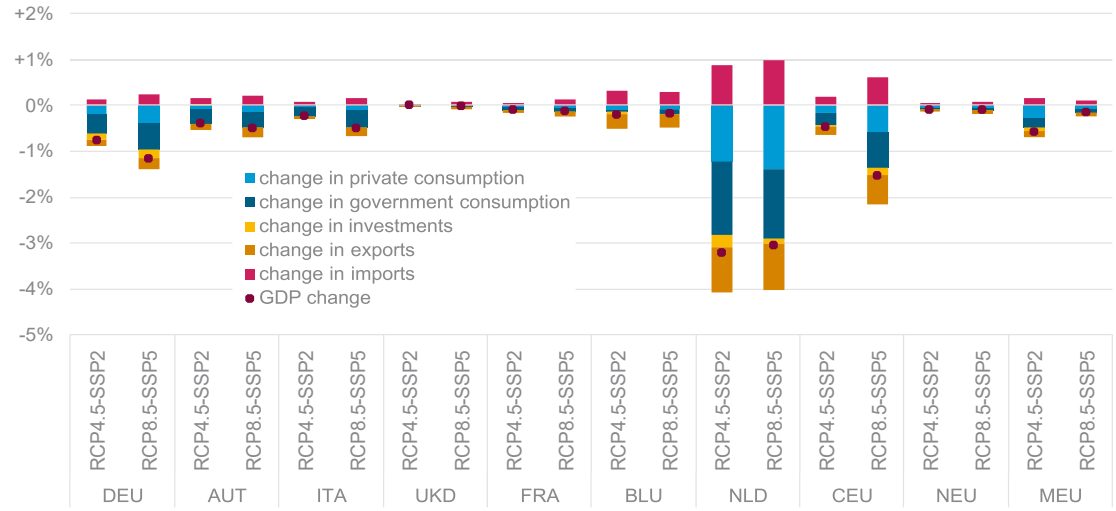

Figure 2.7.4: Decomposition of GDP effects for changes in private consumption, government consumption, changes in investments, and changes in exports and imports (stacked bars), as well as showing the net effect (dot) for model regions and for the two tipping point scenario combinations RCP4.5-SSP2 and RCP8.5-SSP5.

With a focus on the public household, government welfare decreases as government income decreases from various sources, but especially from the factor tax income (see Figure 2.7.5). This is because the destruction of capital triggers a scarcity effect of that factor and thus implies its rent to increase. As a consequence, the employment of this factor decreases and thereby reducing the tax base for the factor tax. With lower income, government consumption necessarily needs to decrease as well yielding a reduction of government welfare.[18] While we refer to the public and the private households as two separate agents, one has to be careful about interpreting government welfare: as public consumption to a very large extent includes the provision of public goods and services, it is highly relevant for the private household and its welfare too. In addition, the increase of relief payments via transfers due to higher climate change damages reduces the government's disposable income.Moreover, the negative effect on the private household's welfare can be partly absorbed by these transfers. Given the national practices of handling ex-post relief payments, transfers in the higher emission scenario (RCP8.5-SSP5) are twice as high as in the lower emission scenario (RCP4.5-SSP2) for Germany, Italy and the CEU region. Low transfers also apply for the Northern EU region (NEU), the MEU region and Austria.

[18] Note that this is only true given the modelling choice of not allowing to incur public debts.

*This project has received funding from the European Union's Horizon 2020 research and innovation programme under the Grant Agreement No **776479.***

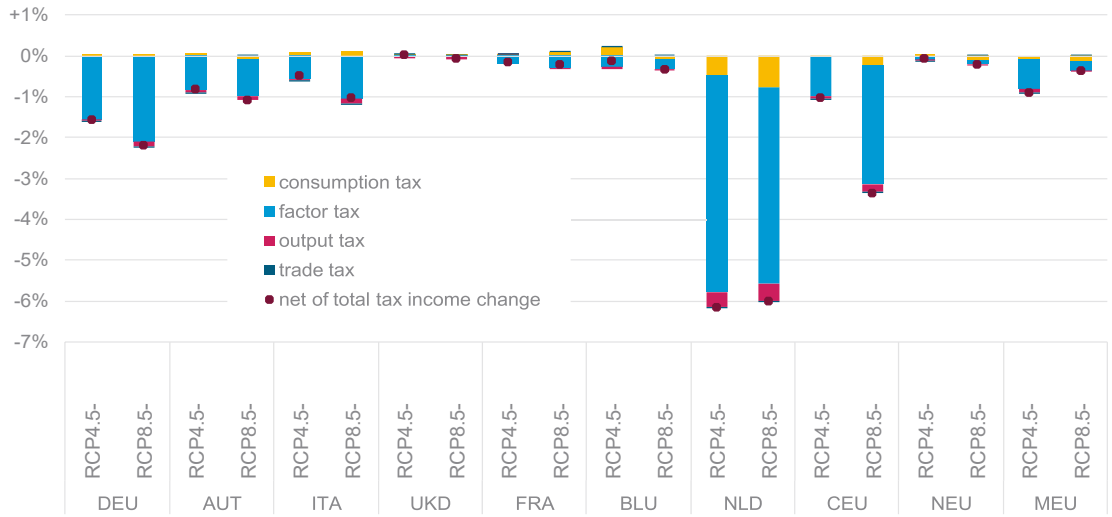

Figure 2.7.5: Decomposition of tax income change for consumption, factor, output and trade tax (stacked bars), as well as for the net of total tax income change (dot) for model regions and for the two tipping point scenario combinations RCP4.5-SSP2 and RCP8.5-SSP5.

As the reduction in consumption tends to be smaller in the RCP4.5-SSP2 than in the RCP8.5-SSP5 scenario, the effect on the consumption tax (the tax that is applied to all goods that are either used as intermediate input in production or for final demand use) is also smaller in the lower emission scenario for Austria and the Netherlands. For some other regions (BLU, NEU and MEU) the effect is even slightly positive in the lower emission scenario, but turns negative in the RCP8.5-SSP5 scenario. As the negative shock on factor prices also affects the competitiveness in production, most regions see a decrease in production quantities, which again lowers the specific tax base and thus the income source for the government. The trade tax income change is only minor and direction depends on whether a country's reduction in exports or increase in imports prevail. Overall, however, the net of tax income changes remains negative in all regions and scenario combinations.

2.8. Climate induced economic shocks

This assessment is based upon the application of two macro-economic assessment models used in the COACCH project: the ICES CGE model and the CLIMRISK model (for models characterization see COACCH D2.1 (Bosello and Parrado, 2018). Both models eventually describe the impacts of climate change on the "regional" economic performance, but while GDP effects in the ICES model are derived through a full description of market functioning, those assessed by CLIMRISK are based on the use of reduced-form damage functions. It is thus particularly interesting to compare the outcomes from these two different approaches. Furthermore, complementarity across the two modelling methodologies is also given by the fact that, while ICES can be more precise in capturing market dynamics, the uncertainty analysis of CLIMRISK can be richer spatially and more complex.

*This project has received funding from the European Union's Horizon 2020 research and innovation programme under the Grant Agreement No **776479.***

2.8.1. Definition of a tipping point

The tipping point of climate induced economic shocks can be defined as a point at which unprecedented shocks are experienced that could significantly destabilize the economy. In the deliverable D3.2: Tipping point likelihood in the SSP/RCP space, the following conditions were explored as potential candidates for socio-economic tipping points through the use of the integrated assessment model (IAM) CLIMRISK:

1. A loss of €10 million in (2015 PPP) at the local level (0.5ºx0.5º)
2. A 5% annual loss of GDP at the local level (0.5ºx0.5º)
3. A "Very High" Multivariate Risk Index (MVRI), which means that at the local level a threshold of 4ºC or more in annual temperatures is exceeded, annual precipitation declines with at least 10%, and economic impacts exceed 5% of local GDP.

Among these, the second "candidate", GDP loss, is also the one more closely related to the macroeconomic underpinning of the ICES CGE model. On the one hand, GDP effects are the typical higher order economic impact indicators produced by CGE models, on the other hand they fit better than the other two to the geographical resolution of ICES based upon (NUTS2/1) administrative units rather than spatial-explicit areas ("grids" like in CLIMRISK). GDP losses will be thus used to characterize the economic tipping point with the ICES model. More specifically, the analysis performed under COACCH D2.7 is used to highlight when and where under all the SSPs/RCPs combinations considered, and the joint occurrence of the impacts cathegories analyzed, EU NUTS areas can experience a GDP loss larger than 5%.

The CLIMRISK model could perform a richer analysis considering that, the above-mentioned measures may not adequately relate to the country or location- specific tipping points as the threshold is set uniformly for the entire grid. In other words, the loss of €10 million or 5% loss of local GDP is not placed into perspective of past economic impact experience of a specific location.

In order to more accurately measure the occurence of climate-induced economic tipping point, we use a measure of the time of emergence of impacts (ToEI) of climate change, a concept closely related to the time of emergence (ToE) in climate sciences. Namely, the ToE can defined as the point in time where the observed climate signal diverges significantly from the defined baseline period signal (King et al., 2015). Hawkins & Sutton (2012) further explore the long-term inter-annual temperature variability for various GCMs and estimate the ToE of climate change for each of them.A similar methodology was applied by Mora et al. (2013) where authors identify the first year of where extreme temperatures exceed the natural climate variability of the post-industrial revolution era. ToEI can be used to estimate the first year in which impacts exceed a set past impact threshold. Exceeding such thresholds of high damages can signal that a tipping point is reached and an economic shock from climatechange may occur. More specifically, we aim to examine where, when, and under which climate conditions such damages occur in Europe.

*This project has received funding from the European Union's Horizon 2020 research and innovation programme under the Grant Agreement No **776479.***

2.8.2. Identifying tipping points with CLIMRISK

The estimation procedure for the time of emergence of impacts can be defined as follows. Let X denote the logarithms of an economic time series[19]:

Equation 1

$$\boldsymbol{X} = \{\boldsymbol{x_1}, \boldsymbol{x_2}, \dots, \boldsymbol{x_n}\}$$

This data can be on any cross-sectional scale if it represents a time-series of economic output. The annual economic time-series of output data was collected from the Maddison Database (Bolt, Inklaar, de Jong, & Luiten van Zanden, 2017). The data for most countries is available since year 1950, providing a historic period of over 50 years for the computation of the ToEI of climate change.

The past economic output time series can be decomposed into a trend component ($\boldsymbol{\tau}$) and a cyclical component ($\boldsymbol{c}$):

Equation 2

$$\boldsymbol{x_n} = \boldsymbol{\tau_n} + \boldsymbol{c_n}$$

The decomposition can be done using a set of filters common in macroeconomic analysis of business cycles (Mills, 2003). The filters include Hodrick-Prescott (Hodrick & Prescott, 1997), Christiano-Fitzgerald (Christiano & Fitzgerald, 2003) and Baxter King filters (Baxter & King, 1999)**.** The cyclical components constitute a time-series $\boldsymbol{C}$:

Equation 3

$$\boldsymbol{C} = \{\boldsymbol{c_1}, \boldsymbol{c_2}, \dots, \boldsymbol{c_n}\} \quad \textbf{, where } \boldsymbol{C} \in \textbf{R}$$

We can obtain a set of past negative output deviations from the long-term trend by further isolating the negative values of the time series of the cyclical component. We label this set $\boldsymbol{C^-}$ and it represents a set of negative deviations of the economy from the long-term trend:

Equation 4

$$\boldsymbol{C^-} = \{\boldsymbol{c_1}, \boldsymbol{c_2}, \dots, \boldsymbol{c_m}\} \quad \textbf{, where } \boldsymbol{C} \in \boldsymbol{R^-}$$

The set of shocks estimated for any given European country is stored as a vector of values which can be compared against a user-defined historic shock threshold.

Next, the time series estimates of future impacts, defined as D, is required for comparison against past shocks. The future impact projections are generated through the CLIMRISK IAM. CLIMRISK is a global IAM that assesses the dynamic economic impacts of climate change at the 0.5◦x0.5◦ scale for various socioeconomic and climate change projections.[20] Formally, future impacts are defined as follows:

[19] Economic output could refer to total output, sectoral, firm level output or other.
[20] The full description of the CLIMRISK model can be found in D2.1.

*This project has received funding from the European Union's Horizon 2020 research and innovation programme under the Grant Agreement No **776479.***

Equation 5

$$D = \{d_{t}, d_{t+1} \ldots, d_{t+z}\}$$

, where t and z are the first and last year for which the projections are available and t > n, implying that the first year of impact projections must be after the last year of past observed impacts.

The ToEI is estimated by comparing the distribution of past economic shocks with the projected climate impacts:

Equation 6

$$\boldsymbol{ToEI} = \boldsymbol{t} + \sum_{\boldsymbol{i}=\boldsymbol{0}}^{\boldsymbol{z}} \boldsymbol{b_i}$$

, where $\boldsymbol{b_i}$ is a Boolean value for year i indicating whether the impact projections have exceeded a pre-determined shock threshold. Formally, it is defined as follows:

Equation 7

$$b_i = \begin{cases} 0 & for\ d_t\ 2: c^* \\ 1 & for\ d_t < c^* \end{cases}$$

, where $\boldsymbol{c}^*$ represents a percentile value from the set $\boldsymbol{C}^-$ that is first sorted by magnitude of shocks. In this report, the threshold is set to 95th percentile of the past economic shocks as a representation of extreme impacts.

Contributing factors and occurrence of tipping point

The occurrence of the tipping point (ToEI) is heavily dependent on the choice of the impact threshold. The threshold represents a draw from the pool of past economic impacts of a specific location. Relatively high values (>95th percentile) representing high past impacts are more difficult to be exceeded by future developments of climate change.

The occurrence is also determined by the impact projections which are, in turn, determined by the climate and socioeconomic projections. The results are available for many climate (RCP 2.6, RCP 4.5, RCP 6.0 and RCP 8.5) and socio-economic scenario combinations (SSP1, SSP2, SSP3, SSP4, SSP5). Fossil fuel driven developments (eg.SSP5) are likely to lead to high levels of economic growth but also high exposure and higher climate risk. Such a development is expected to shorten the ToEI and lead to unprecedented impacts sooner within the century.

The climate projections are made using MAGICC, a reduced-complexity model of climate change widely used in the research community to project future climate impacts (Meinshausen et al., 2011)21. The MAGICC annual global temperature

[21] For more information, please refer to Deliverable 3.2 ST8

*This project has received funding from the European Union's Horizon 2020 research and innovation programme under the Grant Agreement No **776479.***

projections represent the difference in annual mean temperatures with respect to year 1900. Future temperatures are drawn probabilistically by imposing a triangular probability distribution for the climate sensitivity parameter in MAGICC. This triangular distribution in question is centred around a lower limit of 1.5ºC, an upper limit of 4.5ºC and a mean value of 3ºC for climate sensitivity (IPCC, 2014). This distribution of temperatures is the source of uncertainty in the model and presents the likely developments of future climate that is commonly found in the literature (Stocker et al., 2013).

The UHI effect is another contributing factor to the ToEI of emergence and its inclusion in the model contributes to the likelihood of the tipping point occurence. Namely, urban areas are expected to experience higher impact due to climate change than non-urban areas as cities account for about 80% of global GDP and about 50% of global population (Dobbs et al., 2011; Re, 2004). In addition, urban cells are expected to experience higher local temperatures due to the replacement of natural surfaces with structures of higher thermal capacity (concrete, asphalt etc.), leading to local climate change effects (Estrada et al., 2017).

Macroeconomic implications

The implications of exceeding the ToEI in Europe could be unprecedented as the climate impacts have the potential to exceed past economic impacts in many areas under certain climate and economic scenarios.

The time of emergence of impacts (ToEI) in Europe is expected to occur past year 2100 in case of strict climate mitigation policy, as plotted in **Errore. L'origine riferimento non è stata trovata.**. However, this threshold can be exceeded in Western Europe and parts of Scandinavia after 2060 in the case of RCP 8.5 – SSP5 “business-as- usual” policymaking. The significantly later occurrence of ToEI under the RCP 2.6 scenario suggests that abiding by the climate policy consistent with the Paris Agreement can significantly reduce the risk of ToEI occurrence. More extreme realizations of annual mean global temperatures would contribute to the occurrenceof the ToEI tipping point as the projected climate impacts would be higher. An important observation from the results presented in **Errore. L'origine riferimento nonè stata trovata.** is that most developed countries in Europe are facing a higher risk of ToEI due to their history of relatively minor economic shocks compared to the otherEU and non-EU countries. This observation is inherently present in the model as ToEI is a measure that is relative to past economic shocks.

*This project has received funding from the European Union’s Horizon 2020 research and innovation programme under the Grant Agreement No **776479.***

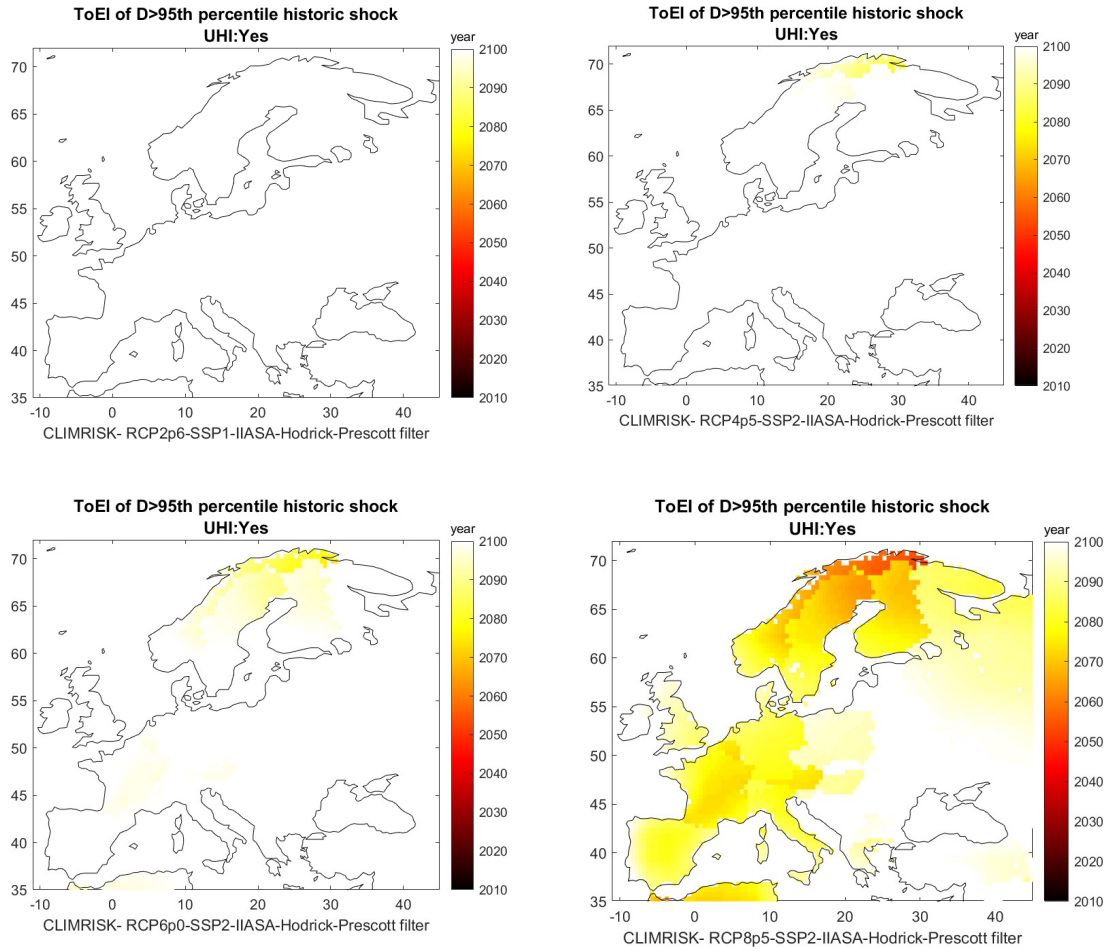

Figure 2.8.1: Climate scenario implications for the occurrence of ToEI under RCP 2.6 – SSP1, RCP 4p5 – SSP2, RCP 6p0 – SSP2 and RCP 8.5 – SSP5 scenarios. indicating the importance of global annual temperature increase in the occurrence of a tipping point. Under the Paris Climate Agreement, the ToEI is not expected to emerge within the current century. Threshold: 95th percentile.

The ToEI is also heavily dependent on the choice of the impact threshold. When a lower threshold of 75th percentile impacts is selected, the ToEI occurs sooner. This is illustrated in Figure 2.8.2.

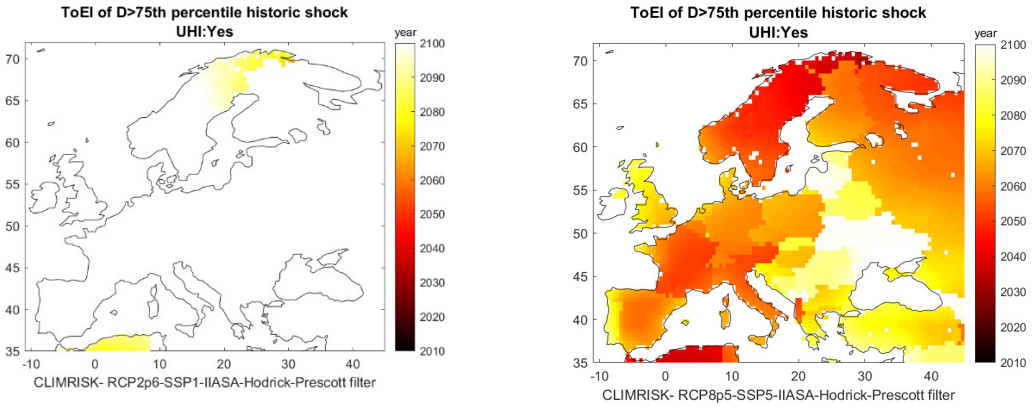

Figure 2.8.2: Climate scenario implications for the occurrence of ToEI under RCP 2.6 – SSP1 and RCP 8.5 – SSP5 scenarios and an impact threshold equivalent to the 75th percentile of past impacts.

*This project has received funding from the European Union's Horizon 2020 research and innovation programme under the Grant Agreement No **776479.***

The advantages of a local scale CLIMRISK model are apparent from Figure 2.8.3 where city-cell level ToEI estimates across various shock thresholds are presented. The risk level is indicated by the steepness of the line; the steeper the line, the later the specific shock threshold is exceeded. For example, the ToEI of 90th percentile of past impacts for Stockholm is around year 2065 whereas for Madrid it is past 2100 under the RCP 8.5 – SSP5 scenario combination. The ToEI can be delayed by several decades by applying a stringent emission mitigation policy in line with the Paris Agreement(RCP 2.6) and even through moderate mitigation policy (eg. RCP 4.5), as is indicated by steeper slopes of the curves in Figure 2.8.3 (left panel). In such a way, policymakers can buy significant amounts of time for climate adaptation strategies to come into play.

The results indicate a noticeable distribution of ToEI across European cities and can be explored for any other European city within the model.

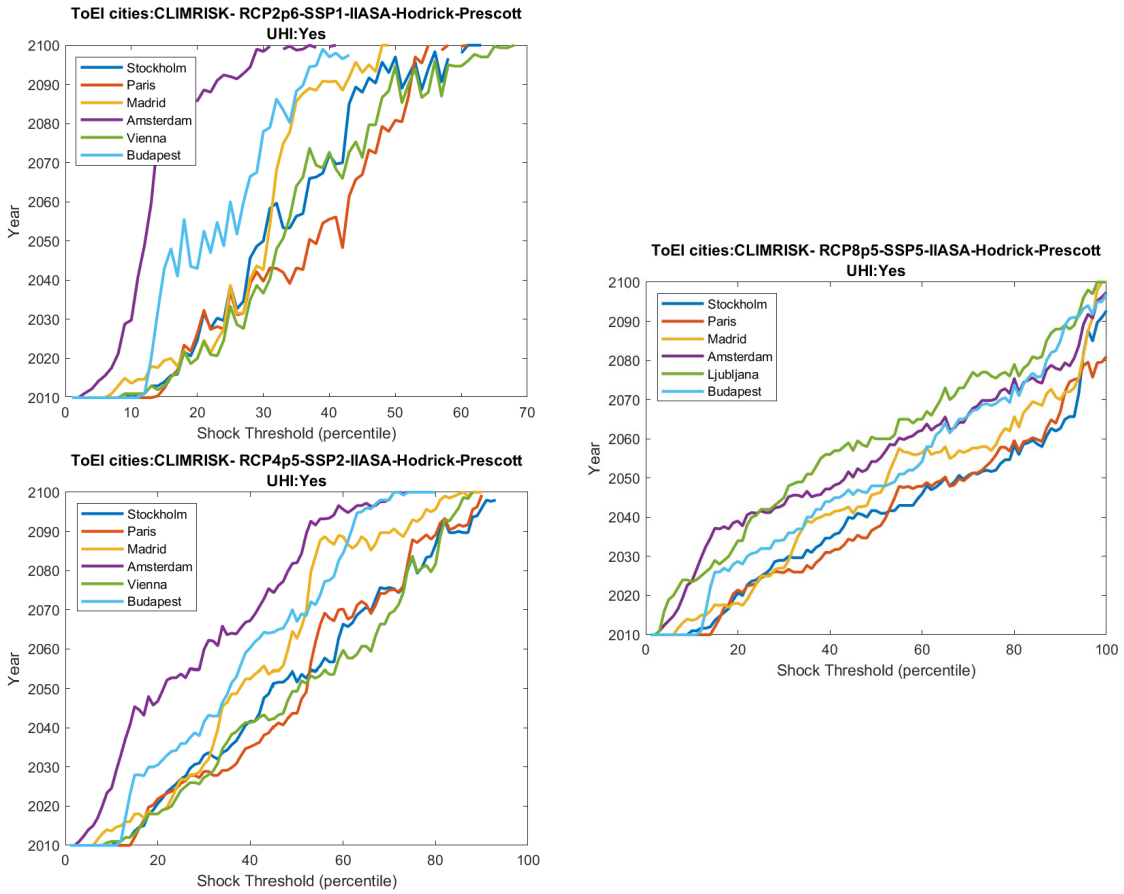

Figure 2.8.3: Time of emergence of impacts (ToEI) of climate change for various European city-cells in the 21st century for RCP 2.6 – SSP1, RCP 4.5 – SSP2 and RCP 8.5 – SSP5 scenario combinations.

The occurence of the ToEI tipping points can be verified through a metric of probability of emergence of impacts (PoEI). PoEI measures the likelihood of the impact threshold being exceeded in the given year. In the context of CLIMRISK, for each of the

*This project has received funding from the European Union's Horizon 2020 research and innovation programme under the Grant Agreement No **776479.***

500 MAGICC climate model runs, we count the number of times each cell's climate impact estimate exceeds the previously defined extreme shock, providing a probability of exceeding a threshold economic shock by a given year or PoEI. Some PoEI results are presented in Figure 2.8.4 for various RCP/SSP scenario combinations. Under the RCP 2.6 – SSP1 scenario, following the Paris Agreement, no probabilistic climate runs lead to the exceedance of the ToEI threshold of 95th percentile of past impacts. Moderate climate mitigation lead to ToEI realizations, specifically in Scandinavia and parts of Western-Europe (RCP 4.5 and RCP 6.0). Under the RCP 8.5 scenario, most of Europe could exceed the ToEI in at least 10% of probabilistic runs, with Scandinavia and Western-Europe approaching 100% ie. all runs exceeding ToEI before year 2100.

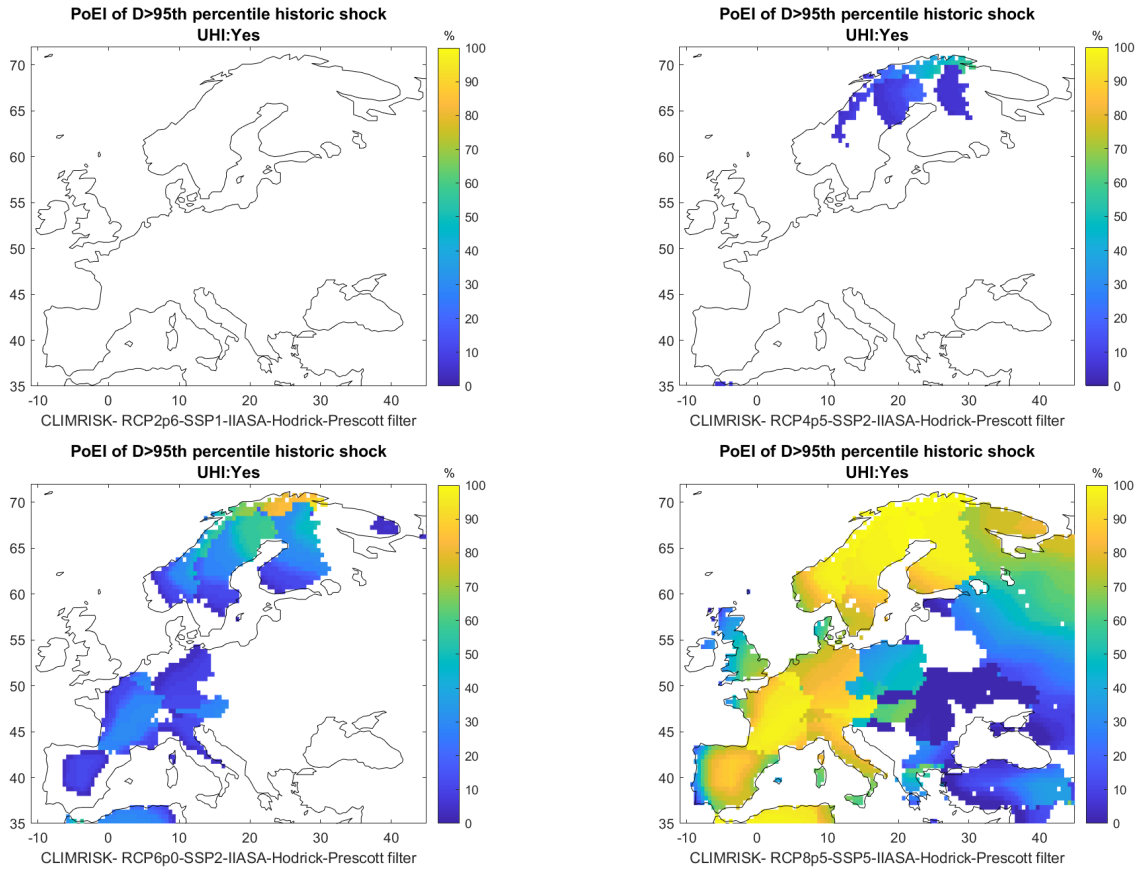

Figure 2.8.4: Probability of emergence of impacts (PoEI) measures the likelihood that the climate impacts exceed a set impact threshold across all simulation runs (95th percentile).

2.8.3. Identifying tipping points with ICES

The ICES CGE model analizes the following set of climate change impacts (seeCOACCH D2.7 (Bosello et al. 2020)): on energy demand, on energy supply, on labour productivity, on agriculture, on forestry, on fisheries, of sea-level rise, of riverine floodsincluding effects on transportation network.

What is presented in this section are the results of the economic assessment when all the impacts are jointly implemented as specific input shocks to the economic model.

*This project has received funding from the European Union's Horizon 2020 research and innovation programme under the Grant Agreement No **776479.***

The implementation strategy is briefly described here, while for more extensive information on the methodology and on the input data used, the interested reader is addressed to COACCH D2.7.

- Climate change impacts on fisheries are summarized by changes in catches that have been implemented into the ICES model as changes in the productivity of the natural resource input of the representative regional fish industry.
- Climate change impacts on agriculture are represented by changes in yields, than are implemented in the CGE model as changes in changes in the productivity of the land primary production factor used by the representative agricultural firms in each of the ICES region.
- Climate change impacts on forestry are represented by changes in net physical wood production per hectare and are then implemented in the ICES model as changes in the productivity of the natural resource input used by the regional representative timber (logging) industry.
- Climate change impacts on river floods are summarized by the expected annual damages determined for three macro-areas of activity: industrial, commercial and residential and by the exposed population. These impacts have been implemented into the ICES model as loss of capital and labour productivity respectively.
- Climate change impacts on transportation are measured by the direct infrastructural expected annual damage to road assets. They have been implemented in the ICES model as a proportional and uniform loss in the productivity of the labour and capital production factors used by the road transportation sector.
- Climate change impacts on wind and hydro power supply derive from projections using econometrically estimated supply to temperature elasticities. Changes in enery supply are then implemented in the ICES model as a proportional and uniform change in the productivity of the capital and labour factors of production used by the regional wind-power sectors.
- Climate change impacts on energy demand are obtained combining econometrically estimated demand to temperature elasticities with high-resolution climatic projections. Demand for electricity, petroleum products,and natural gas is projected for four economic activities: agriculture, industry, services and residential. In the case of the former three activities changes in demand are simulated acting on the energy efficiency (productivity) in those sectors. Changes in residential energy demand are implemented as exogenous shocks to household energy expenditure while keeping the household budget constraint unchaged.
- Climate change impacts on labour productivity are estimated applying a fixed-effects panel regression method linking sectoral GVA per working population to temperature. The estimated coeficients are then used to perform future projections on the basis of future temperature trends. In the ICES model labour productivity impacts are implemented directly as changes in the productivity of labour in the agricultural and industrial sectors.

*This project has received funding from the European Union's Horizon 2020 research and innovation programme under the Grant Agreement No **776479.***

Each of the impacts, and accordingly, their joint implementation in the economic model, are detailed for 9 combinations of SSPs and RCPs, chosen to enable disentangling the effect of the social-economic from that of climatic drivers. The combinations are:

- SSP1 RCP2.6 (s1r26 in figures)
- SSP1 RCP4.5 (s1r45 in figures)
- SSP2 RCP2.6 (s2r26 in figures)
- SSP2 RCP4.5 (s2r45 in figures)
- SSP2 RCP6.0 (s2r60 in figures)
- SSP3 RCP2.6 (s3r26 in figures)
- SSP3 RCP4.5 (s3r45 in figures)
- SSP5 RCP4.5 (s5r45 in figures)
- SSP5 RCP8.5 (s5r85 in figures)

Furthermore, to better account for uncertainty, input impact data[22] deriving from each single sectoral assessment study are specified according to a possible “low”, “medium” and “high” realization of the damage. The range deterimination method varies across studies. For instance, in the case of sea-leve rise different assumption on ice melting dynamics (low, medium and high) are used. In the case of agriculture the ranges are provided chosing realization from the climate model producing the highest and the lowest yield losses.

Two observations are in order. Firstly, we recognize that in doing so we are mixing different types of uncertainty (for instance environmental response uncertainty and climate model uncertainty). But our aim is to span and represent the full range of results from COACCH exercise. For the sake of completeness we merge the different uncertainty sources from different studies. Secondly,on a different token, we also recognize that we are not providing a complete characteriation of the uncertainty related to social-economic responses. Athough this is partly captured by analyzing different SSPs that in the model are associated to different assumptions on technological progress and substitution elasticities, we are not performing a full sensitivity analysis on all the behavioral parameter. This however would have required a very complex and too burdensome computational exercise.

For the sake of compactness we report results just for two sample years, 2050 and 2070.[23]

Macroeconomic implications

Table 2.8.1 reports the number of EU NUTS regions (over a total of 138 modeled) where the loss is larger than the 5% of GDP. Figure 2.8.5Figure 2.8.5 indicates which the regions are, Figure 2.8.6 maps the regions for the “high impact” case.

[22] With the exception ofclimate change impacts on enery demand and supply and labour supply.
[23] Full results include information 2020 - 2070 in 5-year time steps.

*This project has received funding from the European Union’s Horizon 2020 research and innovation programme under the Grant Agreement No **776479.***

Table 2.8.1: Number of EU regions with a GDP loss larger or equal to 5%

Scenario combination	*2050*			*2070*		
	Low impact	*Medium impact*	*High impact*	*Low impact*	*Medium impact*	*High impact*
s1r26	-	-	3	1	4	42
s1r45	-	-	2	4	6	27
s2r26	-	-	3	1	4	33
s2r45	-	-	2	6	6	39
s2r60	-	1	1	25	31	41
s3r26	-	-	1	2	3	27
s3r45	-	-	2	8	11	60
s5r45	-	-	2	7	8	31
s5r85	1	3	7	15	16	57

Before 2050 no region exhibits a loss equal or larger than 5%. In 2050, if impacts would stay at the low end of estimates, only the combination of SSP5-RCP8.5 originates that loss in one region: Marche in Italy. The economic loss is driven by lossof labour productivity and sea-level rise. If impacts would fall in the high range of estimates, the SSP5-RCP8.5 produces the highest number of regions (7) reaching the economic tipping point. Three regions are Italian: Marche, Veneto, Tuscany. Major impact driver for Veneto and Tuscany is sea-level rise. It is so also for Malta, Cyprusand Latvia. In Rumenia also labour productivit loss plays an important role.

In 2070, under low end impacts, the SSP1-RCP2.6 combination produces 1 tipping point region, SSP2-RCP6.0 25. In the high end impact case a minimum of 27 regions in the SSP1-RCP4.5 and SSP3-RCP2.6 combinations, to a maximum of 60 regions in the SSP3-RCP4.5 combination display a regional GDP loss larger than 5%.

As expected, the RCP6.0 and RCP8.5 climate scenarios, with the stronger climate signal, tend to depict the higher number of regions meeting the tipping point. Similarly, a larger number of regions meets the tipping points in the SSP1 and SSP5 social economic scenarios that feature higher GDP growth than in SSP3 and 2, and, therefore, also a higher exposure of capital stock and assets to climate change risk. However, this is not always the case especially when impacts are in the high end of estimates. This non-monotonicity from low to high-end climate scenarios is particularlyevident comparing the 42 tipping point regions of the SSP1-RCP2.6 against the 27 ofthe SSP1-RCP4.5 combination. Non monotonicity from low to high-exposure social- economic scenarios emerges comparing the 27 regions meeting the tipping poin in the SSP1-RCP4.5 against the 39 of the SSP2-RCP4.5 or the 60 of the SSP3-RCP4.5 combinations. The first behaviour is due to the compensating effect of responses from the agriculture and forestry sectors. With stronger climate change, crop and forestry yield losses are lower (in some cases they are negative, i.e. gains) due to the CO_2 fertilization effects[24]. Accordingly, GDP losses are also lower. The second behaviour, is

[24] It is worth highlighting that these data come from the analysis performed with the EPIC model. Results from the LPJmL model are more pessimistic featuring larger yield losses, or lower gains, in all the regions. In this exercise however, the results from EPIC have been used as they covered the full

*This project has received funding from the European Union's Horizon 2020 research and innovation programme under the Grant Agreement No **776479.***

induced by the different model parameterization used to calibrate the SSPs (see COACCH MS8 (Bosello et al. 2019)). Moving from SSP1 to SSP3 three key behavioral parameters, namely the efficiency in clean energy production, the elasticity of substitution between electric and non electric energy input, the substitutability between domestic and imported commodities are progressively reduced. These factors, in particular the latter, that can be interpreted as a restriction, or higherfriction, in international trade, introduce more rigidity in market adjustment to external shocks. What shown, is that a more "flexible" system can eventually experience lower macroeconomic costs than a more "rigid" one, even though the latter is less exposed. The regional distribution of highly impacted regions emphasizes the predominance of Southern European and coastal areas,which depends upon the predominance of asset losses associated to sea-level rise.

Eventually this exercise emphasizes the following messages. Considering a "medium impact" case, as expected, regions meeting the chosen social-economic tipping point are considerably more in high climate-change than in low climate-change scenarios. Nonetheless, the situation blurs when the possible "high end" of the impact uncertainty range is considered. In this case, also low climate change scenarios can be troublesome, with many areas meeting the tipping point in RCP2.6 and 4.5 in a way comparable to what occurs in RCP6.0 or 8.5. The partly confounding factor at work, is the smoothing effect of impacts on agriculture where CO2 fertilization decreases yield losses in higher temperature scenarios. This highlights the particular care that needs tobe used in the interpretation of aggregated results where the "averaging effect" can hide huge losses. The possibility of high losses in low tempertature RCPs also stresses the importance to reduce emission as much as possible as, given the uncertainty, "every degree matters". Mitigation is thus essential to reduce to an acceptable level the chances of these localized high losses. Finally, adaptation also can play an important role. In the exercise it is noted that more flexibility (larger substitutability across energy and non energy input or across domestic and imported commodities) tends to reduce the number of regions reaching the tipping point, even though more assets could be at risk compared with lower exposure, but more "rigid" scenarios. Although very rough, this is an indication that building adaptive capacity and flexibility is fundamental to address climate shocks. Then, this general adaptability should be supported by ad hoc adaptation measures that can tackle, more directly, specificimpacts.

combination of SSPs-RCPs of the project. D2.7 reports a comparison indicating the potential implications of using LPJmL input data.

*This project has received funding from the European Union's Horizon 2020 research and innovation programme under the Grant Agreement No **776479.***

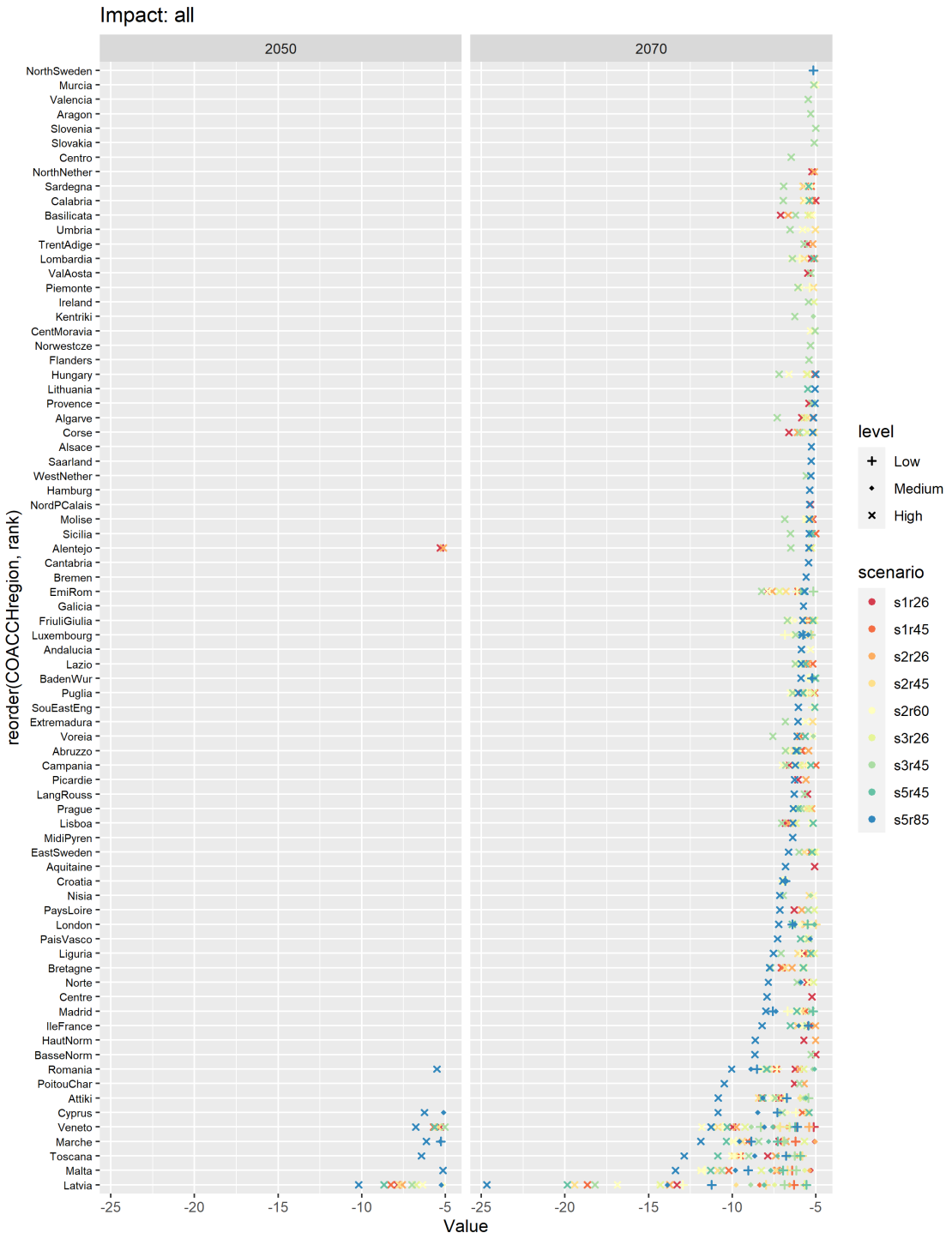

Figure 2.8.5. EU regions highlighting a loss larger than 5% of regional GDP under the different combination of SSP-RCPs

*This project has received funding from the European Union's Horizon 2020 research and innovation programme under the Grant Agreement No **776479.***

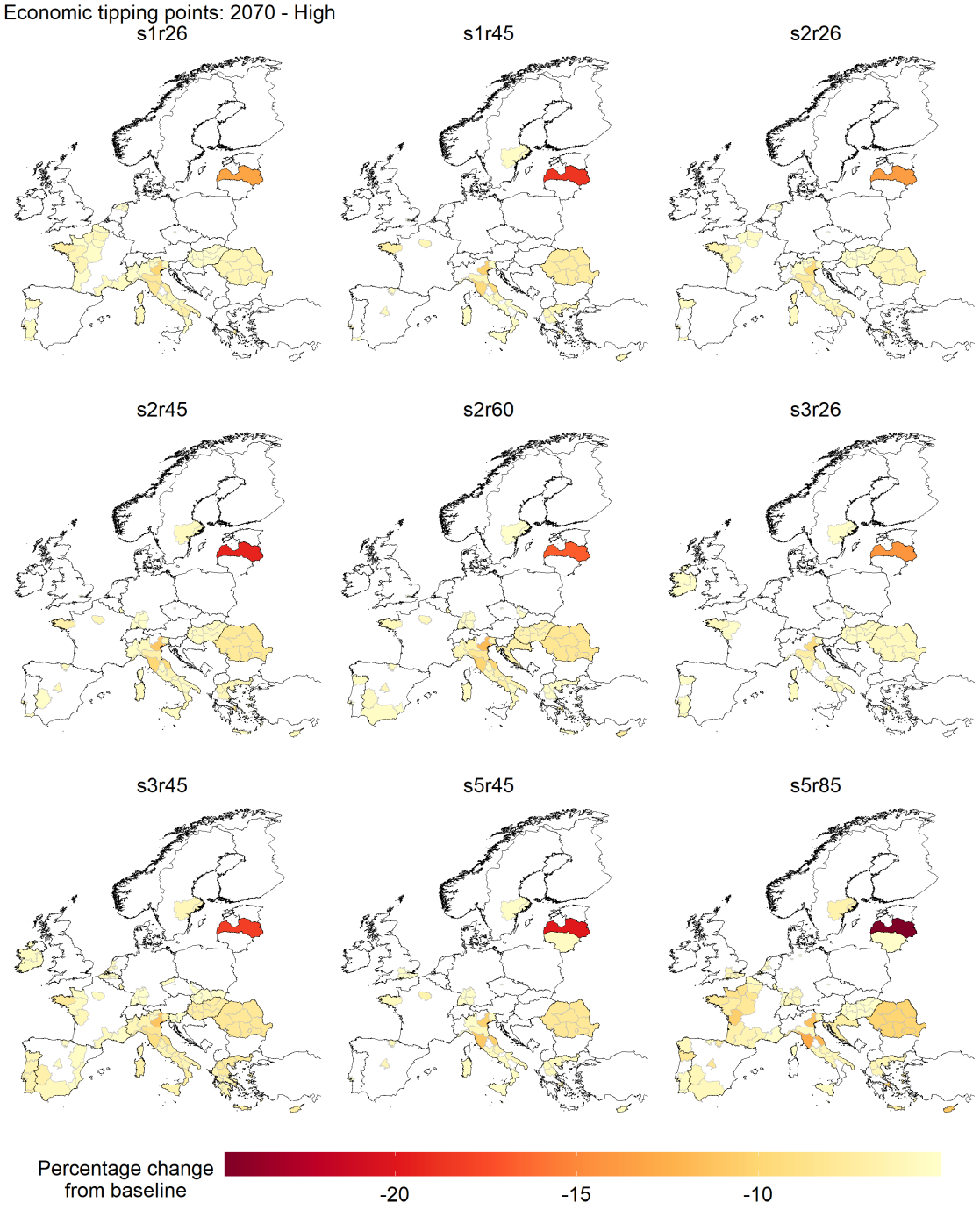

Figure 2.8.6. EU regions highlighting a loss larger than 5% of regional GDP under the different combination of SSP-RCPs, high impact case, year 2070.

*This project has received funding from the European Union's Horizon 2020 research and innovation programme under the Grant Agreement No **776479.***

2.9. Electricity system failures

Executive Summary

In our assessment of a socio-economic tipping point of major blackouts due to increasing wildfires, we use a risk-based approach to assessing the possible current and future impacts and effects on European countries. We build off of work in Scoccimarro et al. (2020) which outlined the potential for natural conditions leading to the tipping point (decreasing precipitation leading to long drought periods, followed by heatwaves), finding that much of the land area in Europe could see extreme increase in wildfire probability by the end of the century under different RCP scenarios, including areas which until now have little experience dealing with such threats.

In this work, we begin by expanding on the biophysical dimension of the hazard, highlighting an exponential increase in dryness of fuels for wildland fires with increasing temperatures, thus emphasizing the likely underestimation of fire risk until now, and its likelihood of becoming ever more common in the future. Recent research into the drivers of forest health, particularly an exponential relationship of temperature to drying times for fuels in forests, inform the application of a Forest Drought Stress Index (FDSI) to Europe, originally developed by Williams et al (2013) focusing on the western United States. Using ERA5 and EURO-CORDEX precipitation and temperature data, we estimate changes in extreme drought for the rest of the century for RCP 2.6, 4.5 and 8.5, highlighting extreme events with a focus on wildfire risk.

We then turn to exposure as the second component of risk; focusing on blackouts due to fires, we derive a method for assessing potential exposure in terms ofvalue added at risk (VAaR), based on previous studies of blackouts using production- function approaches, and project our estimates forward to future SSP scenarios using CGE modeling results. We quantify the VAaR in terms of gross value added (GVA) lost per hour of blackout per capita, and find that across Europe, VAaR is expected to increase strongly under three of four SSP projections, due to a marked increase in manufacturing sector activity in all but SSP3 modelled worlds. We downscale these estimates to NUTS2 level, finding that GVA loss per hour ranges widely, with mean values of between 6 and 13 EUR / capita, but with high variance (maximum values range between 45 and 96 EUR / capita).

To move towards a determination of areas more or less likely to be at risk in the future to blackouts caused by wildfire, in Section 3.9 we propose a new index of potential risk based on a combination of the FDSI hazard indicator and GVA lossexposure indicator. Normalizing and combining these two indicators additively produces an index which highlights areas likely to have high future exposure andincreasing risk (See Figure 2.9.1).

*This project has received funding from the European Union's Horizon 2020 research and innovation programme under the Grant Agreement No **776479.***

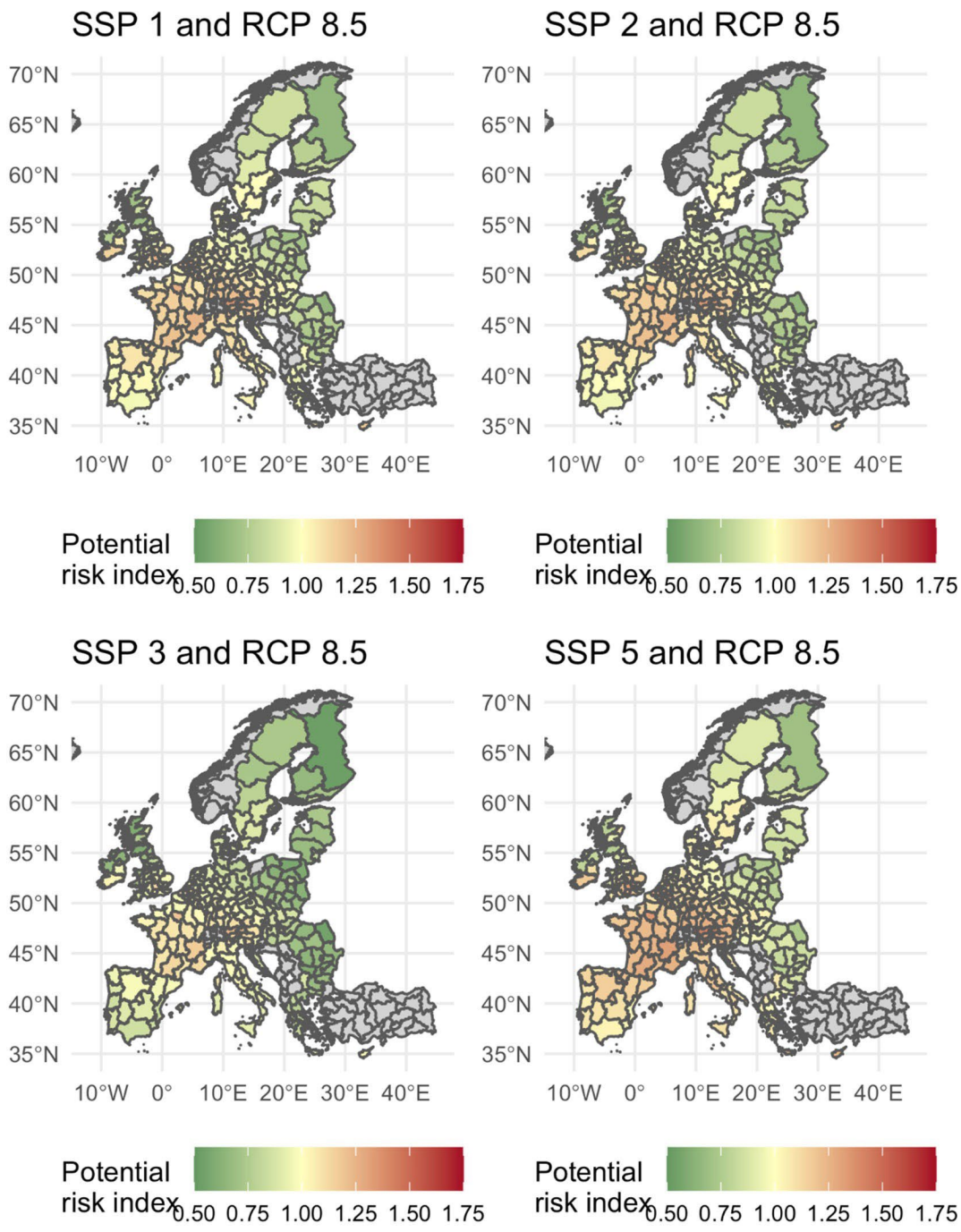

Figure 2.9.1. Potential future risk index (derived from hazard + exposure indicators) for RCP 8.5 model runs, for SSPs 1, 2, 3 and 5. Higher values indicate higher risk.

Our results show that while areas of the EU typically known from previous research to be vulnerable to fires due to increasing temperature and decreasing precipitation (e.g. the Iberian peninsula and Mediterranean region), also central Europe and northern latitudes may see increased risk potential in the future, while generally, Eastern Europe has lower potential index values.

*This project has received funding from the European Union's Horizon 2020 research and innovation programme under the Grant Agreement No **776479.***

We complete our discussion of risk with a focus on the potential vulnerability to such blackouts with an overview of key traits of the electricity sector which will impact the eventual losses due to wildfires in the future. The structure and composition of the electricity supply and transmission network, in terms of grid size, complexity and interconnections, as well as the generation plants that connect to it, will be a defining characteristic of eventual vulnerability, along with the potential stranded assets which may occur in terms of conventional electricity generation depending on future investment and energy policy.

Thus, decision-makers should recognize that the impending threat of major wildfires in Europe can be avoided by accelerating their plans for investing in renewable energy. And here it is of utmost importance to include all new technologies in the planning process, as the energy sector is of significant importance, both in termsof economic relevance and greenhouse gas emissions. Our research, pointing out the acuteness of this risk, can thus serve as an important additional motivation for an acceleration of investments in renewable energy.

Introduction

Expected impacts of climate change in Europe are likely to be the source of significant stressors for the electricity system as time progresses. As put forward in Deliverable 3.2 (Scoccimarro et al. 2020), a steady supply of electricity has become a basic necessity, with the European electricity system and its complexity of a pan-European network connecting hundreds of thousands of devices being no exception. This is not a startling assertion; a number of potential impacts on the electricity system have been identified in the past, ranging from difficulties for generation arising from a lack of cooling water (Behrens et al. 2017) to increasing demand to power air conditioning during periods of increasingly hot summer periods (Mima and Criqui2015). The European Environment Agency (2017) highlighted the vulnerability of energy infrastructure to windstorm, heat, drought and flood hazards, expecting increasing impacts from all in the future. As reported by Scoccimarro et al. (2020) , these four hazards have been listed as the cause of 30% of the major blackouts since 1965 as defined by Bompard et al. (2013), with the main stressors being windstorms and heat waves (causing 28% of all blackouts).

Amidst these expected impacts, two events in 2019 highlighted the potential for yet another hazard to affect the availability of electricity: large-scale wildfires. The incidence of fires in Australia and California in the US which resulted in several major, lengthy blackouts demonstrated the potential of a new hazard to disrupt stable electricity supply. Even absent an active fire, the California case demonstrates that risk aversion to such events leads to actions which cause interruptions to the electricity supply in the form of planned fire-prevention power outages (Johnson 2019).

In the following section, we build upon the work in Scoccimarro et al. (2020) which identified the likelihood of such wildfire events occurring and elaborate uponthe climate and weather conditions seen as a precursor to this risk. We define a tipping point in relation to the increase of major blackouts within a disaster risk framework, which brings together three components of hazard (here climateconditions leading to increased fire incidence), exposure (in terms of potential gross

*This project has received funding from the European Union's Horizon 2020 research and innovation programme under the Grant Agreement No **776479.***

value added of European countries potentially lost) and vulnerability (dependent on the electricity generation and supply system, discussed in Section 3.9) to such an event.

In practice, having defined the tipping point, we identify the biophysical conditions necessary for fire events to occur. Then we estimate the evolution of this future risk, that turned out to be exponential. As a third step we assess the EU's potential exposure to such increasing blackout risk in the future, under a variety of climate, policy and electrification scenarios. Using a production function approach, we were able to highlight the value of lost electricity production and, from this, to inferthe potential value added at risk due to power outages for EU member states. We conclude with a discussion of vulnerability of the electricity system to both the causes and occurrence of wildfire, based on factors which alternatively may mitigate or exacerbate potential future damages, and provide indications of areas of changing future risk.

2.9.1. Definition of tipping point

As mentioned, reliable supply of electricity is essential for meeting basic production and consumption needs in Europe. While the electricity supply system has commonly experienced minor and brief outages in the past (Martinez-Anido et al. 2012), the impacts of climate change will likely exacerbate these disruptions. This can be due to impacts on both electricity supply and demand, as well as mitigation policy responses which may increase electrification of industrial sectors and therefore increase vulnerability to events like large scale electricity blackouts, which up to now have been rare in the European context.

Demonstrated by the experiences in Australia and California, wildfire hazard has presented itself as a potential major driver of such an event. Needless to say, the underlying conditions – drought and heatwaves - required to cause a fire, pose themselves significant stress on electricity supply and demand. The electricity sector itself may exacerbate the potential for wildfire hazard, as seen in California, where power lines and electrical equipment are a leading cause of fires (Penn 2017), and as a result preemptive blackouts occurred with increasing regularity over large scales in recent years (Vartabedian 2019).

Compared to previous ones, changing climate conditions could lead to much larger and lengthier blackouts. Such repeated major blackouts could have dire socio- economic consequences for a variety of sectors of the economy and the population asa whole. Large manufacturing sites already consume huge amounts of power for industrial processes; electrification of e.g. the iron and steel sectors will likely increase this dependence on electricity. Existing emergency power generators are not built to cope with blackouts that may last multiple hours or days, such generators usually employ diesel engines, leading to increased local air and noise pollution, and entailing high fixed and marginal costs coupled with low reliability due to their limited use. Electrification of other sectors in line with meeting climate goals, such as the envisagedelectrification of transport, could also exacerbate the effects of a blackout as compared to today's society. Wildfire impacts and associate blackouts additionally can impact private households via loss of property and life, also evident in recent major

*This project has received funding from the European Union's Horizon 2020 research and innovation programme under the Grant Agreement No **776479.***

fires, where in California, more than nine thousand structures were destroyed and several hundred lives were lost (CAL FIRE 2017, Gorman 2019).

We define this specific SETP based on the work of Bompard et al. (2013). A major blackout is defined as an event which affects a population larger than 1,000,with a duration longer than one hour, where the affected population times the duration is greater than 1,000,000 person-hours. As an example the failure of just one transmission line with 100 kV or more, which typically can supply over 100,000 people with electricity, would fall within the definition of a major blackout as specified by Bompard et al. (2013) when the repair of the line takes longer than ten hours, a likely condition if destroyed by a wildfire. Due to increase of major blackouts, companies andthe population may increase precautions, in particular through purchase of emergency power generators or installations of rooftop PV and batteries, leading to a structurally different society with regard to either or both the reliability of the electricity system and its makeup.

Will Europe also experience major blackouts in its electricity system from wildfires as has occurred recently the U.S. and Australia? Although failures of a large power station often trigger major blackouts, e.g. in Australia as mentioned above, the Organization for Security and Co-operation in Europe (2016) sees the preservation of the "functionality, continuity, and integrity of electricity transmission networks" as the main challenge for "protecting electricity networks from natural hazards". This is justified as the failure of a large network can cause much bigger blackouts than the failure of one power plant. Hence, we analyze impacts of an increasing number of wildfires on the transmission system.

Most transmission systems in Europe are of the overhead type. The total length of overhead lines with above>100 kV in Europe is 265,359 km, and only 35,098 km of transmission lines (cables) are underground (Eurelectric 2013). The EU has 1.82 million km^2 of forest area which accounts for slightly more than 42 % of EU land area (Eurostat 2020). Large transmission lines are usually planned such that they connect power plants and load centers directly, i.e. on the shortest way possible with one peculiarity. Planners prefer to put extended infrastructure into forest area so that they have to negotiate, for example for the right of way and payments, only with a low number of owners per area which is easier and cheaper than negotiating with a large number of farmers. Hence, the density of transmission lines over forest area will be higher than over other area types. To be on the safe side (i.e. to determine a lower bound) we assume that only 42% of transmission lines are over forests. How many separatetransmission lines are in the forests? The transmission lines end at interconnection points to the low-voltage distribution networks (Eurelectric 2013). These latter distribution networks are the "final mile" in the delivery of electricity to the customers. In Europe, 99.6% of all customers get their electricity through distribution networks which are linked through 10,713 interconnection points with the transmission network. Thus, the transmission network comprises 10,713 transmission lines to these interconnection points. We can assume that 42% of these lines will be in forest area,
i.e. 4,496 lines.

*This project has received funding from the European Union's Horizon 2020 research and innovation programme under the Grant Agreement No **776479.***

The average European load is 360 GW[25], varying between about 230 GW in summer and up to 530 GW in winter. Thus, the average connection point has a load of 34 MW and serves 25,000 customers. The total number of customers in the EU is 263,370,337, i.e. about one customer per two people in the EU. Destruction of one of these 4,496 lines can on average affect 25,000 customers or 50,000 people. As the repair of transmission lines can take many hours up to several days, the destruction of one of these lines can cause a major blackout as defined by Bompard.

In 2019 the total area affected by wildfires in the EU was about 8000 km^2 (Earth-i 2019) or 0.43% of the total forest area of 1.82 million square kilometers in the EU (Eurostat 2020). If we assume an even distribution of the 4,496 transmission lines that connect to the distribution points, then wildfires in 2019 could have destroyed lines in 0.43% of the total forest area, or 4,496 x 0.43/100 or about 20 such lines. However, often the area under overhead lines is cleared and other precautions may exist to protect the overhead lines. To take this into account we assume that only 10% of the transmission lines are at risk to be destroyed by wildfires, i.e. the wildfires in 2019 might have destroyed just 2 of the connecting lines to the distribution networks. An increase in wildfires will increase the fraction of destroyed forest (which was at 0.43% in 2019) and thus put more transmission lines at risk, the destruction of each of which could – on average – cause an electricity blackout SETP according to our definition following Bompard (2013). We find that our probably cautious calculation identified the risk of two SETPs in 2019, with risk of wildfires rising in the future also raising the risk for a higher number of SETPs of major blackouts in the EU.

In the following sections, we further investigate the occurrence – and possible impacts – of the SETP as discussed above. We begin with an analysis of the increasing hazard risk in the form of forest fire incidence. We then address the amount of assets exposed to such a blackout risk using a macroeconomic approach to estimate future gross value added potentially lost per hour. We then conclude with a discussion on vulnerability, and a first indication of areas potentially at risk in the future via a combination of a hazard and exposure indicator.

2.9.2. Contributing factors and occurrence of tipping point

Exponential increase of wildfires hazard potential

Brown et al. (2020) describe climate change as an enabler of wildfires: “Increasing temperature trends enable longer and more extreme fire seasons. California (as well as all of the West) has had significantly enhanced fuel aridity due to anthropogenic increases in temperature and vapor pressure deficit over the past several decades. This can also be seen in the increasing number of days of fire weather season length based on fire danger indicators.” Jolly et al. (2015) come to similar conclusions and see wildfire surges as a signal of a “weather-induced pyrogeographic shift”. They show that between 1979 to 2013 the fire weather seasons have lengthened across 29.6 million km2 (25.3%) of the Earth’s vegetated surface, resulting in an 18.7% increase in global mean fire weather season length. These authors also

[25] data from Entso-E, www.entsoe.eu

*This project has received funding from the European Union’s Horizon 2020 research and innovation programme under the Grant Agreement No **776479.***

show a doubling (108.1% increase) of global burnable area affected by long fire weather seasons (> 1.0 standard deviation above the historical mean) and an increasedglobal frequency of long fire weather seasons across 62.4 million km2 (53.4%) during the second half of the study period. Williams et al. (2019) also find warming as the driving factor for increasing summer forest-fire burned areas, due to increased atmospheric aridity. They highlight a robust interannual relationship between atmospheric vapor pressure deficit (VPD) and forest fires, suggesting that nearly all therecent increase in damaged area by fires from 1972 to 2018 was driven by increased VPD, and that the response of eventual burned area to VPD is exponential.

Vapor pressure increases exponentially with temperature (the Magnus formula, see below), and evaporation. Drying of fuel also increases linearly with vapor pressure, meaning that it increases exponentially with temperature. In summary, increasing warming is increasingly impactful on fires.

Wildfires become devastating if they destroy forests, i.e. living matter. Initial small wildfires, e.g. caused by lightning or human acts, can develop into devastating wildfires if they begin in an area with a suitable mixture of dry fuels. Fuels have very different drying times, characterized by the length of time until the fuel moisture (FM) is sufficiently evaporated. These are (Stavros et al. 2014) the 1-hr FM (e.g. grass or pine needles on the ground), 10-hr FM (sticks up to 2.5 cm in diameter), 100-hr FM (or FM100, branches of 2.5 to 7.6 cm diameter), and 1000-hr FM (or FM1000, logs greater than 7.6 cm in diameter) in the United States National Fire Danger Rating System (NFDRS) (Lute and Keane 2006). The explanation for the significance of these characterizations by Weill (2018) is that “Grasses are 1-hour fuels, sometimes called light fuels, or flashy fuels. If the weather becomes hot and dry, they become just as dryas the surrounding atmosphere in about an hour. Trees and dead logs are usually 100 or 1000-hour fuels; it takes much longer before they're ready to burn.” Hence, earlierin the season, blazes tend to be grass fires that are easier to get under control. The more types of fuel get dried the more catastrophic the wildfires can become. Power lines can spark flames in dry grass, starting a fire. How big it becomes depends on the availability of fuels with lots of mass. Areas with a suitable composition of fuels can be small, for example the area around a fallen dead tree, i.e. for example 100 square meters. Extended heatwaves would drastically shorten drying times (Table 2.9.1). Table 2.9.1 shows the decrease of drying times from the initial value at 20°C if temperature increases; here shown for a maximal value of 45°C. For example, if a big piece of wood needs 500 hours for drying at 20°C, it would dry within 122 hours at 45°C. The most convenient equation for calculation of the saturated vapor pressure is the Magnus formula, which is recommended by the WMO (2012):

$$VPsat = 6.112^{17.62\mathrm{t}/243.12+\mathrm{t}}$$

with t in [°C] and VPsat in [hPa].

Table 2.9.1: Temperature, saturated vapor pressure and decrease of drying times for fuel, derived from the Magnus formula.

Temperature t [°C]	20	25	30	35	40	45

*This project has received funding from the European Union’s Horizon 2020 research and innovation programme under the Grant Agreement No **776479.***

VPsat [hPa]	23	32	42	56	74	96
FM100 [hours]	100	74	55	42	32	25
FM500 [hours]	500	369	275	208	158	122
FM1000 [hours]	1000	738	551	416	317	243

In reality, drying times decrease even faster than shown because evaporation increases almost linearly with the drying force VPD, which is the difference between the saturation vapor pressure VPsat and the actual vapor pressure VP (i.e. VPD = VPsat – VP) (Mackay and van Weesenbeck 2014). This difference is the driving force for drying, because fuel can only dry, independent of the temperature, as long as the relative humidity is below 100%. The lower the relative humidity, the faster the drying. Through this process an increase of temperature causes further acceleration of drying because relative humidity decreases with temperature.

This indicates that the process of drying of fuel proceeds in two stages. If temperature increases, it increases the saturation vapor pressure VPsat which increases evaporation which in turn increases the actual vapor pressure until either VPD becomes zero and stops further evaporation or until most matter in a forest is dried, which also almost totally stops further evaporation. Wind and diffusion carry away water vapor, again increasing VPD and making room for new evaporation. Additionally, temperature increase decreases relative humidity thus also increasing vapor pressure deficit. In extended periods of dryness, drying also of thick logs and other material occurs that is slow to dry and has kept some water. Due to this exponential process, wildfires can also burn thick logs after extended periods of hot temperature and thus can become catastrophic. This process was confirmed by Lewis et al. (2020) in an analysis of the Australian McArther Forest Fire Danger Index. While this index combines many dependent variables, these authors found that extended periods of well-below normal precipitation, followed by heatwaves, are the main driving factor of major wildfires.

The description of the two stages of drying indicates that the relationship inTable 2.9.1 could be improved to also include relative humidity in the drying times, which is a measure for actual vapor pressure depending on temperature t, i.e.

$$relative\ humidity_{\mathrm{t}} = \frac{actual\ vapor\ pressure_{\mathrm{t}}}{VPsat_{\mathrm{t}}}$$

Having an exponential factor in the saturated vapor pressure (see equation (1)) and thus also in the vapor pressure deficit should be alarming because this implies that seemingly low increases of temperature can unexpectedly trigger catastrophic events. This is empirically confirmed by Abatzoglou and Williams (2016): “Anthropogenic increases in temperature and vapor pressure deficit significantly enhanced fuel aridity across western US forests over the past several decades and, during 2000–2015, contributed to 75% more forested area experiencing high (over 1 standard deviation higher than the mean) fire-season fuel aridity and an average of nine additional days per year of high fire potential. Anthropogenic climate change accounted for ∼55% of observed increases in fuel aridity from 1979 to 2015 across western US forests,

This project has received funding from the European Union’s Horizon 2020 research and innovation programme under the Grant Agreement No **776479.**

highlighting both anthropogenic climate change and natural climate variability as important contributors to increased wildfire potential in recent decades." In their review Allen et al. (2010) conclude there exists "the potential for amplified tree mortality due to drought and heat in forests worldwide".

Regarding the temperature increase that is necessary to increase VPD such that drying times for FM1000 become short, Williams et al. (2019) specify that "During 1896–2018, October–November Tmax increased significantly (at a 95% confidencelevel) by 1.67 °C, driving an increase in VPD of 1.21 hPa (+14.6%). This positive trend in the latter, in VPD, was not statistically significant, however, due to high interannual to decadal variability in fall temperature and humidity. VPD did increase significantly (again, with 95% confidence) during 1948–2018, and this trend is almost entirely responsible for the decrease in FM1000 during this time."

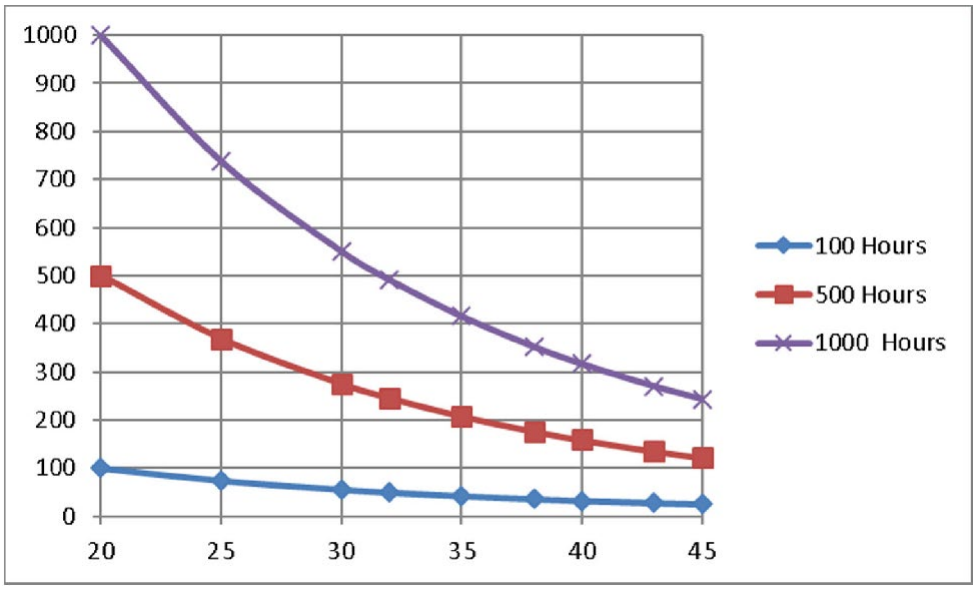

Figure 2.9.2. Shortening of drying times in hours (y-axis) of different types of fuel (FM100, FM500, FM1000) with temperature in °C (x-axis)

An extended analysis for the South Western United States gave the same result, according to Williams et al. (2013). For climate data during 1896-2007, combinations of warm-seasons vapor pressure deficit and cold-season precipitation account for 82% of the tree-ring-derived forest drought stress index variability ($p<0.0001$, 95% confidence: $0.74<=R^2<=0.88$). They define a forest drought-stress index FDSI as

$$FSDI = 0.44[zscore(\ln(P_{\mathrm{ndj\ m}}))] - 0.56(zcore(\frac{VPD_{\mathrm{aso}} + VPD_{\mathrm{mjj}}}{2}))$$

with $P_{\underline{\mathrm{ndjfm}}}$ precipitation of November and December preceding the present year and January, February and March from the present year and likewise $VPD_{\underline{\mathrm{aso}}}$ the vapor pressure deficit from August, September and October of the preceding year and VPD_{mjj} the vapor pressure deficit of the present year in May, June and July. The terms in this

*This project has received funding from the European Union's Horizon 2020 research and innovation programme under the Grant Agreement No **776479.***

equation describe the availability of water depending on precipitation and

*This project has received funding from the European Union's Horizon 2020 research and innovation programme under the Grant Agreement No **776479.***

evaporation. The results by Williams et al. (2019) "indicate a strong exponential relationship between forest drought-stress and satellite measurements of forest and woodland area burned by wildfire" and: "If the vapor-pressure deficit continues increasing as projected by climate models, the mean forest drought-stress by the2050s will exceed that of the most severe droughts in the past 1,000 years."

Developing a hazard estimate for Europe based on a Forest Drought Stress Index

To estimate future fire hazard potential, we apply the forest drought stress index developed by Williams et al. (2013) to bias-corrected climate model outputs for the EU up to 2100. The FDSI utilizes VPD, derived from temperature and humidity estimates, and precipitation over different periods of the year to determine drought stress correlating with forest fire activity. In order to generate a consistent time series ofboth VPD and precipitation for Europe, we use historic weather data from ERA5 and future scenarios from EURO-CORDEX model runs to identify the change in both variables due to climate change. Specifically, we calculate a 25 year (1980-2005) average representative year based on ERA5 precipitation, average temperature, and dew point temperature. We then determine the difference between a modelled historical period from climate model runs and the future periods to 2100, which is thenadded to the real historical average derived from ERA5 data to create a consistent timeseries of daily estimates for precipitation and temperatures from 1980-2100.

To calculate the FDSI, we use Eq. 1 above to derive saturated vapor pressure (using average daily temperature) and vapor pressure (using dew point temperature) for the ERA5 data. However, the EURO-CORDEX data utilized did not contain dew point temperature, but did contain relative humidity, which was then converted to dew point temperature via the following:

$$dew\ point\ temp = \frac{243.12 \log\left(\frac{Relative\ humidity}{100} VP_{\text{sat}}\right)}{\log\left(\frac{Relative\ humidity}{100} VP_{\text{sat}}\right) - 17.62 \log(6.112)}$$

After creating the consistent 1980 – 2100 dataset, precipitation and derived VPD were aggregated for the relevant periods (see Williams' equation above) into an FDSI index for the years 1981-2100 (1980 is dropped due to lack of data from 1979). The FDSI is normalized for each grid cell for the entire time series, and functions such that severity is based on difference to the historical mean value for a given point. Thus, to examine future possible drought severity, we first calculate ensemble mean FDSI values for each year, and then find for 30 year periods (2011-2040, 2041-2070, 2071- 2100) the cutoff FDSI value for the 10th percentile (as negative values are indicative of drought). We then determine how far (in terms of number of standard deviations) these 30-year extremes lie from the 1981-2010 average.

The results of the FDSI calculation for RCP 4.5 and RCP 8.5 (based on 3 models each) can be found in Figure 2.9.3, and Figure 2.9.4; the associated climate model runs utilized can be found in Table 2.9.2. Results for RCP 2.6 – for which only one model run

*This project has received funding from the European Union's Horizon 2020 research and innovation programme under the Grant Agreement No **776479.***

was available and thus serving more as an indication of the future distribution of events – are included in Figure 5.2.1.

As expected, higher RCPs lead to more severe fire risk later in the century, particularly in southern regions. However, these increasing risks also appear in central Europe, extending well into northern Germany. In terms of Northern Europe, themodel results do not indicate that e.g. northern Sweden and Finland would see drastic increases in risk, while Norway could see increased incidence of fire, particularly later in the century under RCP 8.5. However, the southern portions of Scandinavia and the Baltics are projected to face increasing extremes in all periods of all RCP scenarios in our model assessment.

Figure 2.9.5 depicts the changing distribution of extreme events for our model results over all three RCPs. While RCP 2.6 results are further from the historical mean in the near future period (2011-2040), the chosen model remains relatively stationary over the century but projects lower extreme FDSI values (which are interpreted as being worse for forests) for the near future than do the results of RCPs 4.5 (middle panel) or 8.5 (bottom). In a similar analysis on burned area in Europe under RCP 2.6 and 8.5 scenarios, Wu et al (2015) found that in both RCPs, up until circa 2040 the change in burnt area in two models (LPJ-GUESS and LPJmL) is identical; only thereafter do clear differences begin to emerge between the two, growing towards the end ofthe century, with little change after 2040 in RCP 2.6. This is in accord with the results from our Figure 2.9.5, but it should be emphasized that there are only a small subset ofthe models available for different RCP ensembles, used to present a first test of suchan approach to estimate hazard changes. For a more robust assessment, an enlarged ensemble of climate model results for all RCPs along with discussion of their varying storylines and implications is required.

*This project has received funding from the European Union's Horizon 2020 research and innovation programme under the Grant Agreement No **776479.***

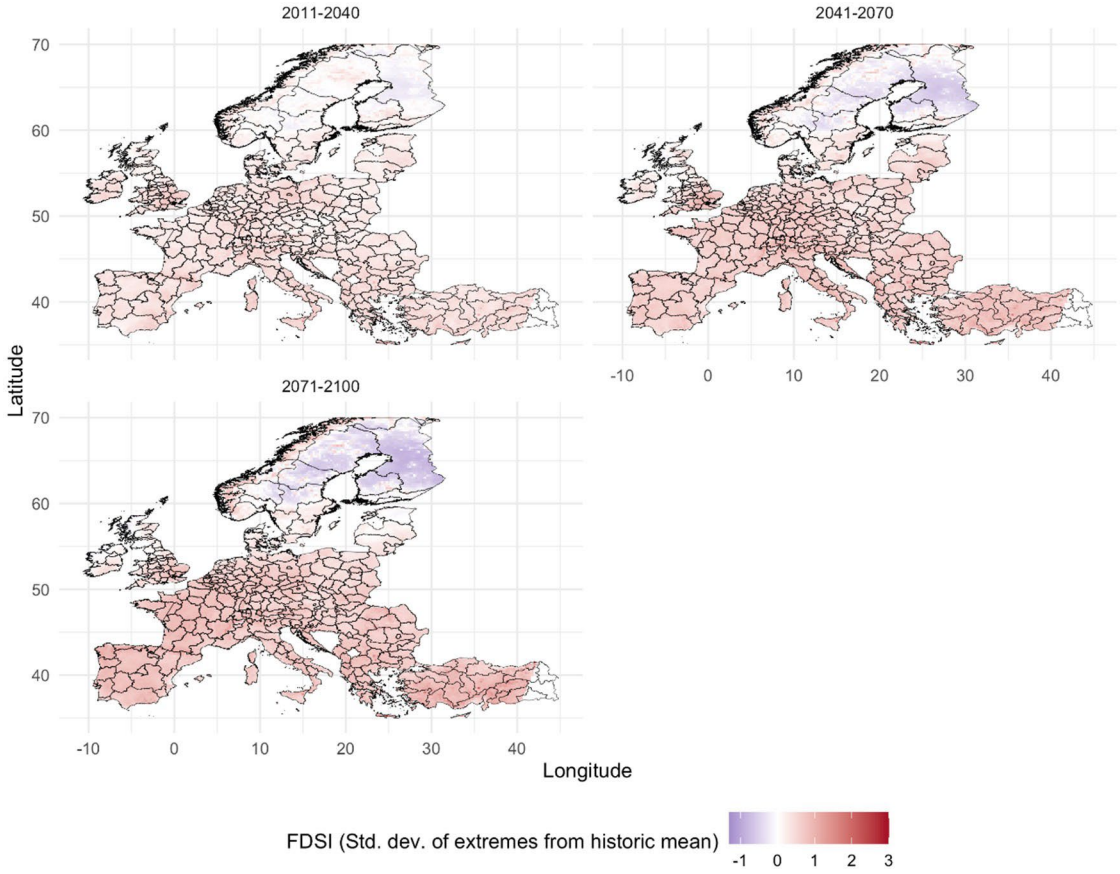

Figure 2.9.3. Increase in extreme drought, expressed as the 10th percentile FDSI values for a 30-year period for RCP 4.5, based on ERA5 and EURO-CORDEX model runs, for EU regions from 2007 to 2100. Increases are expressed as the number of standard deviations away from the historical mean value.

Table 2.9.2. Climate model runs used in hazard calculation

Model	RCP 2.6	RCP 4.5	RCP 8.5
Max Planck Institute Earth system model (r1i1p1)		X	X
EC-Earth Atmosphere-Ocean General Circulation Model (r12i1p1)	X	X	X
IPSL-CM5 Climate Model (r1i1p1)		X	X

*This project has received funding from the European Union's Horizon 2020 research and innovation programme under the Grant Agreement No **776479.***

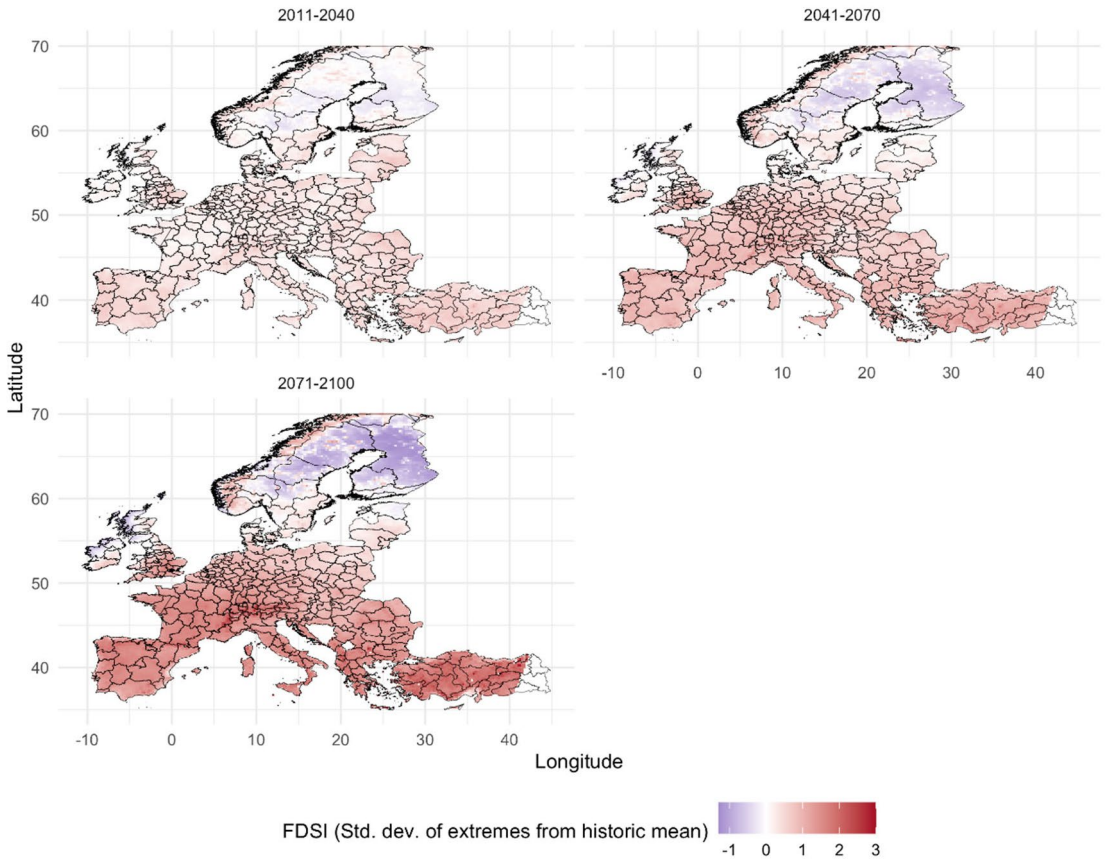

Figure 2.9.4. Increase in extreme drought, expressed as the 10th percentile FDSI values for a 30-year period for RCP 8.5, based on ERA5 and EURO-CORDEX model runs, for EU regions from 2007 to 2100. Increases are expressed as the number of standard deviations away from the historical mean value.

*This project has received funding from the European Union's Horizon 2020 research and innovation programme under the Grant Agreement No **776479.***

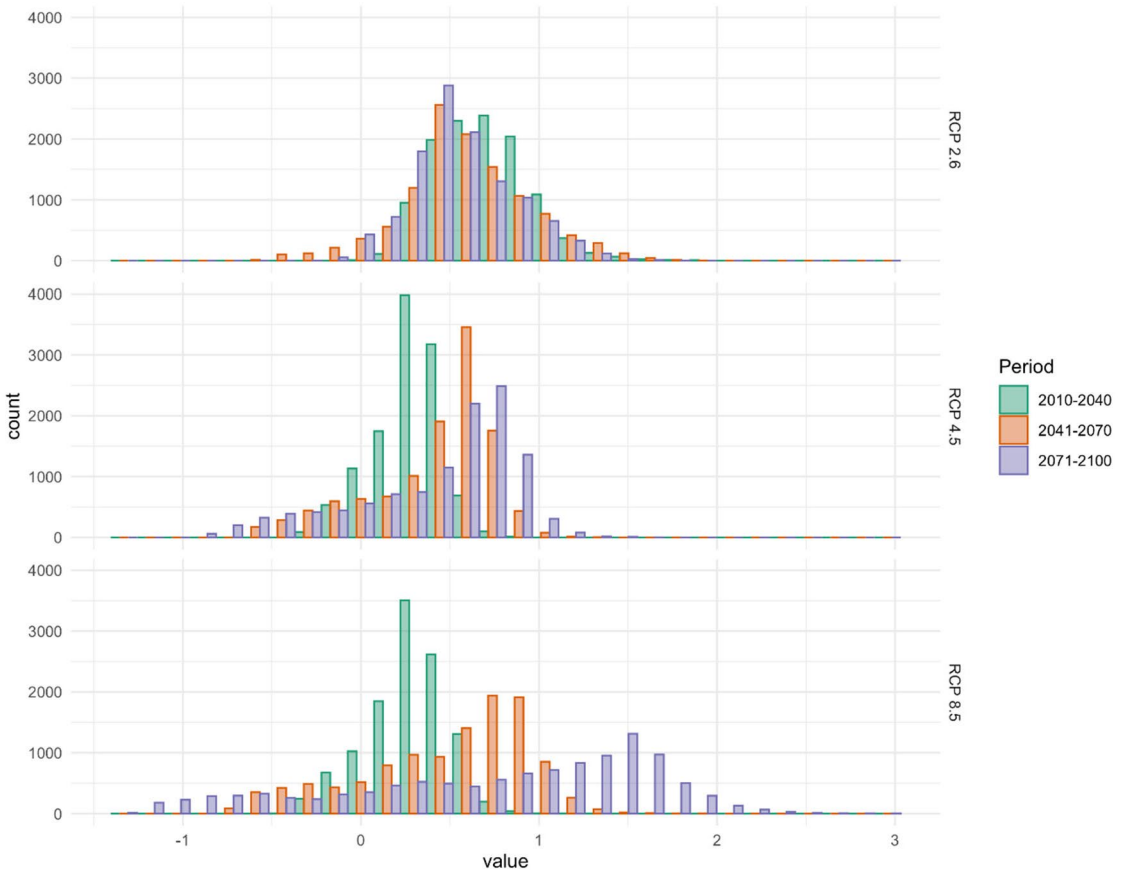

Figure 2.9.5. Histogram of the model results for increases in extreme drought, expressed as the 10th percentile FDSI values over 30-year periods. Increases are expressed as the number of standard deviations away from the historical mean value. The top panel shows the distribution of results for the RCP 2.6 model run, the middle for RCP 4.5 and bottom for RCP 8.5. RCP 2.6 FDSI results are initially a higher level than RCP 4.5 and 8.5 but remain concentrated around the starting distribution over subsequent time periods, while the tails of the other RCP distributions spread widely, indicating increasing extreme event severity.

2.9.3. Macroeconomic implications

Section 2.9.2 addressed the incidence of fires potentially leading to blackouts, but macroeconomic implications are additionally heavily dependent on the exposure of EU countries to such hazard. We here attempt to provide a first estimate of the potential value-added of EU countries at risk to large-scale blackout events caused by climatic conditions and subsequent wildfires.

Development of a blackout exposure indicator

Several approaches have been taken in the literature to assess the economic exposure to and impacts of blackout events, which have varied widely in focus, methods, and results. The common indicator at the basis of the evaluation of historical or future blackouts, is the value of lost load (VoLL) a monetary indicator of the costs associated with electricity interruption, typically expressed in monetary units overpower units e.g. Dollars per kWh. From there, measurement approaches vary widely, from direct assessments via event studies, surveys of likely direct costs or willingnessto pay to avoid future events, to indirect approaches such as production function

*This project has received funding from the European Union's Horizon 2020 research and innovation programme under the Grant Agreement No **776479.***

approaches or revealed preferences. Production function studies use macroeconomic statistics to determine sectoral production functions and derive the drop in production following a lack of an essential element of production (in this case, an electricity input). Revealed preferences methods attempt to derive the VoLL from investment behavior of households and firms by assessing the mitigation costs for blackout risk, e.g. via purchases of generators or batteries, or structuring of uninterruptable supply contracts (Schröder and Kuckshinrichs 2015).

Eventually we base our analysis on a production function approach. We are aware of the limitations of the method. It "linearizes" the importance of an input (in our case electricity) in the resulting sector output. There can be however cases when a production factor, that builds a small share of the output value, is anyway essential being used in a critical step of the industrial process. This aspect is not fully captured.
Furthermore, the method cannot fully account for time dynamics which are also relevant. For instance, blackout costs are higher at the beginning, then increase, but at a decreasing rate (e.g. loss of refrigerated or frozen stock in supermarkets happens early on in a blackout event, not continuously over time periods). Furthermore, different sectors may not be active during a blackout period and thus would experience no loss. Accordingly, the production function method can overstate possible impacts.

However, studies based on past-event evidence, surveys of direct costs or willingness to pay are extremely context-specific, subject to the format of questioning (i.e. survey or questioning which may bias results), with large discrepancies between e.g. willingness-to-pay versus willingness-to-accept results. Conversely, the production function approach provides a standard, easily applicable method which can be carried out at large scale, as is the case here. It also facilitates linking with assessing future economies as described in Section 1.1.2.

A production function approach uses macroeconomic data from (sub)national Input-Output tables to construct sectoral production functions (which imply demand functions for the final products) and estimate the consequences of blackouts due to lost firm production (Toll 2007, de Nooij et al. 2007). The approach recognizes that electricity is a vital input to production, thus the lack of this input factor leads to a dropor complete ceasing of production (Schröder and Kuckshinrichs 2015).

As the typical approach focuses on the value of lost load as a relation between output and physical electricity (typically GVA / electricity input in kWh), assessments can derive the GVA component of VoLL by using a production function (typically a Cobb-Douglas model) to predict VoLL for each sector, as follows:

$$\ln(Q) = \alpha + \beta_1 \ln(M) + \beta_2 \ln(K) + \beta_3 \ln(L) + \beta_4 \ln(E)$$

where *M* are intermediate inputs, *K* capital, *L* labor, and *E* electricity (London Economics 2013). This can then be used to estimate VoLL econometrically via regression.

The following assumptions also apply to the method: firm production can be shifted to another time period, and electricity can be partially substituted by other

*This project has received funding from the European Union's Horizon 2020 research and innovation programme under the Grant Agreement No **776479.***

inputs (de Nooij et al. 2007). A further assumption of the basic approach is that the timing and duration of a blackout is irrelevant (Leahy and Toll 2010).

Basing our analysis on a production function approach, we obtain data on electricity use in EU countries by sector using Input-Output data generated from the GTAP9 database[26]: we first calculate the estimated dependence of sector value added on an electricity input, incorporating estimates of the electricity intensity of sectoral gross value added and the active working time of sectors. The result is a national-level estimate of the amount of GVA lost from every hour of a blackout's duration, downscaled to NUTS2 regional level based on proportion of national GDP.

Finally, as we discuss the possible effects of climate impacts in the future under various climate-economic scenarios, we apply our results to the economies modeled in Section 1.1.2, and include considerations of the effect of increasing electrification of key sectors (e.g. transport and industry) which are often deemed necessary to meet climate targets.

Method

Table 2.9.3: Sectoral electricity dependence and working hours per year assumptions used in analysis.

Sector	Electricity dependence of GVA (Linares and Rey 2013)	Working hours per year (de Nooji et al. 2007)
Agriculture	40%	8,760
Energy	90%	8,760
Manufacturing	90%	8,760
Food, beverages and tobacco	90%	6,240
Pulp and paper	90%	6,240
Fertilizers	90%	8,760
Chemicals	90%	8,760
Chemical products	90%	6,240
Building materials	90%	6,240
Basic metals	90%	8,760
Metal products	90%	6,240
Rubber and plastic	90%	6,240
Construction	40%	2,600
Transport	90%	3,650
Services	80%	2,860

Using national macroeconomic data from the GTAP9 database, we first calculate sectoral gross value added (GVA), which is equal to sector output minus the sum of all intermediate inputs. To determine the amount of GVA potentially at risk of loss due to a blackout we take up the approach of Linares and Rey (2013), who estimate the electricity dependence of GVA by sector. By doing so, our approach partially addresses the limitation of the production function approach in adequately reflecting the importance of the electricity input. We use the estimates of Linares and Rey (found in Table 2.9.3) as a baseline estimate for determining current GVA at risk.

Determining the percentage reduction in GVA due to a loss of electricity in a sector's production thus becomes a simple equation:

[26] We use data from the GTAP database and not from other sources (e.g. EUROSTAT) due mainly to the consistency of the data over time and across countries. National data sources may classify sectors differently, and data sources such as EUROSTAT were found to have numerous missing values for our study year. Additionally, using GTAP data provides an easy linkage to the SSP scenarios assessed in Section 1.1.2.

*This project has received funding from the European Union's Horizon 2020 research and innovation programme under the Grant Agreement No **776479.***

$$\%\ reduction\ in\ GVA = \frac{GVA_j * electricity\ dependence}{GVA_j}$$

with the total country GVA at risk defined as:

$$GVA\ at\ risk = \sum \%\ reduction\ in\ GVA_j * \left(\frac{GVA_j}{\sum GVA_J}\right)$$

where J is the set of all sectors in a country, which results in a weighted sum of the GVA potentially lost in each sector of a country's economy. This result represents the estimated GVA at risk for the national economy without electricity for an entire year.

To find the potential loss relevant for blackout time periods of a matter of hours (and thus estimate potential impacts for blackouts occurring at different times of the day or week), we use estimates of sectoral active working time from de Nooji et al. (2007) to calculate GVA loss per hour as follows:

$$GVA\ loss\ per\ hour = \frac{(GVA_j * electricity\ dependence)}{active\ hours}$$

Calculating the GVA loss per hour, linked to the active hours of each sector, also allows for temporal differentiation in terms of the timing of a blackout. In the main results below, we estimate the potential GVA loss per hour given the occurrence of a blackout during a working weekday, followed by estimates of varying value added at risk for weeknights and weekend periods.

The above calculation steps result in an estimate of the 'current' (to the GTAP data base year of 2011) exposure. However, of greater interest is the possible future risk, given likely substantial structural changes to national economies, depending on socio-economic factors and climate policy initiatives. To address this, we utilize the results of Section 1.2, which uses a dynamic computable general equilibrium model to assess likely future structures of the economy in a manner consistent with SSP storylines and corresponding SPA (shared climate policy assumptions) scenarios chosen as reference by the COACCH project. Using projected 2050 sectoral activity levels from the WEGDYN model, we re-calculate the sectoral GVA at risk due to blackouts for modelled economies under SSP1, 2, 3 and 5 pathways.

Among the many assumptions driving the SSPs and SPAs (see Table 5.1.3 and Table 5.1.4), the electricity dependence of GVA is not explicitly addressed. We thus introduce an 'Increased Electrification' scenario, to reflect the probable rising dependence on electricity inputs in all parts of society as a key factor for production of outputs. As changing shares of electricity use in sectors may be driven not only byinput needs, but also price, we utilize a study by Mai et al. (2018) focusing on electric technology adoption. While the report is focused on US industry, it is useful in its disentangling electrification and technology adoption from the changing share of electricity in final energy demand due to changes in exogenous factors e.g. energy prices or climate / other policies. The authors estimate that by 2050, electrification of

*This project has received funding from the European Union's Horizon 2020 research and innovation programme under the Grant Agreement No **776479.***

industry will increase by about 2 and 7 percent, commercial between 8 to 12 percent, and transport up to 30%.

Also likely to be an influence on future electrification are indirect impacts in terms of climate-related needs for electricity, namely via increased demand for air conditioning and cooling with rising temperatures. Hotter working conditions could reduce worker productivity, force businesses to temporarily shut down, or run e.g. refrigeration for longer periods to maintain correct temperatures of goods. These higher electricity demands would translate into an increased dependency on electricity to maintain current levels of output. Schleypen et al. (2019) illustrate the heterogeneity of these potential impacts on different sectors across the EU for different energy. They estimate electricity demand due to these factors to rise by between 0.6 to 2% for agriculture, 0.6 to 2.1% for industry, and 13.1 to 40.1% for commercial sectors, varying by RCP and time period.

Due to this rising demand for electricity in terms of GVA dependence both in terms of technological change and increased electrification, as well as the additional climate-related electricity burden, we increase our baseline electricity dependence 10 percentage points for construction, services and agriculture sectors, and five percent for manufacturing and transport (as it is unlikely that transport would genuinely become 100% dependent on electricity across the entirety of the EU, 95% is an ambitious upper bound). The results of this electrification scenario can be seen in Figure 2.9.6 as the 'Increased' scenario.

Results and discussion

Full results for the main set of scenarios and assumptions (current time + projected 2050 economies under various SSPs, for a current and increasing electrification scenario) can be found in Figure 2.9.6. The results are additionally downscaled proportionally to NUTS2 level, using EUROSTAT data on GDP in NUTS2 regions, and can be seen in Figure 2.9.7.

*This project has received funding from the European Union's Horizon 2020 research and innovation programme under the Grant Agreement No **776479.***

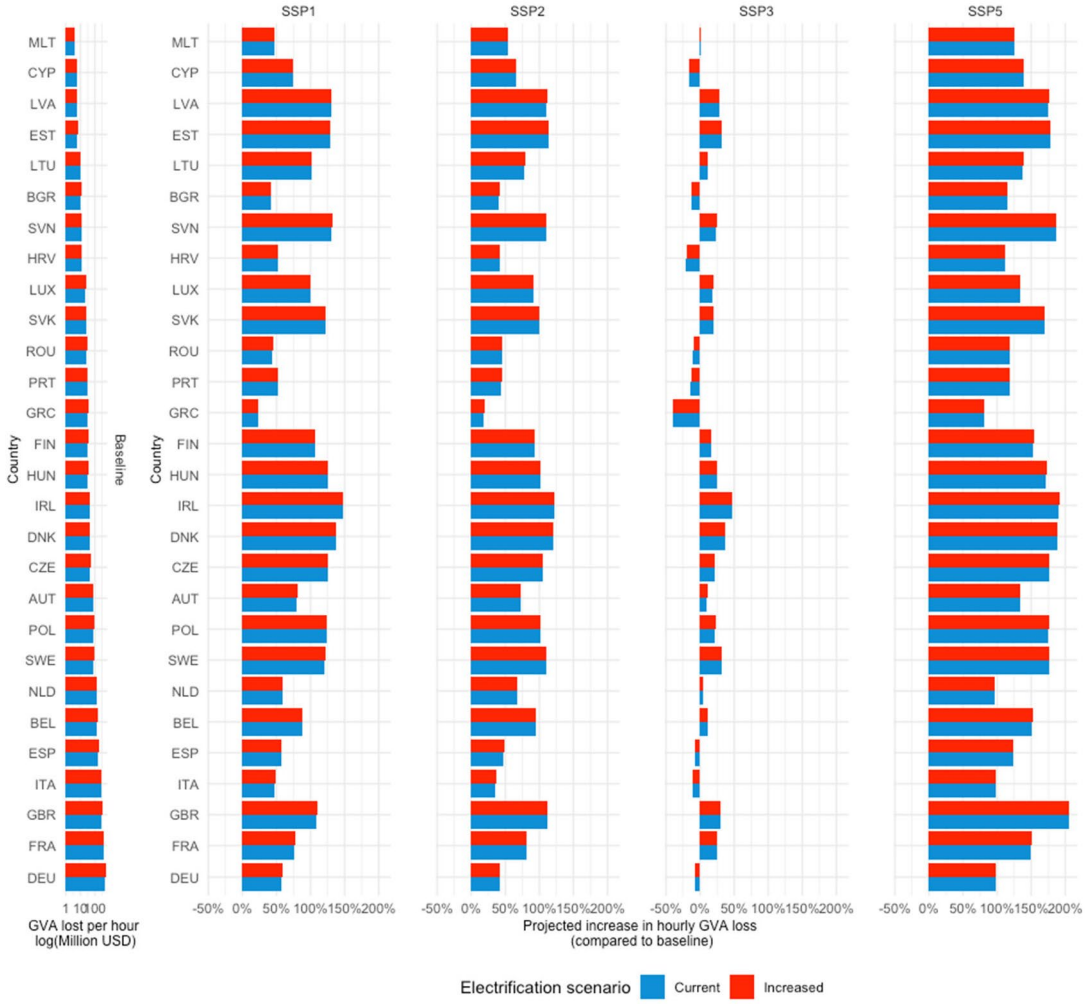

Figure 2.9.6: Potential GVA loss per hour (for EU countries and Great Britain) due to electricity blackouts, for the current economic structure and 2050 economies under SSP1, 2, 3, and 5 assumptions, for two scenarios of electrification. GVA loss potential is depicted for a blackout event occurring during a normal working weekday. In the left panel, the estimated GVA loss per hour for the current period is given in monetary terms, while the four right panels depict the percentage change in GVA loss per hour relative to this baseline.

*This project has received funding from the European Union's Horizon 2020 research and innovation programme under the Grant Agreement No **776479.***

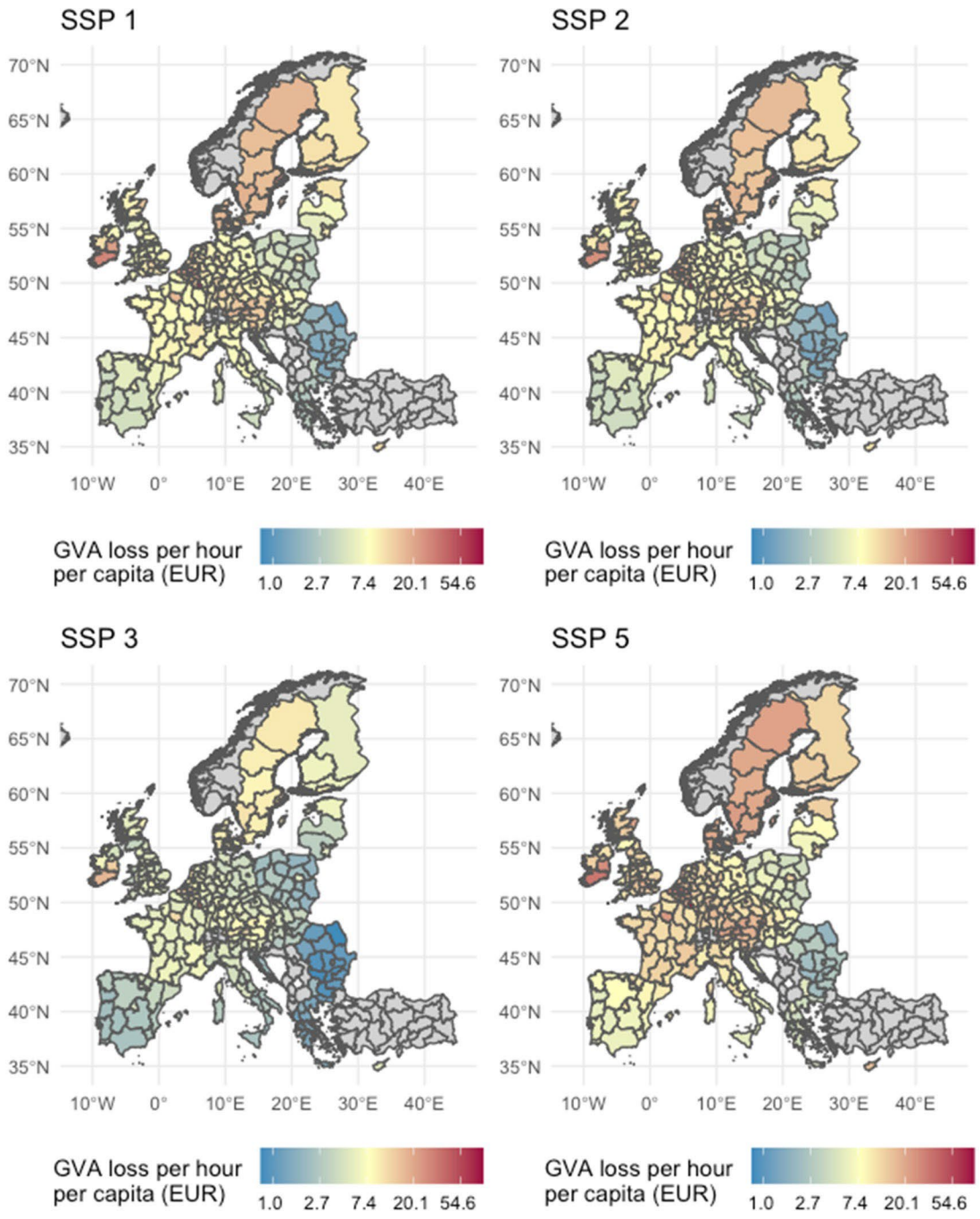

Figure 2.9.7. Potential GVA loss per hour due to electricity blackouts for 2050 economies under SSP1, 2, 3, and 5 assumptions, for the 'current' electrification scenario. National GVA loss is downscaled to regional level using NUTS2 GDP data. The panels indicate GVA loss per hour per capita for each SSP. Luxembourg (not clearly visible) has the highest value in every scenario, ranging between 55 and 85 EUR per hour per capita.

As seen in Figure 2.9.6, which depicts potential GVA loss, the envisaged socio-economic structures resulting from SSP projections lead to huge differences in national exposure to blackout in the model. SSP storylines focused on sustainability (SSP1), the middle of the road scenario (SSP2) and fossil-fueled development (SSP5) all result in

*This project has received funding from the European Union's Horizon 2020 research and innovation programme under the Grant Agreement No **776479.***

much higher potential value added at risk as compared to current levels, while the regional rivalry storyline (SSP3) holds exposure at about today's levels, and for some countries decreasing their exposure. While the SSPs contain different fossil fuel prices, electrification of sectors, growth targets etc., the results of the CGE modeling in Section 1.1.2 – and common to SSPs 1, 2, and 5 – is a drastic increase in activity of a number of manufacturing sectors, especially as compared to the activity levels of SSP
3. Given our assumption that currently, the share of GVA reliant on electricity in manufacturing is 90%, and will likely rise further in the future, the increased manufacturing activity in the future drives the results. Mostly irrespective of the SSP chosen, and the underlying causes for sectoral growth, our model forsees substantial exposure growth by mid-century. The impact of the increasing electrification scenario is limited, as for most large sectors, an extremely high electricity dependence is already assumed in the baseline scenario, and thus, increases are marginal.

Our results are driven mainly by sectoral activity levels of the CGE modeling framework, and do not take into account factors which may reduce blackout exposure. For instance, while electricity supply may expand in the SSP storyline focused on sustainability (SSP1), this epansion and shift to renewables implies large capacities of rooftop PV and local windpower plus batteries, i.e. technologies which are already used in Australia and California for safeguarding electricity supply, and which would reduce blackout vulnerability.

We find the baseline results to be in line with previous estimates of the impacts of blackouts at national level. While studies mainly focus on VoLL, some do further calculate monetary impacts of blackouts on a per-hour basis. De Nooij et al (2007) estimated the cost of a one hour loss of supply for the Netherlands on a weekday to result in a loss of approximately 120 million EUR for firms and government, compared to our baseline estimate for value added at risk (VAaR) of 133 million EUR. For Austria, Bliem (2005) estimates an hourly loss of around 60 million EUR, while our current estimates of VAaR for the country are 75 million EUR. Beyond production function approaches, the econometric model developed by the FP7 project SESAME (called the 'Blackout Simulator') estimates similarly sized effects for e.g. Czechia, with an estimated hourly blackout impact of about 80 million EUR, compared to our estimateof VAaR at 50 million EUR, or Italy with 440 million EUR to our 270 million. It should be noted that the latter estiamtion approach takes a different approach which may bettercapture impacts of e.g. spoilage, delays in restarting production processes, and/or repairs to facilities, among other direct impacts, while we focus more on the indirect impacts through non-availability of electricity in a sector.

The results describe the *potential exposed value added;* actual blackout disaster impacts are predicated upon the existence of a hazard in the form of a climate impact as described in Section 2.9.2, acting on these exposed assets which are in turn vulnerable. Vulnerability as the last third of the risk framework, determines the propensitity for an exposed asset to be damaged. As mentioned, an SSP1 world may lead to increased manufacturing sector activity, but being a sustainable pathway, if it consists of predominately distributed renewable generation with microgrids and battery backups, the eventual risk of a large scale blackout event could be mitigated much more than in an SSP3 or 5 world, with lower exposure but correspondingly

*This project has received funding from the European Union's Horizon 2020 research and innovation programme under the Grant Agreement No **776479.***

higher vulnerability due to a different electricity supply structure. We turn to this issue in further depth in Section 3.9 with a discussion of the vulnerability of future electricity supply and distribution.

Our approach is – as far as can be found – the first attempt to provide forward-looking (in terms of SSP scenarios) projections of blackout impacts; until now, studies have focused on past events, or current risk. Additionally, our research is novel in the application of a common assessment framework to the whole of the EU, departing from the standard of sub-national or national assessments in past studies, and we additionally provide a first effort to downscale results to sub-national levels. Our method allows for easy linking to the modelling framework in Section 1.2 and a first estimate of how exposure to blackout risk may change in the future.

While our analysis is in line with other literature, it is not free of weaknesses, namely the lack of regional differentiation in terms of sector active hours, electricity dependence and corresponding electrification scenario. It is highly likely that a large amount of heterogeneity exists between EU countries in terms of these variables, but estimates of such are lacking. Estimates of sectoral electricity dependence are also rare and not well investigated in the literature, as put forward by Lineares and Rey (2012), presenting opportunities for future research. Most discussion of electrification of industry does not explicitly quantify the increasing share of electricity as an integral input to production, and frequently such a signal from modeling outputs cannot be disentangled from increasing electrification due to changing input prices (e.g. via taxes on fossil fuels, cheaper renewables etc.) or other indirect effects.

3. Discussion and conclusions

3.1. Impacts of migration

Our modelling has shown that under a certain set of assumptions a number of African households and potentially social groups breach the series of socio-economic tipping points. Consequently, the numbers of migrants moving from African regions to Europe will rise over the course of the 21st century. The increases are driven by population and climate change-induced drought magnitude projections in Africa. The results therefore suggest that adaptation policy might consider how these two drivers could be effectively managed. However, it should be noted that these modelling results are grounded in historical data on migration flows. They are therefore based onthe assumption that the probability and conditions of access to European countries faced by migrants from Africa remain similar, on average, to those that have existed in the last 50 years. Clearly, if access restrictions became markedly more severe, the migrant numbers would decline. Conversely, the degree to which states allow their citizens to leave is also assumed to remain similar to that currently existing. Similarly, the validity of the model depends on both the current relative levels of GDP/capita in Africa and Europe persisting over the time period as well as the personal costs to each migrant of moving.

Moreover, we highlight that whilst income and amenity differentials are likely to remain important in informing decisions relating to movements of people, such real-

*This project has received funding from the European Union's Horizon 2020 research and innovation programme under the Grant Agreement No **776479.***

world decisions are likely to be much more complex and determined by a range of social, cultural and economic factors (Black et al., 2011). As highlighted by Boas et al. (2019), future research in this area should embrace this complexity if it is to best inform both adaptation and development policies.

3.2. Financial Tipping Points

There is an increasing recognition that the physical risks of climate change are a financial risk, and this is reflected in recent initiatives by the financial sector andcentral banks. A literature review has assessed the potential financial risks of climate change and used this to qualitatively explore potential transmission pathways including socio-economic tipping points.

The analysis has first looked at sovereign risks and credit ratings. This finds that large-scale climate hazards already affect ratings, and in turn the cost of debt and cost of capital: in extreme cases these can be a direct cause of sovereign defaults. The major credit rating agencies have already identified climate change as a global mega- trend that will impact sovereign creditworthiness. The study has identified potential pathways, whereby climate impacts affect economic and fiscal performance, leading toa major downgrade of sovereign credit ratings, and in turn affecting the cost of debt, the public finances, the cost of capital and levels of investment. These could arise from a series of large climate shocks or major slow-onset risks and could be irreversible. These major downgrade tipping points are unlikely to be a major issue for Europe, but are a potential risk for small island states and LDCs, especially given their less diversified economies and geographies, lower incomes, and lower fiscal flexibility.

The study has also looked at the potential transmission pathways from climate change through to financial markets. Climate change is a risk for the stock of manageable assets and investment returns, and potentially financial market stability. While the effects here could be very large (in financial terms), it is more difficult to see large-scale tipping points, though these could emerge in particular geographical areas or investment or asset classes.

Finally, recent initiatives are addressing these risks by encouraging greater climate related disclosure (in the private sector and in financial institutions). However, greater disclosure could be detrimental for high risk countries or regions, because this transparency is likely to lead to financial market anticipation of future risks. This could mean that a socio-economic tipping point (e.g. for a high-risk country or sector) could actually occur before the physical impacts of climate change occur, i.e. market anticipation could bring forward the timing of localised tipping points.

3.3. Food and Water

Climate change may render agricultural production to not be viable anymore, leading to farms to cease to exist, and thereby triggering rural abandonment. Here, this socio-economic tipping point is defined by agricultural land abandonment, measured as the change in cropland area. We tested the hypothesis that the tipping point of land abandonment occurs with a combination of yield deviations induced by

*This project has received funding from the European Union's Horizon 2020 research and innovation programme under the Grant Agreement No **776479.***

gradual climate change and substantive climate-induced yield drops caused by extreme events. Yield impacts stemming from both gradual climate change and extreme events are a result of the biophysical crop model EPIC and are based on climate model projections with Euro-Cordex downscaling. These served as inputs in thebio-economic model GLOBIOM, to investigate under what magnitude of yield shocks around 2030 and 2050 the socio-economic tipping points of land abandonment occurs.To analyze the implications of local tipping points on a macroeconomic level, weapplied the COIN-INT computable general equilibrium model for 2050.

Amongst the all GCM-RCP-SSP cases analyzed, the largest magnitude of cropland losses due to farmland abandonment found is about 7% for Europe. Theseare not all connected to the strongest forcing scenario (RCP8.5), or a specific SSP,which is in line with the lack in differences in the magnitude of yield shocks observed along the RCP axis in D3.2 of COACCH. Geographical differences were however found. In the five selected cases with the highest farmland abandonment in Europe, land abandonment was highest in the middle and Southern parts of Europe and showed particular concentrations in Southern Spain and Italy. The abandoned farmland foundis a result of the analysis using a partial-equilibrium model that describes the land in economic terms and therefore does not consider how the interplay with other sectors and socio-economic variables may accelerate or discourage the process of land abandonment. Thus the economy-wide and effects were further investigated using themacroeconomic CGE model COIN-INT. From the macroeconomic assessment we find that food prices in Europe slightly increase in most of the analyzed scenarios. We demonstrate that GDP effects might be strongly overestimated, when only capturing the slow-onset effect of climate change on agriculture (i.e. average yield changes), instead of also including extreme events and the resulting changes in cropland availability. Cropland loss due to extreme events could (more than) offset positive effects from long-run (slow onset) higher yields.

*This project has received funding from the European Union's Horizon 2020 research and innovation programme under the Grant Agreement No **776479.***

3.4. Coastal migration

For coastal migration we showed that high migration number that might trigger tipping points in societies do not occur in the EU28 due to its high existing standards of coastal protection, which will avoid large-scale migration even if there would be no further raising of dikes. For other regions, such as the MENA region a one of the main sources of migration into the EU28, the migration thresholds defined in the previous COACCH Deliverable D3.2 could be crossed from RCP6.0 onwards in the 2050s and the 2080s. However, the most important contributing factor is successful adaptation to rising sea-levels. With adaptation, migration numbers are below thresholds in nearly all cases. However, additional autonomous adaptation in the form of migration further avoids impacts. We demonstrate that the simultaneous implementation of planned and autonomous measures is superior to purely planned adaptation. This is in line withthe literature. For some developing regions autonomous adaptation might even be superior to planned adaptation, as planned adaptation needs high (public) investmentsinto grey infrastructure which binds capital that might be used more productively elsewhere in the economy.

We further demonstrate that sectoral effects can be very different between regions, with comparative advantages in foreign trade being a main driver of these differences.

Finally, our analysis shows that the benefits of adaptation might be overestimated when using a no-adaptation scenario as a reference. Since autonomous adaptation will happen in any case (people will migrate if their place of living is regularly flooded), impact assessments of sea level rise should use an autonomous adaptation scenario as a point of reference.

3.5. Adaptation to accelerating sea level rise

Using a stylized model loosely based on the City of Rotterdam, we investigated the interaction between sea level rise and socio-economic mechanisms leading to the SETP of an abrupt drop in the value of real estate (SETP). This resulted in the following insights. For lowly elevated outerdike areas, tipping points due to sea level rise are likely to occur in the 21st century. Transformational response is required to maintain these areas, especially in high-end sea level rise scenarios. For innerdike areas such as the City Centre of Rotterdam with high-end flood protection infrastructure, SETPS can be avoided in the 21st with sound, proactive flood risk management. With poor,reactive flood risk management, SETPs may occur under high end sea level rise even in cities that are currently protected with a very high protection level (1:10,000 year event). The cause for these SETPs under high end SLR scenarios is that the implementation times of the traditional dike heightening measures will become too long compared to rate of sea level rise projected by the end of the 21st century. Hence, the major cause of these SETPs is that the rate of change of the naturalenvironment may exceed societies ability to adapt.

*This project has received funding from the European Union's Horizon 2020 research and innovation programme under the Grant Agreement No **776479.***

3.6. Trade disruptions due to flooding

The question whether river flood disruptions of the European road network may cause SETPs was examined on three spatial levels.

First, at the level of a (member) state, for six European territories we examined whether river floods could cause a major loss of network functionality. We found that there are large differences in network vulnerability between European countries. Among the most vulnerable countries are Albania and Italy. Among the most robust countries are Sweden and the island of Ireland. In each country, some very critical (and flood vulnerable) links were identified. The disruption of these would lead to a disproportionally large loss of network functionality. This analysis is helpful for identification of the most vulnerable road segments in a country. However, a more detailed analysis is required to deal with the uncertainties, including: the resolution of the inundation modelling, the bias towards the historic time series, and the local flood-proofing that is not acknowledged in the current model set-up. This could help to prioritize the investigation in these local weaknesses in the network. This prioritization paves the way for targeted adaptation of the road network at the level of individual road segments, which is an advantage of the object-based approach.

Second, at the level of the national road network of Austria, we examined the economic costs of six unfavourable flood scenarios, which may happen with return period 1:100 year. Under future climate scenarios, the likelihood of these events may increase with a factor 2-10 if no adaptation takes place. The most disruptive scenario costs 101 million euro (pricelevel 2015): 88 million for cars and 13 million for trucks. The major share of costs originates from cancelled trips rather than from detour times. Although these disruptions may be very disruptive and bothersome on the local scale and for particular road users, we did not find convincing evidence that these floods lead to substantial macro-economic disruptions. We reason that the expected 101 million euro of damage is relatively small compared to the total flood losses during large flood events, which can add up to billions of euros.

Third, at the level of an individual car and truck manufacturer we assessed whether river floods could cause a significant disruption of the supply of just-in-time input products to the manufacturer. We found that the risk of the manufacturer or any of the suppliers being hit by a river flood is more substantial than a disruption of the road transport from the supplier to the manufacturer. This suggests that SETPs are more likely to be caused by a flood of the manufacturer itself or a flood at one of the suppliers to the factory than from a flood of the road network connection the supplierssto the manufacturer. Furthermore, the detour times in case of inundation of thepreferred routes from the suppliers to the manufacturer tend to increase in a rather linear fashion. This indicates that the European road network has a high degree of resilience. Nevertheless, these initially linear increases of travel time may be a cause ofSETPs due to four characteristics of the supply chain of the truck and car manufacturer.The first characteristic is that there are legal thresholds limiting the time that a truck driver can drive. If this threshold is exceeded, the driving times increase sharply. The second characteristic is that the time window in which the products can be deliveredto the factory is limited by a staff availability constraint. As a result, any substantial delay (such as resulting from passing the legal driving time threshold) in delivery will

*This project has received funding from the European Union's Horizon 2020 research and innovation programme under the Grant Agreement No **776479.***

directly translate in a full day delay of stock deliveries. The third characteristic is that a delay of one day already creates a problem at the manufacturer because of the very small stocks that are kept. The fourth characteristic is that problems at the manufacturer will spill over to the supplier as well, because the supplier needs a timelyreturn-transport of some package container to successful continue production of the input product. Large supply chain disruptions during the recent COVID-19 crisis confirmthat the car and truck manufacturers are indeed very sensitive to these cascading effects.

Overall, our results suggest that Europe is unlikely to experience a severe (tipping point like) macro-economic shock resulting from decreasing road networkperformance due to river flooding. However, most national road networks have weak parts, disruptions of which may cause damage in the order of 100 million euros. The network of potential candidate country Albania is relatively vulnerable. On a smaller scale, river floods may cause SETPs for specific supply chains working with just-in-time deliveries, although the risk of the production sites or delivering factories being flooded seems to be more substantial than a disruption of the road network.

3.7. Collapse of insurance markets for extreme weather risks

With climate change flood risk is increasing in most European regions inducing higher damages. Whether households insure damages against flooding or not depends on various parameters such as the amount of premiums that need to be paid, the disposable income, the perceived risk of flooding and above all the insurance market system in place. When insurance is not mandatory, but households can voluntarily decide to take up insurance, penetration rates are usually low. With climate change induced increases of premiums, insurance uptake may further decline resulting in a collapse of the insurance market system.

While the tipping point regions identified in the sectoral analysis include regions in Croatia, Bulgaria, Czech Republic, Poland and Portugal, the macroeconomic analysis reveals particularly severe impacts for the Netherlands, the Central European region, Germany, Austria and Italy. The Central European region entails the two tippingregions Czech Republic and Poland. As the other tipping regions Croatia, Bulgaria and Portugal are in a model aggregate with less severely affected regions and regions where no insurance data is available from the DIFI model, we observe comparatively small impacts.

A major difference in the outcomes of analysed regions lies in the insurance market system that is currently in place and we assumed to not change throughout the analysed time horizon (up to 2080). Regions relying on a public-private partnership or a solidarity system, with both systems maintaining mandatory insurance uptake, are among the least affected. These regions include the UK, France and the BLU regions entailing Belgium and Luxembourg. The obligation of insuring against flood risk implies that there is no uncovered risk and households do not need to reduce savings to finance repair costs nor do governments have to issue compensation payments.

Overall, we find that welfare effects largely exceed the effects on GDP indicating on the one hand the productive potential of natural disasters and on the

*This project has received funding from the European Union's Horizon 2020 research and innovation programme under the Grant Agreement No **776479.***

other hand the importance of distinguishing between different economic indicators. While the destruction of productive capital is a clear negative driver for economic growth, the reconstruction of damaged assets enter positively in calculation of GDP. Thus, the adverse shock is partly absorbed by creating demand for reconstruction. Nevertheless, the indicator welfare might better represent the situation when analysing the effects of natural disasters such as flooding.

3.8. Climate induced economic shocks

The time of emergence of impacts (ToEI) of climate change measures the first year in which climate impacts exceed a desired threshold of paste economic shocks. Unlike the more traditional impact measures (absolute monetary & relative to GDP), the ToEI relates future climate impacts to past economic shocks thereby placing climate impacts in the context of past economic experience.

The ToEI results imply that economically stable, developed countries are equally or more at risk from climate change than less economically stable, developing countries. This conclusion follows from the way ToEI is modelled. Namely, for the observations with less severe past GDP shocks, the past GDP impact threshold is lower thereby making it more likely for future impacts to exceed this pre-determined value. This result is at odds with the result that developed countries are “safer” in the face of climate change due to high levels of economic development, an observation commonlyfound using more traditional impact measures. ToEI methodology suggests that it can also be expected that the developed countries could more likely perceive the effects ofclimate change impacts as severe shocks to their economies than it is the case for the developing countries with a vast experience in political conflict and economic crises.

The ToEI methodology is flexible and can be applied to different impact studies not necessarily related to climate change or Europe. The user is free to define an impact threshold of interest and the size of the past impact pool, as long as sufficient data is available. Through the local-scale integrated assessment model (IAM) CLIMRISK,we have shown that country-level impact data can be used to project ToEI estimates on a 0.5 degree * 0.5 degree grid in Europe. The advantages of local scale past shock data can only be utilised by applying the ToEI methodology to a model of an equal or higher spatial resolution.

The key conclusion of the ToEI analysis of climate induced economic shocks is that even moderate mitigation effort can delay the ToEI by several decades, as was witnessed by the difference in ToEI projections for RCP 4.5 and RCP 8.5. In Europe, Scandinavian countries and Western-Europe could experience a significant delay in the ToEI from around 2080 to well past 2100 for most parts. Abiding by the Paris Agreement would delay the effects even further into the 22nd century, however this is not studied in detail in the current study that focuses on the 21st century.

The analysis on climate-induced economic shocks has been also conducted with the ICES macroeconomic NUTS2 model. The assessment aims to identify how many regions and where economic shocks are larger than the 5% of regional GDP. The macroeconomic perspective of the ICES model enables to capture market adjustments triggered by climate change impacts. Furthermore, it does not rely upon reduced form climate change damage functions, but analyses the economic consequence of each

*This project has received funding from the European Union’s Horizon 2020 research and innovation programme under the Grant Agreement No **776479.***

single climate change impact through its effect on the quantity and quality of production factors or changes in consumer preferences. The exercise is thus an interesting complement of the CLIMRISK assessment. The evaluation is performed for the 9 SSP-RCP scenario combinations of the COACCH project. For each, the uncertainty range is represented considering a “low”, “medium” and “high” impact case. Major findings are the following: considering a “medium impact” case, regions in the EU meeting the chosen social-economic tipping point are considerably more in high climate-change (16-31 out of th total of 138) than in low climate-change scenarios (4- 8).

Nonetheless, the situation blurs when the possible “high end” of the impact uncertainty range is considered. In this case, also in low climate change scenarios many EU areas meet the tipping point in RCP2.6 and 4.5 (27-60) in a way comparable to what occurs in RCP6.0 or 8.5 (41-57). The factor at work, is the smoothing effect of impacts on agriculture where CO2 fertilization decreases yield losses in higher temperature scenarios. This highlights the particular care that needs to be used in the interpretation of aggregated results where the “averaging effect” can hide huge losses. The possibility of high losses in low tempertature RCPs also stresses the importance to reduce emission as much as possible as, given the uncertainty, “every degree matters”. Mitigation is thus essential to reduce to an acceptable level the chances of these localized high losses. Finally, adaptation also can play an important role. In the exercise it is noted that more economic “flexibility” (larger substitutability across energy and non energy input or across domestic and imported commodities) tends to reduce the number of regions reaching the tipping point, even though more assets could be at risk compared with lower exposure, but more “economically rigid” scenarios. Although very rough, this is an indication that building adaptive capacity and flexibility is fundamental to address climate shocks.

3.9. Electricity system failures

While in Section 2.9 we address the hazard (wildfires occurrence) and exposure (value added at risk) facets of the typical disaster risk triangle, an open issue is the potential future vulnerability of electricity production and distribution, with vulnerability of the system being its susceptibility to harm (IPCC 2014) or ability to cope with, resist, and recover from a disaster. Below we discuss two factors, stranded asset risk and the changing electricity sector, which could significantly influence the future system’s vulnerability and resilience, followed by final conclusions anddiscussion.

Divestment in the energy sector and stranded assets

Assets in the electricity sector are rapidly becoming obsolete due to a technological paradigm change which implies departure from fossil fuels. Projections of the role of new technologies such as renewable electricity sources coupled with solid-state power electronics and high voltage direct current transmission lines presentthe possibility of decreasing demand for all types of fossil fuels. Renewable electricity generation decreases demand for coal and gas, adoption of electric vehicles decreases

*This project has received funding from the European Union’s Horizon 2020 research and innovation programme under the Grant Agreement No **776479.***

demand for oil, new HVAC systems (heating, ventilation, air conditioning) decrease demand for oil and gas from buildings.

Additionally, as electricity from PV and wind is now cheaper for most parts of the world than the marginal costs of electricity from coal power plants, the latter are in fact also stranded assets, leading to avoidance of costs due to major maintenance, thereby increasing the vulnerability of the fossil power sector. Many power plants in Australia are not reliable, either due to age or due to poor quality, contributing to the numerous blackouts in the electricity sector and accelerating the uptake of renewable energy. Now, with the additional impact of large wildfires on the electricity sector in Australia, investors redirect investments to renewable energy; another development that is not reversible.

Investment companies, in their effort to avoid losses due to investment in stranded assets are globally beginning to ban investments in thermal power plants. Again, this gives rise to a positive exponential loop with PV, batteries and wind power, as more orders for these technologies cause prices to decrease, making investments here ever more attractive. Financing organizations are divesting from fossil fuel assets to avoid large financial losses and to support climate mitigation, with recent reports that institutions managing over 11 trillion USD in assets have committed todivestment, an increase from 52 billion USD in 2014 (Fortuna 2020). Divestment is mainly being driven by the rising penetration of renewable electricity generation, as well as the recognition that increasing climate risk could be closely linked to investment risk, leading to a likely significant reallocation of capital (Chalmers 2020). Thus, the problem of stranded assets in the electricity system may increase in the future. Accordingly, risks from stranded assets are analyzed even for central banks' financial stability, Bolton et al. (2020). These authors describe "green swan" risks, potentially extremely financially disruptive events that could be behind the next systemic financial crisis. The authors emphasize that this complex, multifaceted problem requires coordinating actions among many players including governments, the private sector, civil society and the international community.

This likely divestment and shift to renewable generation capacity coupled with long-distance, high-power transmission could present a large issue, where investing in soon-to-be-stranded assets becomes economically or socially unattractive, potentially leading to reduced investment into maintenance and upkeep of current generation and transmission and subsequent rising potential of such systems triggering blackouts or wildfires given the increasing periods of drought and heatwaves. Given the amount and ubiquity of assets affected by technological change, if so much investment is put into a qualitatively different form of asset, this is an opportunity for both a decrease of emissions of greenhouse gases and building up an electricity infrastructure that is far more robust with respect to impending damage from large wildfires.

Reducing vulnerability to blackouts from fires via a changing electricity sector

Contrary to the previous discussion of both biophysical and socio-economic conditions which could exacerbate both the incidence of wildfires and subsequent blackouts, the necessary modernization of electricity generation and distribution could have a mitigating effect on the incidence of wildfire hazard and the severity of

*This project has received funding from the European Union's Horizon 2020 research and innovation programme under the Grant Agreement No **776479.***

subsequent blackout effects. Climate policies which encourage distributed renewable generation of electricity and the use of battery backups may lessen the risk of climate-induced blackouts and provide additional stability to the grid. Improving grid reliability via decreasing its length and complexity has been proposed, although the potential is mixed; while more interconnected European grids have experienced four times the number of faults as those less interconnected, they are considered as significantly more reliable based on reliability indicators for the bulk of their distribution, because they perform better in three dimensions: systematically lower ENS (estimation of energy not supplied), TLP (total loss of power) and RT (restoration time). Thus, these faults have smaller impacts (Martinez-Anido et al 2012). However, the authors do note that reliability indicators are not well-suited to discussing rare, extreme events, e.g. blackouts due to wildfire. Of the three sub-indicators mentioned, RT would be most important with reference to the criterion of "major blackout". Climate policies encouraging local renewable generation, microgrids and battery storage could reduce the size and impacts of blackout events caused by climate conditions, compared to the current system, but may have differential effects on society, due to their expense (Mulkern 2019). Solar PV is already seen as a mitigating factor in preventing blackouts from fires in Australia (Parkinson 2019), and the use of large-scale battery installations may help to address shortfalls in supply caused by insufficient cooling of thermal generation due to drought or upswings in demand due to heatwaves (Suba 2020).

Linking hazard, exposure, and vulnerability

Each facet of risk – hazard, vulnerability, and exposure – jointly contributes to the eventual impact on a system, and while our current findings by no means allow to paint a comprehensive picture of future blackout risk, our assessment of changing wildfire risk as well as relative change in exposure do allow for emphasizing future areas of concern. From Deliverable 3.2 we found the possibility of extreme increases inwildfire occurrence, not only in drier, more southern latitudes or areas typically known for seasonal fires, but also in central and parts of northern Europe especially in the second half of the century. However, as the present wildfires in Siberia demonstrate, such impacts could come much faster than is generally thought. This again illustrates the effect of sudden overwhelming impacts from exponential relationships, here between temperature increase and drying of fuels.

At the same time, we find in this work that almost universally, exposure to blackouts caused by fires is likely to increase in the future, for the most part irrespective of the specific socioeconomic scenario. The scale of exposure increase differs significantly between an SSP3 future, or SSP1 or 2, which all see less of an increase in exposure than SSP5, but it does not seem probable that in any case, exposure to blackouts will decrease to any large degree, neither for the EU as a whole nor for individual countries.

However, within that space there are relative winners and losers. Italy and Spain are two countries which face the dual burdens of very high or extreme increases in fire risk in the future in almost all scenarios, combined with some of the highest GVA loss potential exposure (over 100 million EUR per hour in both nations), which will in all likelihood increase substantially in the future; ranging from around 35% in SSP2 to

*This project has received funding from the European Union's Horizon 2020 research and innovation programme under the Grant Agreement No **776479.***

between 100 to 125% in SSP5. Conversely Greece, a country with similar fire risk, sees a much lower increase in future exposure change, which for SSP1 and 2 remains below 25%, the lowest increase in Europe. The modelling in Section 1.2 would see Greece in an SSP4 world with a reduction in exposure of over 25%, and in an SSP5 world, it is the only modelled country with exposure increase below 100% of current values. Portugal, Romania, Bulgaria, and Croatia also have a less severe increase than Spain or Italy, but still almost double the increase in exposure in SSP1 and 2 compared to Greece.

There are also a number of countries which could see a drastic rise in exposure without a corresponding increase in fire risk, such as Great Britain, Ireland, parts of central Europe e.g. Czechia and to a lesser extent Hungary.

To better understand and visualize the potential future risk, we build upon the exposure and hazard indicators described in Section 2.9 by combining them into an index of potential blackout risk due to fire. In a similar approach to e.g. Williges et al (2017), Nelson et al. (2010), we intersect the two indicators spatially to identify areasof higher or lower potential future risk, creating a differential index for Europe. Each indicator is normalized to fall between zero and one, with low hazard / exposure being zero and the inverse being one. We then add the two dimensions, thus producing a maximum potential risk value of two. Table 3.9.1 depicts the link between each indicator (hazard and exposure) and the normalized index, and depicts the qualitative interpretation for the resulting index. The results can be seen in Figure 3.9.1 and Figure 3.9.2 for RCPs 4.5 and 8.5 (respectively). The results for RCP 2.6 are provided in Figure 5.2.2.

Table 3.9.1. Depiction of the potential future risk index and correlation between original values (FDSI changes and GVA loss) to normalized values.

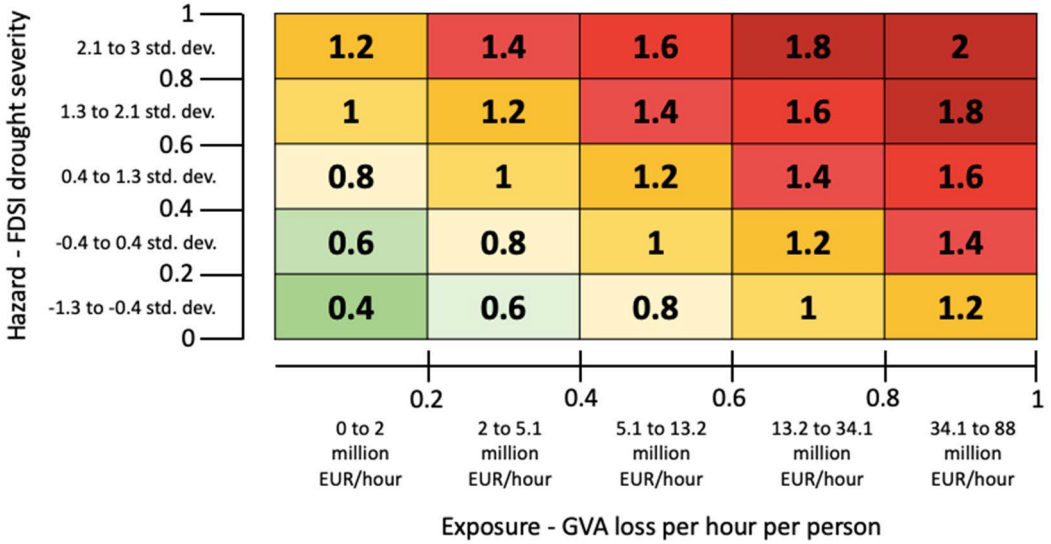

*This project has received funding from the European Union's Horizon 2020 research and innovation programme under the Grant Agreement No **776479.***

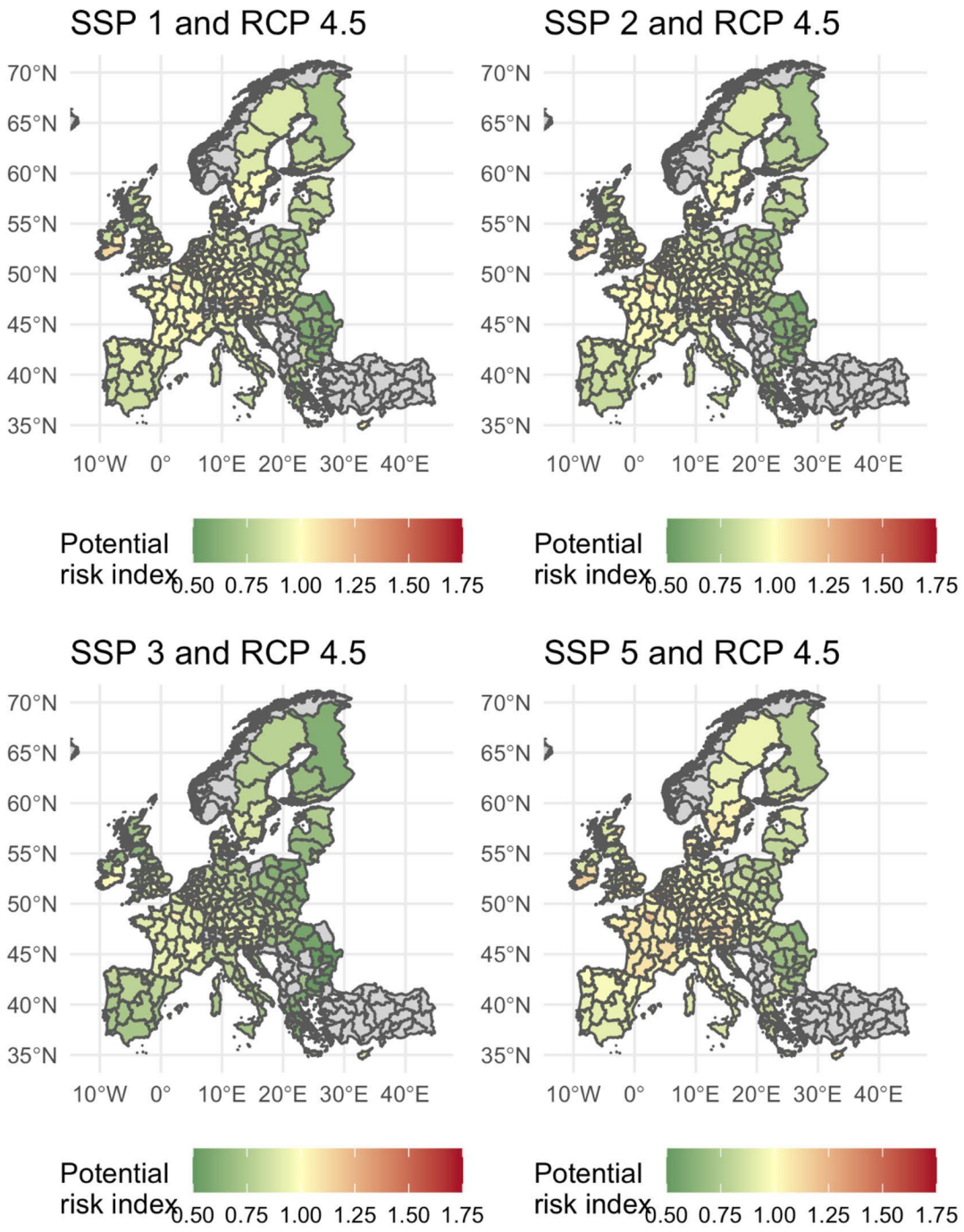

Figure 3.9.1. Potential future risk index (derived from hazard + exposure indicators) for RCP 4.5 model runs, for SSPs 1, 2, 3 and 5. Higher values indicate higher risk.

*This project has received funding from the European Union's Horizon 2020 research and innovation programme under the Grant Agreement No **776479.***

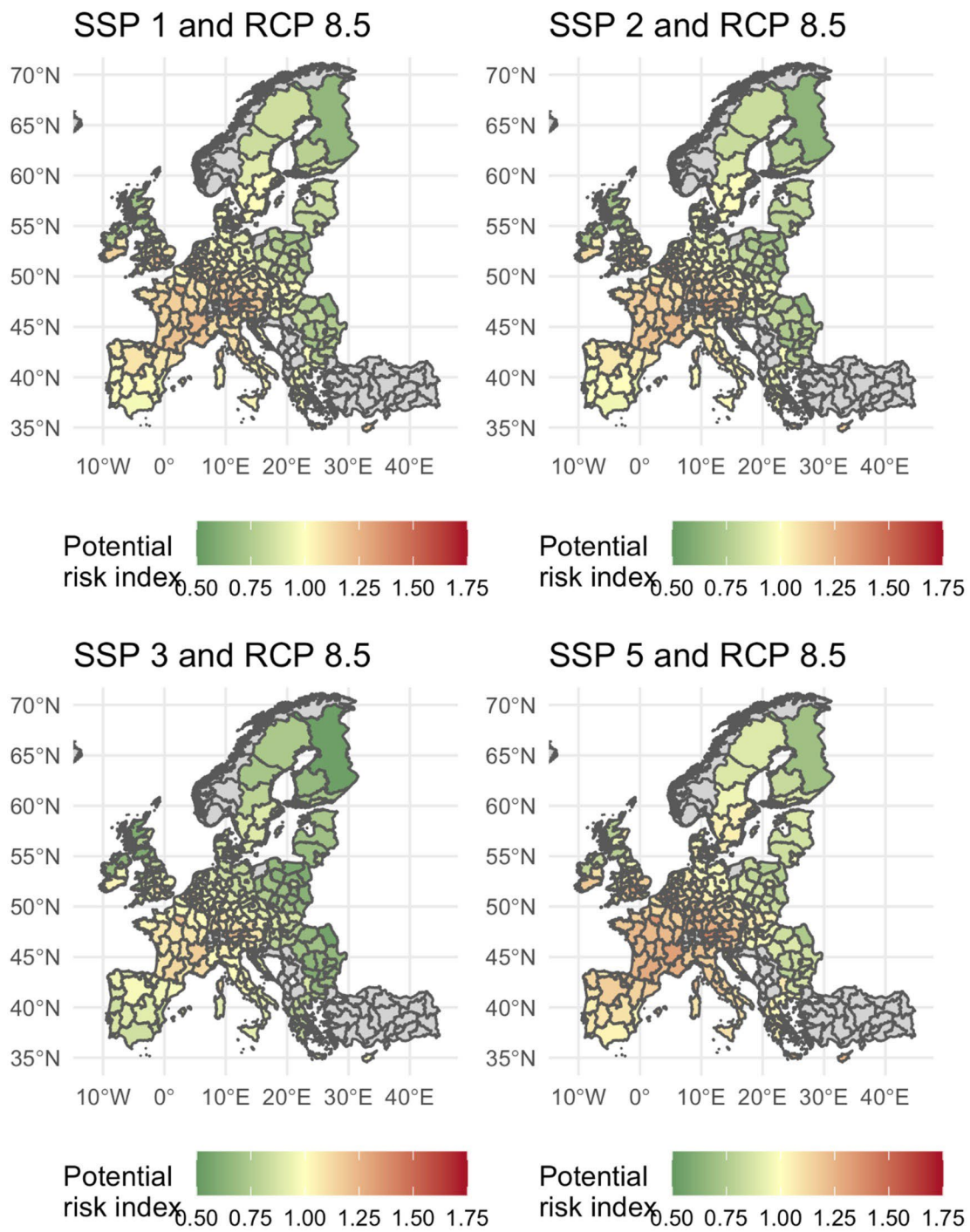

Figure 3.9.2. Potential future risk index (derived from hazard + exposure indicators) for RCP 8.5 model runs, for SSPs 1, 2, 3 and 5. Higher values indicate higher risk.

As seen in the resulting index of hazard and exposure, RCP 8.5 scenarios result in the highest potential risks for the majority of Europe over all SSPs, with the exception of Scandinavia, which model results predict would fare worse under a RCP 2.6 scenario. In the results of RCPs 4.5 and 8.5, extreme drought events in the region grow closer to the historical mean as the century progresses (likely due to increased

*This project has received funding from the European Union's Horizon 2020 research and innovation programme under the Grant Agreement No **776479.***

precipitation across all seasons near the end of the century, while in RCP 2.6 the region sees less change in precipitation (a common trend in RCP 2.6 for the most part, leading to the more uniform slight increase in drought risk, but no large changes and lack of an increase over time) (Rajczak and Schär 2017).

The results indicate that outside of an SSP3 scenario with limited rise in exposure, the highest potential risks will exist for the Iberian peninsula andMediterranean region, but also more central and northern regions (e.g. increases in southern Scandinavian regions), while Eastern Europe will be less effected, due to bothmilder hazard increase and less projected exposure in comparison to the rest of theEU. The results are robust across most SSPs and RCPs, but the reader should bereminded that we present only a small subset of possible RCP ensembles, and further expansion of the model runs incorporated would be beneficial to confirm the robustness of hazard increase.

It must be repeated, however, that this is only part of the risk equation, and a key missing factor discussed above remains vulnerability. As shown, the future structure of the electricity system could have a major influence on both the incidence of fire hazard and the resilience (or conversely vulnerability) to extreme blackouts. But too much is still unknown about the future grid and sectoral structure as well as the differential vulnerability of a distributed renewables-based system versus centralized interconnected grids. At present, areas of greater or lesser degree of potential risk can be identified and emphasized, in terms of increasing awareness and encouraging future planning, while research and experience will continue to evolve in terms of vulnerability to blackout.

Conclusions

A seemingly small effect, the slow increase of temperature, has had sudden and unexpected strong effects on human systems in Australia and in California. Given the nature of the two most important driving forces, periods with below-average rainfall and occasional strong heat waves with their exponential impact on availability of fuel for wildfires, such impacts on society and economy are also becoming highly likely for Europe. Due to the exponential behavior, no problem seems to exist for a long time and then, very suddenly, the problem becomes overwhelming.

In our assessment of a socio-economic tipping point of major blackouts due to increasing wildfires, we use a risk-based approach to assessing the possible current impacts and effects on European countries. Beginning with Deliverable 3.2, we outline the hazard component of this risk, here being climate conditions (decreasing precipitation leading to long drought periods, followed by heatwaves) leading to enhanced wildfire risk, finding that much of the land area in Europe could see extreme increase in wildfire probability by the end of the century under different RCP scenarios, including areas which until now have little experience dealing with such threats.

In this work, we began by expanding on the biophysical dimension of the hazard, highlighting an exponential increase in dryness of fuels for wildland fires with increasing temperatures, thus emphasizing the likely underestimation of fire risk until now, and its likelihood of becoming ever more common in the future. We then turn to exposure as the second component of risk, as a lack of exposed assets to such fires

*This project has received funding from the European Union's Horizon 2020 research and innovation programme under the Grant Agreement No **776479.***

would result in minimal risk. Focusing on blackouts due to fires, we derive a method for assessing potential exposure in terms of value added at risk, based on previous studies of blackouts using production-function approaches, and project our estimates forward to future SSP scenarios using CGE modeling results. We find that across Europe, VAaR is expected to increase strongly under three of four SSP projections, due to a marked increase in manufacturing sector activity in all but SSP3 modelled worlds.

We complete our discussion of risk with a focus on the potential vulnerability to such blackouts with an overview of key traits of the electricity sector which will impact the eventual losses due to wildfires in the future. The structure and composition of the electricity supply and transmission network, in terms of grid size, complexity and interconnections, as well as the generation plants that connect to it, will be a defining characteristic of eventual vulnerability, along with the potential stranded assets which may occur in terms of conventional electricity generation depending on future investment and energy policy.

Australia and California reacted rapidly – both economically and politically – and in much the same way by installing large amounts of PV and by installing large numbers of batteries of a size that did not exist before. The use of big batteries by utilities came unexpectedly and was met with skepticism (Bullis 2014), however, demand for batteries has become so high that now about 10 companies have factories of comparable size and this transformation of both the energy sector and the transportation sector will become more all-encompassing. This then is a positive feedback loop between production and installation. Batteries are now beginning to replace some distributional grids, which then decreases the vulnerability of the electricity system to large wildfires. This development cannot easily be reversed.

Climate change is much more difficult for thermoelectric plants than for PV and wind power. Thermoelectric plants are more susceptible to several impacts of climate change, due to a lack of water and decrease of efficiency if the temperature of water for cooling increases. Due to better economics, as electricity from thermoelectric plants is now considerably more expensive than electricity from PV and wind, governments can more easily fulfill their greenhouse gas emission obligations. Accordingly, new construction of thermoelectric plants increases the amount of soon- to-be stranded assets.

Thus, decision-makers should recognize that the impending threat of major wildfires in Europe can be avoided by accelerating their plans for investing in renewable energy. And here it is of utmost importance to include all new technologies in the planning process, as the energy sector is of significant importance, both in termsof economic relevance and greenhouse gas emissions. Our research, pointing out the acuteness of this risk, can thus serve as an important input for an acceleration of investments in renewable energy.

Many questions exist in this sector, but the major pathway advice is obvious and comparatively easy to implement due to its favorable economic and, mostly, political advantages – accelerate investments in renewable energy, both in central power stations and decentralized, with batteries, both central and decentralized.

*This project has received funding from the European Union's Horizon 2020 research and innovation programme under the Grant Agreement No **776479.***

4. References

Abatzoglou, J.Tl & Williams, A.P. (2016). Impact of anthropogenic climate change on wildfire across western US forests. *Proceedings of the National Academy of Sciences of the United States of America*, *113*(42), 11770-11775. doi:10.1073/pnas.1607171113

Acclimatise, Climate Finance Advisors, and Four Twenty Seven. (2017). Lenders' Guide for considering climate risk in infrastructure investments. Investment Guide for Climate Risk. Retrieved from https://climatefinanceadvisors.com/wp-content/uploads/2018/01/Investment-Guide_1.8-single-hi-q_17012018.pdf

ACEA, (2020, 1 June). Interactive map: Production impact of COVID-19 on the European auto industry. Retrieved from https://www.acea.be/

Aerts, J. (2018). A review of cost estimates for flood adaptation. *Water, 10*(11): 1646. doi:10.3390/w10111646

Aguiar, A., Narayanan, B., & McDougall, R. (2016). An overview of the GTAP 9 Data Base. *Journal of Global Economic Analysis 1*, 181–208. doi:10.21642/JGEA.010103AF

Alfieri, L., Feyen, L., Dottori, F., & Bianchi, A. (2015). Ensemble flood risk assessment in Europe under high end climate scenarios. *Global Environmental Change, 35*, 199-212. doi:10.1016/j.gloenvcha.2015.09.004

Allen, C. D., A. K. Macalady, H. Chenchouni, D. Bachelet, N. McDowell, M. Vennetier, T., … Cobb, N. (2010). A global overview of drought and heat-induced tree mortality reveals emerging climate change risks for forests. *Forest Ecology and Management, 259* (4), 660-684. doi.org/10.1016/j.foreco.2009.09.001

Armington, P.S. (1969). A theory of demand for products distinguished by place of production (Une theorie de la demande de produits differencies d'apres leur origine) (Una teoria de la demanda de productos distinguiendolos segun el lugar de produccion). *Staff Papers - International Monetary Fund, 16*, 159. doi:10.2307/3866403

Balkovic, J., R. Skalsky, et al. (2009). D2100 of the cc-tame project: Database and data strategy report. Technical report.: 24.

Bamber, J. L., Oppenheimer, M., Kopp, R. E., Aspinall, W. P., & Cooke, R. M. (2019). Ice sheet contributions to future sea-level rise from structured expert judgment. *Proceedings of the National Academy of Sciences of the United States of America*, *166*(23), 11195–11200. doi: 10.1073/pnas.1817205116

Banton, C. (2020, Feb 4). Just in Time (JIT). In Investopedia. Retrieved from https://www.investopedia.com/terms/j/jit.asp

Behrens, P., van Vliet, M. T. H., Nanninga, T., Walsh, B., & Rodrigues, J. F. D. (2017). Climate change and the vulnerability of electricity generation to water stress in the European Union. *Nature Energy 2*, 17114. doi:10.1038/nenergy.2017.114

*This project has received funding from the European Union's Horizon 2020 research and innovation programme under the Grant Agreement No **776479.***

Black, R., Arnell, N., & Dercon, S. (2011) Migration and global environmental change – Review of drivers of migration. *Global Environmental Change, 21*, S3–S11. doi: 10.1016/j.gloenvcha.2011.10.005

Black, R., Bennett, S.R.G., Thomas, S.M., & Beddington, J.R. (2011). Climate change: migration as adaptation. *Nature, 478*, 447–449. doi: 10.1038/478477a

Bliem, M (2005). Eine makroökonomische Bewertung zu den Kosten eines Stromausfalls im österreichischen Versorgungsnetz. IHSK Discussion Paper. Institute for Advanced Studies, Carinthia, Austria.

Boas, I, Farbotko, C, Adams, H, Sterly, H, Bush, S, van der Geest, K, … Hulme, M. (2019). Climate migration myths, *Nature Climate Change, 9* (12), 901-903. doi.org/10.1038/s41558-019-0633-3

Boere, E., Valin, H., Bodirsky, B., Baier, F., Balkovic, J., Batka, M., Folberth, C., Karstens, K., Kindermann, G., Krasovskii, A., Leclere, D., Wang, X., Weindl, I., Havlik, P. & Lotze-Campen, H. (2020). Impacts on agriculture including forestry & fishery. Deliverable D2.2, COACCH H2020 Project.

Bompard, E., Huang, T., Wu, Y., & Cremenescu. M. (2013). Classification and trend analysis of threats origins to the security of power systems. *Electrical Power and Energy Systems, 50,* 50–64. doi: 10.1016/j.ijepes.2013.02.008

Bosello et al. (2020). D2.7. Macroeconomic, spatially-resolved impact assessment. Deliverable of the H2020 COACCH project.

Bosello et al. (2018). MS8. ICES NUTS-2 model calibrated on the selected set of scenarios. Milestone of the H2020 COACCH project.

Bosello F., Eboli, F., & Pierfederici, R. (2012). *Assessing the economic impacts of climate change. An updated CGE point of view*, Working Papers 2012.02, Fondazione Eni Enrico Mattei.

Bosello, F., & De Cian, E. (2014). Climate change, sea level rise, and coastal disasters. A review of modeling practices. *Energy Economics, 46*, 593–605. doi: 10.1016/j.eneco.2013.09.002

Bosello, F. & Parrado, R. (2018). D2.1 Protocol of information exchange flow and model integration. Deliverable of the H2020 COACCH project.

Bosello, F., & Standardi, G., (2015). *A sub-national CGE model for the European Mediterranean countries* (Working Paper No. RP0274), CMCC Research Papers. CMCC, Lecce (Italy).

Bosello, F., Nicholls, R. J., Richards, J., Roson, R., & Tol, R. S. J. (2012). Economic impacts of climate change in Europe: Sea-level rise. *Climatic Change*, *112*(1), 63–81. doi: 10.1007/s10584-011-0340-1

Botzen, W. J. W., Aerts, J. C. J. H., & van den Bergh, J. C. J. M. (2009). Dependence of flood risk perceptions on socioeconomic and objective risk factors. *Water Resources Research*, *45*(10), 1–15. doi:10.1029/2009WR007743

*This project has received funding from the European Union's Horizon 2020 research and innovation programme under the Grant Agreement No **776479.***

Brown, T., Leach, S., Wachter, B., & Gardunio, B. (2020). The northern California 2018 extreme fire season. In S. C. Herring, , N. Christidis, A. Hoell, M. P. Hoerling, & P. A. Stott (Eds.) Explaining extreme events of 2018 from a climate perspective. *Bulletin of the American Meteorological Society*, 101 (1), S1–S128. doi:10.1175/BAMS-ExplainingExtremeEvents2018.1.

Bruin, K. de, Hubert, R., Evain, J., Clapp, C., Stackpole Dahl, M., & Bolt J. (2019). Physical climate risk. Investor needs and information gaps. CICERO Climate Finance – ClimINVEST project. Retrieved from https://www.cicero.oslo.no/en/publications/internal/2884

Bryant, B. P., & Lempert, R. J. (2010). Thinking inside the box: A participatory, computer-assisted approach to scenario discovery. *Technological Forecasting and Social Change*, *77*(1), 34–49. doi: 10.1016/j.techfore.2009.08.002

Bullis, K. (2014). Does Musk's gigafactory make sense? MIT Technology Review. Retrieved from https://www.technologyreview.com/s/526126/does-musks-gigafactory-make-sense/

CAL FIRE (2017). Incident Archive. Retrieved from https://www.fire.ca.gov/incidents/2017/

Chalmers, S. (2020). World's largest fund manager BlackRock cuts thermal coal exposure on climate concerns. ABC News. Retrieved from https://www.abc.net.au/news/2020-01-15/worlds-largest-fund-manager-to-cut-thermal-coal-exposure/11869300

Ciscar, J.C., Feyen, L., Soria, A., Lavalle, C., Raes, F., Perry, M., ... Ibarreta, D. (2014). *Climate impacts in Europe*. The JRC PESETA II Project. JRC Scientific and Policy Reports, EUR 26586EN.

CISL (2018) University of Cambridge Institute for Sustainability Leadership (CISL). Sailing from different harbours: G20 approaches to implementing the recommendations of the Task Force on Climate-related Financial Disclosures. Cambridge, UK: the Cambridge Institute for Sustainability Leadership. Retrieved from https://www.cisl.cam.ac.uk/resources/publication-pdfs/cisl-tcfd-report-2018.pdf

Climate Transparency (2017). Financing the transition from brown to green: how to track country performance towards low carbon, climate resilient economies. Climate Transparency Secretariat and ODI, Berlin, Germany. Retrieved from http://www.climate-transparency.org/wp-content/uploads/2017/12/Financing_the_transition.pdf

Covington, H. & Thamotheram, R. (2015). The case for forceful stewardship (Part 1): The financial risk from global warming (January 19, 2015). Available at SSRN: https://ssrn.com/abstract=2551478 or doi:10.2139/ssrn.2551478

Dai, H.-C., Zhang, H.-B., & Wang, W.-T. (2017). The impacts of U.S. withdrawal from the Paris Agreement on the carbon emission space and mitigation cost of China, EU, and Japan under the constraints of the global carbon emission space. *Advances in Climate Change Research*, *8* (4), 226–234. doi:10.1016/j.accre.2017.09.003

de Jong, G. (2007). Value of freight travel-time savings. In: D.A. Hensher & K.J. Button (Eds.), *Handbooks in Transport, Volume 1: Handbook of Transport Modelling* (pp.649-663). Emerald Group. doi:10.1108/9780857245670-041

*This project has received funding from the European Union's Horizon 2020 research and innovation programme under the Grant Agreement No **776479.***

De Nederlandsche Bank (2017). Waterproof? An exploration of climate-related risks for the Dutch financial sector. Retrieved from https://www.dnb.nl/en/binaries/Waterproof_tcm47-363851.pdf?2019061816

de Nooij, M., Koopmans, C., Bijvoet, C. (2007). The value of supply security: The costs of power interruptions: Economic input for damage reduction and investment in networks. *Energy Economics, 29*, 277–295. doi:10.1016/j.eneco.2006.05.022

DeConto, R. M. & Pollard, D. (2016). Contribution of Antarctica to past and future sea-level rise. *Nature, 531*, 591–597. doi:10.1038/nature17145

Dietz, S., Bowen, A., Dixon, C. & Gradwell, P. (2016). 'Climate value at risk' of global financial assets. *Nature Climate Change, 6*, 676–679. doi:10.1038/nclimate2972

Earth-i. (2019). Europe's 2019 wildfires already exceed last year's blazes. Retrieved from https://earthi.space/blog/europe-wildfires-2019

Eboli F., Parrado R. & Roson R. (2010). Climate-change feedback on economic growth: Explorations with a dynamic general equilibrium model. *Environment and Development Economics, 15*, 515-533. Retrieved from www.jstor.org/stable/44379339

Economist Intelligence Unit (2015) The cost of inaction the value at risk from climate change. Retrieved from https://eiuperspectives.economist.com/sites/default/files/-The%20cost%20of%20inaction_0.pdf

Eurelectric. (2013). Union of the Electricity Industry. Power Distribution in Europe – Facts & Figures. Retrieved from https://www3.eurelectric.org/powerdistributionineurope/

European Environment Agency (2017). Climate change, impacts and vulnerability in Europe 2016. EEA Report No 1/2017. An indicator-based report. ISSN 1977-8449.

Eurostat. (2019). 43% of the EU is covered with forests. *Eurostat News.* Retrieved from https://ec.europa.eu/eurostat/web/products-eurostat-news/-/EDN-20190321-1

Feo-Valero, M., García-Menéndez, L. & Garrido-Hidalgo, R. (2011). Valuing freight transport time using transport demand modelling: A bibliographical review. *Transport Reviews: A Transnational Transdisciplinary Journal, 31* (5), 625-651. doi:10.1080/01441647.2011.564330

Filatova, T. (2014). Market-based instruments for flood risk management: A review of theory, practice and perspectives for climate adaptation policy. *Environmental Science & Policy, 37*, 227–242. doi:10.1016/j.envsci.2013.09.005

Fortuna, C. (2020). 2019 Divestment year In review. Clean Technica. Retrieved from https://cleantechnica.com/2020/01/02/2019-divestment-year-in-review/

Frank, S., Böttcher, H., Gusti, M., Havlík, P., Klaassen, G., Kindermann, G. & Obersteiner, M. (2016). Dynamics of the land use, land use change, and forestry sink in the European Union: The impacts of energy and climate targets for 2030. *Climatic Change, 138*(1-2), 253--266. doi: 10.1007/s10584-016-1729-7

*This project has received funding from the European Union's Horizon 2020 research and innovation programme under the Grant Agreement No **776479.***

Frank, S., Schmid, E., Havlík, P., Schneider, U. A., Böttcher, H., Balkovic, J. & Obersteiner, M. (2015). The dynamic soil organic carbon mitigation potential of European cropland. *Global Environmental Change, 35*, 269--278. doi:10.1016/j.gloenvcha.2015.08.004

Fricko, O., Havlik, P., Rogelj, J., Klimont, Z., Gusti, M., Johnson, N., … Riahi, K. (2017). The marker quantification of the Shared Socioeconomic Pathway 2: A middle-of-the-road scenario for the 21st century. *Global Environmental Change 42*, 251–267. doi:10.1016/j.gloenvcha.2016.06.004

Gorman, S. (2019). Year's most destructive California wildfire declared extinguished after two weeks. Reuters. Retrieved from https://www.reuters.com/article/us-california-wildfire/years-most-destructive-california-wildfire-declared-extinguished-after-two-weeks-idUSKBN1XI0BA

Grinsted, A. (2020, May 12). Here's how the expert estimates of future sea level rise (Horton et al., 2020) compare to other sea level rise projections" [Twitter Post, updated version in reply 8:15 AM]. Retrieved from: https://twitter.com/AGrinsted/status/1260091186573914113

Haer, T., Botzen, W. J. W., de Moel, H., & Aerts, J. C. J. H. (2017). Integrating household risk mitigation behavior in flood risk analysis: An agent-based model approach. *Risk Analysis*, *37*(10), 1977–1992. doi:10.1111/risa.12740

Hainmueller, J. & Hiscox, M. J. (2007). Educated preferences: Explaining attitudes toward immigration in Europe. *International Organization*, *61* (2), 399-442. https://www.jstor.org/stable/4498150

Hanley, S. (2020). Neoen commits to building 600 MWh battery In Victoria. CleanTechnica. Retrieved from https://cleantechnica.com/2020/04/07/neoen-commits-to-building-600-mwh-battery-in-victoria/

Haraguchi, M., & Lall, U. (2015). Flood risks and impacts: A case study of Thailand's floods in 2011 and research questions for supply chain decision making. *International Journal of Disaster Risk Reduction, 14*, 256–272. doi:10.1016/j.ijdrr.2014.09.005

Hauer, M.E. (2017). Migration induced by sea-level rise could reshape the US population landscape. *Nature Climate Change, 7*(5), 321-325. doi:10.1038/nclimate3271

Hauer, M.E., Fussell, E., Mueller, V., Burkett, M., Call, M., Abel, K. ,… Wrathall, D. (2019). Sea-level rise and human migration. *Nature Reviews Earth & Environment, 1*, 28-39. doi:10.1038/s43017-019-0002-9

Havlík, P., Valin, H., Herrero, M., Obersteiner, M., Schmid, E., Rufino, … Notenbaert, A. (2014). Climate change mitigation through livestock system transitions. *Proceedings of the National Academy of Sciences of the United States of America*, *111*(10), 3709--3714. doi:10.1073/pnas.1308044111

Herrero, M., Havlík, P., Valin, H., Notenbaert, A., Rufino, M. C., Thornton, P. K., & Obersteiner, M. (2013). Biomass use, production, feed efficiencies, and greenhouse gas emissions from global livestock systems, *Proceedings of the National Academy of Sciences of the United States of America, 110*(52), 20888--20893. doi:10.1073/pnas.1308149110

*This project has received funding from the European Union's Horizon 2020 research and innovation programme under the Grant Agreement No **776479.***

Hinkel, J., & Nicholls, R.,J. (2020). Responding to sea level rise. *The Bridge, 50*(1), 50–58. Retrieved from https://www.nae.edu/228938/Responding-to-Sea-Level-Rise

Hinkel, J., Lincke, D., Vafeidis, A. T., Perrette, M., Nicholls, R. J., Tol, R. S. J., … Levermann, A. (2014). Coastal flood damage and adaptation costs under 21st century sea-level rise. *Proceedings of the National Academy of Sciences of the United States of America, 111*(9), 3292–3297. doi:10.1073/pnas.1222469111

Hino, M., Field, C.B., & Mach, K.J. (2017). Managed retreat as a response to natural hazard risk. *Nature Climate Change, 7* (5), 364-370. doi:10.1038/nclimate3252

Hof, A., van Vuuren, D., Watkiss, P., & Hunt, A. (2018). D1.5 Impact and policy scenarios co-designed with stakeholders. Deliverable of the H2020 COACCH project.

Huizinga, J., de Moel, H., & Szewczyk, W. (2017). *Global flood depth-damage functions. Methodology and database with guidelines.* European Union. Retrieved from https://doi.org/10.2760/16510

ICBS and SOAS (2018). Climate change and the cost of capital in developing countries. Available at http://unepinquiry.org/publication/climate-change-and-the-cost-of-capital-in-developing-countries/

IEA (2018). *World energy outlook 2018*. Paris: International Energy Agency.

IOM (2018). *Mapping human mobility and climate change in relevant national policies and institutional frameworks*. Geneva: International Organization for Migration.

IOM (2019). *International Migration Law N°34 - Glossary on Migration*. Geneva: International Organization for Migration.

IPCC (2014). Climate change 2014: Synthesis report. Contribution of Working Groups I, II and III to the Fifth Assessment Report of the Intergovernmental Panel on Climate Change [Core Writing Team, R.K. Pachauri and L.A. Meyer (Eds.)]. Geneva, Switzerland: IPCC.

IPCC (2019). IPCC Special Report on the Ocean and Cryosphere in a Changing Climate [H.-O. Pörtner, D.C. Roberts, V. Masson-Delmotte, P. Zhai, M. Tignor, E. Poloczanska, K. Mintenbeck, A. Alegría, M. Nicolai, A. Okem, J. Petzold, B. Rama, N.M. Weyer (Eds.)]. Geneva, Switzerland: IPCC.

Iqbal, K., & Roy, P. K. (2015). Climate change, agriculture and migration: Evidence from Bangladesh. *Climate Change Economics, 06* (02), 1550006. doi:10.1142/S2010007815500062

Johnson, A. (2019, October 23). Fire safety power blackouts begin for as many as a half-million in California. NBCnews. Retrieved from https://www.nbcnews.com/news/us-news/fire-danger-again-threatens-power-800-000-across-california-n1070351

Jolly, W.M.A., Cochrane, M.A., Freeborn, P.H., Holden, Z.A., Brown, T.J., Williamson, G.J., & Bowman, D.M.J.S. (2015). Climate-induced variations in global wildfire danger from 1979 to 2013. *Nature Communications, 6*, 7537. doi:10.1038/ncomms8537

*This project has received funding from the European Union's Horizon 2020 research and innovation programme under the Grant Agreement No **776479.***

Kemp-Benedict, E., Lamontagne, J., Laing, T., & Drakes, C. (2019). Climate impacts on capital accumulation in the small island state of Barbados. *Sustainability, 11* (11), 3192. doi:10.3390/su11113192

Kesten, H. (1982). *Percolation theory for mathematicians*.Boston, MA: Birkhäuser. doi:10.1007/978-1-4899-2730-9. ISBN 978-0-8176-3107-9

Kindermann, G. E., McCallum, I., Friz, S. & Obersteiner, M. (2008). A global forest growing stock, biomass and carbon map based on FAO statistics. *Silva Fennica, 42*(3): 387-396. doi:10.14214/sf.244

Klein, R. J. T., Midgley, G. F., Preston, B. L., Alam, M., Berkhout, F. G. H., Dow, K., … Thomas, A. (2015). Adaptation opportunities, constraints, and limits. In *Climate Change 2014 Impacts, Adaptation and Vulnerability: Part A: Global and Sectoral Aspects*. New York, NY: Cambridge University Press.

Koubi, V., Spilker, G., Schaffer, L., & Böhmelt, T. (2016). The role of environmental perceptions in migration decision-making: evidence from both migrants and non-migrants in five developing countries. *Population and Environment, 38*(2), 134–163. doi:10.1007/s11111-016-0258-7

Kubik, Z., & Maurel., M. (2016). Weather shocks, agricultural production and migration: Evidence from Tanzania. *The Journal of Development Studies, 52*(5): 665–80. doi:10.1080/00220388.2015.1107049

Kunreuther, H., & Pauly, M., 2004. Neglecting disaster: Why don't people insure against large losses? *Journal of Risk and Uncertainty, 28*, 5-21. doi:10.1023/B:RISK.0000009433.25126.87

Kwadijk, J. C. J., Haasnoot, M., Mulder, J. P. M., Hoogvliet, M. M. C., Jeuken, A. B. M., van der Krogt, R. A. A., … de Wit, M. J. M. (2010). Using adaptation tipping points to prepare for climate change and sea level rise: a case study in the Netherlands. *Wiley Interdisciplinary Reviews: Climate Change*, *1*(5), 729–740. https://doi.org/10.1002/wcc.64

Kwakkel, J. H. (2017). The exploratory modeling workbench: An open source toolkit for exploratory modeling, scenario discovery, and (multi-objective) robust decision making. *Environmental Modelling and Software*, *96*, 239–250. doi:10.1016/j.envsoft.2017.06.054

Le Bars, D., Drijfhout, S., & de Vries, H. (2017). A high-end sea level rise probabilistic projection including rapid Antarctic ice sheet mass loss. *Environmental Research Letters*, *12*(4), 044013. doi:10.1088/1748-9326/aa6512

Le Den, X., Persson, M., Benoist, A., Hudson, P., de Ruiter, M., de Ruig, L., & Kuik, O. (2017). *Insurance of weather and climate related disaster risk: Inventory and analysis of mechanisms to support damage prevention in the EU*. Luxembourg: Publications Office of the European Union. doi:10.2834/40222

Leahy, E., & Tol, R.S.J. (2010). *An estimate of the value of lost load for Ireland*. ESRI Working Paper No. 357. Dublin: The Economic and Social Research Institute (ESRI),.

*This project has received funding from the European Union's Horizon 2020 research and innovation programme under the Grant Agreement No **776479.***

Lewis, S. C., Blake, S. A. P., Trewin, B,. Black, M. T., Dowdy, A. J., Perkins-Kirkpatrick, S. E., King, A. D., & Sharples. J. J. (2020). Deconstructing factors contributing to the 2018 fire weather in Queensland, Australia. In: S. C. Herring, N. Christidis, A. Hoell, M. P. Hoerling, & P. A. Stott, (Eds.), Explaining extreme events of 2018 from a climate perspective. *Bulletin of the American Meteorological Society, 101* (1), S1–S128, doi:10.1175/BAMS-ExplainingExtremeEvents2018.1

Linares, P., & Rey, L. (2013). The costs of electricity interruptions in Spain. Are we sending the right signals? *Energy Policy, 61*, 751–760. doi:10.1016/j.enpol.2013.05.083

Lincke, D., & Hinkel J. (2018): Economically robust protection against 21st century sea-level rise. *Global Environmental Change 51*, 67-73. doi:10.1016/j.gloenvcha.2018.05.003

Lincke, D., and Hinkel J. (forthcomming): Coastal migration due to 21st century sea-level rise [unpublished manuscript].

London Economics (2013). *The value of lost load (VoLL) for electricity in Great Britain*. London: London Economics.

Lutes, D.C., & Keane, R.E. (2006). Fuel load (FL) sampling method. USDA Forest Service Gen. Tech. Rep. RMRS-GTR-164-CD. 2006. Retrieved from https://www.fs.fed.us/rm/pubs/rmrs_gtr164/rmrs_gtr164_06_fuel_load.pdf

Maccaferri, S., Cariboni, F., & Campolongo, F. (2012). *Natural catastrophes: risk relevance and insurance coverage in the EU*. JRC Scientific and Technical Reports. Luxembourg: Publications Office of the European Union. doi:10.2788/ 93626

Mackay, D., & van Wesenbeeck I. (2014). Correlation of chemical evaporation rate with vapor pressure. *Environmental Science & Technology, 48*, 10259–10263. doi:10.1021/es5029074

Mai, T., Jadun, P., Logan, J., McMillan, C., Muratori, M., Steinberg, D., ... Nelson, B. (2018). *Electrification futures study: Scenarios of electric technology adoption and power consumption for the United States*. Golden, CO: National Renewable Energy Laboratory. NREL/TP-6A20-71500. Retrieved from https://www.nrel.gov/docs/fy18osti/71500.pdf.

Marchiori L., Maystadt J., & Schumacher, I. (2012). The impact of weather anomalies on migration in sub-Saharan Africa. *Journal of Environmental Economics and Management, 63*, 355–374. doi:10.1016/j.jeem.2012.02.001

Martínez-Anido, C. B., Bolado, R., de Vries, L., Fulli, G.,Vandenbergh, M., & Masera. M. (2012). European power grid reliability indicators, what do they really tell? *Electric Power Systems Research, 90*, 79-84. doi:10.1016/j.epsr.2012.04.007

McSweeney, C. F., & Jones, R. G. (2016). How representative is the spread of climate projections from the 5 CMIP5 GCMs used in ISI-MIP? *Climate Services, 1*, 24-29, doi:10.1016/j.cliser.2016.02.001

Mercer (2015). *Investing in a time of climate change*. Retrieved from www.mercer.com/ri/climate-change-study

*This project has received funding from the European Union's Horizon 2020 research and innovation programme under the Grant Agreement No **776479.***

Mima, S., & Criqui, P. (2014). The costs of climate change for the European energy system, An assessment with the POLES model. *Environmental Modeling and Assessment, 20*, 303–319. doi:10.1007/s10666-015-9449-3

Moody's Investors Service (2016a). Understanding the impact of natural disasters: Exposure to direct damages across countries, 28 November 2016. Retrieved from https://www.eenews.net/assets/2016/11/30/document_cw_01.pdf

Moody's Investors Service (2016b). Small island credit profiles resilient to near term climate shocks, but climate trends pose longer-term risks, 5 December 2017. Retrieved from https://www.moodys.com/research/Moodys-Medium-term-climate-change-vulnerabilities-factored-into-small-island--PR_376346

Moody's Investors Service (2017). How Moody's assesses the physical effects of climate change on sovereign issuers, 7 November 2016. Retrieved from https://www.eticanews.it/wp-content/uploads/2017/01/Moodys-climate-change-and-sovereigns-November-7.pdf

Morton, A. (2019). Just a matter of when': the $20bn plan to power Singapore with Australian solar. *The Guardian*. Retrieved from https://www.theguardian.com/environment/2019/jul/14/just-a-matter-of-when-the-20bn-plan-to-power-singapore-with-australian-solar

Mulkern, A. C. (2019). Are blackouts here to stay? A look into the future. Scientific American, E&E news on November 15, 2019.

Müller, C., Elliott, J., Chryssanthacopoulos, J., Deryng, D., Folberth, C., Pugh, T. A. M., & Schmid, E. (2015). Implications of climate mitigation for future agricultural production, *Environmental Research Letters, 10*, 125004. doi: 10.1088/1748-9326/10/12/125004.

Myers, N. (1997). Environmental refugees. *Population and Environment, 19*, 167–182. doi:10.1023/A:1024623431924

Narayanan, B., Aguiar, A., & McDougall, R. (2012). *Global trade, assistance, and production: The GTAP 8 data base*. Center for Global Trade Analysis, Purdue University.

Naumann, G., Alfieri, L., Wyser, K., Mentaschi, L., Betts, R. A., Carrao, H., … Feyen. L. (2018). Global changes in drought conditions under different levels of warming. *Geophysical Research Letters, 45*, 3285–3296. doi:10.1002/2017GL076521

Nelson, R., Kokic, P., Crimp, S., Martin, P., Meinke, H., Howden, S.M., de Voil, P. & Nidumolu, U. (2010). The vulnerability of Australian rural communities to cliamte variability and change: part 2 – integrating impacts with adaptive capacity. *Environ. Sci. Policy 13*, 18-27.

Nerem, R. S., Beckley, B. D., Fasullo, J. T., Hamlington, B. D., Masters, D. & Mitchum, G. T. (2018). Climate-change–driven accelerated sea-level rise detected in the altimeter era. *Proceedings of the National Academy of Sciences of the United States 115* (9), 2022-2025. doi:10.1073/pnas.1717312115

*This project has received funding from the European Union's Horizon 2020 research and innovation programme under the Grant Agreement No **776479.***

NGFS [Network for Greening the Financial System] (2019). A call for action: Climate change as a source of financial risk. Retrieved from https://www.banque-france.fr/sites/default/files/media/2019/04/17/ngfs_first_comprehensive_report_-_17042019_0.pdf

Nordhaus W. D. (2017). Revisiting the social cost of carbon. *Proceedings of the National Academy of Sciences of the United States*, *114* (7) 1518-1523. doi:10.1073/pnas.1609244114

O'Neill, B.C., Kriegler, E., Riahi, K., Ebi, K.L., Hallegatte, S., Carter, T.R., Mathur, R., & van Vuuren, D.P. (2014). A new scenario framework for climate change research: the concept of shared socioeconomic pathways. *Climatic Change 122*, 387–400. doi:10.1007/s10584-013-0905-2

OECD (2015). *The economic consequences of climate change*. Paris: OECD Publishing. doi:10.1787/9789264235410-en.

OECD (2016). *Financial management of flood risk*. Paris: OECD Publishing. doi:10.1787/9789264257689-en

Organization for Security and Co-operation in Europe (OSCE). 2016. Protecting Electricity Networks from Natural Hazards. OSCE, Vienna, Austria. www.osce.org

Parrado R., De Cian E. (2014). Technology spillovers embodied in international trade: Intertemporal, regional and sectoral effects in a global CGE framework. *Energy Economics, 41*, 76-89. doi:10.1016/j.eneco.2013.10.016

Parrado, R., Bosello, F., Delpiazzo, E., Hinkel, J., Lincke, D., & Brown, S. (2020). Fiscal effects and the potential implications on economic growth of sea-level rise impacts and coastal zone protection. *Climatic Change, 160*, 283–302. doi:10.1007/s10584-020-02664-y

Pedersen, J. (1995). Drought, migration and population growth in the Sahel: The case of the Malian Gourma: 1900–1991. *Population Studies, 49* (1), 111-126. doi:10.1080/0032472031000148276

Penn, I. (2017, October 17). Power lines and electrical equipment are a leading cause of California wildfires. LATimes. Retrieved from https://www.latimes.com/business/la-fi-utility-wildfires-20171017-story.html

Penn, I., Hepler, L., & Eavis, P. (2019, December 6). PG&E reaches $13.5 billion deal with wildfire victims. New York Times. Retrieved from https://www.nytimes.com/2019/12/06/business/energy-environment/pge-wildfire-victims-deal.html

Pérez Blanco, C.D., & Standardi, G. (2019). Farm waters run deep: A coupled positive multi attribute utility programming and computable general equilibrium model to assess the economy wide impacts of water buyback. *Agricultural Water Management, 213*, 336-351. doi:10.1016/j.agwat.2018.10.039

*This project has received funding from the European Union's Horizon 2020 research and innovation programme under the Grant Agreement No **776479.***

Peters, J.C. (2016). The GTAP-Power data base: Disaggregating the electricity sector in the GTAP data base. *Journal of Global Economic Analysis, 1* (1), 209–250. doi:10.21642/JGEA.010104AF

Pieters, M. (2004). *Rand Europe report TR-110-AVV*. Prepared for the AVV Transport Research Centre. Cambrige UK: Rand Europe.

Platts (2014). *UDI World Electric Power Plants Data Base (WEPP)*. Washington, DC.

PRA (2015). The impact of climate change on the UK insurance sector: A climate change adaptation report by the Prudential Regulation Authority. Available at https://www.bankofengland.co.uk/-/media/boe/files/prudential-regulation/publication/impact-of-climate-change-on-the-uk-insurance-sector.pdf?la=en&hash=EF9FE0FF9AEC940A2BA722324902FFBA49A5A29A

Prishchepov, A. V., Müller, D., Dubinin, M., Baumann, M. & Radeloff, V. C. (2013). Determinants of agricultural land abandonment in post-Soviet European Russia. *Land Use Policy*, 30, 873–884. doi:10.1016/j.landusepol.2012.06.011

Rajczak, J. and C. Schär (2017). Projections of Future Precipitation Extremes Over Europe: A Multimodel Assessment of Climate Simulations. *JGR Atmospheres 122*(20) 10773-10800.

RAND (2004). Hoofdonderzoek naar de reistijdwaardering in het vervoer van goederen over de weg (Main survey into the value of time in freight transport by road). Gerard de jong, Sjoerd Bakker. Retrieved from https://www.rand.org/pubs/technical_reports/TR110.html.

Rigaud, K.K., et al. (2018). Groundswell: preparing for internal climate migration, World Bank, Washington, DC, USA, Technical report.

Romain,H., Evain, J. & Nicol, M. (2019). Getting started on physical climate risk analysis in finance - Available approaches and the way forward. ClimINVEST project. Etrieved from https://www.i4ce.org/wp-core/wp-content/uploads/2018/12/I4CE-ClimINVEST_2018_Getting-started-on-physical-climate-risk-analysis.pdf

Rosenzweig, C., Elliott, J., Deryng, D., Ruane, A. C., Müller, C., Arneth, A., … Jones, J. W. (2014). Assessing agricultural risks of climate change in the 21st century in a global gridded crop model intercomparison. *Proceedings of the National Academy of Sciences of the United States, 111*(9), 3268-3273. doi:10.1073/pnas.1222463110

Schinko, T., Bednar-Friedl, B., Steininger, K.W., & Grossmann, W.D. (2014). Switching to carbon-free production processes: Implications for carbon leakage and border carbon adjustment. *Energy Policy 67*, 818–831. doi:10.1016/j.enpol.2013.11.077

Schleypen, J.R., Dasgupta, S.., Borsky, S., Jury, M., Ščasný, M., Bezhanishvili, L. (2019). D2.4 Impacts on Industry, Energy, Services, and Trade. Deliverable of the H2020 COACCH project.

Schröder, T., & Kuckshinrichs, W. (2015). Value of lost load: An efficient economic Indicator for power supply security? A literature review. *Frontiers in Energy Research, 3,* 55. https://doi.org/10.3389/fenrg.2015.00055

*This project has received funding from the European Union's Horizon 2020 research and innovation programme under the Grant Agreement No **776479.***

Scoccimarro, E., Steininger, K.W., Watkiss, P.. Boere, E., Hunt, A., Linke, D., … Chaves Montero, MdM. (2020). D3.2. Tipping point likelihood in the SSP/RCP space. Deliverable of the H2020 COACCH project.

Shukla, P.R., Skea, J., Slade, R., van Diemen, R., Haughey, E., Malley, J., Pathak, M., J. Portugal Pereira (2019). Technical Summary, 2019. In: P.R. Shukla, J. Skea, E. Calvo Buendia, V. Masson-Delmotte, H.-O. Pörtner, D. C. Roberts, … J. Malley, (eds.) *Climate change and land: an IPCC special report on climate change, desertification, land degradation, sustainable land management, food security, and greenhouse gas fluxes in terrestrial ecosystems*. In press.

Skalský, R., Tarasovicova, Z., Balkovic, J., Schmid, E., Fuchs, M., Moltchanova, E., Kindermann, G. & Scholtz, P. (2008). *GEO-BENE global database for bio-physical modeling v. 1.0 (Concepts, methodologies and data)*, Technical report. Laxenburg, Austria: IIASA.

South Pole Group (2016). Final report potential impact of climate change on financial market stability, Report to the German Federal Ministry of Finance. Zurich. Retrieved from https://yoursri.com/media-new/download/20161021-bmf-final-english.pdf

Standard & Poor's (2014). Climate change is a global mega-trend for sovereign risk. Retrieved from https://www.maalot.co.il/publications/GMR20140518110900.pdf

Standard & Poor's (2015a). The heat is on: How climate change can impact sovereign ratings. Retrieved from https://www.spglobal.com/ratings/en/research/articles/151125-the-heat-is-on-how-climate-change-can-impact-sovereign-ratings-9425836

Standard & Poor's (2015b). Climate change will likely test the resilience of corporates' creditworthiness to natural catastrophes. Retrieved from http://www.actuarialpost.co.uk/downloads/cat_1/SP_Climate%20Change%20Impact%20On%20Corporates_Apr212014.pdf

Standard & Poor's (2015c). Storm alert: Natural disasters can damage sovereign creditworthiness. Retrieved from https://unepfi.org/pdc/wp-content/uploads/StormAlert.pdf

Standard & Poor's (2017). How environmental and climate risks and opportunities factor Into global corporate ratings - An update. Retrieved from https://www.spratings.com/documents/20184/1634005/How+Environmental+And+Climate+Risks+And+Opportunities+Factor+Into+Global+Corporate+Ratings+-+An+Update/5119c3fa-7901-4da2-bc90-9ad6e1836801

Stavros, E. N., Abatzoglou, J. T., McKenzie, D., & Larkin, N. K. (2014). Regional projections of the likelihood of very large wildland fires under a changing climate in the contiguous Western United States. *Climatic Change, 126*, 455-468. doi:10.1007/s10584-014-1229-6

Sterl, A., van den Brink, H., de Vries, H., Haarsma, R., & van Meijgaard, E. (2009). An ensemble study of extreme storm surge related water levels in the North Sea in a changing climate. *Ocean Science*, *5*(3), 369–378. doi:10.5194/os-5-369-2009

*This project has received funding from the European Union's Horizon 2020 research and innovation programme under the Grant Agreement No **776479.***

Suba, R. (2020). How Tesla's big battery saved South Australia from 3 major blackouts. Teslarati. Retrieved from https://www.teslarati.com/tesla-big-battery-south-australia-3-blackouts/

TCFD (2017). Recommendations of the Task Force on Climate-related Financial Disclosures. Retrieved from https://www.fsb-tcfd.org/wp-content/uploads/2017/06/FINAL-2017-TCFD-Report-11052018.pdf

TCFD (2019). Task Force on Climate-related Financial Disclosures: Status Report. 2019 report. Retrieved from https://www.fsb-tcfd.org/publications/tcfd-2019-status-report/

Thober, J., Schwarz, N., & Hermans, K. (2018). Agent-based modeling of environment-migration linkages: a review. *Ecology and Society, 23*(2), 41. doi:10.5751/ES-10200-230241

Tol, R. S. J. (1995). The damage costs of climate change: Toward more comprehensive calculations. *Environmental and Resource Economics, 5*, 353–374. https://doi.org/10.1007/BF00691574

Tol, R. S. J. (2007). *The value of lost load*. ESRI Working Paper, No. 214. Dublin: The Economic and Social Research Institute (ESRI).

Tol, R. S. J. (2018). The economic impacts of climate change. *Review of Environmental Economics and Policy, 12* (1), 4–25. doi: 10.1093/reep/rex027

van Ginkel, K. C. H., Botzen, W. J. W., Haasnoot, M., Bachner, G., Steininger, K. W., Hinkel, J., … Bosello, F. (2020). Climate change induced socio-economic tipping points: Review and stakeholder consultation for policy relevant research. *Environmental Research Letters*, *15*(2), 023001. doi: 10.1088/1748-9326/ab6395

van Ginkel, K. C. H., Dottori, F., Alfieri, L., Feyen, L., and Koks, E. E. (2020). Direct flood risk assessment of the European road network: An object-based approach. *Natural Hazards and Earth System Sciiences* {under review]. doi.org/10.5194/nhess-2020-104

Vartabedian, R. (2019, October 28). *Intentional blackouts of this magnitude are unprecedented in California history*. Los Angeles Times.

Vorrath. S. (2019). *Cannon-Brookes, "Twiggy" Forrest lead capital raise for world's biggest solar project*. RenewEconomy. Retrieved from https://reneweconomy.com.au/cannon-brookes-twiggy-forrest-lead-capital-raise-for-worlds-biggest-solar-project-57623/

VPÖ2025+ (2009). VERKEHRSPROGNOSE ÖSTERREICH 2025+, Endbericht Teil/Kapitel 3: Beschreibung des Verkehrsmodells (Personenverkehr und Güterverkehr). Wien.

Ward, P. J., Jongman, B., Aerts, J. C. J. H., Bates, P. D., Botzen, W. J. W., Dlaz Loaiza, A., … Winsemius, H. C. (2017). A global framework for future costs and benefits of river-flood protection in urban areas. *Nature Climate Change, 7,* 642-646*.* doi:10.1038/nclimate3350

Wardman, M., Chintakayala, V.P.K. & de Jong, G.C. (2016). Values of travel time in Europe: Review and meta-analysis. *Transportation Research Part A: Policy and Practice, 94*, 93-111. doi:10.1016/j.tra.2016.08.019

*This project has received funding from the European Union's Horizon 2020 research and innovation programme under the Grant Agreement No **776479.***

Weill, A. (2018). Fuel matters: Why wildfire behavior depends on what's burning. KQED (belongs to Northern California Public Broadcasting). Retrieved from https://www.kqed.org/science/1928625/_trashed-35

Williams, A. P., C.D. Allen, A. K., Macalady, D., Griffin, C.A., Woodhouse, D.M., Meko, T. W., … McDowell, G. (2013). Temperature as a potent driver of regional forest drought stress and tree mortality. *Nature Climate Change, 3*, 292–297. doi:10.1038/nclimate1693

Williams, A.P., Abatzoglou, J.T., Gershunov, A., Guzman-Morales, J., Bishop, D.A., Balch, J.K., & Lettenmaier, D.P. (2019). Observed impacts of anthropogenic climate change on wildfire in California. AGU100. *American Geophysical Union*, 7 (8), 892-910. doi:10.1029/2019EF001210

Williams, J. R. (1995), The EPIC model, in V. P. Singh, (Ed), *Computer models of watershed hydrology* (p. 909-1000). Highlands Ranch, CO.: Water Resources Publications.

Williges, K., Mechler, R., Bowyer, P. & Balkovic, J. (2017). Towards an assessment of the adaptive capacity of the European agricultural sector to droughts. *Climate Services, 7,* 47-63.

Winsemius, H.C., Aerts, J.C.J.H., Van Beek, L.P.H., Bierkens, M.F.P., Bouwman, A., Jongman, B., … Ward, P.J. (2016). Global drivers of future river flood risk. *Nature Climate Change, 6*, 381–385. doi:10.1038/nclimate2893

World Bank (2019). Gross savings (% of GDP) | Data [WWW Document]. Retrieved from https://data.worldbank.org/indicator/NY.GNS.ICTR.ZS (accessed 5.29.20).

World Bank. (2020). Price level ratio of PPP conversion factor (GDP) to market exchange rate | Data. Retrieved from https://data.worldbank.org/indicator/PA.NUS.PPPC.RF?end=2011&start=2011&view=bar

World Meteorological Organization (2012). Commission for instruments and methods of observation. CIMO Expert Team on Standardization. First Session. Geneva, Switzerland. 26 – 29 November 2012. CIMO/ET-Stand-1/Doc. 10, (20.XI.2012)

Wu, M., Knorr, W., Thonicke, K., Schurgers, G., Camia, A. & Arneth, A. (2015). Sensitivity of burned area in Europe to climate change, atmospheric CO_2 levels and demography: A comparison of two fire-vegetation models. *JGR Biogeosciences, 120*(11), 2256-2272.

*This project has received funding from the European Union's Horizon 2020 research and innovation programme under the Grant Agreement No **776479.***

5. Appendix

5.1. Detailed description of the COIN-INT model

5.1.1. Regional and sectoral aggregations

Table 5.1.1: COIN-INT model region aggregates

Aggregated region	Model code	Comprising GTAP9 regions
Germany	DEU	Germany
Austria	AUT	Austria
Italy	ITA	Italy
UK	UKD	UK
France	FRA	France
Belgium and Luxemburg	BLU	Belgium, Luxemburg
Netherlands	NLD	Netherlands
Central EU 27 + Switzerland	CEU	Czech Republic, Hungary, Poland, Slovenia, Slovakia, Switzerland
Northern EU 27+ Liechtenstein, Norway and Iceland	NEU	Sweden, Ireland, Denmark, Finland, Norway, Estonia, Latvia, Lithuania, Rest of EFTA (*Liechtenstein, Iceland*), Rest of the world (*Antarctica, French Southern Territories, Bouvet Island, British Indian Ocean Territory*)
Mediterranean and South-eastern EU 27	MEU	Cyprus, Greece, Malta, Spain, Portugal, Bulgaria, Croatia, Romania, Albania, Rest of Europe (*Bosnia and Herzegovina, Macedonia, Serbia and Montenegro, Faroe Islands, Gibraltar, Monaco, San Marino*)
North America	NAM	USA, Canada, Rest of North America (*Bermuda, Greenland, Saint Pierre and Miquelon*)
Australia and New Zealand	AUZ	Australia, New Zealand
Eurasian countries	ERA	Russian Federation, Kazakhstan, Belarus, Ukraine, Armenia, Georgia, Kyrgyzstan, Rest of former Soviet Union (*Tajikistan, Turkmenistan, Uzbekistan*), Rest of Eastern Europe (*Moldova*)
Emerging economies- Asia	ECA	Hong Kong, Singapore, South Korea, Japan
Turkey	TUR	Turkey, Israel
China	CHN	China
India	IND	India
South-East Asia	SEA	Bangladesh, Thailand, Indonesia, Vietnam, Pakistan, Tunisia, Malaysia, Taiwan, Philippines, Cambodia, Lao People's Democratic Republic, Rest of South-East Asia (*Myanmar, Timor-Leste*), Sri Lanka, Rest of South Asia (*Afghanistan, Bhutan, Maldives*), Rest of East Asia (*Korea, Macau*), Rest of Oceania, Nepal, Brunei Darussalam, Mongolia
Latin America (w/o Venezuela)	LAM	Brazil, Mexico, Argentina, Bolivia, Guatemala, Honduras, Nicaragua, Peru, Rest of South America, Chile, Colombia, Dominican Republic, Ecuador, El Salvador, Paraguay, Uruguay, Costa Rica, Panama, Rest of Central America, Trinidad and Tobago, Caribbean (*Anguilla, Antigua and Barbuda, Aruba, Bahamas, Barbados, British Virgin Islands, Cayman Islands, Cuba, Dominica, Grenada, Haiti, Montserrat, Netherlands Antilles, Saint Kitts and Nevis, Saint Lucia, Saint Vincent and Grenadines, Turks and Caicos Islands, Virgin Islands (US)*), Jamaica, Puerto Rico

*This project has received funding from the European Union's Horizon 2020 research and innovation programme under the Grant Agreement No **776479.***

Aggregated region	Model code	Comprising GTAP9 regions
Oil exporting countries (OPEC: Middle East and Africa + Venezuela)	OIE	Saudi Arabia, United Arab Emirates, Egypt, Nigeria, Venezuela, Rest of North Africa (*Algeria, Lybia*), Rest of Western Asia (*Iraq, Lebanon, Palestinian Territory, Occupied, Syrian Arab Republic (Syria), Yemen*), Azerbaijan, Iran, Bahrain, Kuwait, Oman, Qatar, Morocco, Rest of South Central Africa, Jordan
Africa	AFR	South Africa, Benin, Burkina Faso, Cameroon, Cote d'Ivoire, Ghana, Guinea, Senegal, Togo, Tunisia, Rest of West Africa, Central Africa, Ethiopia, Kenya, Madagascar, Malawi, Mauritius, Mozambique, Namibia, Rwanda, Tanzania, Uganda, Zambia, Zimbabwe, Rest of Eastern Africa, Botswana, Rest of South African Customs Union

Table 5.1.2: COIN-INT model sector aggregates (superscripts 1-5 denote attribution to one of the five groups: 1. Resource using sectors, 2. Agricultural sectors, 3. Refined petroleum and coal products, 4. Process-emission generating sectors, 5. Non-resource using sectors)

Acronym	Sector aggregates in the model	Comprising GTAP9 sectors
AGC [2]	Agricultural products -crops	Agricultural sectors (1-8)
AGL [2]	Agricultural products -livestock	Agricultural sectors (9-12)
FOF [1]	Forestry and Fishery	forestry (13) and fishing(14)
COA [1]	Coal	Coal Mining (15)
OIL [1]	Crude Oil	Oil extraction (16)
GAS [1]	Natural Gas	Natural Gas extraction (17), manufacture of gas, distribution, steam and hot water supply (44)
OMN [1]	Other mining	other mining (18)
ELY [5]	Electricity	Production, collection and distribution of electricity (share of 43)
FBT [5]	Foodstuffs and feedingstuffs, beverages and tobacco products	All food processing sectors (19-25), beverages and tobacco products (26)
TWO [5]	Textile industry and other manufacturing	Textiles (27), Wearing apparel (28), Leather products (29), Wood products (30), Manufacture of paper products and publishing (31), Other Manufacturing: includes recycling (42)
OME [5]	Machinery, data processing equipment, electronic and optical products, Electronic Equipment, Motor, Motor vehicles and parts and other Transport Equipment	Other Machinery & Equipment: electrical machinery and apparatus n.e.c., medical, precision and optical instruments, watches and clocks (41), Electronic Equipment: office, accounting and computing machinery, radio, television and communication equipment and apparatus (40), Motor, Motor vehicles and parts: cars, lorries, trailers and semi-trailers (38), Other Transport Equipment: Manufacture of other transport equipment (39)
P_C [3]	Refined oil products	Petroleum, coal products (32)
CRP [4]	Chemical industry	Chemical, rubber, plastic products (33)
MIS [4]	Manufacture of other non-metallic mineral products, precious and non-ferrous metals, of basic iron and steel and casting and fabricated metal	Manufacture of other non-metallic mineral products (34), precious and non-ferrous metals (36), Manufacture of basic iron and steel and casting (35), fabricated metal products (37)

*This project has received funding from the European Union's Horizon 2020 research and innovation programme under the Grant Agreement No **776479.***

Acronym	Sector aggregates in the model	Comprising GTAP9 sectors
	products	
WAT [5]	Transport –Water	Water (49)
AIT [5]	Transport –Air	Air (50)
LAT [5]	Transport – Land	Other Transport (including road and rail transport) (48)
SER [5]	Other services and utilities	Water (45), Trade: all retail sales; wholesale trade and commission trade; hotels and restaurants; repairs of motor vehicles and personal and household goods; retail sale of automotive fuel (47), financial services (52), post and telecom (51), Recreational & service activities (55), dwellings (57) real estate & other business (54)
PIN [5]	Private insurance	insurance (53)
OSG [5]	Public services	other services (government): public administration (56)
CON [5]	Construction	construction (46)

5.1.2. Specification of production sectors, final demand and foreign trade

As given in Table 5.1.2, COIN-INT features a multitude of different production sectors. All of them are implemented as nested constant elasticity of substitution (CES) production functions. These CES functions, however, differ for different groups of sectors to capture key characteristics of production technologies (for details see Schinko et al., 2014). These groups are:

1. **Resource using sectors**: Coal Extraction, Oil Extraction, Gas Extraction, Other Mining, Forestry & Fishery. These sectors all use limited natural resource to operate. These sectors thus provide raw materials to the market.
2. **Agricultural sectors**: Agricultural crop and agricultural livestock sectors, using land as production factor. Land is exclusively used by these two sectors.
3. **Refined petroleum and coal products**: This sector aggregate uses fossil raw materials to produce refined fossil fuels (essentially oil and coal).
4. **Process-emission generating sectors**: Sectors that emit process-emissions, i.e. greenhouse gas emissions that do not originate from the combustion of fossil fuels but stem from chemical processes in the production. This group comprises the Iron & Steel sector, non-metallic minerals (including cement) as well as the chemical industry.
5. **Non-resource using sectors**: This groups comprises all remaining sectors.

In addition to the described sectoral structure, the Electricity sector is further divided into 12 sub-sectors according to the GTAP-POWER database (Peters, 2016). The 12 sub-sectors represent seven base-load electricity generation technologies (Nuclear, Coal, Gas, Wind, Hydro, Oil, Other) as well as four peak-load technologies (Gas, Hydro, Oil, Solar). In addition there is a transmission and distribution-sector.

Final demand is generated as follows: Within the EU there are two representative households in each region. First, a private household which is endowed with the production factors skilled labour, unskilled labour, capital as well as natural resources

*This project has received funding from the European Union's Horizon 2020 research and innovation programme under the Grant Agreement No **776479.***

(fossil resources, land and CO_2 emission allowances). These factors and resources are provided to the market and thus create income. The resulting income is spent for either consumption or investment (savings), subject to a fixed savings rate. Private consumption is specified as a nested CES consumption function. Second, in each EU regions there is also a public household, which collects taxes and provides transfers to the private household. Net-tax income is used to finance the supply of public services; i.e. government consumption, which is specified as a Leontief consumption function (i.e. fixed expenditure shares within the consumption bundle). Tax rates are assumed to be fixed, thus government income is flexible. By default transfers to the private household are assumed to scale linearly with tax income.

Foreign trade is implemented according to the Armington assumption (Armington, 1969). Hence, each region treats domestically produced goods and imported goods differently, subject to sectorally differentiated elasticities of substitution from GTAP9. Foreign trade is closed by assuming a fixed current account balance, which grows with GDP. The current account is balanced via net-capital inflows of opposite sign (i.e. the capital account).

5.1.3. Dynamics

COIN-INT is available in two variants: a static comparative version which models snapshots of 2011, 2030 and 2050, as well as a recursive dynamic version that explicitly models the pathway of economic development in 5-year times steps from 2015 to 2050.

In the comparative static variant the supply of production factors and resources is exogenously scaled up according to the quantitative indicators of the Shared Socioeconomic Pathways (SSPs; O'Neill et al., 2014). Total factor productivity is determined endogenously to meet the SSP-specific GDP growth rates.

In the dynamic recursive variant time steps are modelled explicitly, which are connected via the following equation of capital accumulation: $K_{t+1} = K_t*(1-\delta) + I_t$. This equation reads as follows. The capital stock (K) of the next year period (t+1) is determined by the current year (t) capital stock, minus deprecation according to the depreciation rate (δ), plus current period Investments (I). The recursive dynamic model specification implicitly assumes myopic behaviour of all economic agents, that is, they do not include future expectations in their decision but optimize within the current period. Depreciation rates and 2011 regional capital stocks are taken from GTAP9. In order to prevent very strong/weak capital accumulation until 2050 due to possible high/low investment levels in the benchmark year 2011, the savings rate is assumed to converge in all regions to 25% until 2050 (based on World Bank (2019)). The endogenously derived capital stock thus drives the availability of the production factor capital (i.e. the annual capital rent of the capital stock). The availability of labour is given exogenously via the growth of the working age population in each region, according to SSPs. Total factor productivity is determined endogenously to meet the SSP-specific GDP growth rates. Land availability is exogenous, according to SSPs. Natural resource supply (including fossil fuels) is determined endogenously.

*This project has received funding from the European Union's Horizon 2020 research and innovation programme under the Grant Agreement No **776479.***

5.1.4. Baseline calibration

COIN-INT is calibrated to all SSP-RCP-combinations from the COACCH modelling protocol (Hof et al., 2020). The calibration process involves two steps.

In **step 1** the SSP-Baselines are calibrated; i.e. socio-economic developments without any additional climate policy as given in 2011 are constructed. The socio-economic development is driven by exogenously given population growth, endogenous total factor productivity (TFP) changes, exogenously given autonomous energy efficiency improvements (AEEI, based on Dai et al. (2017)) as well as exogenously given electricity generation cost digressions. Fossil fuel supply is set endogenously to meet the SSP-specific fossil fuel price forecast (for SSP2 this is based on IEA (2018)). In step 1 SSP2 is selected as a central case and deviations from SSP2 parameters are introduced for calibrating other SSPs (i.e. SSP1, SSP3 and SSP5). Parameters are set in a way such that the CO_2 emissions calculated by COIN-INT come close to the IIASA SSP marker-scenarios' CO_2 emissions (Fricko et al., 2017); see Figure 5.1.1 (note that CO_2 emissions from land use changes are not included in the model). For a full overview on the parameter settings of the SSP-Baseline calibration see Table 5.1.3.

In **step 2** the SSPs are combined with RCPs by introducing a set of "Shared Policy Assumptions" (SPAs). These are: CO_2-pricing, subsidies for climate neutral Iron & Steel production (for sector MIS) as well as standards (which are assumed to increase the share of renewable electricity as well as flexibility in power generation and consumption). Note, that in the calibration process the CO_2-price is determined endogenously such that the exact emission pathway as given by the RCPs are reached. Note, that emission reduction obligations are set exogenously for each region. The reduction targets have been determined based on step 1 of the calibration procedure: Global emissions from step 1 are used to calculate a global emission reduction requirement to meet the given RCP. The same relative emission reduction requirement is then applied to all model regions uniformly. This means that each region fulfills the same relative emission reduction in a future year (relative to the respective Baseline emissions from step 1). The endogenously derived CO_2 prices are regionally different, with the exception of the EU with one shared price and emission allowance framework (EU-ETS). Figure 5.1.2 shows the global average CO_2 prices in 2050 (weighted by regional emissions) for all COACCH SSP-RCP-combinations. As expected, CO_2 prices need to be higher, the lower the RCP, and need to be lower in more sustainable SSPs. For further details on the assumptions on SPAs, see Table 5.1.4.

*This project has received funding from the European Union's Horizon 2020 research and innovation programme under the Grant Agreement No **776479.***

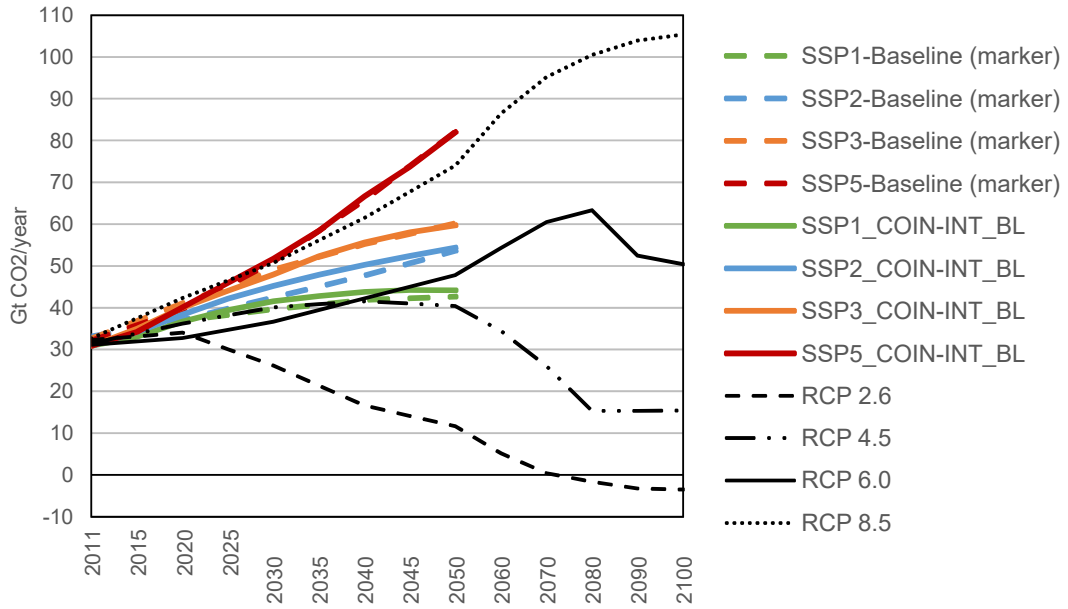

Figure 5.1.1: Comparison of CO_2 emissions of the COIN-INT Baseline scenarios (COIN-INT_BL) and the IIASA SSP marker-scenarios (step 1).

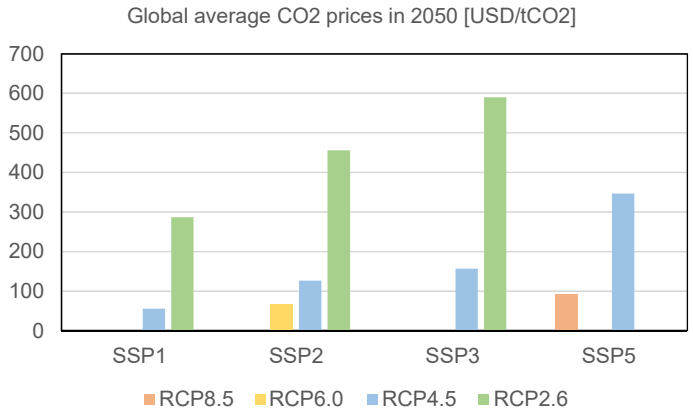

Figure 5.1.2: Global average CO_2 prices for all COACCH SSP-RCP combinations (weighted by regional emissions).

*This project has received funding from the European Union's Horizon 2020 research and innovation programme under the Grant Agreement No **776479.***

Table 5.1.3: SSP calibration parameter settings in COIN-INT

	Sustainability—Taking the green road	**Middle of the road**	**Regional rivalry—A rocky road**	**Fossil-fueled development—Taking the highway**
Parameter	**SSP1**	**SSP2**	**SSP3**	**SSP5**
Fossil fuel price forecast	=SSP2 (Actually no reason for increasing/decreasing exogenously the given fossil fuel price forecast. In SSP1 demand for fossil fuels is lower than in SSP2. If supply would not react, this would lead to lower prices, however in such a sustainable world supply should also adjust (i.e. decrease) due to expectations of the suppliers.)	following WEO (2018) "current policies scenario" until 2050: Coal: -0.3% p.a. Oil: +1.5% p.a. Gas: +1.4% p.a.	>SSP2, due to high demand: +0.5% p.a.	>>SSP2, due to high demand: +1% p.a.
AEEI (in non-ELY sectors)	>SSP2: +1% p.a.	2-5% p.a., depending on region (developed versus developing) and energy type (based on Dai et al. 2017)	<<SSP2: developed regions: -1% p.a. Developing regions: -2.5% p.a. (gas: 0%)	<SSP2: developed regions: -0.5% p.a. Developing regions: -0.5% p.a.
Electricity generation cost digression p.a. (on all non-energy intermediate inputs and production factors)	>SSP2: +1% p.a. for all non-fossil ELY generation technologies; -2% p.a. for fossil ELY generation (risk markup)	Hydro: 0.25% (i.e. 10% in 2050) Other: 0.47% (i.e 20% in 2050) Wind: 1.79% (i.e. 100% in 2050) Solar-PV: 2.38% (i.e. 150% in 2050) Nuclear: 0.47% (i.e. 20% in 2050) Fossil: 0% (i.e. 0% in 2050)	<SSP2: by 20% lower than SSP2 values to reflect slow technological change (for renewables); for fossils=SSP2	= SSP2 for renewables; 0.25% for fossils (i.e. 10% in 2050) to reflect fossil fuel tech-driven world
change elasticity of substitution within energy bundle	>SSP2: SSP2 * 2 to reflect technological change	default GTAP (0.16)	=SSP2	=SSP2
change elasticity of substitution within peak load bundle	>SSP2: SSP2 * 5 to reflect technological change	default GTAP-POWER (0.472)	=SSP2	=SSP2
change elasticity of substitution within base load bundle	>SSP2: SSP2 * 2 to reflect technological change	default GTAP-POWER (1.386)	=SSP2	=SSP2

*This project has received funding from the European Union's Horizon 2020 research and innovation programme under the Grant Agreement No **776479.***

	Sustainability—Taking the green road	**Middle of the road**	**Regional rivalry—A rocky road**	**Fossil-fueled development—Taking the highway**
Parameter	**SSP1**	**SSP2**	**SSP3**	**SSP5**
elasticity of substitution between base- and peak-load bundles	>SSP2: 2	default GTAP-POWER (0)	=SSP2	=SSP2
Armington elasticity	>SSP2: increased by 1/4 to reflect stronger global integration	default GTAP	<SSP2: reduced by 1/4 to reflect regional rivalry	>SSP2: increased by 1/4 to reflect stronger global integration
cost-neutral change in private consumption expenditure shares (coal, oil, gas, refined petroleum products, land and air transport, electricity)	coal, oil, gas, p_c: -40% land transport: -40% air transport: -30% electricity: +5%	coal, oil, gas, p_c: -20% land transport: -20% air transport: -20% electricity: +5%	default GTAP expenditure shares	default GTAP expenditure shares
technological change in iron and steel sector: switch from current technology to EAF (electric arc furnace)	=SSP2	stylized backstop technology for MIS (based on Mayer et al., 2019), which is 25% more costlier than conventional, but needs more capital and electricity instead of coke input	=SSP2	=SSP2
increase elasticity of substitution between (LK) and E-nest (technological improvement)	>SSP2: +0.7	Koesler and Schymura (2015): between 0.3 and 1.3; +0.3	Koesler and Schymura (2015): between 0.3 and 1.3;	Koesler and Schymura (2015): between 0.3 and 1.3;

*This project has received funding from the European Union's Horizon 2020 research and innovation programme under the Grant Agreement No **776479.***

	Sustainability—Taking the green road	**Middle of the road**	**Regional rivalry—A rocky road**	**Fossil-fueled development—Taking the highway**
Parameter	**SSP1**	**SSP2**	**SSP3**	**SSP5**
increase elasticity of substitution between energy and non-energy input in consumption function of private household (technological improvement and change of lifestyle)	>SSP2: +0.7	default: 0.2 +0.3	default: 0.2	default: 0.2

*This project has received funding from the European Union's Horizon 2020 research and innovation programme under the Grant Agreement No **776479.***

Table 5.1.4: SPA calibration parameter settings in COIN-INT

	Sustainability—Taking the green road	**Middle of the road**	**Regional rivalry—A rocky road**	**Fossil-fueled development—Taking the highway**
	SSP1	**SSP2**	**SSP3**	**SSP5**
subsidy for clean MIS production (steel)	RCP2.6 '50% subsidy of clean MIS in Europe 30% subsidy of clean MIS in ROW-regions 'RCP4.5: 25% subsidy of clean MIS in Europe 15% subsidy of clean MIS in ROW-regions RCP6.0: 15% subsidy of clean MIS in Europe 10% subsidy of clean MIS in ROW-regions	RCP2.6 '50% subsidy of clean MIS in Europe 30% subsidy of clean MIS in ROW-regions 'RCP4.5: 25% subsidy of clean MIS in Europe 15% subsidy of clean MIS in ROW-regions RCP6.0: 15% subsidy of clean MIS in Europe 10% subsidy of clean MIS in ROW-regions	RCP2.6 '50% subsidy of clean MIS in Europe 30% subsidy of clean MIS in ROW-regions 'RCP4.5: 25% subsidy of clean MIS in Europe 15% subsidy of clean MIS in ROW-regions RCP6.0: 15% subsidy of clean MIS in Europe 10% subsidy of clean MIS in ROW-regions	RCP2.6 '50% subsidy of clean MIS in Europe 30% subsidy of clean MIS in ROW-regions 'RCP4.5: 25% subsidy of clean MIS in Europe 15% subsidy of clean MIS in ROW-regions RCP6.0: 15% subsidy of clean MIS in Europe 10% subsidy of clean MIS in ROW-regions
increase elasticity of substitution between (LK) and E-nest [this has to be interpreted as a policy; e.g. energy efficiency standard in production]	Koesler and Schymura (2015): between 0.3 and 1.3; RCP2.6: '+1 RCP4p5: +0.8 other RCPs: +0	Koesler and Schymura (2015): between 0.3 and 1.3; RCP2.6: '+1 RCP4p5: +0.8 other RCPs: +0	Koesler and Schymura (2015): between 0.3 and 1.3; RCP2.6: '+1 RCP4p5: +0.8 other RCPs: +0	Koesler and Schymura (2015): between 0.3 and 1.3; RCP2.6: '+1 RCP4p5: +0.8 other RCPs: +0
increase elasticity of substitution between energy and non-energy input in consumption function of private household (policy interpreted as energy efficiency standards for home appliances and awareness raising)	default: 0.2 RCP2.6: '+1 RCP4p5: +0.8 other RCPs: +0	default: 0.2 RCP2.6: '+1 RCP4p5: +0.8 other RCPs: +0	default: 0.2 RCP2.6: '+1 RCP4p5: +0.8 other RCPs: +0	default: 0.2 RCP2.6: '+1 RCP4p5: +0.8 other RCPs: +0
CO2 price	endogenous s.t. given RCP is met	endogenous s.t. given RCP is met	endogenous s.t. given RCP is met	endogenous s.t. given RCP is met

*This project has received funding from the European Union's Horizon 2020 research and innovation programme under the Grant Agreement No **776479.***

5.2. Electricity system failures – blackout-fire risk for RCP 2.6

The analysis of fire risk and its future development in our analysis is based on the Forest Drought Stress Index (FDSI). Based on sufficient model runs available only for the analysis of RCP 4.5 and 8.5, the respective analysis is presented in Section 2.9. For RCP 2.6, results were available from the runs of one model only, which is why these results are at best a first indication of the potential risk. Nevertheless, we provide these results here in the Appendix for clarity and informational purposes.

Hazard modeling for RCP 2.6

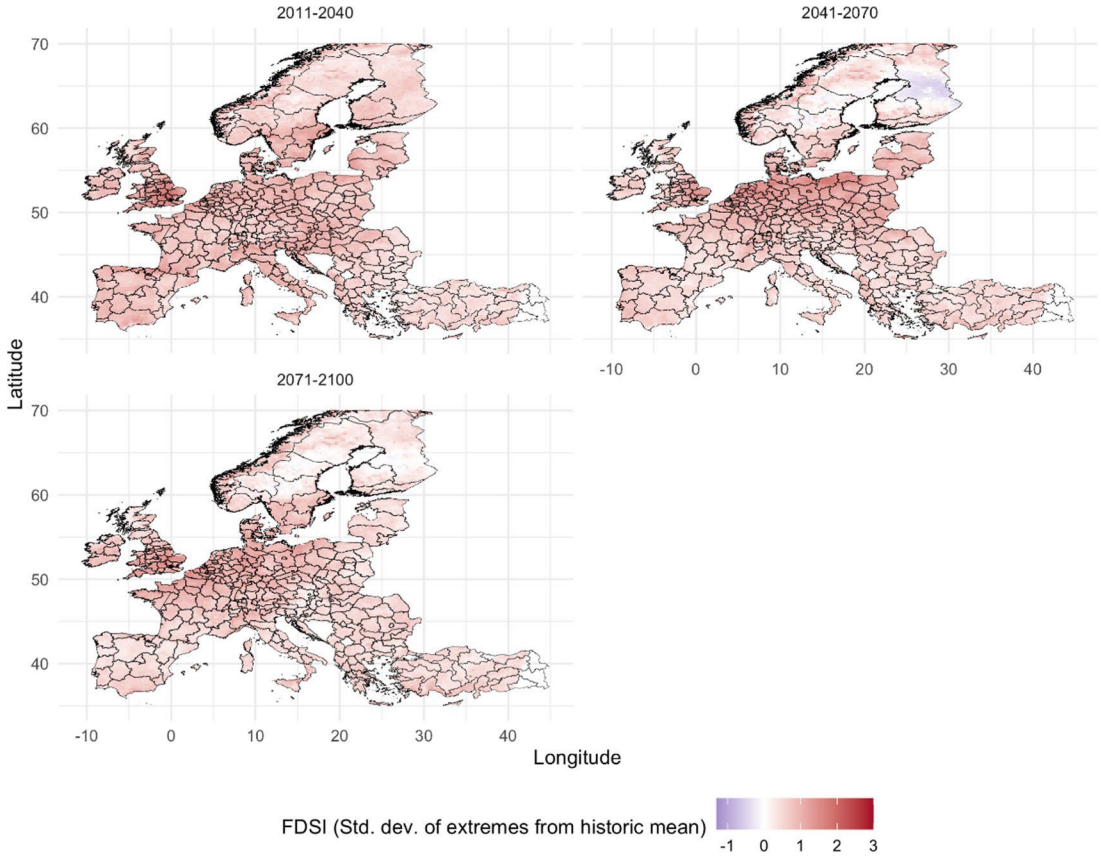

Figure 5.2.1. Increase in extreme drought, expressed as the 10th percentile FDSI values for a 30-year period for RCP 2.6, based on ERA5 and EURO-CORDEX model runs, for EU regions from 2007 to 2100. Increases are expressed as the number of standard deviations away from the historical mean value.

At first glance, results from RCP 2.6 (Figure 5.2.1) appear more severe than for RCPs 4.5 and 8.5 (Figure 2.9.3 and Figure 2.9.4). Several causes could be underlying the issue, the first being lack of a model ensemble from which to draw results, with the analysis therefore being based on a single model only. Due to data availability, only one model run could be constructed for RCP 2.6, as compared to the three models of the other RCPs. As can be seen in the top histogram in Figure 2.9.5, the chosen model remains relatively stationary over the study time period, but projects lower extreme

*This project has received funding from the European Union's Horizon 2020 research and innovation programme under the Grant Agreement No **776479.***

FDSI values (which are interpreted as being worse for forests) for the near future than do the results of RCPs 4.5 (middle panel) or 8.5 (bottom). The distribution of values for RCP 2.6 is much more concentrated between zero and one standard deviation from the historical mean and does not rise over time. This is consistent with other fire modelling which shows RCP 2.6 following the same trend as RCP 8.5 up to about 2040, and then levelling off in terms of burnt area (Wu et al. 2015). The initially high results for RCP 2.6 may also be driven by the determination of FDSI based on precipitation in the months from November to March. While in higher RCPs (particularly 8.5) summer seasonal rainfall is heavily reduced, there is less reduction in the fall and winter months, compared to e.g. RCP 2.6 which sees less rainfall loss in summer but greater inthe other seasons, as well as more uniform changes (or lack thereof) across Europe, rather than the large reductions in rainfall in southern latitudes contrasting more mild changes in northern regions in RCP 4.5 and 8.5 model runs. (Rajczak and Schär 2017).

Combined Hazard-Exposure Index for RCP 2.6

*This project has received funding from the European Union's Horizon 2020 research and innovation programme under the Grant Agreement No **776479.***

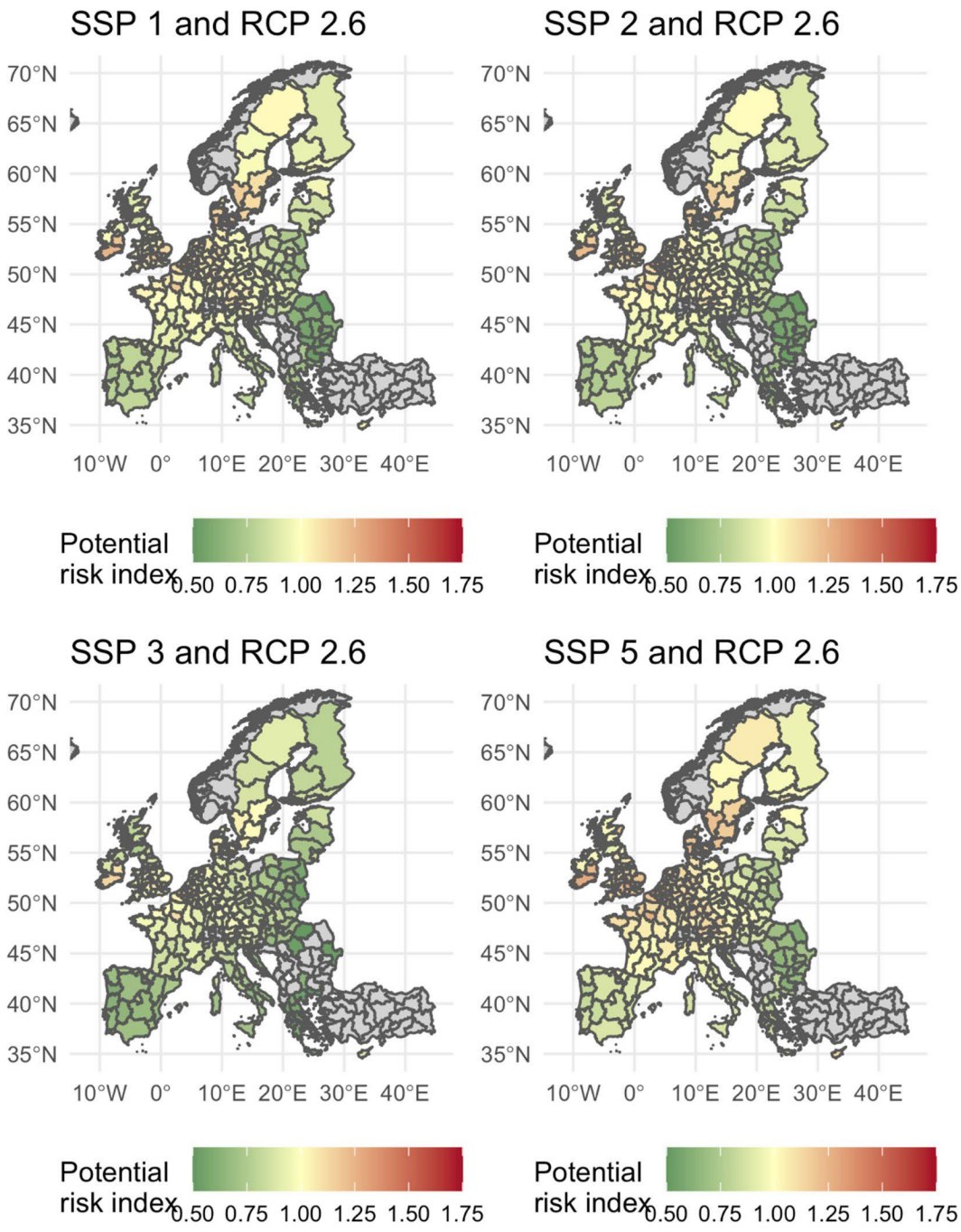

Figure 5.2.2. Potential future risk index (derived from hazard + exposure indicators) for RCP 2.6 model runs, for SSPs 1, 2, 3 and 5. Higher values indicate higher risk.

*This project has received funding from the European Union's Horizon 2020 research and innovation programme under the Grant Agreement No **776479.***